VNIVERSITAT DE VALÈNCIA

Programa de Doctorado en
Biomedicina y Farmacia

STUDY OF THE SYSTEMIC INFLAMMATION ASSOCIATED TO PRIMARY HYPERCHOLESTEROLEMIA, ITS MODULATION AND ITS IMPACT IN ATHEROSCLEROSIS

ROLE OF CXCL16/CXCR6 AXIS IN ABDOMINAL AORTIC ANEURYSM FORMATION

TESIS DOCTORAL

PRESENTADA POR:

AIDA COLLADO SÁNCHEZ

Directores:

María Jesús Sanz Ferrando
Laura Piqueras Ruiz

VALENCIA, Mayo 2019

VNIVERSITAT DE VALÈNCIA Facultat de Medicina i Odontologia

Dña. María Jesús Sanz Ferrando, Catedrática del Departamento de Farmacología de la *Universitat de València* y **Dña. Laura Piqueras Ruiz**, Investigadora adscrita al Instituto de Investigación Sanitaria INCLIVA y Profesora asociada del Departamento de Farmacología de la *Universitat de València*.

HACEN CONSTAR:

Que el trabajo titulado: "*Study of the systemic inflammation associated to primary hypercholesterolemia, its modulation and its impact in atherosclerosis. Role of CXCL16/CXCR6 axis in abdominal aortic aneurysm formation*", presentado por la Licenciada **Aida Collado Sánchez** para obtener el grado de doctor, ha sido realizado en el Departamento de Farmacología de la Facultad de Medicina y Odontología de la *Universitat de València*, bajo nuestra dirección y asesoramiento.

Concluido el trabajo experimental y bibliográfico, autorizamos la presentación y la defensa de esta Tesis Doctoral para que sea juzgada por el Tribunal correspondiente.

Valencia, 23 de mayo de 2019

Fdo. Dra. María Jesús Sanz Ferrando

Directora

Fdo. Dra. Laura Piqueras Ruiz

Directora

La presente Tesis Doctoral ha sido financiada gracias a los siguientes proyectos y becas:

PROYECTOS

- "Nuevas dianas farmacológicas para el tratamiento de la EPOC y sus comorbilidades vasculares". Entidad financiadora: Conselleria de Educación, Investigación, Cultura y Deporte de la Generalitat Valenciana (PROMETEO II/2013/014). Duración, desde: Junio 2013 hasta: Diciembre 2016. Investigador responsable: **Esteban J. Morcillo Sánchez**.
- "Estudio de los mecanismos moleculares y celulares en la disfunción endotelial asociada a enfermedades con inflamación sistémica que podrían inducir desórdenes cardiovasculares". Entidad financiadora: Conselleria de Educación, Investigación, Cultura y Deporte, Dirección General de Política Científica. Generalitat Valenciana. Ayudas complementarias para proyectos de I+d para grupos de calidad (GVACOMP2014-006). Duración, desde: Julio 2014 hasta: Diciembre 2014. Investigador responsable: **María Jesús Sanz Ferrando**.
- "Modulación Inmunofarmacológica de la Inflamación Sistémica asociada a Desordenes Metabólicos. Búsqueda de nuevas dianas terapéuticas y síntesis de fármacos novedosos". Entidad financiadora: Ministerio de Economía y Competitividad (SAF2014-57845-R). Duración, desde: Enero 2015 hasta: Junio 2018. Investigador responsable: **María Jesús Sanz Ferrando** y **Juan Francisco Ascaso Gimilio**.
- "Modulación farmacológica del sistema inmune como diana clave en la prevención de la enfermedad cardiovascular asociada a desórdenes metabólicos. Síntesis de fármacos novedosos". Entidad financiadora: Ministerio de Economía y Competitividad (SAF2017-89714-R). Duración, desde: Julio 2018 hasta: Diciembre 2020. Investigador responsable: **María Jesús Sanz Ferrando** y **Juan Francisco Ascaso Gimilio**.
- "Identificación de nuevos mecanismos implicados en la angiogénesis e inflamación en pacientes obesos. Modulación por ligandos de receptores nucleares constitutivos de androstano". Entidad financiadora: Instituto de Salud Carlos III (PI18/00209).

Duración, desde: Enero 2019 hasta: Diciembre 2021. Investigadora responsable: **Laura Piqueras Ruiz**.

- "Estudio de nuevos mecanismos inflamatorios y angiogénicos asociados a la obesidad grave mórbida; Papel del eje CXCR3 y los receptores nucleares ROR". Entidad financiadora: Instituto de Salud Carlos III (PI15/00082). Duración, desde: Enero 2016 hasta: Diciembre 2018. Investigadora responsable: **Laura Piqueras Ruiz**.

BECAS

- Contrato Predoctoral PROMETEO. Título del proyecto: Nuevas dianas farmacológicas para el tratamiento de la EPOC y sus comorbilidades vasculares. PROMETEO II/2013/014. Entidad financiadora: Conselleria de Educación, Investigación, Cultura y Deporte de la Generalitat Valenciana. 2013-2016. Duración, desde: Noviembre 2014 hasta: Junio 2016. Investigador responsable: **Esteban J. Morcillo Sánchez**.
- Beca Predoctoral del Programa VALi+d concedida por la Conselleria de Educación, Investigación, Cultura y Deporte de la Generalitat Valenciana. ACIF/2016/424. Duración, desde: Julio 2016 hasta: Octubre 2017.
- Contrato Predoctoral: Título del proyecto: Modulación farmacológica del sistema inmune como diana clave en la prevención de la enfermedad cardiovascular asociada a desórdenes metabólicos. Síntesis de fármacos novedosos. Entidad financiadora: Ministerio de Economía y Competitividad (SAF2017-89714-R). Duración, desde: Julio 2018 hasta: Diciembre 2020. Investigador responsable: **María Jesús Sanz Ferrando** y **Juan Francisco Ascaso Gimilio**.
- Beca para la realización de una estancia de contratados predoctorales en centros de investigación fuera de la Comunidad Valenciana de la Conselleria de Educación, Investigación, Cultura y Deporte. Convocatoria 2017. Duración, desde: 1 Julio 2017 hasta: 30 Septiembre 2017. *King's College. Faculty of Life Sciences & Medicine*. Investigador responsable: **Aleksandar Ivetic**.

A lo largo de esta Tesis Doctoral se han obtenido las siguientes publicaciones:

- **Collado, A.**, Perez-Alós, L., Escudero, P., Piqueras, L., Blanes, J.I. and Sanz, M.J. (2015). El ratón deficiente en apolipoproteína E (apoE-/-), un modelo traslacional para el estudio de la aterosclerosis. *Angiología*. **67**:342-51.
- Escudero, P., Martinez de Maranon, A., **Collado, A.**, Gonzalez-Navarro, H., Hermenegildo, C., Peiro, C., Piqueras, L. and Sanz, M. J. (2015a). Combined sub-optimal doses of rosuvastatin and bexarotene impair angiotensin-II-induced arterial mononuclear cell adhesion through inhibition of Nox5 signaling pathways and increased RXR/PPARalpha and RXR/PPARgamma interactions. *Antioxid Redox Signal* **22**(11): 901-920.
- Martorell, S., Hueso, L., Gonzalez-Navarro, H., **Collado, A.**, Sanz, M. J. and Piqueras, L. (2016). Vitamin D Receptor Activation Reduces Angiotensin-II-Induced Dissecting Abdominal Aortic Aneurysm in Apolipoprotein E-Knockout Mice. *Arterioscler Thromb Vasc Biol* **36**(8): 1587-1597.
- Marques, P.†, **Collado, A.†**, Escudero, P., Rius, C., González, C., Servera, E., Piqueras, L. and Sanz, M. J. (2017). Cigarette Smoke Increases Endothelial CXCL16-Leukocyte CXCR6 Adhesion In Vitro and In Vivo. Potential Consequences in Chronic Obstructive Pulmonary Disease. *Front Immunol* **8**. **†These authors have contributed equally to this work as first authors**.
- Plens-Galaska, M., Szelag, M., **Collado, A.**, Marques, P., Vallejo, S., Ramos-González, M., Wesoly, J., Sanz, M.J., Peirró, C. and Bluyssen Hans A. R. (2018). Genome-Wide Inhibition of Pro-atherogenic Gene Expression by Multi-STAT Targeting Compounds as a Novel Treatment Strategy of CVDs. *Front Immunol* **5**.
- **Collado, A.**, Marques, P., Domingo, E., Perello, E., Gonzalez-Navarro, H., Martinez-Hervas, S., Real, J. T., Piqueras, L., Ascaso, J. F. and Sanz, M. J. (2018a). Novel Immune Features of the Systemic Inflammation Associated with Primary Hypercholesterolemia: Changes in Cytokine/Chemokine Profile, Increased Platelet and Leukocyte Activation. *J Clin Med* **8**(1).

- **Collado, A.**, Marques, P., Escudero, P., Rius, C., Domingo, E., Martinez-Hervas, S., Real, J. T., Ascaso, J. F., Piqueras, L. and Sanz, M. J. (2018b). Functional role of endothelial CXCL16/CXCR6-platelet-leucocyte axis in angiotensin II-associated metabolic disorders. *Cardiovasc Res* **114**(13): 1764-1775.
- Marques, P. **†**, **Collado, A. †**, Martinez-Hervas, S., Domingo, E., Benito, E., Piqueras, L., Real, J. T., Ascaso, J. F. and Sanz, M. J. (2019). Systemic Inflammation in Metabolic Syndrome: Increased Platelet and Leukocyte Activation, and Key Role of CX3CL1/CX3CR1 and CCL2/CCR2 Axes in Arterial Platelet-Proinflammatory Monocyte Adhesion. *J Clin Med* **8**. **†These authors have contributed equally to this work as first authors**.

AGRADECIMIENTOS

En primer lugar agradecer a mis directoras de Tesis, Mª Jesús y Laura, por acogerme con los brazos abiertos desde el primer día, por todo lo que me han enseñado en estos últimos años, y sobre todo por el tiempo empleado en mí.

Agradecer también a todos mis compañeros de laboratorio: Luisa, Rebeca, Laura, Nuria y Paqui y en especial a Patrice y Elena, por amenizar las muchas horas que hemos pasado juntos trabajando. Del mismo modo, querría dar las gracias a mis compañeros del laboratorio de Londres, Izaj, Justin y en especial a Alex, porque en tan poco tiempo me hicieron sentir una más del grupo: gracias por esos tres productivos y maravillosos meses.

Dar las gracias al resto de mi familia de Valencia: María, Carlos, Blanca, Bea, Susana y Elena(s), porque durante todos estos años siempre habéis estado ahí, en lo bueno y en lo malo; por muchos años más. También agradecer a mi familia de acogida de Londres, en especial a Rosa y Rafa, porque con vosotros esos tres meses fueron infinitamente mejores.

También doy las gracias a mis amigos de Albacete: Javi, Juan, Bea, Jorge y Nico, porque siempre estáis ahí desde hace más de 20 años y los que nos quedan.

Una mención especial es para Laura porque, aunque estés a miles de kilómetros de distancia, siempre te he sentido a mi lado. Gracias por todo, por tus consejos y sobre todo porque casi te has leído tantas veces esta Tesis Doctoral como yo.

Quiero dar las gracias a mis padres: Manuel y Aurora, porque sin ellos jamás habría llegado donde estoy, y por supuesto a mis hermanas Ester e Irene, porque pase lo que pase, siempre están ahí. ¡Os quiero!

Por último, pero no por ello menos importante, dar un GRACIAS en mayúsculas a Miguel, porque has sido el pilar fundamental durante toda la tesis, porque has estado siempre presente, en los mejores y peores momentos y porque esta Tesis Doctoral tiene mucho de ti. ¡Muchas gracias!

Gracias a todos los que están, estarán, pero sobre todo muchas gracias a los que ya no están. Si he llegado hasta aquí es gracias a cada uno de vosotros.

Para Miguel

ÍNDICE / INDEX

LIST OF ABBREVIATIONS

AAA – Abdominal aortic aneurysm

AAM – Alternative-activated macrophages

ACE – Angiotensin-converting enzyme

ADAM – A disintegrin and metalloproteinase

ADH – Autosomal dominant hypercholesterolemia

Ang-II – Angiotensin-II

ANOVA – Analysis of variance

APC – Allophycocyanin

ApoB – Apolipoprotein B

ApoE – Apolipoprotein E

AT_1 **–** Angiotensin-II receptor type 1

AT_2 **–** Angiotensin-II receptor type 2

BMI – Body mass index

BSA – Bovine serum albumin

BV – Brilliant violet

CAM – Cell adhesion molecules

CCL – C-C motif ligand

CCR3 – C-C chemokine receptor type 3

CD – Cluster of differentiation

cDNA – Complementary DNA

CF – 5-carboxyfluorescein

CX_3CR1 – Fractalkine receptor

DAB – 3, 3'-diaminobenzidine

DBP – Diastolic blood pressure

DMEM – Dulbecco's modified eagle's medium

EBM-2 – Endothelial cell basal medium-2

EDTA – Ethylenediaminetetraacetic acid

EGM-2 – Endothelial growth medium-2

ELISA – Enzyme-linked immunosorbent assay

ENA-78 – Epithelial-neutrophil activating peptide-78

eNOS – Endothelial nitric oxide synthase

ESL-1 – E-selectin ligand-1

FACS – Fluorescence-activated cell sorting

FBS – Fetal bovine serum

FcεRIα – High-affinity IgE receptor

FGF – Fibroblast growth factor

FITC – Fluorescein isothiocyanate

FSC – Forward scatter

GAPDH – Glyceraldehyde 3-phosphate dehydrogenase

GFP – Green fluorescence protein

GM-CSF – Granulocyte-macrophage colony-stimulating factor

GOT – Glutamic-oxalacetic transaminase

GPCR – G protein-coupled receptors

GPT – Glutamate-pyruvate transaminase

GROα – Growth-regulated oncogene α

HBSS – Hank's balanced salt solution

HDL – High-density lipoprotein

HEPES – 4-(2-hydroxyethyl)-1-piperazineethanesulfonic acid

HIF-1 – Hypoxia-inducible factor-1

HRP – Horseradish peroxidase

HUAEC – Human umbilical arterial endothelial cells

ICAM – Intercellular adhesion molecule

IFNγ – Interferon γ

Ig – Immunoglobulin

IL – Interleukin

IU – International units

LDL – Low-density lipoprotein

LDLox – Oxidized low-density lipoprotein

LDLR – Low-density lipoprotein receptor

LFA-1 – Lymphocyte function-associated antigen-1

LIN – Lineage

LPAM-1 – Integrin alpha 4 beta 7

mAb – Monoclonal antibody

Mac-1 – Macrophage-1 antigen

MAdCAM-1 – Mucosal addressin cell adhesion molecule-1

MAPK – Mitogen-activated protein kinase

MCP-1 – Monocyte chemoattractant protein-1

MFI – Mean fluorescence intensity

MIP – Macrophage inflammatory proteins

MMPs – Matrix metalloproteinases

NAD – Nicotinamide adenine dinucleotide

NADP – Nicotinamide adenine dinucleotide phosphate

NAP-2 – Neutrophil-activating peptide-2

NF-κB – Nuclear factor kappa-light-chain-enhancer of activated B cells

NK – Natural killer

NO – Nitric oxide

OFL – Oral fat load

PAC-1 – First procaspase

PB – Pacific blue

PBS – Phosphate-buffered saline

PCR – Polymerase chain reaction

PCSK9 – Proprotein convertase subtilisin/kexin 9

PE – Phycoerythrin

PECAM-1 – Platelet/endothelial cell adhesion molecule-1

PF-4 – Platelet factor-4

PFA – Paraformaldehyde

PH – Primary hypercholesterolemia

PMN – Polymorphonuclear

PRR – Pattern recognition receptors

PSGL-1 – P-selectin glycoprotein ligand-1

qPCR – Quantitative polymerase chain reaction

RANTES – Regulated upon activation, normal T cell expressed and secreted

RAS – Renin-angiotensin system

RBCs – Red blood cells

RhoA – Ras homolog gene family, member A

RT – Reverse transcription

RT-PCR – Reverse transcription polymerase chain reaction

SBP – Systolic blood pressure

SDF-1α – Stromal cell-derived factor-1α

SEM – Standard error of the mean

SMC – Smooth muscle cells

SSC – Side scatter

TACE – The tumor necrosis factor α converting enzyme

TAE – Tris acetate-EDTA

TC – Total cholesterol

TG – Triglycerides

TGF – Transforming growth factor

Th – T helper lymphocytes

TIMP – Tissue inhibitor of metalloproteinases

TLR – Toll-like receptor

TNFα – Tumor necrosis factor α

Treg – Regulatory T lymphocytes

VCAM-1 – Vascular cell adhesion molecule-1

VEGF – Vascular endothelial growth factor

VLA-4 – Very late antigen-4

VLDL – Very low-density lipoprotein

XO – Xanthine oxidase

LISTA DE ABREVIATURAS

AAA – Aneurisma aórtico abdominal

ADAM – Proteasas con dominio metaloproteasa y desintegrina

ADH – Hipercolesterolemia autosómica dominante

Ang-II – Angiotensina-II

ApoB – Apolipoproteína B

ApoE – Apolipoproteína E

AT_1 – Receptor de angiotensina-II de tipo 1

AT_2 – Receptor de angiotensina-II de tipo 2

CCL – Ligando del motivo C-C

CCR3 – Receptor de quimiocinas C-C de tipo 3

CD – Cúmulo de diferenciación

CT – Colesterol total

ECA – Enzima conversora de angiotensina

ENA-78 – Péptido activador de neutrófilos epiteliales-78

eNOS – Óxido nítrico sintasa endotelial

ESL-1 – Ligando 1 de E-selectina

FcεRIα – Receptor de IgE de alta afinidad

FGF – Factor de crecimiento de fibroblastos

GM-CSF – Factor estimulante de colonias de granulocitos y monocitos

GPCR – Receptores acoplados a proteína G

GROα – *Growth-regulated oncogene α*

HIF-1 – Factor 1 inducible por hipoxia

HP – Hipercolesterolemia primaria

ICAM – Molécula de adhesión intercelular

IFNγ – Interferón γ

Ig – Inmunoglobulina

IL – Interleucina

LDL – Lipoproteínas de baja densidad

LDLox – Lipoproteínas de baja densidad oxidadas

LDLR – Receptor de lipoproteínas de baja densidad

LFA-1 – Antígeno 1 asociado a función linfática

LPAM-1 – Integrina alfa 4 beta 7

MAC – Moléculas de adhesión celular

Mac-1 – Antígeno 1 asociado a macrófagos

MAdCAM-1 – Molécula de citoadhesión adresina mucosal-1

MAPK – Proteína quinasas activadas por mitógenos

MCP-1 – *Monocyte chemoattractant protein-1*

MEC – Quimiocina epitelial asociada a la mucosa

MIP – Proteína inflamatoria de macrófagos

MMPs – Metaloproteasas de matriz

NAD – Dinucleótido de nicotinamida y adenina

NADP – Nicotinamida adenina dinucleótido fosfato

NAP-2 – Proteína activadora de neutrófilos-2

NF-κB – Factor nuclear potenciador de las cadenas ligeras kappa de las células B activadas

NK – *Natural killer*

NO – Óxido nítrico

PCSK9 – Proteía convertasa subtilisina/kexina 9

PECAM-1 – Molécula de adhesión de célula endotelial/plaqueta-1

PF-4 – Factor plaquetario-4

PMN – Polimorfonucleares

PRR – Receptores de reconocimiento de patrones

PSGL-1 – Ligando 1 de la glicoproteína P-selectina

RANTES – *Regulated upon activation, normal T cell expressed and secreted*

RhoA – Familia de genes homólogos de Ras, miembro A

SDF-1α – Factor derivado de células estromales-1α

SRA – Sistema renina-angiotensina

TACE – Enzima convertidora del factor de necrosis tumoral α

TGF – Factor de crecimiento transformante

TIMP – Inhibidores de metaloproteasas de matriz

TLR – Receptor tipo *toll*

TNFα – Factor de necrosis tumoral α

VCAM-1 – Molécula de adhesión vascular-1

VEGF – Factor de crecimiento vascular endotelial

VLA-4 – *Very late antigen-4*

VLDL – Lipoproteínas de muy baja densidad

XO – Xantina oxidasa

LISTADO DE FIGURAS / LIST OF FIGURES

LISTADO DE TABLAS / LIST OF TABLES

RESUMEN / ABSTRACT

RESUMEN

La hipercolesterolemia primaria (HP) es un desorden metabólico caracterizado por unos elevados niveles circulantes de lipoproteínas de baja densidad (LDL), así como por una inflamación sistémica de bajo grado, que puede finalmente dar lugar al desarrollo de aterosclerosis. Debido a la escasa información que se tiene de la enfermedad a nivel inmunológico, hemos caracterizado el comportamiento de diferentes mediadores solubles y celulares de la inflamación y sus posibles consecuencias. Para ello se ha empleado sangre completa de 22 pacientes con HP y 21 controles de semejante edad. En todos ellos se ha analizado la sangre por citometría de flujo para determinar la activación leucocitaria y plaquetaria, la proporción de las distintas subpoblaciones leucocitarias, así como la formación de agregados plaqueta-leucocito, junto con la determinación de los niveles plasmáticos de diferentes marcadores solubles. De hecho, los pacientes con HP presentaron mayores porcentajes de monocitos de tipo 3 (Mon 3), linfocitos Th2 y Th17 y plaquetas y leucocitos activados que los controles. Asimismo, se detectaron mayores niveles circulantes de interleucina (IL)-8/CXCL8, CCL2, fractalquina/CX_3CL1 e IL-6 que se correlacionaron positivamente con los niveles de lípidos característicos de la HP: apolipoproteína B (apoB), LDL y colesterol total (CT). Sin embargo, los pacientes con HP mostraron niveles plasmáticos inferiores de las citocinas anti-inflamatorias IL-4 e IL-10 que los correspondientes controles.

Por otro lado, la disfunción endotelial constituye una de las primeras etapas de la aterogénesis, promoviendo la adhesión y posterior migración leucocitaria hacia el foco inflamatorio. El factor de necrosis tumoral α (TNFα) es una de las citocinas principales en la hipercolesterolemia; por esta razón se han explorado las consecuencias funcionales de la presencia de elevados niveles de TNFα en los pacientes con HP. Así, se ha estudiado mediante cámara de flujo la adhesión plaqueta-leucocito y leucocito sobre el endotelio arterial estimulado o no con TNFα, observándose una mayor adhesión leucocitaria al endotelio disfuncional en los pacientes con HP. Ello sugiriere una posible asociación entre la inflamación sistémica y el desarrollo de enfermedades cardiovasculares en este desorden metabólico.

Al mismo tiempo, y para saber si la ingesta de una sobrecarga lipídica oral de una preparación comercial de triglicéridos de cadena larga con una proporción ω6/ω3 >20/1, logra disminuir la inflamación sistémica, se administró a pacientes con HP y se repitió el estudio de todos los parámetros anteriores a las 4 horas de su ingesta, observándose una disminución de la activación plaquetaria así como una disminución en la adhesión leucocitaria al endotelio disfuncional. Se pudo observar que la administración de esta sobrecarga lipídica tuvo un efecto beneficioso en el estado protrombótico y proinflamatorio en los pacientes con HP.

Así mismo, se detectaron elevados niveles circulantes de eotaxina-1/CCL11 y eotaxina-3/CCL26 en los pacientes con HP. Ya que ambas quimiocinas señalizan exclusivamente a través del receptor CCR3, el cual se expresa de manera constitutiva en los eosinófilos, se llevó a cabo un estudio en profundidad de la expresión del receptor en diferentes poblaciones leucocitarias, tanto en pacientes como en controles.

La aterosclerosis es una de las principales causas de morbilidad y mortalidad en países desarrollados que presenta varias similitudes histopatológicas con la inflamación crónica. Para entender el papel que desempeña en su desarrollo el eje CCL11/CCR3, se generaron ratones deficientes en apolipoproteína E (apoE$^{-/-}$) y el receptor de eotaxina-1 (CCR3; apoE$^{-/-}$CCR3$^{-/-}$). Se evaluó el impacto de una dieta aterogénica en la formación de la placa de ateroma en ratones apoE$^{-/-}$CCR3$^{+/+}$ y ratones apoE$^{-/-}$CCR3$^{-/-}$. Los ratones apoE$^{-/-}$CCR3$^{+/+}$ y apoE$^{-/-}$CCR3$^{-/-}$ sometidos a una dieta hipercolesterolémica durante dos meses mostraron un claro desarrollo de lesión aterosclerótica en aorta caracterizada por un mayor contenido en colágeno, *core* necrótico, células de la musculatura lisa vascular, macrófagos y linfocitos T que aquellos sometidos a una dieta control. Los ratones apoE$^{-/-}$CCR3$^{-/-}$ sometidos a dieta aterogénica mostraron mayor lesión aterosclerótica y mayor contenido en colágeno e infiltración de macrófagos y linfocitos T que los ratones que presentaban el receptor CCR3 (apoE$^{-/-}$CCR3$^{+/+}$). La expresión de eotaxina-1 en la lesión de los ratones apoE$^{-/-}$CCR3$^{+/+}$ en ambiente hipercolesterolémico fue mucho mayor que la detectada en los ratones apoE$^{-/-}$CCR3$^{-/-}$ en las mismas condiciones. Esto sugieren que el eje eotaxina-1 (CCL11)/CCR3 podría ejercer un efecto protector en el desarrollo del proceso aterosclerótico.

El aneurisma aórtico abdominal (AAA) es una importante causa de muerte en nuestro país, afectando principalmente a varones mayores de 65 años de edad. Actualmente no existe tratamiento preventivo ya que la falta de conocimiento sobre los mecanismos responsables de la iniciación, propagación y ruptura del AAA aún hoy en día son desconocidos. Uno de los causantes de la patología es la angiotensina-II (Ang-II), principal péptido efector del sistema renina-angiotensina, la cual es utilizada *in vivo* para inducir la enfermedad en modelos experimentales de ratones apoE$^{-/-}$. En el estudio se ha empleado el fármaco antihipertensivo losartán, el cual actúa como antagonista selectivo del receptor de Ang-II de tipo 1 (AT_1), a la dosis de 30 mg/kg/día. Tras 28 días de tratamiento, se pudo comprobar cómo la dosis de 30 mg/kg/día lograba atenuar la formación, el desarrollo y el diámetro del AAA inducida con Ang-II, así como la infiltración de linfocitos T, macrófagos, la neovascularización, células CXCR6^{+} y la expresión de ARNm de quimiocinas y mediadores proangiogénicos como *Mcp-1/Ccl2*, *Vegf*, *Cxcl16* y su receptor *Cxcr6*. Estos resultados nos inducen a sugerir que una monoterapia con losartán a una dosis de 30 mg/kg/día podría ser susceptible de convertirse en una nueva y segura herramienta terapéutica en el control del AAA.

Para estudiar el papel del eje CXCL16/CXCR6 en el desarrollo del AAA, se generaron ratones con el receptor CXCR6 no funcional (apoE$^{-/-}$CXCR6$^{GFP/GFP}$). En aquellos animales deficientes en la función de CXCR6 se observaron resultados similares a los ratones apoE$^{-/-}$ tratados con losartán. Por tanto, la modulación farmacológica del eje CXCL16/CXCR6 podría impactar beneficiosamente en el desarrollo del AAA asociado a alteraciones del sistema renina-angiotensina.

ABSTRACT

Primary hypercholesterolemia (PH) is a metabolic disease characterized by high circulating levels of low-density lipoproteins (LDL), as well as a low-grade of systemic inflammation, which can eventually lead to the development of atherosclerosis. Due to the limited information of the immunological component of the disease, we have characterized the behavior of different immunological cell populations, the soluble inflammatory mediators and their possible consequences in PH. Whole blood of 21 age-matched controls and 22 patients with PH was used. In all of them, the blood was analyzed by flow cytometry to determine platelet, and leukocyte activation, percentage of leukocyte subpopulations, the formation of platelet-leukocyte aggregates as well as the circulating levels of different soluble inflammatory mediators. PH patients presented a higher percentage of type 3 monocytes (Mon 3), Th2 and Th17 lymphocytes, activated platelets, and leukocytes than controls. Similarly, circulating interleukin (IL)-8/CXCL8, CCL2, fractalkine/CX_3CL1, and IL-6 levels positively correlated with key lipid features of PH: apolipoprotein B (apoB), LDL and total cholesterol (TC); whereas negative correlations were found for IL-4 and IL-10.

Endothelial dysfunction is one of the first stages of atherogenesis, promoting the adhesion and the subsequent leukocyte migration to the inflammatory focus. Tumor necrosis factor α (TNFα) is one of the central cytokines in hypercholesterolemia; for this reason, the functional consequences of high levels of TNFα in PH patients have been studied. Thus, platelet-leukocyte and leukocyte adhesion on the arterial endothelium stimulated or not with TNFα have been assessed using a flow chamber. Indeed, greater leukocyte adherence to the dysfunctional endothelium was observed in patients than in control subjects suggesting a possible link between systemic inflammation and the development of cardiovascular diseases in this metabolic disorder.

To explore whether the intake of an oral fat load (OFL) with a commercial preparation of long-chain triglycerides (ω6/ω3 ratio >20/1) has an impact on inflammation, this OFL was administered to PH patients, and the different parameters were determined 4 hours later. A decrease in platelet activation as well as in leukocyte adhesion to the dysfunctional endothelium was detected. Therefore, the administration of this OFL may have a beneficial impact on the control of the pro-thrombotic and proinflammatory state in patients with PH.

Likewise, high circulating levels of eotaxin-1/CCL11 and eotaxin-3/CCL26 were detected in patients with PH. Both mediators signal exclusively through the CCR3 receptor, which is expressed constitutively in eosinophils. Therefore, an in-depth study of the expression of the receptor in different leukocyte populations was carried out, both in PH patients and in control volunteers.

Atherosclerosis is one of the leading causes of morbidity and mortality in developed countries that presents several histopathological similarities with chronic inflammation. To understand the role of the CCL11/CCR3 axis in its development, mice deficient in apolipoprotein E ($apoE^{-/-}$) and the eotaxin-1 receptor (CCR3; $apoE^{-/-}CCR3^{-/-}$) were generated. The impact on the atheroma plaque formation of an atherogenic diet was evaluated in $apoE^{-/-}CCR3^{+/+}$ and $apoE^{-/-}CCR3^{-/-}$ mice. The $apoE^{-/-}CCR3^{+/+}$ and $apoE^{-/-}CCR3^{-/-}$ mice under a hypercholesterolemic diet for two months showed a clear development of atherosclerotic lesion in the aorta characterized by a higher content of collagen, necrotic *core*, vascular smooth muscle cells, macrophages, and T lymphocytes than those subjected to a control diet. The $apoE^{-/-}CCR3^{-/-}$ mice subjected to an atherogenic diet showed greater atherosclerotic lesion and higher collagen content and infiltration of macrophages and T lymphocytes than the mice that express the CCR3 receptor ($apoE^{-/-}CCR3^{+/+}$). The expression of eotaxin-1 in the lesion of the $apoE^{-/-}CCR3^{+/+}$ mice in a hypercholesterolemic environment was much higher than that detected in the $apoE^{-/-}CCR3^{-/-}$ mice under the same conditions. This suggests that the eotaxin-1 (CCL11)/CCR3 axis may exert a protective effect in the development of the atherosclerotic process.

Abdominal aortic aneurysm (AAA) is an important cause of death in developed countries, affecting mainly men over 65 years old. Currently, there is no preventive treatment because of the lack of knowledge regarding the mechanisms involved in AAA initiation, progression, and rupture. One of the causes of this pathology is linked to angiotensin-II (Ang-II), the main effector peptide of the renin-angiotensin system. Ang-II is used *in vivo* to induce the disease in experimental models of $apoE^{-/-}$ mice. The study has used the anti-hypertensive drug losartan, which acts as a selective antagonist of the Ang-II receptor type 1 (AT_1), at a dose of 30 mg/kg/day. After 28 days of treatment, losartan was able to reduce Ang-II-induced AAA formation and diameter. The infiltration of T lymphocytes, macrophages, neovascularization, $CXCR6^+$ cells, and the mRNA expression of pro-angiogenic mediators

such as *Mcp-1/Ccl2*, *Vegf*, *Cxcl16*, and its receptor, *Cxcr6* were clearly impaired. These results suggest that a monotherapy with losartan at a dose of 30 mg/kg/day may become a new and safe therapeutic tool in the control of AAA.

In order to study the role of the CXCL16/CXCR6 axis in the development of AAA, mice deficient in CXCR6 receptor function (apoE$^{-/-}$CXCR6$^{GFP/GFP}$) were generated. In those animals deficient in CXCR6 functionality, similar results to those observed in apoE$^{-/-}$ mice treated with losartan were detected. Therefore, pharmacological modulation of CXCL16/CXCR6 axis may positively affect AAA development linked to disorders associated with the renin-angiotensin system.

1. INTRODUCCIÓN

1.1 INFLAMACIÓN SISTÉMICA Y ENFERMEDADES CARDIOVASCULARES

1.1.1 El proceso inflamatorio

La inflamación es una respuesta fisiológica común, localizada y protectora de los tejidos vascularizados, que se genera ante la presencia de los denominados "agentes inflamatorios" o perturbaciones severas de la homeostasis, como patógenos, exposición a contaminantes o señales endógenas como células dañadas. La inflamación es, por lo tanto, un mecanismo de defensa vital para el organismo (Chen *et al.* 2018).

La respuesta inflamatoria comienza con el reconocimiento de un daño tisular, desencadenando una respuesta innata que permite el reconocimiento de los agentes extraños o de las células dañadas, promoviendo la reparación tisular y/o eliminando el agente extraño, manteniendo así la salud e integridad del organismo (Soehnlein *et al.* 2010). Sin embargo, esta función de defensa puede fallar en algunos casos, en los cuales se genera una respuesta incontrolada que puede derivar de esta manera en una patología (Ashley *et al.* 2012).

Así mismo, la inflamación es clave en el desarrollo de numerosas enfermedades y desórdenes complejos que incluyen el cáncer y las enfermedades autoinmunes, metabólicas, neurodegenerativas y cardiovasculares (Murakami *et al.* 2012, Wu *et al.* 2018). En función de diversos parámetros como la sintomatología clínica, la persistencia del daño y la naturaleza de la reacción inflamatoria —a su vez, relacionada con la subclase predominante de leucocito—, se distingue tradicionalmente entre inflamación aguda e inflamación crónica (Moro-García *et al.* 2018).

La inflamación aguda es la respuesta innata a corto plazo del organismo ante la presencia de un agente extraño. Se caracteriza por la presencia de plaquetas y neutrófilos, un aumento del flujo sanguíneo y la acumulación de líquidos en la zona afectada, lo que produce los síntomas propios de la inflamación: el dolor, la hinchazón, la pérdida de función y el ardor (Ross 2017). Por lo general, durante las respuestas inflamatorias agudas, los eventos e interacciones celulares y moleculares minimizan eficazmente las lesiones o infecciones inminentes. Este proceso de mitigación contribuye a la restauración de la homeostasis tisular y a la resolución de la inflamación aguda (Chen *et al.* 2018). No obstante, si se produce un fallo en los mecanismos para eliminar el tejido dañado, se desencadena la aparición de la denominada inflamación crónica, una forma aberrante y prolongada de respuesta protectora,

con prevalencia de otros fenómenos bioquímicos y tipos celulares como los monocitos, los macrófagos y los linfocitos, y contribuye a una variedad de enfermedades inflamatorias crónicas como son las enfermedades cardiovasculares, aterosclerosis, diabetes tipo 2, artritis reumatoide, enfermedades autoinmunes y cáncer (**Figura 1**) (Chen *et al.* 2018, Moro-García *et al.* 2018). Además, se ha observado que la presencia de hipertensión o humo de tabaco predisponen la prolongación de la cronicidad inflamatoria en las enfermedades cardiovasculares (Morris *et al.* 2015).

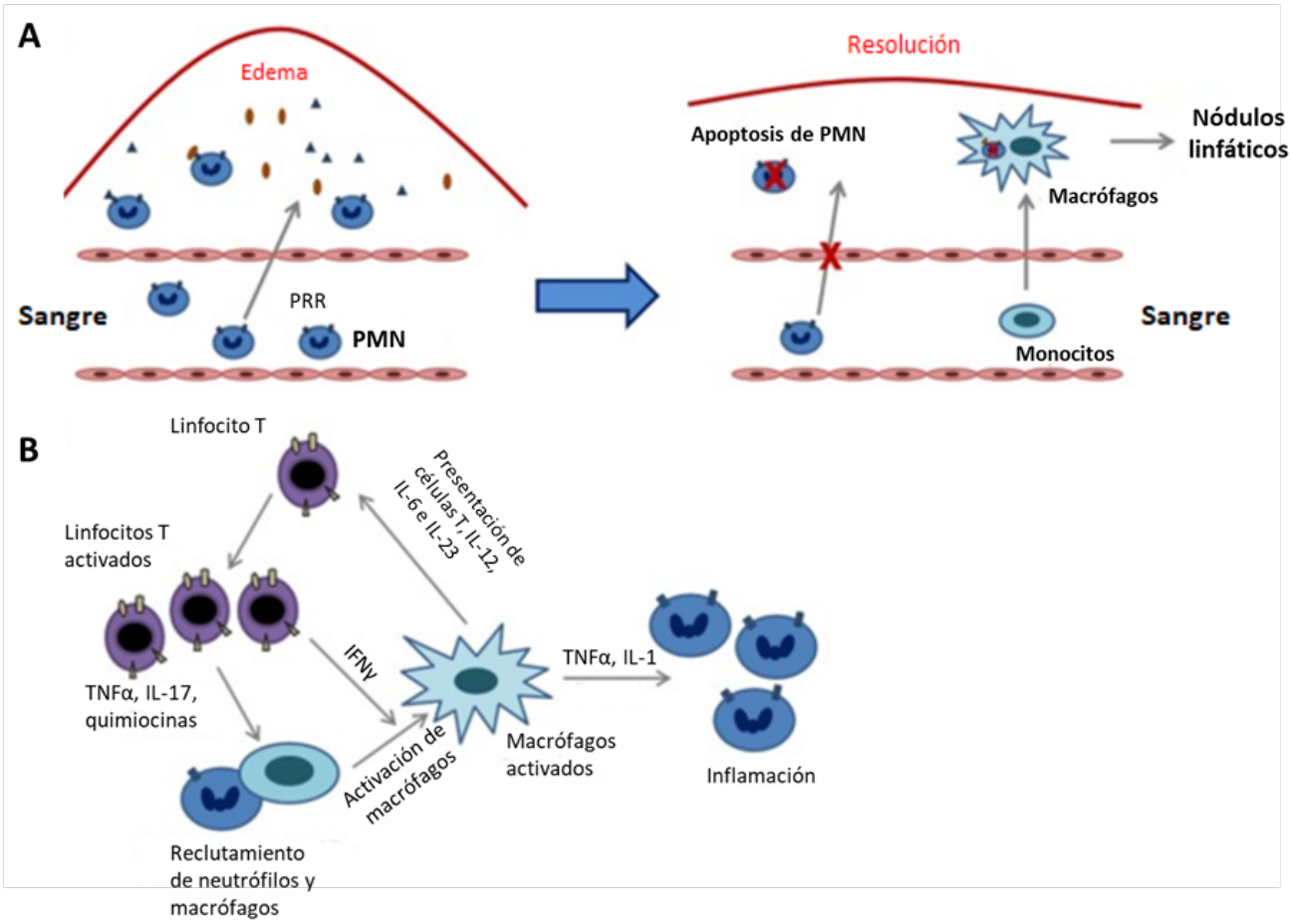

Figura 1. Inflamación aguda *versus* inflamación crónica. El inicio de la inflamación aguda se caracteriza por la acumulación de neutrófilos polimorfonucleares (PMN) y monocitos que se convierten rápidamente en macrófagos tisulares, así como la aparición de edema debido a daños en los tejidos inflamados. Los patrones moleculares asociados al daño y a patógenos son reconocidos por los receptores de reconocimiento de patrones (PRR) y atraen a los PMN al lugar de la infección. Los PMN representan la primera línea de defensa en los tejidos infectados ya que eliminan gran parte de los patógenos o materiales dañinos mediante fagocitosis. Cuando se desencadena la inflamación, los neutrófilos sufren apoptosis y son fagocitados por los macrófagos que migran a los ganglios

linfáticos donde presentarán a los antígenos (**A**). Los linfocitos T activados producen citocinas como el factor de necrosis tumoral α (TNFα), la interleucina (IL)-17 y otras quimiocinas, que reclutan macrófagos y otros mediadores tales como interferón γ (IFNγ) que los activan. Las subpoblaciones de linfocitos T (Th1, Th2, Th17, etc.) producen diversos tipos de citocinas y, a su vez, activan a los macrófagos y estimulan a los linfocitos T a través de la presentación de antígenos, la síntesis y liberación de diferentes citocinas como IL-6, IL-12 e IL-23. Estos macrófagos también liberan TNFα e IL-1 que actúan sobre los neutrófilos (**B**). Adaptado de Moro-García *et al.* 2018.

1.1.1.1 Mediadores de la respuesta inflamatoria

En respuesta a la lesión tisular, el organismo inicia una cascada de señalización bioquímica que estimula una serie de respuestas destinadas a la reparación de los tejidos afectados a través de los mediadores de la inflamación (Chen *et al.* 2018). Estos mediadores de la inflamación, tanto aguda como crónica, son productos químicos que regulan el proceso inflamatorio. Según su origen se clasifican en plasmáticos, celulares o derivados de microorganismos invasores (Muller 2014).

Los mediadores plasmáticos más conocidos están constituidos por las cininas y los sistemas del complemento, de la coagulación y el fibrinolítico. Todos ellos desencadenan la reacción inflamatoria tras el reconocimiento de distintos elementos como células dañadas y toxinas; así mismo, participan en la amplificación de la respuesta inflamatoria atravesando el endotelio hacia el tejido dañado (Muller 2014).

Otros mediadores están preformados y se almacenan en gránulos citoplasmáticos que se liberan con rapidez ante el estímulo inflamatorio. Los más comunes son la histamina, secretada por los mastocitos; el óxido nítrico (NO), los neuropéptidos, citocinas proinflamatorias como el factor de necrosis tumoral α (TNFα), mediadores lipídicos como las prostaglandinas, los leucotrienos, el factor activador de plaquetas o las quimiocinas. Todos ellos contribuyen a amplificar la respuesta inflamatoria, permitiendo por ejemplo un aumento de la permeabilidad local del endotelio (Muller 2014).

Por último, se han descrito mediadores derivados de microorganismos invasores como moléculas vasoactivas, péptidos formilados quimiotácticos y endotoxinas, como los lipopolisacáridos, responsables de la activación del receptor tipo *toll* (TLR) 4. Los receptores TLR pertenecen a un grupo de receptores capaces de reconocer varios patrones moleculares asociados a patógenos en las células inmunes, lo que les permite distinguir organismos

extraños como virus, bacterias, hongos y parásitos de las células anfitrionas (Trussoni *et al.* 2015). Así mismo, diversos componentes o mediadores celulares, entre los que destacan distintos tipos de leucocitos, plaquetas y células endoteliales, también participan en el proceso inflamatorio (Lam *et al.* 2015, Lawrance *et al.* 2017).

Junto con la acción quimiotáctica de las quimiocinas proinflamatorias y de varias moléculas coestimuladoras, se lleva a cabo el reclutamiento leucocitario de neutrófilos, basófilos, eosinófilos, monocitos/macrófagos, y linfocitos T desde el torrente sanguíneo hacia el tejido dañado (Chen *et al.* 2018). De esta manera, los leucocitos activados liberan mediadores inflamatorios; además, tienen la capacidad de adherirse al endotelio, de migrar a su través y, en general, de fagocitar a los agentes patógenos, destruyéndolos (Soehnlein *et al.* 2010, Ashley *et al.* 2012).

Tradicionalmente, se ha adscrito una función homeostática a las plaquetas; sin embargo, cada vez más estudios demuestran su importante papel en el proceso inflamatorio mediante la liberación de quimiocinas, permitiendo llevar a cabo el desarrollo y el progreso de la inflamación a través de un aumento de la interacción de las mismas con el endotelio vascular y los leucocitos circulantes (Lam *et al.* 2015). Gracias en buena medida al gran abanico de moléculas de superficie y mediadores solubles que expresan, las plaquetas son capaces de reconocer, secuestrar y eliminar patógenos, de activar y reclutar leucocitos, así como de modular su comportamiento (Jenne *et al.* 2015).

Por su parte, las células endoteliales producen y liberan al espacio extracelular múltiples mediadores inflamatorios e interactúan con los leucocitos durante la infiltración leucocitaria (Muller 2014).

Finalmente, los leucocitos, las plaquetas y las células endoteliales comparten la presencia, en su superficie, de moléculas de adhesión celular (MAC), que son ligandos de superficie, generalmente glicoproteínas, que llevan a cabo un papel crítico en el mantenimiento de la integridad del tejido y en la migración de las células. Además, regulan procesos importantes como la proliferación celular, la diferenciación y la morfogénesis, y algunas de ellas también actúan como receptores virales (**Tabla 1**) (Gerhardt *et al.* 2015).

Tabla 1. Moléculas de adhesión celular (MAC). Adaptado de Gerhard *et al.* 2015.

Familia	Nombre común	Nomenclatura inmunológica	Función	Expresión celular	Principales ligandos
Selectinas	E-selectina	CD62E	Rodamiento leucocitario	Células endoteliales	ESL-1, PSGL-1 y CD44
	L-selectina	CD62L	Rodamiento leucocitario y señalización	Leucocitos	PSGL-1, CD34 y MAdCAM-1
	P-selectina	CD62P	Rodamiento leucocitario y arresto leucocitario	Células endoteliales y plaquetas	PSGL-1
Inmunoglobulinas (Ig)	ICAM-1	CD54	Adhesión y transmigración	Células endoteliales	LFA-1 y Mac-1
	ICAM-2	CD102	Adhesión y transmigración	Células endoteliales	LFA-1
	VCAM-1	CD106	Arresto leucocitario	Células endoteliales y células del músculo liso	VLA-4
	PECAM-1	CD31	Transmigración	Células endoteliales, plaquetas y leucocitos	PECAM-1 (unión homóloga)
	MAdCAM-1	*Addressin*	Arresto leucocitario	Linfocitos	LPAM-1, L-selectina y VLA-4
Integrinas	VLA-4 ($\alpha_4\beta_1$)	CD49d, CD29	Adhesión y transmigración	Monocitos, linfocitos, eosinófilos y basófilos	VCAM-1, moléculas de la matriz extracelular y MAdCAM-1
	LFA-1 o $\alpha_L\beta_2$	CD11a/CD18	Locomoción y arresto leucocitario	Monocitos y linfocitos	ICAM-1 e ICAM-2
	Mac-1 o $\alpha_M\beta_2$	CD11b/CD18	Arresto leucocitario, locomoción, transmigración y activación	Monocitos y granulocitos	ICAM-1 e ICAM-2
	$\alpha_D\beta_2$	CD11d/CD18	Arresto leucocitario	Linfocitos CD8 y macrófagos	ICAM-3 y VCAM-1

CD, Cúmulo de diferenciación; ESL-1, ligando 1 de E-selectina; PSGL-1, ligando 1 de la glicoproteína P-selectina; ICAM, molécula de adhesión intercelular; VCAM-1, molécula de adhesión vascular-1; PECAM-1, molécula de adhesión de célula endotelial/plaqueta-1; MAdCAM-1, molécula de citoadhesión adresina mucosal-1; LPAM-1, integrina alfa 4 beta 7; VLA-4, *very late antigen*-4; LFA-1, antígeno 1 asociado a función linfática, y Mac-1, antígeno 1 asociado a macrófagos.

1.1.2 Regulación de la infiltración leucocitaria

La infiltración leucocitaria forma parte del mantenimiento homeostático del organismo, y sucede más acusadamente en procesos inflamatorios. Esta cascada de adhesión implica interacciones complejas de los leucocitos con el endotelio que, a su vez, se activa y regula al alza los mecanismos de señalización inflamatoria mediante la liberación de citocinas y quimiocinas inflamatorias. A continuación, los leucocitos se adhieren firmemente al endotelio a través de varias clases de MAC. Una vez que los leucocitos alcanzan una fase de detención, se deslizan hasta alcanzar el arresto completo y son capaces de transmigrar a través de la pared vascular (Shihata *et al.* 2016).

Por un lado, las MAC promueven interacciones directas entre los leucocitos y las células endoteliales, a través de la adhesión célula a célula, o bien entre los leucocitos y la matriz extracelular en la segunda parte del proceso. Estas interacciones promueven un amplio espectro de señalización celular que modula directa o indirectamente la proliferación de células madre, la diferenciación y la morfogénesis (Rahimi 2017, Steinbacher *et al.* 2018). Por su parte, los factores implicados en la quimiotaxis son mediadores químicos solubles de producción local en el área de daño tisular. Su función es atraer un mayor número de leucocitos circulantes al foco inflamatorio y, así mismo, regular la expresión de determinadas MAC. Entre los agentes quimiotácticos más conocidos se encuentran las quimiocinas, cuya relevancia en distintos procesos inflamatorios se discutirá más adelante. Además de ellas, se han descrito agentes quimiotácticos clásicos o inespecíficos como los fragmentos C3a y C5a del complemento, los péptidos bacterianos formilados como el N-formil-metionil-leucil-fenilalanina y las moléculas lipídicas proinflamatorias como el leucotrieno B4, entre otros. Este último, desencadena la adhesión al endotelio, activando y reclutando leucocitos en el sitio de la lesión (Di Gennaro *et al.* 2014).

Las citocinas, proteínas de bajo peso molecular con un importante papel señalizador, son otro grupo de mediadores solubles que participan en la infiltración leucocitaria. Entre ellas destacan citocinas proinflamatorias como el TNFα o la interleucina (IL)-1 que, sin ser propiamente quimiotácticas, promueven la migración leucocitaria a través de la regulación de la expresión de diferentes MAC. El TNFα, producido por monocitos y macrófagos activados, tiene una importancia particular. Ha sido descrito como una citocina pleiotrópica

crítica para el tráfico de células, la inflamación aguda y crónica y la defensa del huésped contra diversos patógenos. Además, se asocia con varias enfermedades autoinmunes e inflamatorias, como la artritis reumatoide, el shock séptico y la enfermedad inflamatoria intestinal. Pese a no ejercer ninguna acción directa sobre los leucocitos, el TNFα participa en diversas funciones biológicas tales como: proporcionar señales para la activación, la diferenciación, la supervivencia y la muerte celular. Además, modula la respuesta inmune y la inflamación en múltiples tejidos y órganos (Fava *et al.* 2018).

1.1.3 Etapas de la infiltración leucocitaria

La respuesta inflamatoria requiere de una serie de fases específicas que demandan la participación de diferentes moléculas y tipos celulares (Moro-García *et al.* 2018). El reclutamiento de estas células en el sitio de la lesión requiere de su desplazamiento a través de la pared del vaso sanguíneo. Tradicionalmente, el proceso de infiltración leucocitaria se ha descrito como compuesto en tres etapas; sin embargo, algunos autores han dividido una de estas etapas en dos, quedando las cuatro actuales: la adhesión primaria o *tethering*, el rodamiento leucocitario o *rolling*, la activación leucocitaria y adhesión firme y, por último, la migración transendotelial (**Figura 2**) (Inoue *et al.* 2011, Gerhardt *et al.* 2015).

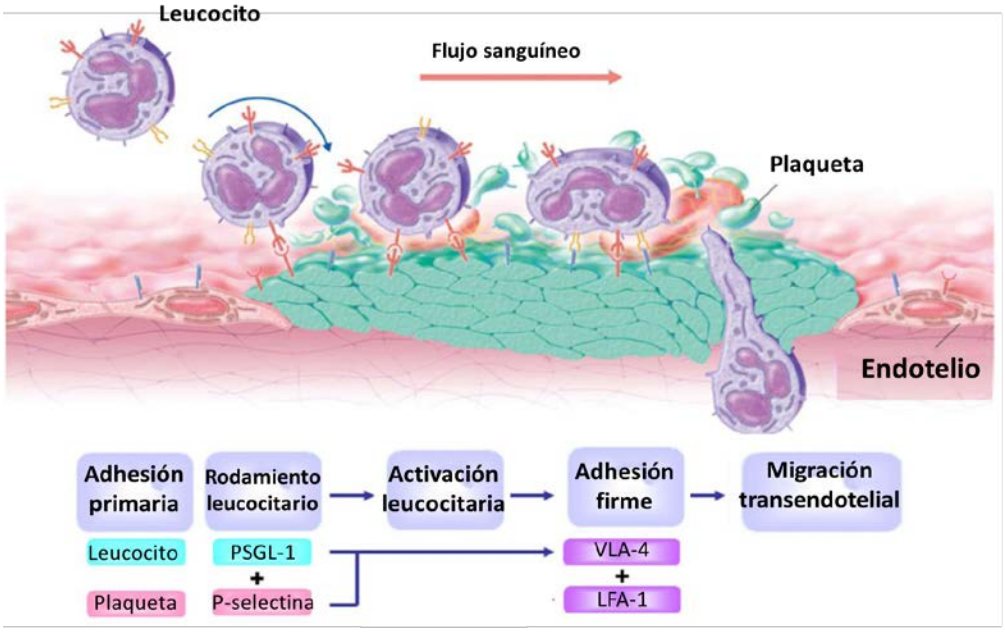

Figura 2. Etapas del proceso de la infiltración leucocitaria. El proceso comienza con el arresto de los leucocitos circulantes del torrente sanguíneo, seguida del rodamiento dependiente de selectinas y la adhesión firme al endotelio. Después de la migración transendotelial, los leucocitos migran hacia el foco inflamatorio. Adaptado de Inoue *et al.* 2011.

1.1.3.1 Adhesión primaria y rodamiento leucocitario

La respuesta inflamatoria requiere que los leucocitos migren dentro y a través de la vasculatura, un proceso que se ve facilitado por su capacidad de cambiar a una morfología polarizada, con una distribución asimétrica de sus receptores (Sreeramkumar *et al.* 2014).

El proceso inflamatorio comienza con una vasoconstricción transitoria debida a la liberación de catecolaminas, serotonina y tromboxano A_2 por diferentes células, seguida de la activación del endotelio debido a la liberación de moléculas proinflamatorias como la bradiquinina, la histamina, el TNFα, la IL-1β o prostaglandinas por parte del tejido dañado (McEver 2010). Esta primera etapa provoca una disminución de la velocidad de los leucocitos en el torrente sanguíneo, aumentando así la frecuencia de interacción entre el endotelio y los mismos (Zabel *et al.* 2015). De esta manera se produce el reconocimiento dependiente del estímulo inductor de la inflamación de los leucocitos que circulan por el torrente sanguíneo, y el endotelio activado, estableciéndose interacciones reversibles entre los receptores de superficie celular de los leucocitos y los ligandos presentes en las células endoteliales, produciéndose una adhesión primaria o laxa que podrá deshacerse si, tras un tiempo, no se desencadenan los mecanismos de adhesión firme, volviendo los leucocitos al torrente circulatorio (Liu *et al.* 2017b).

El rodamiento o *rolling* de los leucocitos sobre la superficie endotelial es uno de los pasos limitantes de la cascada de eventos que supone el proceso inflamatorio. El rodamiento permite a los leucocitos interactuar con las quimiocinas inmovilizadas que inducen el cambio de las integrinas β_2 a conformaciones de alta afinidad, promoviendo el arresto, el fortalecimiento de la adhesión firme, y la migración transendotelial (McEver 2015). La expresión de combinaciones específicas de MAC y de receptores de quimiocinas determina la subpoblación leucocitaria que se interna en el tejido durante el proceso inflamatorio (Ley *et al.* 2007), a su vez mediado por las selectinas, que son lectinas transmembranales dependientes de Ca^{2+}. La L-selectina es expresada por la mayoría de los leucocitos, mientras que E-selectina y P-selectina son expresadas por las células endoteliales activadas y, en el caso concreto de la P-selectina, también por las plaquetas activadas (Ivetic 2018). Todas ellas interaccionan con el ligando 1 de la glicoproteína P-selectina (PSGL-1), así como con otros ligandos glicosilados (Gerhardt *et al.* 2015, McEver 2015). La interacción P-selectina/PSGL-

1 activa las integrinas leucocitarias (Abadier *et al.* 2017). Las uniones entre las selectinas y sus ligandos permiten que los leucocitos se adhieran al endotelio activado (Marki *et al.* 2018). El endotelio tiene un papel muy activo durante el proceso del rodamiento de los leucocitos, el cual es mediado además por integrinas activadas que participan en la mediación de la adhesión celular (Gerhardt *et al.* 2015, Mitroulis 2015).

1.1.3.2 Activación leucocitaria y adhesión firme

Cuando la inflamación persiste en el tiempo tras el reconocimiento del daño, los leucocitos se activan con el propósito de eliminar el foco inflamatorio y se mueven lentamente por el torrente sanguíneo pero no se detienen de manera abrupta, sino que se desaceleran hasta adherirse firmemente al endotelio vascular (Gerhardt *et al.* 2015, Li *et al.* 2015).

El arresto leucocitario durante el rodamiento, convirtiendo la adhesión en firme, está producido por la interacción entre las selectinas y las quimiocinas originadas en el foco de inflamación, desencadenando de esta manera la activación de las integrinas expresadas por los leucocitos (Mitroulis *et al.* 2015). Éstas dirigen su unión a las inmunoglobulinas, como la molécula de adhesión intercelular (ICAM)-1 y la molécula de adhesión vascular-1 (VCAM-1), expresadas en las células endoteliales (McEver 2010, Gerhardt *et al.* 2015). Entre las integrinas de la membrana leucocitaria más relevantes durante esta etapa caben destacar las β_1 (*very late antigen*-4; VLA-4), que regulan el rodamiento y arresto leucocitario al unirse a VCAM-1, y las β_2, donde destacan el antígeno 1 asociado a macrófagos (Mac-1) y el antígeno 1 asociado a función linfática (LFA-1), siendo estas últimas las más importantes en la adhesión firme de los leucocitos al endotelio vascular al unirse a ICAM-1 (Mitroulis *et al.* 2015, Tissino *et al.* 2018). Debido a la adhesión, tanto estas integrinas como las inmunoglobulinas, sus ligandos, sufren un cambio de conformación hacia un estado de activación (Ley *et al.* 2007). A continuación, la extensión del citoplasma celular es promovido por un reordenamiento del citoesqueleto de actina inducido por integrinas; seguido del deslizamiento celular, que es guiado por gradientes intravasculares de quimiocinas a lo largo del endotelio en busca del lugar apropiado para transmigrar desde el vaso hacia el tejido inflamado (Mitroulis *et al.* 2015).

1.1.3.3 Migración transendotelial y quimiotaxis

La transmigración de las células inmunitarias a través de la pared endotelial es el último paso del proceso inflamatorio y permite la migración leucocitaria hacia el foco de inflamación, gracias a una mayor cantidad de agentes quimiotácticos (Mitroulis *et al.* 2015). Para poder abandonar el torrente sanguíneo, los leucocitos deben atravesar el endotelio; dicho proceso dura entre 2 y 5 minutos. Posteriormente, necesitan entre 5 y 15 minutos más para poder atravesar la membrana basal (Ley *et al.* 2007, Kolaczkowska *et al.* 2013).

La transmigración depende de muchos factores diferentes, como la distribución y la densidad de los ligandos de integrina, quimioatrayentes y otras citocinas. En todo el proceso tiene un papel fundamental PECAM-1 (*platelet/endothelial cell adhesion molecule*-1), también conocida como CD31. PECAM-1 se expresa en plaquetas y leucocitos, así como en las células del endotelio vascular donde es un componente principal de la unión intercelular de células endoteliales en lechos vasculares confluentes (Privratsky *et al.* 2011). El mecanismo por el cual PECAM-1 promueve la migración celular parece deberse a la capacidad del complejo PECAM-1/proteína tirosina fosfatasa 2 para alterar el citoesqueleto, tanto por la defosforilación de la quinasa de adhesión focal, como por la alteración de la actividad de la proteína G, RhoA (Collins *et al.* 2012, Lertkiatmongkol *et al.* 2016). Al mismo tiempo, también se requieren integrinas e inmunoglobulinas tales como ICAM-1, ICAM-2 y VCAM-1 para completar el proceso (Kolaczkowska *et al.* 2013).

1.1.4 Quimiocinas

1.1.4.1 Generalidades

El acúmulo local de células del sistema inmune durante el proceso inflamatorio es un proceso complejo que sucede a través de la interacción de los leucocitos y las células endoteliales de la microvasculatura, y cuya regulación depende principalmente de MAC y distintos factores quimiotácticos, capaces de modular la trayectoria de los leucocitos y atraerlos hacia el foco inflamado. De entre estos mediadores destacan las citocinas quimiotácticas o quimiocinas, que desempeñan un papel clave en diferentes enfermedades cardiovasculares (van der Vorst *et al.* 2015b). Durante los últimos veinte años, se ha constatado que las quimiocinas forman una familia de mediadores críticos para la migración

celular durante la vigilancia inmunitaria, la inflamación y la progresión de enfermedades como el cáncer (Minton 2018).

Las quimiocinas son glicoproteínas secretadas de bajo peso molecular (8-12 kDa) que desempeñan un papel clave en el sistema inmune, ya que coordinan la migración de los leucocitos durante la inflamación y la vigilancia inmunitaria (van der Vorst *et al.* 2015a). Todas ellas tienen características estructurales semejantes, y un plegamiento tridimensional característico establecido por puentes disulfuro intramoleculares esenciales para llevar a cabo la interacción con su receptor, y poder actuar localmente mediante mecanismos autocrinos o paracrinos (Blanchet *et al.* 2012, Shang *et al.* 2017). Son sintetizadas y liberadas por las células del sistema inmunitario durante el proceso de la inflamación. Están compuestas por 70-130 aminoácidos y sus funciones homeostáticas incluyen la maduración y el tráfico de leucocitos, el desarrollo, la reparación de tejidos y la angiogénesis (Ransohoff 2009). Originalmente, se estudiaron junto a sus receptores por su papel en el tráfico celular de leucocitos durante la inflamación y la vigilancia inmunológica. Hoy en día se conoce su importancia fisiológica, pero también patológica en procesos de tumorigénesis, metástasis, así como en enfermedades inflamatorias y autoinmunes (Blanchet *et al.* 2012). Son potentes mediadores de la adhesión y migración leucocitaria a través de su interacción con receptores presentes en los leucocitos u otras células inmunes, los cuales están acoplados a proteínas G (GPCR), mediante cambios conformacionales que desencadenan las vías de señalización para llevar a cabo las diversas funciones (Shen *et al.* 2018).

Estos receptores GPCR constan de 7 hélices α transmembranales que rodean una hendidura central y que están conectadas por tres bucles intracelulares y tres bucles extracelulares. El extremo N-terminal y el extremo C-terminal se localizan en la parte extracelular e intracelular, respectivamente (Vass *et al.* 2018). Se clasifican en tres familias diferentes de GPCR: la familia de la rodopsina, la familia de receptores de secretina/glucagón y la familia del receptor metabotrópico para glutamato/sensor de calcio. La región intracelular es la que se encuentra unida a la proteína G, sujeta a su vez a fosforilación regulatoria (Yang *et al.* 2017, Eichel *et al.* 2018).

Hasta el momento se han identificado 43 quimiocinas humanas que participan en diversas enfermedades y sólo 23 receptores de las mismas, lo que indica que un mismo

receptor puede reconocer a varias quimiocinas. Así mismo, una quimiocina puede interactuar con distintos receptores. Actualmente, sólo se conoce un receptor C y un receptor C-X_3-C; mientras que existen diez receptores C-C y seis C-X-C (Blanchet *et al.* 2012, Back *et al.* 2015).

En particular, los receptores de quimiocinas son estructuras altamente dinámicas y la eficacia de la señalización depende en gran medida del contacto discreto con el ligando. La promiscuidad de las quimiocinas y los receptores de quimiocinas, combinada con la señalización sesgada y la modulación alostérica de la activación del receptor, garantiza un reclutamiento y un posicionamiento estrechamente controlados de células individuales dentro del entorno local en un momento dado (Legler *et al.* 2018).

1.1.4.2 Subfamilias estructurales de quimiocinas

Las quimiocinas se clasifican en cuatro subfamilias: C, C-C, C-X-C y C-X_3-C. Todas ellas se caracterizan por la presencia de cuatro residuos de cisteína en la posición N-terminal de la cadena peptídica, salvo las linfoactinas α y β que sólo tienen dos residuos (van der Vorst *et al.* 2015a). La clasificación se basa en el número y la disposición de estos cuatro residuos de cisteína que forman enlaces disulfuro que permiten estabilizar el plegamiento terciario (Zernecke *et al.* 2014).

En la subfamilia de las quimiocinas C o γ, el primer y el tercer residuo de cisteína están ausentes y posee solo un enlace disulfuro. Si hay dos residuos de cisteínas adyacentes se denominan quimiocinas C-C o β y entre ambos residuos de cisteína no se inserta ningún aminoácido. Si los primeros dos de los cuatro residuos de cisteína conservados están separados por un aminoácido variable, se habla de la subfamilia de las quimiocinas C-X-C o α, mientras que si están separados por tres aminoácidos, se trata de la subfamilia C-X_3-C o δ (Koenen *et al.* 2011). Las quimiocinas tipo C-C como MCP-1 (*monocyte chemoattractant protein*-1), RANTES (*regulated upon activation, normal T cell expressed and secreted*) o eotaxina-1 (CCL2, CCL5 y CCL11, respectivamente), actúan sobre los monocitos, los macrófagos, los eosinófilos y participan en las respuestas inflamatorias crónicas; mientras que las quimiocinas C-X-C, como IL-8 (CXCL8), actúan sobre los neutrófilos participando tanto en respuestas inflamatorias agudas como crónicas (**Figura 3**) (White *et al.* 2013, Warner *et al.* 2014, de Munnik *et al.* 2015).

Todas las quimiocinas son solubles, a excepción de la fractalquina (CX_3CL1) y de CXCL16, que normalmente se expresan asociadas a membrana facilitando así la adhesión célula-célula con células que expresan sus receptores afines, que son CX_3CR1 y CXCR6, respectivamente (Scholten *et al.* 2012, Rius *et al.* 2013a).

Además de su clasificación estructural, alternativamente las quimiocinas se pueden dividir de acuerdo a su expresión y actividad funcional. Esta clasificación agrupa a las quimiocinas en tres familias: las quimiocinas proinflamatorias, que son aquellas que se inducen durante el proceso inflamatorio y están involucradas en el reclutamiento leucocitario en el foco inflamatorio; las quimiocinas homeostáticas que se expresan de manera constitutiva en sitios no inflamados y están involucradas en la migración homeostática y el desplazamiento de las células en condiciones fisiológicas tales como la localización de los linfocitos; y las de función mixta que tienen ambas propiedades (Blanchet *et al.* 2012, Stone *et al.* 2017).

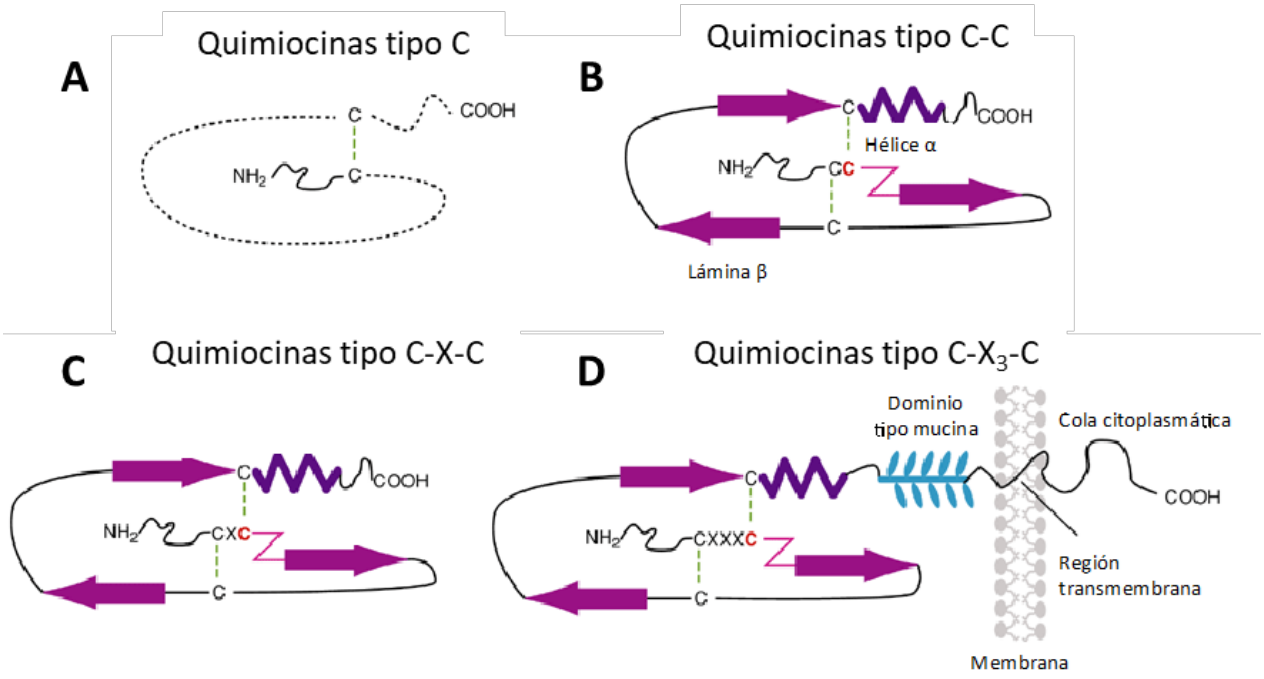

Figura 3. Subfamilias estructurales de quimiocinas. Las quimiocinas se dividen en cuatro subfamilias de acuerdo a la posición relativa de los dos primeros residuos de cisteínas conservados en el extremo N-terminal de la cadena peptídica. Quimiocinas tipo C (**A**), quimiocinas tipo C-C (**B**), quimiocinas tipo C-X-C (**C**) y quimiocinas tipo C-X_3-C (**D**). La C hace referencia a un residuo de cisteína y la X a cualquier aminoácido. Los puentes disulfuro se muestran como líneas discontinuas. El dominio transmembranal de CX_3CL1 está representado por lípidos (en gris). Adaptado de de Munnik *et al.* 2015.

1.2 ATEROSCLEROSIS Y RIESGO CARDIOVASCULAR

1.2.1 Consideraciones generales

Las enfermedades cardiovasculares son la principal causa de muerte y morbilidad en Europa, causando 3,9 millones de muertes al año (Wilkins *et al.* 2017), y a nivel mundial, ya son responsables de más de un 30% de las muertes anuales (Benjamin *et al.* 2017). La Organización Mundial de la Salud (OMS) estima que, para el año 2020, las enfermedades cardiovasculares serán el principal problema socioeconómico a nivel mundial (resolución WHA66.10, OMS, 2013). En los últimos años, y a pesar de los avances en la mejora de la prevención primaria y las nuevas aproximaciones farmacológicas para lograr disminuir los niveles de colesterol en sangre, la adopción de hábitos de vida no saludables han provocado un aumento de la incidencia de la diabetes y la obesidad, lo que hace que las enfermedades cardiovasculares sigan siendo la principal causa de muerte en Estados Unidos, Europa y Asia (Hedrick 2015, Wilkins *et al.* 2017), y por tanto, aumentando la prevalencia de la aterosclerosis, patología subyacente a las enfermedades cardiovasculares (Hedrick 2015, Zimmer *et al.* 2015).

El término aterosclerosis está compuesto a partir de las palabras griegas *athero* (engrudo o papilla grumosa) y *esclerosis*, cuyo significado es endurecimiento. Actualmente se asocia la *aterosis* a la acumulación de lípidos junto a macrófagos, y la *esclerosis* a la formación de una capa fibrosa, la cual está constituida por células de músculo liso, leucocitos y tejido conectivo (Rafieian-Kopaei *et al.* 2014). Es una enfermedad crónica vascular e inflamatoria, caracterizada por la presencia de elevadas concentraciones de lipoproteínas de baja densidad (LDL), lo que provoca la acumulación de lípidos (entre ellos colesterol, ésteres de colesterol y cristales de colesterol), calcio y células inflamatorias, cubiertas por tejido fibroso, como fibras de colágeno y células de la musculatura lisa vascular (Zimmer *et al.* 2015). Esta acumulación se produce en la pared arterial, dando lugar a la formación de las denominadas placas ateroscleróticas o ateroma, y su posterior erosión, que puede terminar en la ruptura de algunas de estas placas vulnerables o de elevado riesgo (Weber *et al.* 2011). Normalmente, la aterosclerosis no se forma en regiones donde el flujo es uniforme y unidireccional como la aorta torácica descendente, sino que tiene lugar en regiones de la vasculatura donde el flujo sanguíneo tiene una mayor complejidad geométrica como curvas

o puntos de ramificación (Nigro *et al.* 2011). Principalmente, se desarrolla en el espacio subendotelial o íntima de arterias elásticas de calibre intermedio, arterias musculares de tamaño medio y vasos de gran calibre. La mayor curvatura del arco aórtico y las zonas de bifurcación de la carótida son lugares donde se producen disrupciones e irregularidades en el flujo sanguíneo, variando así la magnitud y dirección de la fuerza de cizallamiento, siendo propensas a desarrollar disfunción endotelial (Tabas *et al.* 2015).

La aterosclerosis es una enfermedad cuya progresión es asintomática, desarrollándose durante décadas; sólo en las últimas etapas aparecen los síntomas, manifestándose mediante eventos cardiovasculares como infarto de miocardio, infarto cerebral o pérdida de función de las extremidades (Badimon *et al.* 2014).

1.2.2 Bases del proceso aterogénico

La aterogénesis es el proceso de formación de la placa aterosclerótica. Este proceso involucra a las células inmunitarias, principalmente linfocitos T y B, monocitos y macrófagos, y es inducido por un daño en las células endoteliales (Tse *et al.* 2013).

Tradicionalmente, la aterogénesis se ha comprendido como una enfermedad metabólica caracterizada por una obstrucción arterial por depósitos grasos en las paredes de los vasos. De acuerdo con esta visión, la aterosclerosis es el resultado de la acumulación pasiva de colesterol en la pared arterial. Hoy en día se cree que la aterogénesis involucra respuestas bioquímicas y moleculares altamente específicas con interacciones constantes entre varios mediadores celulares. Pese a la presencia de una reacción inflamatoria en cada una de las etapas de la aterosclerosis, desde sus inicios hasta sus manifestaciones terminales, la relación de causa-efecto entre estos dos procesos permanece confusa (Libby 2012, Pant *et al.* 2014).

No obstante, la evidencia científica acumulada relaciona cada vez más la inflamación y sus mecanismos efectores con la patogénesis de la enfermedad. Tanto la inmunidad innata como la adquirida operan durante la aterogénesis y vinculan muchos factores de riesgo tradicionales con funciones arteriales alteradas. Las rutas inflamatorias se han convertido en dianas en la búsqueda de nuevas estrategias terapéuticas y preventivas frente a las enfermedades cardiovasculares (Libby *et al.* 2013).

1.2.2.1 Disfunción endotelial, inicio y evolución de la lesión aterosclerótica

El endotelio vascular es un órgano multifuncional formado por una monocapa de células endoteliales que recubre la superficie interior de los vasos sanguíneos. Éste desempeña un papel fundamental en el mantenimiento de la homeostasis vascular en respuesta a diversos estímulos, así como en la regulación del tono vascular y su estructura, la permeabilidad y la coagulación. Las células endoteliales, además, producen una amplia gama de factores que también regulan la adhesión celular, la proliferación de células del músculo liso y la inflamación a través de la regulación de numerosos mediadores, como el factor de relajación y contracción derivado del endotelio, las MAC, las citocinas y las quimiocinas (Cho *et al.* 2018). Por tanto, las alteraciones en la fisiología del endotelio de las paredes de las arterias de gran tamaño provocan su activación, también conocida como disfunción endotelial, que es un importante contribuyente en la progresión de diversas enfermedades cardiovasculares, renales y metabólicas crónicas (Gimbrone *et al.* 2016, Zhang *et al.* 2018).

Esta primera etapa del proceso aterosclerótico da lugar a la expresión de diferentes quimiocinas, citocinas y MAC encargadas de interaccionar con los leucocitos y las plaquetas. Además, está involucrada en la progresión de la formación de la placa y complicaciones en el proceso aterosclerótico (Weber *et al.* 2011, Zernecke *et al.* 2014).

La disfunción endotelial se manifiesta por una alteración en la biodisponibilidad del NO, debida o bien a una reducción de la producción de la enzima óxido nítrico sintasa endotelial (eNOS) o, más frecuentemente, a un aumento de la producción de las especies reactivas del oxígeno. El NO, especialmente el derivado de la eNOS, ejerce normalmente efectos protectores sobre la pared del vaso, relacionados con la activación endotelial, la inflamación, el crecimiento vascular y la fibrosis (Vanhoutte *et al.* 2017).

Este desequilibrio lleva a una alteración en las propiedades vasomotoras arteriales mediada por NO, endotelina-1, angiotensina-II (Ang-II) y prostaglandinas, entre otros, provocando que las LDL se transporten hacia la pared del vaso, abandonen el torrente sanguíneo y comiencen a acumularse en la íntima (Deanfield *et al.* 2007). Por el contrario y alternativamente, la “teoría del transporte masivo” establece que el transporte de ciertas sustancias bioactivas, como las LDL, desde la circulación hasta la pared del vaso podría ser

promovido en sitios de flujo turbulento debido a un contacto intenso y prolongado entre las células endoteliales vasculares y la sangre (Kwak *et al.* 2014).

La activación de las células endoteliales en los lugares de la vasculatura propensos a lesiones ateroscleróticas promueve la activación de las MAC y las quimiocinas, que median el reclutamiento de monocitos circulantes. La acumulación de monocitos y macrófagos en la pared de las arterias de gran calibre conduce a la inflamación crónica y al desarrollo y progresión de la aterosclerosis (Ley 2011).

Los monocitos y macrófagos tisulares, así como las células endoteliales y las células del músculo liso, generan radicales libres que oxidan las LDL a su forma oxidada (LDLox), dando lugar a la síntesis de partículas proinflamatorias como quimiocinas y MAC, generando un fenotipo proinflamatorio y protrombótico que precede al desarrollo del proceso aterosclerótico, creando una respuesta inflamatoria innata en la íntima (Weber *et al.* 2011, Chen *et al.* 2015). Debido a la correlación directa entre la concentración de LDL en suero y la cantidad de lipoproteínas acumuladas en la lesión, su nivel en sangre puede considerarse como un indicador de aterogénesis (Mestas *et al.* 2008, Rafieian-Kopaei *et al.* 2014).

La inflamación comienza cuando el endotelio vascular es activado y se induce la expresión de MAC, como E-selectina, P-selectina, ICAM-1 o VCAM-1, que favorecen la adhesión de los leucocitos circulantes, en especial monocitos y linfocitos T, y su migración desde la luz hacia la íntima (Chen *et al.* 2015). Mientras tanto, se secretan quimiocinas quimioatrayentes como MCP-1 y otras, que atraen a monocitos, a linfocitos, a mastocitos y a neutrófilos a la pared arterial. Al mismo tiempo, las células del músculo liso que se encuentran en la íntima secretan factor de crecimiento derivado de plaquetas, proteoglicanos, colágeno y fibras elásticas, permitiendo la migración de los leucocitos del endotelio al espacio subendotelial donde se acumularán (Insull 2009).

1.2.2.2 Formación de la estría grasa

Los monocitos se acumulan en la íntima, donde se desencadena su transformación en macrófagos, en los cuales se produce un aumento de la expresión de los receptores *scavenger* o “basurero”, que llevan a cabo la unión con las LDLox. En un esfuerzo por eliminar dichas lipoproteínas, los macrófagos las reconocen a través de estos receptores basurero, las internalizan mediante endocitosis e, incapaces de degradarlas, las acumulan en el citoplasma,

transformándose así en las células espumosas características del ateroma, promoviendo el desarrollo de las lesiones ateroscleróticas (Chen *et al.* 2015, Gao *et al.* 2017). La captación de las LDLox produce la activación de los macrófagos, que secretan a su vez mayor número de factores quimiotácticos e interleucinas, permitiendo incrementar la llegada de leucocitos circulantes al espacio subendotelial o la íntima (Libby 2012), por mediación de diferentes factores como el factor estimulante de colonias de granulocitos y macrófagos, el TNFα o la IL-1β (Chen *et al.* 2015). Tanto la IL-1β como el TNFα estimulan la producción local del factor de crecimiento de fibroblastos y el factor de crecimiento derivado de plaquetas, los cuales son fundamentales para la formación y complicación de la placa de ateroma. En concreto, el TNFα es producido por las células endoteliales activadas y produce la migración y proliferación de las células del músculo liso de la media a la íntima (Sprague *et al.* 2009).

La acumulación de células inflamatorias en la membrana arterial interna intensifica el proceso inflamatorio local debido a la secreción de especies reactivas de oxígeno, citocinas inflamatorias y metaloproteasas, que aceleran el desarrollo de las lesiones ateroscleróticas. Así mismo, las quimiocinas y sus receptores son instrumentales para orquestar la afluencia de leucocitos a la pared vascular, y también parecen regular las funciones inmunitarias (Zernecke *et al.* 2010). Las acumulaciones subendoteliales de células espumosas y linfocitos T dan lugar a la denominada lesión aterosclerótica precoz o estría grasa (Rafieian-Kopaei *et al.* 2014).

1.2.2.3 Acumulación de células de la musculatura lisa en el espacio subendotelial

Las plaquetas activadas, los macrófagos y las células endoteliales liberan quimiocinas y factores de crecimiento que estimulan la proliferación de células de músculo liso y su acumulación en la íntima (Weber *et al.* 2011).

La lipoproteína lipasa, secretada por el endotelio, promueve la proliferación de las células de músculo liso. Este proceso implica la activación de la proteína quinasa C, que promueve la producción de matriz extracelular por las células de músculo liso, permitiendo la progresión hacia una placa aterosclerótica estable. En este contexto, el factor de crecimiento transformante (TGF)-β ha sido implicado en la producción de colágeno; así mismo, promueve la diferenciación de las células del músculo liso. La señalización de TGF-β es crítica para el mantenimiento de la vasculatura adulta y juega un papel importante en la

mediación del equilibrio entre la inflamación y el crecimiento de la placa fibrosa en la aterosclerosis. También se sabe que el TGF-β inhibe la proliferación de las células de músculo liso junto con interferón γ (IFNγ). Actuando en tándem, todos estos factores conducen a la formación de una gruesa capa de tejido conjuntivo sobre un núcleo rico en lípidos, dando lugar a lo que se conoce como placa fibrosa (Chen *et al.* 2016).

La visión tradicional de las células del músculo liso en la aterosclerosis sostiene que su proliferación aberrante promueve la formación de la placa, pero que su presencia en las placas avanzadas es completamente beneficiosa, previniendo, por ejemplo, la ruptura de la placa fibrosa. Sin embargo, este punto de vista está basado en la idea de que existe una población homogénea de células de músculo liso dentro de la placa, que puede identificarse por separado de otras células en el ateroma, particularmente macrófagos, utilizando marcadores inmunohistoquímicos estándar. Esta idea ha sido puesta en duda al demostrarse la existencia de una elevada heterogeneidad entre las células del músculo liso, y su capacidad de modificar su fenotipo. Así, su proliferación puede ser beneficiosa durante la aterogénesis, y no solo en las lesiones avanzadas; mientras que su apoptosis y senescencia, así como la presencia de células similares a macrófagos derivadas de células del músculo liso, puede promover la inflamación (**Figura 4**) (Bennett *et al.* 2016).

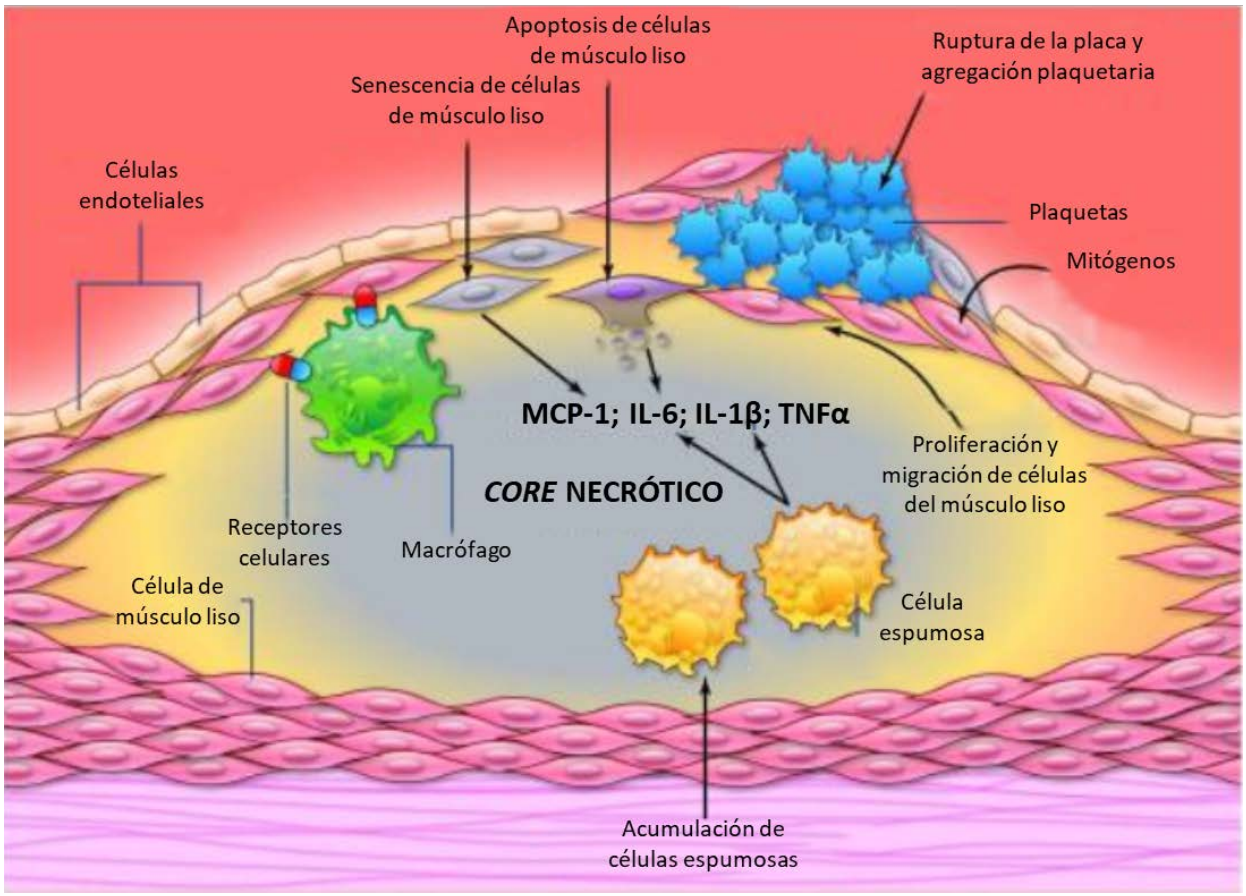

Figura 4. Esquema que ilustra la serie de procesos que experimentan las células del músculo liso en las placas ateroscleróticas avanzadas. Adaptado de Bennett *et al.* 2016.

1.2.2.4 La lesión avanzada: placa fibrosa

La progresión de la estría grasa conduce a la formación de la placa fibrosa. Las lesiones ateroscleróticas avanzadas se caracterizan por la acumulación de lípidos, de células apoptóticas, en especial macrófagos, células de músculo liso y células espumosas formadas tras la fagocitosis de moléculas lipídicas oxidadas, de restos celulares y de material extracelular en la lesión, dando lugar a lo que se conoce como núcleo o *core* necrótico, cuya formación se ve favorecida por el estado de inflamación crónica. Las placas que presentan un mayor *core* necrótico y una capa fibrosa de espesor fino son las que tienen un mayor riesgo de ruptura (de Vries *et al.* 2016), ya que éstos están asociados con la aterogénesis, y su propagación contribuye a la expansión de la placa aterosclerótica (**Figura 5**) (Seimon *et al.* 2009, Kojima *et al.* 2017). El engrosamiento de la pared arterial se compensa inicialmente

con una dilatación gradual, hasta alcanzar un límite en el que la lesión se introduce en el lumen, provocando un estrechamiento progresivo del vaso con riesgo de síntomas isquémicos (Ross 1999, Badimon *et al.* 2014, Bennett *et al.* 2016).

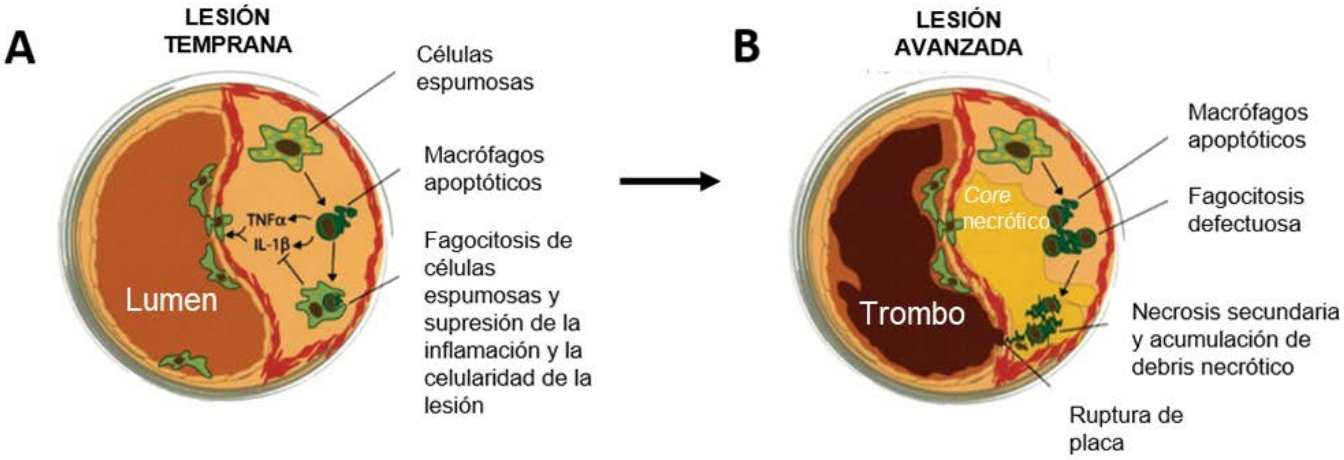

Figura 5. Consecuencias funcionales de la apoptosis de los macrófagos en las lesiones ateroscleróticas tempranas y avanzadas. En las lesiones tempranas (**A**), los monocitos que examinan la pared vascular son reclutados en la placa. Los monocitos se diferencian a macrófagos en áreas donde las lipoproteínas modificadas y remanentes se retienen en la matriz extracelular. Los macrófagos se convierten en células espumosas al ingerir lipoproteínas oxidadas (LDLox) y almacenar estos lípidos en su interior. Las células espumosas activadas secretan una variedad de citocinas proinflamatorias y eventualmente sufren apoptosis. La eliminación rápida de las células apoptóticas conduce a la supresión de la respuesta proinflamatoria. El efecto global es una reducción en la celularidad y el tamaño de la lesión. En las lesiones avanzadas (**B**), los macrófagos apoptóticos no se eliminan eficazmente sino que se acumulan y sufren una necrosis secundaria. La acumulación de desechos necróticos promueve la inflamación, la inestabilidad de la placa y la trombosis aguda. Adaptado de Seimon *et al.* 2009.

Al mismo tiempo, se produce la formación de nuevos vasos sanguíneos o angiogénesis en la placa aterosclerótica. Este es un proceso dinámico regulado por un delicado balance entre factores angiogénicos y angioestáticos (Camare *et al.* 2017).

Un elevado número de factores participan en la regulación de la angiogénesis en las áreas ateroscleróticas, siendo uno de los más importantes la hipoxia. En los tejidos mamíferos, la hipoxia es uno de los estímulos angiogénicos más potentes ya que regula la expresión de una gran variedad de genes implicados en la angiogénesis. En el contexto aterogénico, este proceso facilita la demanda de oxígeno en el ateroma (Camare *et al.* 2017). En las placas ateroscleróticas, la difusión de O_2 local en la luz arterial puede ser insuficiente debido al engrosamiento y la inflamación de la íntima. Las condiciones hipóxicas promueven

la liberación de factores angiogénicos e inflamatorios que estimulan la formación de nuevos vasos a partir de los *vasa vasorum* (Sluimer *et al.* 2009, Marsch *et al.* 2013). Esta neovascularización permite suministrar nutrientes y promueve la infiltración de macrófagos, el engrosamiento de la pared vascular, la deposición de lípidos, la inflamación y la progresión de la lesión aterosclerótica (Moreno *et al.* 2012, Camare *et al.* 2017). Además, aumenta el riesgo de sufrir hemorragias intraplaca y favorece el flujo de mediadores inflamatorios (de Vries *et al.* 2016).

El factor 1 inducible por hipoxia (HIF-1) media la apoptosis e incrementa la formación de nuevos vasos sanguíneos mediante el control de la expresión y la liberación de factores angiogénicos como el factor de crecimiento vascular endotelial (VEGF) (Jain *et al.* 2018). Además, la formación de nuevos vasos sanguíneos requiere de la activación endotelial, lo cual involucra la interacción entre VEGF y su receptor VEGFR2 (**Figura 6**) (Cheng *et al.* 2013, Camare *et al.* 2017).

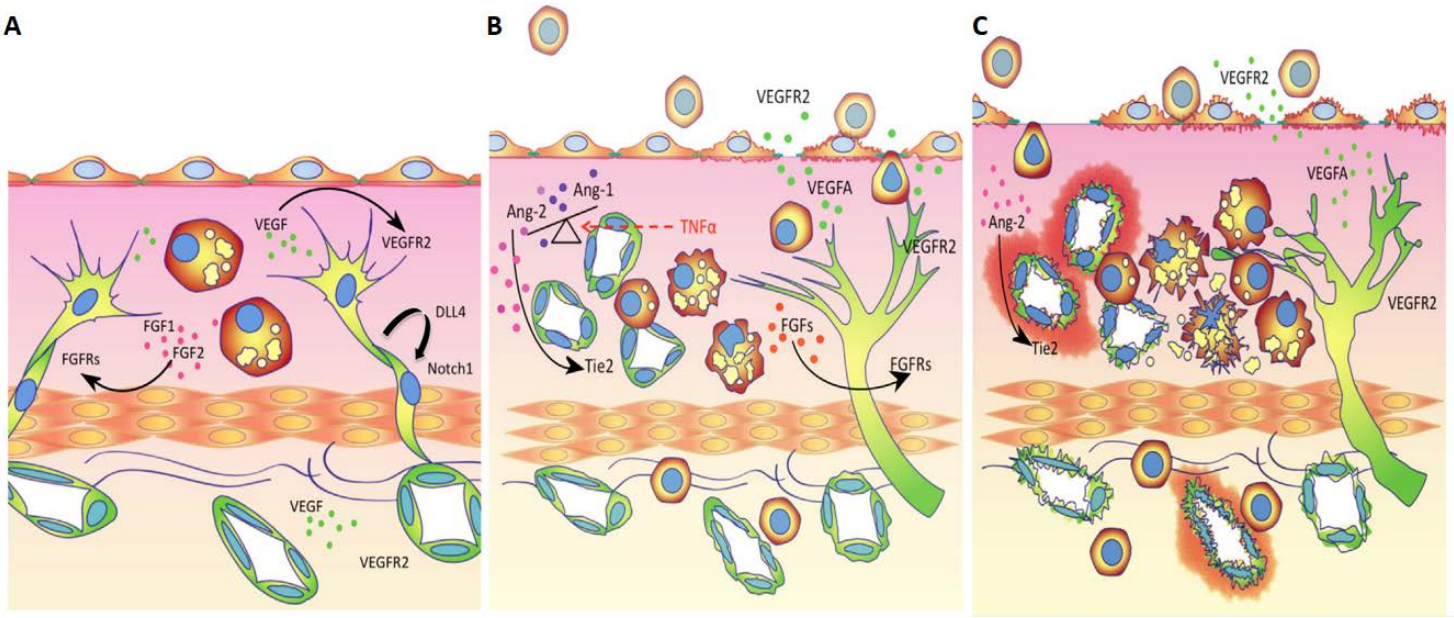

Figura 6. El proceso de angiogénesis en el desarrollo de la placa aterosclerótica. En la primera fase (**A**), el crecimiento de la íntima alcanza un punto en el que la hipoxia en la región central desencadena una respuesta mediada por el factor de crecimiento vascular endotelial (VEGF), induciendo la neovascularización. La secreción del factor de crecimiento de fibroblastos (FGF)-1 y (FGF)-2 por los diferentes componentes de la placa aterosclerótica produce la activación del receptor de FGF permitiendo con ello la proliferación y migración de las células endoteliales en sinergia con la estimulación de VEGF. En la segunda fase (**B**), los altos niveles de angiopoyetina-I, FGF y VEGF aseguran la supervivencia y la expansión de la neovasculatura, proporcionando de esta manera una segunda ruta de entrada a las células inflamatorias además de la entrada principal a través del

endotelio luminal. Esto amplifica el estado inflamatorio de la placa aterosclerótica y, en respuesta a factores inflamatorios como el TNFα, aumenta la relación angiopoyetina-II/angiopoyetina-I, y promueve la inflamación mediante la activación de las MAC e induciendo la pérdida de la integridad de las uniones célula-célula en cooperación con altos niveles persistentes de VEGF. En la fase final (**C**), se compromete la permeabilidad endotelial, y la falta de contactos pericito-célula endotelial permite la hiperproliferación y desdiferenciación funcional del endotelio, lo que resulta en hemorragias intraplaca y el debilitamiento adicional de la lesión avanzada. Adaptado de Cheng *et al.* 2013.

Con el tiempo, la placa fibrosa se vuelve delgada y débil debido a la actividad que llevan a cabo las células inflamatorias, así como la activación de las metaloproteasas de matriz (MMPs), provocando la ruptura o ulceración en los sitios más finos (Ruddy *et al.* 2016). Al mismo tiempo, la inflamación crónica disminuye la concentración de elastina y colágeno en el endotelio debido al incremento en la apoptosis de las células del músculo liso de la íntima. Esto reduce la integridad y resistencia de la capa fibrosa que cubre la placa trombogénica en contacto con la sangre (de Vries *et al.* 2016).

Las MMPs son un grupo de enzimas proteolíticas secretadas por macrófagos, células endoteliales y células inflamatorias, capaces de degradar las proteínas que forman la matriz extracelular, facilitando la migración celular y la liberación de factores de crecimiento embebidos en la matriz extracelular (Camare *et al.* 2017). Además, pueden llevar a cabo la degradación del colágeno presente en los espacios intercelulares. Tienen un papel relevante en procesos como la curación de heridas, la angiogénesis y la metástasis de células tumorales (Coronato *et al.* 2012).

Durante el proceso aterosclerótico, llevan a cabo el debilitamiento de la pared arterial provocando la ruptura de la lámina elástica interna, induciendo la agregación plaquetaria y la trombosis vascular (Nording *et al.* 2015). En la placa fibrosa, las MMP-2 y MMP-9 degradan proteoglicanos, colágeno de tipo IV, fibronectina, elastina y laminina, destruyendo así la matriz de proteínas de la capa y aumentando las probabilidades de ruptura (Ruddy *et al.* 2016). Además de las MMPs, se ha observado que otras citocinas proinflamatorias, como el IFNγ, producido por las células T, inhibe la síntesis de colágeno por las células del músculo liso en combinación con otras moléculas inflamatorias como la IL-1β o el TNFα (Rafieian-Kopaei *et al.* 2014).

La lesión vulnerable tiene varias características estructurales y funcionales que la distinguen de la placa estable. Así, la lesión inestable tiene un *core* necrótico más grande (más del 40% del volumen de la placa) y mayoritariamente acelular, compuesto de cristales de colesterol, ésteres de colesterol, lípidos oxidados, fibrina, eritrocitos y sus remanentes (grupo hemo, hierro, hemoglobina) y macrófagos apoptóticos. La capa fibrosa es delgada, carente de células del músculo liso y colágeno, y está infiltrada por células proinflamatorias. Además, en la lesión inestable se observa un aumento en la neovascularización. Estos nuevos vasos tienen una integridad débil, lo que lleva a la fuga sanguínea y hemorragias recurrentes. Estas hemorragias proveen eritrocitos al *core* necrótico, donde se degradan; promoviendo la inflamación y el estrés oxidativo. Al mismo tiempo, diversas células inflamatorias se extravasan de estos nuevos vasos y se infiltran en el tejido adventicio, donde promueven la inflamación crónica. En resumen, la desestabilización de la placa es un proceso evolutivo que comienza en las etapas ateroscleróticas tempranas y cuya progresión se ve influenciada por muchos factores, incluyendo la neovascularización, las hemorragias intraplaca, la formación de cristales de colesterol, la inflamación, el estrés oxidativo y la actividad proteasa dentro de la placa (Chistiakov *et al.* 2015).

Diversos eventos de riesgo mortal, como el infarto de miocardio o el accidente cerebrovascular isquémico, son provocados por una ruptura súbita de las placas ateroscleróticas vulnerables. Distintos factores biomecánicos, hemodinámicos y físicos contribuyen a la desestabilización de la placa. Así, la aterotrombosis puede ser causada por dos tipos de daño superficial: la ruptura de la placa o la erosión endotelial. Se cree que esta ruptura es causada por una pérdida de la estabilidad mecánica, a menudo debida a una reducción en la resistencia a la tracción de la cubierta de colágeno que envuelve la placa. La erosión endotelial, por otro lado, podría ocurrir tras un daño al endotelio instigado por una alteración metabólica o inmunitaria. Por otra parte, la microcalcificación dentro de la capa fibrosa (típicamente de 10 μm de diámetro) puede facilitar la ruptura de la placa a través del aumento local de la tensión que conduce al despegamiento (Hansson *et al.* 2015). Sin embargo, la ruptura de la placa es frecuentemente subclínica, ya que las células del músculo liso reparan el daño y reorganizan el trombo asociado. De hecho, las placas avanzadas muestran con frecuencia evidencias de múltiples rupturas y reparaciones, que finalmente resultan en un estrechamiento luminal. La reparación exitosa de la placa requiere que las

células del músculo liso proliferen y sinteticen matriz extracelular, ambas propiedades alteradas por la muerte y la senescencia celular. De hecho, el equilibrio de la proliferación celular y la migración frente a la apoptosis y la senescencia celular determina el fenotipo de las células del músculo liso en la placa aterosclerótica. El papel y la regulación de estos procesos es crucial tanto para la aterogénesis como para la estabilidad de la placa (Bennett *et al.* 2016).

Tras la ruptura, estas placas ricas en lípidos exponen estructuras vasculares o componentes del *core* necrótico a la circulación, lo que causa la activación de la cascada de coagulación y, a la vez, el reclutamiento de plaquetas y células inflamatorias circulantes. La interacción entre los componentes de la placa expuestos, los receptores de plaquetas y los factores de coagulación conduce a la activación y agregación plaquetaria y la consecuente formación de un trombo superpuesto que, de bloquear el lumen arterial, llevaría al sufrimiento de síndromes isquémicos agudos (Badimon *et al.* 2014).

Mientras que tanto la inflamación innata como la adaptativa han emergido progresivamente como la fuerza que conduce estos procesos, se sabe mucho menos acerca del papel de las células polimorfonucleares (PMN), en general, y los neutrófilos, en particular. Se piensa que las PMN juegan un papel crucial en promover la vulnerabilidad de la placa a través de la liberación de diferentes enzimas como las MMPs. De hecho, los niveles circulantes de PMN y sus productos se han estudiado como posibles marcadores de la inestabilidad de la placa; así mismo, se están explorando distintos fármacos cuya diana terapéutica sería modular la activación de las PMN (Carbone *et al.* 2015).

El proceso completo de la formación de la placa de ateroma se resume en la **Figura 7** (Ross 1999).

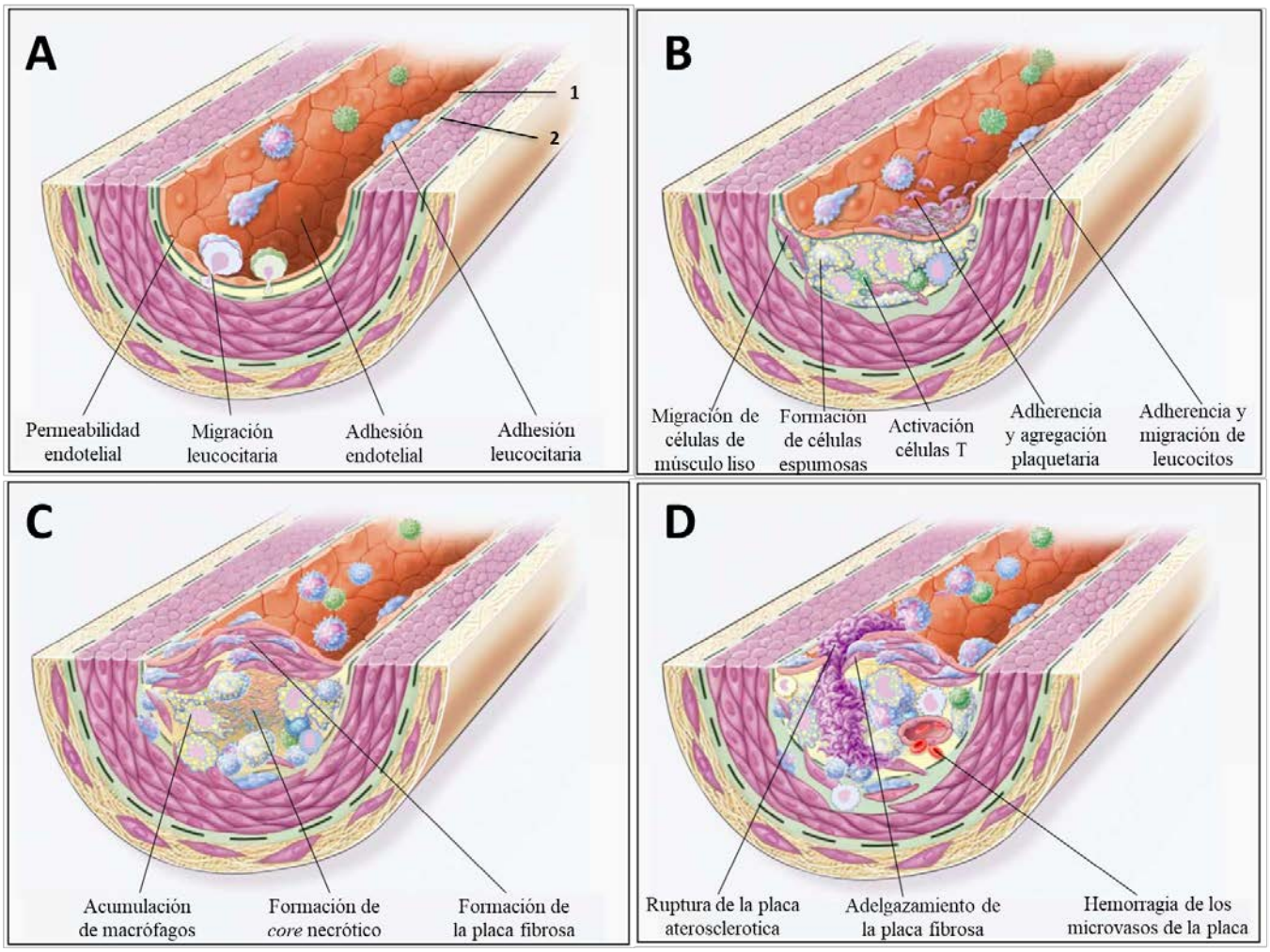

Figura 7. Formación de la placa de ateroma. Tanto en las arterias como en las válvulas, la placa de ateroma se forma por debajo del endotelio (**1**), concretamente en la íntima (**2**). Esta lesión se inicia con la adhesión de LDL en la íntima, causando la activación de las células endoteliales atrayendo a las plaquetas y a los monocitos, estos últimos migran hacia la íntima donde se diferencian a macrófagos (**A**). A medida que va avanzando la lesión, ciertas quimiocinas provocan la migración de células de la musculatura lisa vascular, que se desplazarán hacia la superficie de la lesión; mientras, los macrófagos captan LDLox de la lesión formando las células espumosas. La lesión avanza, causando la infiltración de linfocitos T en la íntima (**B**). Finalmente, una vez la placa de ateroma está formada, comienza la síntesis de tejido fibroso, como colágeno, que estará cubierto por la capa de células de la musculatura lisa vascular migradas anteriormente. Además, algunas células espumosas ya formadas mueren por apoptosis formando lo que se conoce como *core* necrótico, cristales de colesterol que causan el endurecimiento de las arterias y válvulas (**C**). Por último, las placas fibrosas inestables del ateroma, producen la ruptura o ulceración de la placa, y puede conducir rápidamente a la trombosis. Por lo general, se produce en sitios de adelgazamiento de la cubierta fibrosa que cubre la lesión avanzada. El debilitamiento de la placa fibrosa se debe a la afluencia y activación continua de los macrófagos, que liberan metaloproteasas de matriz (MMPs) y otras enzimas proteolíticas en estos sitios. Estas enzimas causan la degradación de la matriz, lo que puede conducir a una hemorragia del *vasa vasorum* o del lumen de la arteria y dar como resultado la formación de trombos y la oclusión de la misma (**D**). Imagen modificada de Ross, 1999.

1.2.3 Las plaquetas en el proceso aterosclerótico

Las plaquetas circulantes son células inflamatorias anucleadas formadas por subpoblaciones con diferente edad, estado de maduración y tamaño (Bakogiannis *et al.* 2017). Éstas desempeñan diversas funciones en la biología vascular y la homeostasis, donde son los mediadores esenciales que desencadenan la cascada de la coagulación, a través de tres procesos principales: activación, adhesión y agregación (Manne 2017, Periayah *et al.* 2017). Además, presentan un papel importante en la patogénesis de la trombosis (Mancuso *et al.* 2017). Sin embargo, en los últimos años han sido reconocidas como centinelas clave y células efectoras que regulan las respuestas del huésped a muchas señales inflamatorias e infecciosas más allá de la hemostasia primaria, actuando como mediadores en la inmunidad y la inflamación (Lam *et al.* 2015).

Al mismo tiempo, las plaquetas contribuyen a la iniciación y propagación de los procesos inflamatorios locales y sistémicos. En ocasiones, estos pueden estar regulados y aumentar las respuestas efectivas del huésped mientras que en otros entornos, la activación plaquetaria exagerada, la adhesión, la agregación y la secreción pueden contribuir al entorno sistémico nocivo y a resultados clínicos adversos (Manne 2017).

Cuando se interrumpe la integridad del endotelio vascular, diversos elementos macromoleculares del subendotelio vascular quedan expuestos y son fácilmente accesibles para las plaquetas (Periayah *et al.* 2017). Durante el proceso aterogénico, se ha observado que las plaquetas activadas no solo participan en eventos trombóticos sino que también juegan un papel esencial en el desarrollo de lesiones ateroscleróticas. Expresan en su superficie numerosos receptores de membrana que median la activación plaquetaria, la adhesión y la agregación en los sitios de lesión vascular (Papapanagiotou *et al.* 2016, Manne 2017). Tras su activación, las plaquetas liberan más de 300 mediadores proinflamatorios diferentes, que incluyen citocinas quimiotácticas almacenadas en los gránulos intracelulares, para modular la inflamación (Blanchet *et al.* 2012, Golebiewska *et al.* 2015). La mayoría de éstos se almacenan en gránulos α y otros, como la serotonina, se almacenan en gránulos densos (Manne 2017). Entre ellos caben destacar el factor plaquetario-4 (PF-4)/CXCL4, RANTES/CCL5, la proteína activadora de neutrófilos-2 (NAP-2)/CXCL7, el factor derivado de células estromales-1α (SDF-1α)/CXCL12, GROα (*growth-regulated oncogene*

α)/CXCL1, o el péptido activador de neutrófilos epiteliales (ENA)-78/CXCL5 entre otras, capaces de mediar en la adhesión endotelial de diferentes células, incluidos los monocitos, los neutrófilos, y las células progenitoras (Lievens *et al.* 2011, Bakogiannis *et al.* 2017). Todas ellas son cruciales para la respuesta funcional de las plaquetas. La capacidad de las plaquetas para producir y secretar citocinas, quimiocinas y moléculas relacionadas, bajo el control de vías intracelulares específicas, está íntimamente relacionada con su papel clave en la inflamación. También pueden intervenir en la regeneración y reparación de tejidos porque producen mediadores proangiogénicos (Mancuso *et al.* 2017); bajo condiciones isquémicas agudas, las quimiocinas derivadas de plaquetas pueden promover la movilización de células progenitoras derivadas de la médula ósea y su localización a los sitios de lesión (**Tabla 2**) (Bakogiannis *et al.* 2017).

Tabla 2. Factores secretados por plaquetas. Adaptado de Bakogiannis *et al.* 2017.

Familia	Factor secretado	Célula diana
Molécula de adhesión celular	P-selectina	Leucocitos
Moduladores inflamatorios	Histamina	Células endoteliales y leucocitos
	Serotonina	Monocitos y macrófagos
Quimiocinas	PF-4/CXCL4	Neutrófilos, monocitos y macrófagos
	NAP-2/CXCL7	Neutrófilos
	GROα/CXCL1	Neutrófilos
	ENA-78/CXCL5	Neutrófilos
	SDF-1α/CXCL12	Células progenitoras de la médula ósea
	RANTES/CCL5	Monocitos, eosinófilos, basófilos, células NK y linfocitos T
	MIP-1α/CCL3	Monocitos, eosinófilos, basófilos, células NK y linfocitos T
	MCP-3/CCL7	Monocitos, eosinófilos, basófilos, células NK y linfocitos T
Citocinas	IL-1β e IL-1α	Monocitos, macrófagos, células T, células endoteliales y células del músculo liso
	GM-CSF	Eosinófilos, neutrófilos y macrófagos

Por lo tanto, se ha descubierto que las plaquetas están involucradas en diferentes patologías con componente inflamatorio como la obesidad, la lesión pulmonar aguda o la enfermedad arterial coronaria donde interactúan tanto con células endoteliales como con leucocitos, conduciendo a una diversidad de efectos (van Gils *et al.* 2009).

Así mismo, las plaquetas contienen y liberan MMPs, así como inhibidores de metaloproteasas de matriz (TIMP). Las MMPs/TIMP liberadas por plaquetas, así como las MMPs generadas por otras células dentro del sistema cardiovascular, modulan la función plaquetaria en determinadas condiciones fisiopatológicas. En particular, una respuesta plaquetaria hemostática normal a la lesión de la pared del vaso puede derivar en la formación de un trombo patológico por la liberación de plaquetas y/o por la generación local de algunas MMPs. Además, las plaquetas pueden localizar la producción de MMPs derivadas de leucocitos en sitios de daño vascular, lo que contribuye al desarrollo y complicaciones de la aterosclerosis y a la formación de aneurismas arteriales. Todos estos mecanismos están emergiendo como factores importantes en el proceso de la aterotrombosis (**Figura 8**) (Gresele *et al.* 2017, Manne 2017).

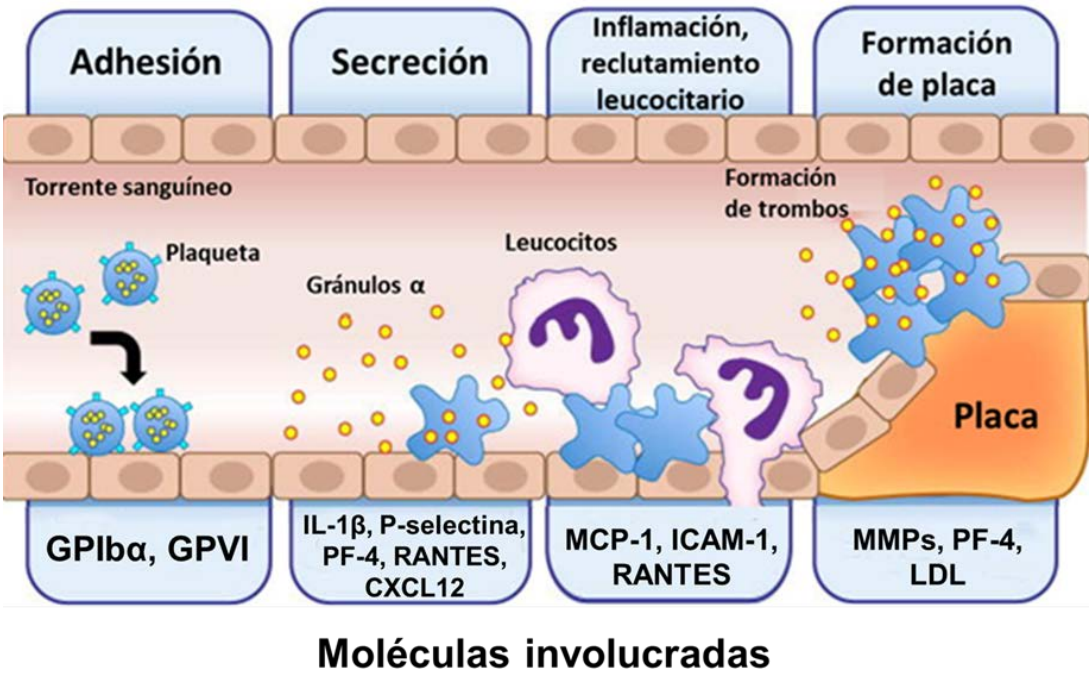

Figura 8. Papel de las plaquetas en la aterosclerosis. Las plaquetas activadas se desplazan a lo largo de la monocapa endotelial a través de GPIbα/P-selectina. Posteriormente, las plaquetas se adhieren al endotelio vascular a través de las integrinas β_3, liberan compuestos proinflamatorios como

IL-1β, CD40L, factor plaquetario-4 (PF-4) y RANTES e inducen la expresión de moléculas de adhesión en las células endoteliales, que ayudan a reclutar leucocitos circulantes. Estos leucocitos transmigran y forman células espumosas a través de la absorción de LDL. En este y en otros mecanismos, las plaquetas proporcionan la base inflamatoria para la formación de la placa y la posterior trombosis tras la rotura de la misma. Adaptado de Manne, 2017.

1.2.4 Factores de riesgo

Numerosos estudios epidemiológicos han identificado diversos factores de riesgo como la edad (mayor incidencia a partir de los 40-50 años), el sexo masculino, la hipertensión, la elevada concentración de LDL, los triglicéridos, el tabaco, la presencia de antecedentes familiares, la obesidad, la diabetes *mellitus* o el haber padecido condiciones de inflamación crónica, como principales factores de riesgo de la aterosclerosis (Wong *et al.* 2016). Todos estos factores varían en prevalencia y potencia, y se suelen presentar de forma combinada en pacientes con aterosclerosis severa, lo que demuestra el carácter multifactorial de la patología (Nahrendorf *et al.* 2015, Smabrekke *et al.* 2016).

1.3 HIPERCOLESTEROLEMIA PRIMARIA

1.3.1 Características generales

La hipercolesterolemia primaria (HP) es un trastorno lipídico caracterizado por elevado niveles plasmáticos de colesterol y LDL. Este trastorno metabólico es heterogéneo a nivel genético y dentro de él se incluye tanto a la hipercolesterolemia familiar, como la hipercolesterolemia no familiar poligénica más frecuente (Langslet *et al.* 2015).

La hipercolesterolemia familiar es una enfermedad monogénica autosómica dominante del metabolismo lipoproteico caracterizada por un aumento notorio de LDL en el torrente sanguíneo (Sniderman *et al.* 2014). Ello provoca la deposición de placa aterosclerótica en las arterias y un marcado riesgo de sufrir enfermedades cardiovasculares a temprana edad como, por ejemplo, aterosclerosis coronaria prematura (Defesche *et al.* 2017). El riesgo de enfermedad coronaria prematura se considera un 20% mayor en pacientes con hipercolesterolemia no tratados que en sujetos control (Sniderman *et al.* 2014).

La hipercolesterolemia familiar pertenece al grupo de hipercolesterolemias autosómicas dominantes (ADH), término reservado a un conjunto de hipercolesterolemias de origen genético ocasionadas por mutaciones en los genes que controlan los niveles de LDL en el torrente sanguíneo. Las ADH se clasifican según el gen que se encuentre mutado (**Tabla 3**) (Sniderman *et al.* 2014).

Tabla 3. Tipos de ADH según la mutación.

Hipercolesterolemias autosómicas dominantes (ADH)	Gen mutado	Prevalencia de la enfermedad	Niveles de LDL (mg/dL)
Hipercolesterolemia familiar heterocigota (ADH-1)	Receptor de LDL (LDLR)	1:300-1:500	350-550
Hipercolesterolemia familiar homocigota (ADH-1)	Receptor de LDL (LDLR)	1:1.000.000	650-1.000
Defecto de la apoB-100 familiar (ADH-2)	Apolipoproteína B (apoB)-100	1:500-1:1.000	350-450
Hipercolesterolemia asociada a mutaciones en PCSK9 (ADH-3)	Proteína convertasa subtisilina/kexina 9 (PCSK9)	<1:2.500	390-550

La hipercolesterolemia familiar heterocigótica es debida a la mutación de uno de los alelos y tiene una prevalencia de 1:300-1:500; por el contrario, en la homocigótica cuya prevalencia es 1:1.000.000, los dos alelos han sufrido una alteración, o bien una heterocigosidad compuesta por dos mutaciones diferentes en el mismo o diferentes genes candidatos.

La mutación más común, presente en el 85-90% de los pacientes con hipercolesterolemia familiar, radica en el gen codificante para el receptor de LDL (LDLR). Este receptor es una glicoproteína localizada en la superficie de los hepatocitos, responsable de eliminar las LDL del torrente sanguíneo mediante la internalización del mismo al interactuar con la apolipoproteína B (apoB)-100. Una vez internalizado, se produce la disociación del complejo LDL-LDLR (Chaudhary *et al.* 2017). Las mutaciones en el gen *LDLR* provocan fallos en los hepatocitos impidiendo eliminar las LDL de manera efectiva del torrente sanguíneo, provocando un incremento en la concentración de LDL y su vida media en la sangre. Las mutaciones en el LDLR provocan diferentes defectos que se pueden clasificar en cinco categorías (**Tabla 4**) (Pejic 2014, Singh *et al.* 2015).

Tabla 4. Principales clases de defectos genéticos del LDLR. Adaptado de Pejic, 2014.

Hipercolesterolemia Familiar − ADH-1	
Clase I	LDLR no sintetizado
Clase II	Alteración en el transporte del LDLR a la superficie celular
Clase III	Alteración en la unión LDL-LDLR
Clase IV	Alteración en la internalización del complejo LDL-LDLR
Clase V	Alteración en el reciclado del LDLR

De estas mutaciones, las más graves son las de clase I, al no sintetizar el LDLR; así como las de clase III, en las que las mutaciones imposibilitan la unión del receptor con las apolipoproteínas B y E (apoB/E) (Angarica *et al.* 2016). En la **Figura 9** se ilustran las diferentes alteraciones que causan la hipercolesterolemia familiar (Sniderman *et al.* 2014).

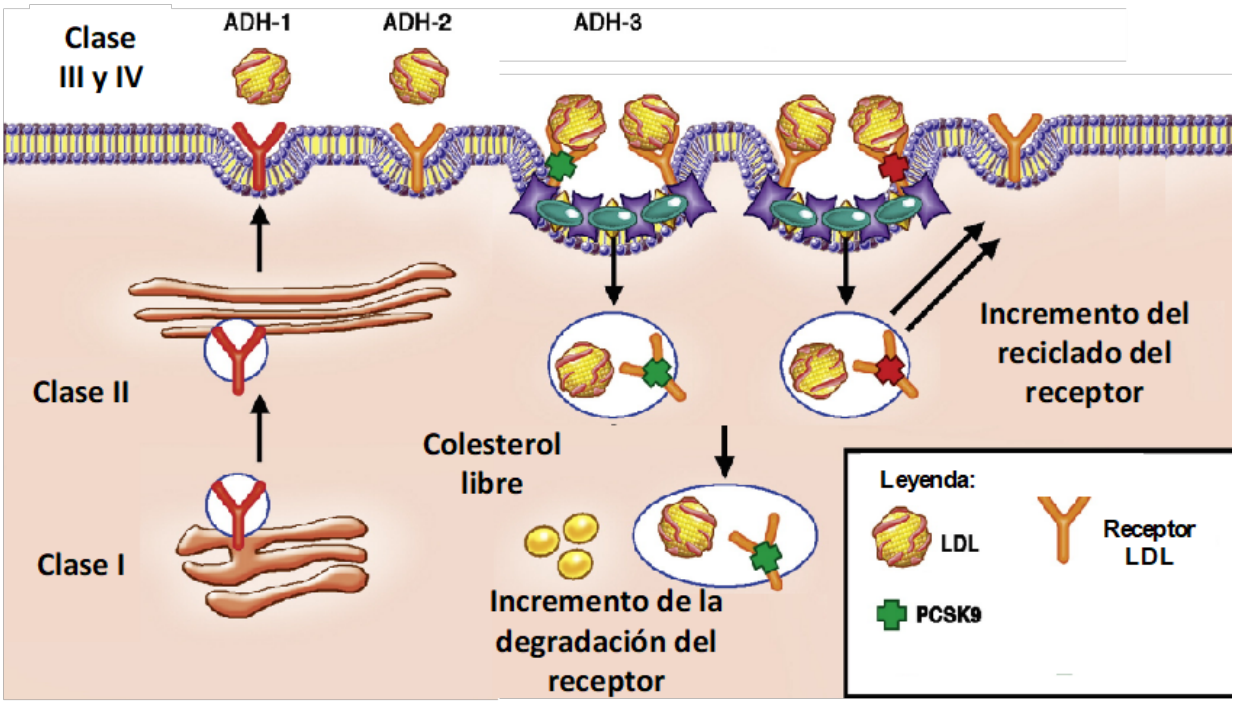

Figura 9. Alteraciones celulares que median la captación de LDL y causan hipercolesterolemia familiar. Descripción de las cinco clases principales de mutaciones que ocurren en el receptor de LDL (LDLR) y que causan hipercolesterolemia familiar (o hipercolesterolemia autosómica dominante [ADH]). En la ADH-1, (**clase I**) las mutaciones genéticas evitan la síntesis de LDLR; (**clase II**) está producida por una alteración en el transporte de LDLR a la superficie celular debido a la salida del retículo endoplasmático de productos codificados genéticamente de manera parcial;

(**clase III**) ocasionada por la unión defectuosa entre la apolipoproteína B (apoB)-100 y el LDLR; (**clase IV**) provocada por fallos en la endocitosis constitutiva del complejo LDL-LDLR; y por último, las de **clase V** (no mostrado para mayor claridad), caracterizadas por fallos en el reciclado del LDLR internalizado. La ADH-2 está causada por mutaciones en el gen de la *APOB-100*, impidiendo la unión de la apoB-100 al LDLR. Por último, la ADH-3 está causada por mutaciones en el gen *PCSK9* con ganancia de función, favoreciendo la eliminación del LDLR. *En rojo, se muestra la mutación de pérdida de función; en verde, la ganancia de función*. Adaptado de Sniderman *et al.* 2014.

La apolipoproteína B-100 defectuosa familiar es un trastorno genético autosómico dominante del metabolismo de los lípidos asociado con la hiperlipidemia y el riesgo elevado de aterosclerosis (Andersen *et al.* 2016). La apoB-100 está presente en la superficie del LDL y permite la unión con su receptor. Las mutaciones en el gen *APOB*, producidas en el cromosoma 2p23-24, son menos frecuentes, ocurriendo en el 5-10% de los casos de hipercolesterolemia (Pejic 2014, Singh *et al.* 2015), con una prevalencia de 1:1.000 (Ahmad *et al.* 2012), y provocan que el LDLR tenga una afinidad reducida por la apoB-100, aumentando así la concentración de LDL en sangre (Pejic 2014).

Por otra parte, la ganancia de función del gen de la proteína convertasa subtisilina/kexina 9 (*PCSK9*) es inusual y ocurre en menos de un 5% de los casos de pacientes con hipercolesterolemia (Pejic 2014). PCSK9 es la enzima responsable de la eliminación del LDLR de la superficie del hepatocito; por tanto, un aumento en su expresión promueve la degradación del LDLR, conllevando así a un incremento de los niveles de LDL en sangre (Chaudhary *et al.* 2017).

Se ha observado que los pacientes con hipercolesterolemia en condiciones de ayuno tienen una mayor concentración de partículas remanentes debido a una lipemia postprandial alterada; lo que, a su vez, es consecuencia del defecto en el LDLR, que elimina las lipoproteínas de densidad intermedia o las de muy baja densidad (VLDL) (Pedro *et al.* 2013).

1.3.2 Inflamación sistémica en la HP

El estrés oxidativo juega un papel fundamental en el desarrollo de las enfermedades cardiovasculares como la aterosclerosis en cualquiera de sus etapas, y está implicado en la patogénesis de la disfunción endotelial (Real *et al.* 2010b). Algunas enzimas clave en este proceso y expresadas en la vasculatura son la xantina oxidasa (XO), la NADH/NADPH, y la eNOS, cuya expresión y actividad está sujeta a una regulación transcripcional, traduccional

y post-traduccional, incluyendo su acetilación, fosforilación y sumoilación (Didion 2017). Un incremento en la actividad de estas enzimas y de las especies reactivas del oxígeno presentes en las paredes arteriales promueven el exceso de estrés oxidativo; al mismo tiempo, una reducción en la biodisponibilidad de NO también agrava el proceso, ya que éste reacciona con el anión superóxido y lo neutraliza (Real *et al.* 2010b, Miyazaki *et al.* 2017). Estos cambios pueden provocar alteraciones en la estructura y funcionalidad de las células endoteliales y contribuir al inicio de la progresión de la placa aterosclerótica (Cortes *et al.* 2014, Rafieian-Kopaei *et al.* 2014). En diferentes estudios se ha observado que los pacientes con HP presentan un mayor estrés oxidativo, en especial aquellos que presentan comorbilidades cardiovasculares, así como un incremento de la inflamación sistémica. En concreto, se ha observado un incremento en la XO, así como en el factor nuclear (NF)-κB (Real *et al.* 2010a, Mollazadeh *et al.* 2018).

Al mismo tiempo, se han estudiado diversos marcadores inflamatorios en pacientes con hipercolesterolemia familiar, detectándose elevados niveles plasmáticos de IL-1, IL-6 (Real *et al.* 2010a), IL-8, proteína inductora de IFNγ-10/CXCL10 y TNFα (Holven *et al.* 2014, Cortes *et al.* 2016), así como de la proteína C reactiva (Gokalp *et al.* 2009) y de las LDLox (Real *et al.* 2010b). Curiosamente, también se ha visto un incremento de la expresión de RANTES/CCL5 en células mononucleares de niños con hipercolesterolemia, pero no de adultos, donde sí se advirtió un aumento en la transcripción de la proteína inflamatoria de macrófagos-1α (MIP-1α)/CCL3 (Holven *et al.* 2006, Cortes *et al.* 2016).

Una de las citocinas de mayor relevancia en la HP es el TNFα, ya que interviene tanto en el inicio como en el desarrollo de la lesión aterosclerótica, reclutando y activando células inflamatorias a través de la inducción de la expresión de MAC y liberación de quimiocinas (Tousoulis *et al.* 2016). Estudios previos han descrito la sobreexpresión del mensajero de dos receptores de TNFα, TNFR1 y TNFR2, así como del ligando inductor de apoptosis relacionado con TNFα, TRAIL o CD40, en los leucocitos mononucleares de pacientes con hipercolesterolemia (Holven *et al.* 2014).

1.3.3 Tratamiento actual y perspectivas de futuro

Las guías clínicas actuales para la prevención de enfermedades cardiovasculares determinan que el objetivo principal del tratamiento para los pacientes con

hipercolesterolemia es lograr reducir los niveles de LDL en sangre en más de un 50% mediante el uso de estatinas (Piepoli *et al.* 2018). La monoterapia con estatinas puede llegar a reducir los niveles de LDL hasta un 60%; sin embargo, estos niveles no son suficientes en pacientes con hipercolesterolemia acompañada de comorbilidades como diabetes o enfermedades cardiovasculares (Sniderman *et al.* 2014), o pacientes con hipercolesterolemia familiar homocigota (Liu *et al.* 2017a).

Para conseguir una mayor disminución de los niveles de LDL, como alternativa a las estatinas se pueden emplear la ezetimiba, la niacina, los fibratos o los secuestrantes de ácidos biliares. Una terapia combinada puede lograr hasta un 30% adicional de reducción. En los casos en los que la terapia farmacológica no funciona, se puede emplear la aféresis de las lipoproteínas, eliminando de esta manera las lipoproteínas apoB-asociadas del plasma (Tavori *et al.* 2013, Sniderman *et al.* 2014).

En el año 2013 fue aprobado por la Administración de Alimentos y Fármacos de Estados Unidos (*Food and Drug Administration*; FDA), así como por la Agencia Europea del medicamento (EMEA), lomitapida, el medicamento huérfano oral de uso diario para el tratamiento de la hipercolesterolemia familiar. Este fármaco actúa como inhibidor de la proteína microsomal de transferencia de triglicéridos, cuya función es llevar a cabo la síntesis de VLDL, y es la proteína clave que permite el ensamblaje de las lipoproteínas que contienen apoB, así como su secreción (Berberich *et al.* 2017, Liu *et al.* 2017a). La inhibición de esta proteína logra disminuir los niveles de quilomicrones y VLDL y por consiguiente reducir en hasta un 38% los niveles de LDL en sangre. Sin embargo, la administración de este fármaco da lugar al desarrollo de algunos efectos secundarios como complicaciones gastrointestinales y hepatotoxicidad (Sniderman *et al.* 2014, Berberich *et al.* 2017).

Actualmente, se han comenzado a usar como terapias alternativas los inhibidores de la enzima PCSK9 (Horton *et al.* 2009). Para inhibir esta enzima en el contexto de la hipercolesterolemia familiar, hoy en día se emplean anticuerpos monoclonales. De hecho, se han observado unas reducciones drásticas de los niveles de LDL en sangre, llegando a ser de hasta un 75%, siendo similar estos niveles en la apoB (Sniderman *et al.* 2014, Baum *et al.* 2018). Igualmente, se han empleado vías alternativas para bloquear la expresión de la PCSK9

mediante el uso de ARN de interferencia, logrando reducir los niveles en sangre de PCSK9 y de LDL en hasta un 70% y un 50% respectivamente (Fitzgerald *et al.* 2014).

1.3.4 Receptor de quimiocinas CC de tipo 3 (CCR3)

El receptor de quimiocinas CC de tipo 3 (CCR3) o CD193 es un receptor acoplado a proteínas G que pertenece a la subfamilia de clase A de receptores semejantes a rodopsina. Está formado por 350 aminoácidos y contiene un motivo de siete regiones hidrofóbicas (Willems *et al.* 2010).

1.3.4.1 Expresión de CCR3

El receptor CCR3 se expresa en la superficie celular de los eosinófilos (Daugherty *et al.* 1996, Ponath *et al.* 1996), mastocitos (de Paulis *et al.* 2001), basófilos (Uguccioni *et al.* 1997), linfocitos Th2 (Miyagaki *et al.* 2010), y de las células de músculo liso de las vías respiratorias (Saunders *et al.* 2009). Su expresión puede ser constitutiva o inducida temporalmente por citocinas específicas como IL-4 (Turner *et al.* 2018). La expresión de CCR3 en mastocitos es intracelular y éste se almacena en gránulos, transportados a la superficie celular mediante la implicación del receptor de IgE de alta afinidad (FcεRIα) tras la señalización por otros receptores; en los eosinófilos y en los linfocitos Th2, la localización de CCR3 siempre es la superficie celular (Forsythe *et al.* 2003, Willems *et al.* 2010). De todos los tipos celulares donde se expresa el receptor CCR3, el mayor nivel de expresión se encuentra en los eosinófilos, donde se pueden llegar a acumular hasta $5*10^4$ receptores por célula (Elsner *et al.* 2004).

1.3.4.2 Funciones de CCR3

El receptor CCR3 está implicado en enfermedades alérgicas y se cree que desempeña un papel fundamental en todo el proceso alérgico.

Este receptor es promiscuo y puede ser activado por diferentes quimiocinas, aunque su potencia y eficacia puede variar entre los distintos ligandos. Actualmente se conocen los siguientes agonistas naturales: RANTES/CCL5, eotaxina-1/CCL11, eotaxina-2/CCL24, eotaxina-3/CCL26, MCP-3/CCL7, MCP-2/CCL8, MCP-4/CCL13, CCL14, MIP-1δ/CCL15 y MEC/CCL28 (quimiocina epitelial asociada a la mucosa). Estos ligandos, además de llevar

a cabo la quimiotaxis de células $CCR3^+$, inducen en los eosinófilos la polimerización de actina, el flujo intracelular de calcio y su degranulación en el foco inflamatorio, liberando radicales libres y moléculas citotóxicas, y promoviendo de esta manera la inflamación. Asimismo, en los basófilos promueven la liberación de mediadores inflamatorios como histamina y leucotrienos (Forsythe *et al.* 2003, Willems *et al.* 2010). De todas ellas, las quimiocinas con mayor capacidad quimiotáctica de eosinófilos son las eotaxinas-1, 2 y 3 (CCL11, CCL24 y CCL26, respectivamente), las cuales son ligandos exclusivos del receptor CCR3 (Ahmadi *et al.* 2016).

1.3.4.3 Familia de las eotaxinas

Hasta la fecha, se han definido tres miembros en la familia de las eotaxinas, como se ha comentado anteriormente: eotaxina-1/CCL11, eotaxina-2/CCL24 y eotaxina-3/CCL26. Todas ellas se unen y activan CCR3 pero tienen un bajo nivel de homología y parecen exhibir diferentes funcionalidades fisiológicas (Ahmadi *et al.* 2016).

La quimiocina CCL11 o eotaxina-1 es una molécula de tipo C-C que, en su estructura, posee dos residuos de cisteína adyacentes en su posición N-terminal (Willems *et al.* 2010). Se trata de una proteína quimiotáctica de eosinófilos (Rankin *et al.* 2000, Blanchet *et al.* 2012), basófilos (Yamada *et al.* 1997) y linfocitos Th2 (Sallusto *et al.* 1997). Además, se ha detectado su presencia en lesiones ateroscleróticas (Blanchet *et al.* 2012). Es liberada por varios tipos celulares como eosinófilos, linfocitos, macrófagos, condrocitos, fibroblastos, células de músculo liso, células endoteliales y epiteliales (Ahmadi *et al.* 2016).

El gen de la eotaxina-1 está bien conservado entre diferentes especies y se expresa de manera constitutiva en distintos tejidos como son el intestino, el nódulo linfático, el timo, la piel, el corazón, el riñón y la glándula mamaria (Luster *et al.* 1997, Salcedo *et al.* 2001).

En enfermedades inflamatorias caracterizadas por una elevada infiltración de eosinófilos como el asma, la poliposis nasal, la sinusitis, la rinitis, la colitis ulcerosa o la enfermedad de Crohn, la quimiocina CCL11 juega un papel biológico importante; además, participa en el remodelado vascular (Salcedo *et al.* 2001).

La eotaxina-2 o CCL24 fue clonada y descrita por primera vez en el año 1997. Pese a su baja homología con CCL11, presenta efectos sorprendentemente similares a los de

eotaxina-1 en eosinófilos humanos y basófilos. Es producida principalmente por fibroblastos, células epiteliales y macrófagos, y sus principales células dianas son eosinófilos, linfocitos T y basófilos (Ahmadi *et al.* 2016).

La eotaxina-3, CCL26, se expresa en el corazón humano, el tejido ovárico y, más concretamente, en los fibroblastos dérmicos y las células endoteliales. Esta quimiocina ejerce su función quimiotáctica sobre eosinófilos y basófilos, y su producción está mediada por IL-4 e IL-13, mediadores de la respuesta de linfocitos Th2. Hasta la fecha, se sabe poco sobre la función y relevancia biológica de CCL26 en comparación con los otros dos miembros de la familia (Ahmadi *et al.* 2016).

1.3.4.4 CCR3 y enfermedades cardiovasculares

En estudios previos, se ha observado que existe una sobreexpresión de eotaxina-1 y de su receptor CCR3 en la lesión aterosclerótica, tanto de pacientes como en modelos animales. La eotaxina-1 se localiza predominantemente en células del músculo liso, mientras que su receptor CCR3 se presenta principalmente en regiones ricas en macrófagos y también una minoría de mastocitos ha demostrado inmunopositividad para el receptor CCR3 (Haley *et al.* 2000). Sin embargo, el papel del eje CCL11/CCR3 en el desarrollo de la aterosclerosis aún no se conoce con exactitud (Haley et al. 2000, Kraaijeveld et al. 2007, Blanchet et al. 2012).

1.4 ANGIOTENSINA-II

1.4.1 Consideraciones generales

La angiotensina-II (Ang-II) es una hormona octopeptídica y el principal péptido efector del sistema renina-angiotensina (SRA), que juega un papel fundamental en la homeostasis vascular y renal (Zhang *et al.* 2017, Eguchi *et al.* 2018). El SRA es un sistema complejo compuesto de una cascada de enzimas, péptidos y receptores, que regula el volumen de sangre y la resistencia vascular sistémica. Tiene tres componentes principales: la renina, la Ang-II y la aldosterona, que actúan para elevar la presión arterial de una manera más prolongada en respuesta a distintas situaciones, como una disminución en la presión

renal o una reducción en la presencia de sal en el túbulo distal (Fountain *et al.* 2018). Así mismo, el SRA es conocido por estar involucrado en la patogénesis de la hipertensión y la aterosclerosis (Nehme *et al.* 2017).

La Ang-II se obtiene a partir de la conversión de la Ang-I, que no posee actividad propia, por la enzima conversora de angiotensina (ECA). A su vez, Ang-I proviene de la proteólisis del angiotensinógeno, una globulina α_2 circulante de origen hepático, por medio de la actividad de la renina (**Figura 10**) (Sata *et al.* 2010, Balakumar *et al.* 2014). La ECA es una enzima de membrana de tipo 1 localizada no solo en la superficie de células endoteliales, sino también en otros tejidos como el corazón, el músculo estriado, los pulmones y el riñón (Zhang *et al.* 2017, Zhao *et al.* 2017). De esta manera, la Ang-II puede producirse en diferentes lechos, como por ejemplo el riñón, el corazón y el pulmón, donde ejerce un control local independiente de la Ang-II transportada por el torrente sanguíneo (Zhang *et al.* 2017). No obstante, el endotelio vascular es el mayor productor de Ang-II; en los vasos sanguíneos se han encontrado todos los componentes del SRA salvo la propia renina, lo que parece indicar que la producción local de la Ang-II en el intersticio vascular depende de los niveles de renina circulante (Sahay *et al.* 2012).

Alternativamente, la Ang-I se puede transformar en Ang-II por rutas enzimáticas diferentes que no requieren la ECA a nivel de tejidos. Por un lado, a partir de angiotensinógeno, gracias a la acción del factor activador tisular del plasminógeno y la tonina (de la Serna 2014). Por otro lado, también se puede producir a partir de la Ang-I, gracias a la acción de la quimasa y la catepsina G. Estas rutas alternativas representan un 40% del total de producción de la Ang-II humana (Daniels 2014, Bertoncello *et al.* 2015).

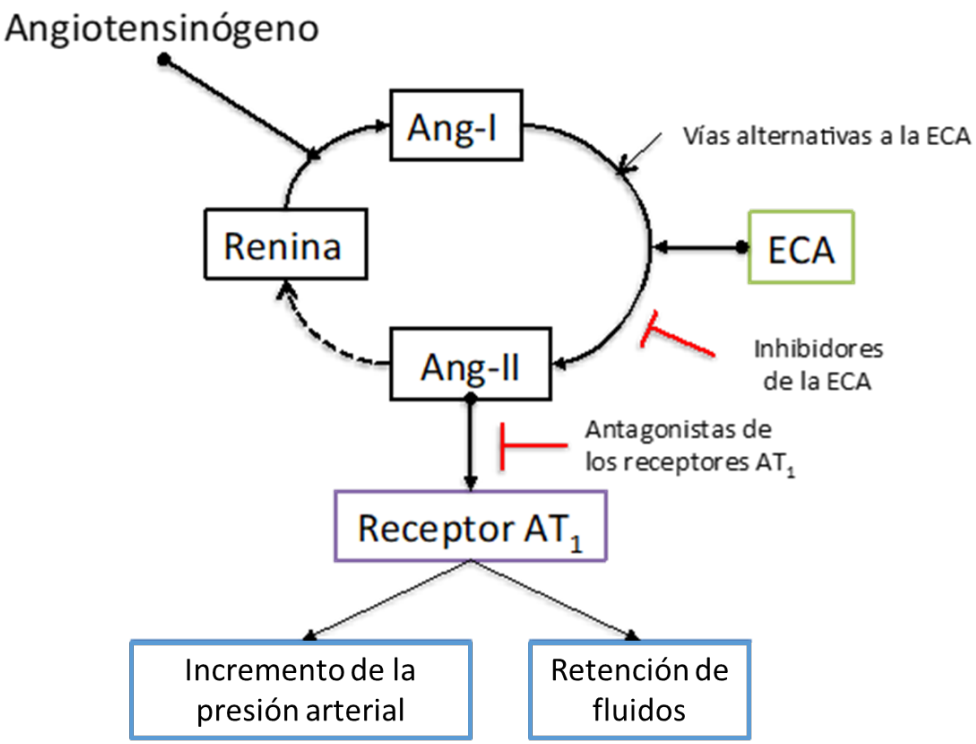

Figura 10. Esquema de la síntesis de angiotensina-II (Ang-II) y el sistema renina-angiotensina.

1.4.2 Funciones de la Ang-II

La Ang-II lleva a cabo diversas funciones fisiológicas que permiten regular la presión sanguínea y la homeostasis a través de diversos efectos que alteran la función de órganos como el corazón, el riñón, la glándula adrenal, la vasculatura y el sistema nervioso central. La estimulación crónica o sobreestimulación con la Ang-II provoca daños en las funciones renales y en el sistema cardiovascular (Balakumar *et al.* 2014). Asimismo, otras de las funciones que desempeña son la modulación de algunas respuestas inmunitarias e inflamatorias como la quimiotaxis, la proliferación y diferenciación de los monocitos en macrófagos, así como la inducción del crecimiento, la migración y la mitosis de las células del músculo liso mediante el aumento de la síntesis de colágeno tipo I en fibroblastos, produciendo una disminución del grosor de la pared vascular (Cuevas *et al.* 2015).

La presencia de la Ang-II en la respuesta inflamatoria de la pared arterial se ha descrito en enfermedades cardiovasculares como la aterosclerosis o la hipertensión, donde tiene un papel importante en el fallo y el remodelado cardiaco, la diabetes y en respuestas

inflamatorias (Ferrario *et al.* 2017). Concretamente, en el proceso aterosclerótico, la Ang-II estimula la disfunción endotelial, la expresión de MMPs, así como la estimulación del inhibidor del activador del plasminógeno-1 y la regulación de la expresión de VEGF, que promueve la angiogénesis adventicia. Todo ello provoca la desestabilización de la placa aterosclerótica y una alteración en el balance fibrinolítico (Sata *et al.* 2010).

En concreto, se ha demostrado que la Ang-II promueve importantes alteraciones estructurales y funcionales mediante la activación de distintos procesos celulares, especialmente en las células de la musculatura lisa vascular y las células endoteliales (Piqueras *et al.* 2000, Alvarez *et al.* 2001, Brasier *et al.* 2002, Volpe *et al.* 2002, Alcazar *et al.* 2003, Alvarez *et al.* 2004, Watanabe *et al.* 2005, Mateo *et al.* 2006, Abu Nabah *et al.* 2007, Mateo *et al.* 2007). De este modo, la Ang-II es un potente modulador del proceso aterogénico, induciendo la producción de quimiocinas, citocinas inflamatorias y especies reactivas del oxígeno, así como un aumento en la expresión de distintas MAC (Piqueras *et al.* 2000, Alvarez *et al.* 2001, Brasier *et al.* 2002, Alvarez *et al.* 2004, Mateo *et al.* 2006, Mateo *et al.* 2007, Rius *et al.* 2013b).

Durante muchos años, se han empleado los moduladores del SRA esencialmente para controlar la hipertensión en un contexto clínico. No obstante, se ha demostrado recientemente que estos moduladores tienen otras propiedades pleiotrópicas independientes de sus efectos antihipertensivos, por ejemplo como potenciadores de la cognición (Jackson *et al.* 2018).

1.4.3 Caracterización de los receptores de la Ang-II

Las acciones desempeñadas por la Ang-II son mediadas principalmente por los receptores de angiotensina de tipo 1 (AT_1) y de tipo 2 (AT_2), los cuales pertenecen a la familia de receptores acoplados a proteínas G (de Kloet 2017). Los receptores AT_1 están distribuidos en numerosos tejidos adultos como el sistema cardiovascular, los riñones, las glándulas suprarrenales, el hígado, el cerebro y los pulmones (Ellis *et al.* 2012, Jackson *et al.* 2018). Dentro del sistema cardiovascular, en los vasos sanguíneos, los receptores AT_1 se encuentran principalmente en las células de la musculatura lisa vascular, en las células endoteliales y en la adventicia (Nehme *et al.* 2017). También se expresan en los leucocitos circulantes, principalmente en monocitos y polimorfonucleares (Rasini *et al.* 2006). Por su parte, los

receptores AT_2 se expresan durante la vida fetal y en determinadas zonas del cerebro y del riñón en el adulto (Sumners *et al.* 2015, de Kloet 2017).

1.4.3.1 Efectos mediados por los receptores AT_1 y AT_2

El receptor AT_1 promueve diversas vías de señalización intracelular que resultan en una vasoconstricción generalizada, especialmente pronunciada en las arteriolas eferentes de los glomérulos renales, disfunción endotelial, un aumento de la liberación de noradrenalina, potenciando los efectos simpáticos; la estimulación de la reabsorción tubular proximal de Na^+, la secreción de aldosterona en la corteza suprarrenal y el crecimiento celular en el corazón y las arterias (Kawai *et al.* 2017, Eguchi *et al.* 2018). La Ang-II, a través de la estimulación del receptor AT_1, media múltiples funciones cardiovasculares, metabólicas y de comportamiento, incluida la respuesta a distintos factores de estrés. Además, a través de la interacción con su receptor AT_1, induce la adhesión al endotelio de monocitos y neutrófilos mediante el aumento de la expresión de E-selectina, P-selectina, ICAM-1, y VCAM-1 en células endoteliales (Grafe *et al.*, 1997, Piqueras 2000, Alvarez 2004). Posteriormente se detectó que también era capaz de inducir la síntesis y generación de quimiocinas tanto solubles como asociadas a membrana capaces de intervenir en el reclutamiento leucocitario (Mateo 2006, Naim Abu Nabah 2004, Naim Abu Nabah 2007, Rius eta al 2013b). En estudios posteriores, se constató que en las arterias, la expresión de TNFα era necesaria para promover la adhesión selectiva de células mononucleares inducida por Ang-II (Mateo *et al.* 2007, Rius *et al.* 2013b). Profundizando en las principales rutas de señalización que conducen a la adhesión de leucocitos mononucleares inducida por esta hormona peptídica, se describió que el aumento vascular de los niveles de especies reactivas del oxígeno a través de Nox5 provocaba la activación de RhoA y diversas rutas de señalización redox-sensibles (Alvarez & Sanz 2001, Rius et al 2013b, Escudero et al 2015). De hecho, la activación de RhoA regula la de miembros de la familia de las MAPK, tales como la p38-MAPK y ERK1/2 siendo capaz la primera de modular la transcripción de varios genes a través de la transactivación del factor NF-κB (Rius et al 2010, Rius et al. 2013b, Escudero et al 2015).

Los efectos cardiovasculares de los receptores AT_2 son opuestos en cierta medida a los de los receptores AT_1. El receptor AT_2 está sobreexpresado en lesiones ateroscleróticas, proporcionando una protección endógena a procesos inflamatorios, oxidativos y apoptóticos.

Los efectos beneficiosos mediados por el receptor AT_2 pueden potenciarse aún más mediante la intervención farmacológica empleando alguno de sus agonistas selectivos, recientemente desarrollados (Kaschina *et al.* 2017). Además, se ha descrito la existencia de receptores diferentes a los anteriores, como AT_3, AT_4 y otros, que no han sido completamente caracterizados; algunos de ellos son específicos para los metabolitos activos de la Ang-II (Singh *et al.* 2016).

Actualmente, en terapéutica, se emplean fármacos que impiden la síntesis de la Ang-II mediante la inhibición de la ECA (Ouwerkerk *et al.* 2017); así como el uso de antagonistas específicos del receptor AT_1, como el losartán (Sellers *et al.* 2018), o los inhibidores de renina como el aliskiren (Pantzaris *et al.* 2017).

1.4.4 Aneurisma aórtico abdominal

El aneurisma aórtico abdominal (AAA) es la forma más común de aneurisma en la aorta (Davis *et al.* 2015a). Es una enfermedad degenerativa vascular caracterizada por una progresiva dilatación localizada en el tramo abdominal, concretamente en la región infrarrenal, de más del 50% de su tamaño original, de las tres capas de la pared del vaso (íntima, media y adventicia) y su posterior rotura (Davis *et al.* 2015a). Es difícil estimar la incidencia anual pero, en diversos estudios realizados en países occidentales, se ha concluido que la incidencia media de nuevos casos de AAA es de 7,5 por cada 1.000 personas al año (Reite *et al.* 2015).

Aunque algunos trabajos indican que la incidencia del AAA está disminuyendo (Anjum *et al.* 2012), actualmente sigue siendo una importante causa de muerte, especialmente en varones mayores de 50 años donde la prevalencia llega al 5%, aumentándose hasta el 10% cuando se superan los 65 años de edad (Rouchaud *et al.* 2016). Esta prevalencia aumenta de forma paralela al incremento de la esperanza de vida y la disminución de la mortalidad por enfermedades cardiovasculares (Riambau *et al.* 2007). Además de la edad y el sexo masculino, algunos de los factores de riesgo asociados a esta patología son las hipertensión arterial, la hipercolesterolemia, la presencia de enfermedades cardiovasculares como aterosclerosis, la existencia de antecedentes familiares donde se hayan producido fallecimientos o intervenciones por AAA y, especialmente, el tabaquismo

(Michel *et al.* 2011, Davis *et al.* 2015b). El tabaco y la hipertensión además, pueden aumentar el riesgo de ruptura (Howard *et al.* 2015).

El AAA puede ser detectado mediante técnicas de imagen no invasivas (Ruff *et al.* 2016); sin embargo, la falta de conocimientos sobre los mecanismos bioquímicos y celulares responsables de la iniciación, propagación y ruptura del AAA han hecho que, actualmente, no haya un tratamiento farmacológico que permita prevenir el progreso de la enfermedad; al ser asintomática, los diagnósticos en estadios tempranos se ven dificultados (Soto *et al.* 2017). La ecografía abdominal es la técnica de elección para la detección del AAA debido a su alta sensibilidad y especificidad, así como a su seguridad y coste relativamente bajo. La intervención clínica de la misma está limitada a la reparación quirúrgica, que conlleva un riesgo significativo de mortalidad y morbilidad, y no está indicada en pacientes con un AAA pequeño o asintomático (Davis *et al.* 2015b).

La mayoría de los AAA son asintomáticos y se detectan como hallazgos incidentales en la ecografía, la tomografía computarizada abdominal o la resonancia magnética realizada para otros fines. También puede presentarse con dolor abdominal o complicaciones como trombosis, embolización y ruptura. Muchos de los AAA asintomáticos se descubren como una masa abdominal pulsátil en el examen físico de rutina (Reis *et al.* 2017).

Por otro lado, el riesgo de rotura del AAA es la principal causa de muerte, y se asocia con una mortalidad global de entre el 80-90%; sin embargo, si logra detectarse a tiempo, ésta se reduce hasta el 2-6% tras la cirugía reparadora (Davis *et al.* 2015b, Howard *et al.* 2015). La mortalidad se ve aumentada de manera exponencial con el tamaño del AAA (Vijaynagar *et al.* 2013).

En los últimos años, se ha comprobado que la angiogénesis asociada al AAA, así como la expresión de quimiocinas proangiogénicas y metaloproteasas, están asociadas con un mayor riesgo de rotura y complicaciones del mismo (Sano *et al.* 2014, Escudero *et al.* 2015b, Martorell *et al.* 2016). Son características patológicas del AAA la inflamación crónica vascular de la pared aórtica, la degradación progresiva de la matriz extracelular y el incremento de la neovascularización (**Figura 11**) (Davis *et al.* 2015b, Hu *et al.* 2017). Hoy en día se sabe que los procesos inflamatorios contribuyen decisivamente a la degradación de

la matriz extracelular que deriva, a través del remodelado expansivo y el agrandamiento compensatorio, en el AAA (Libby *et al.* 2015).

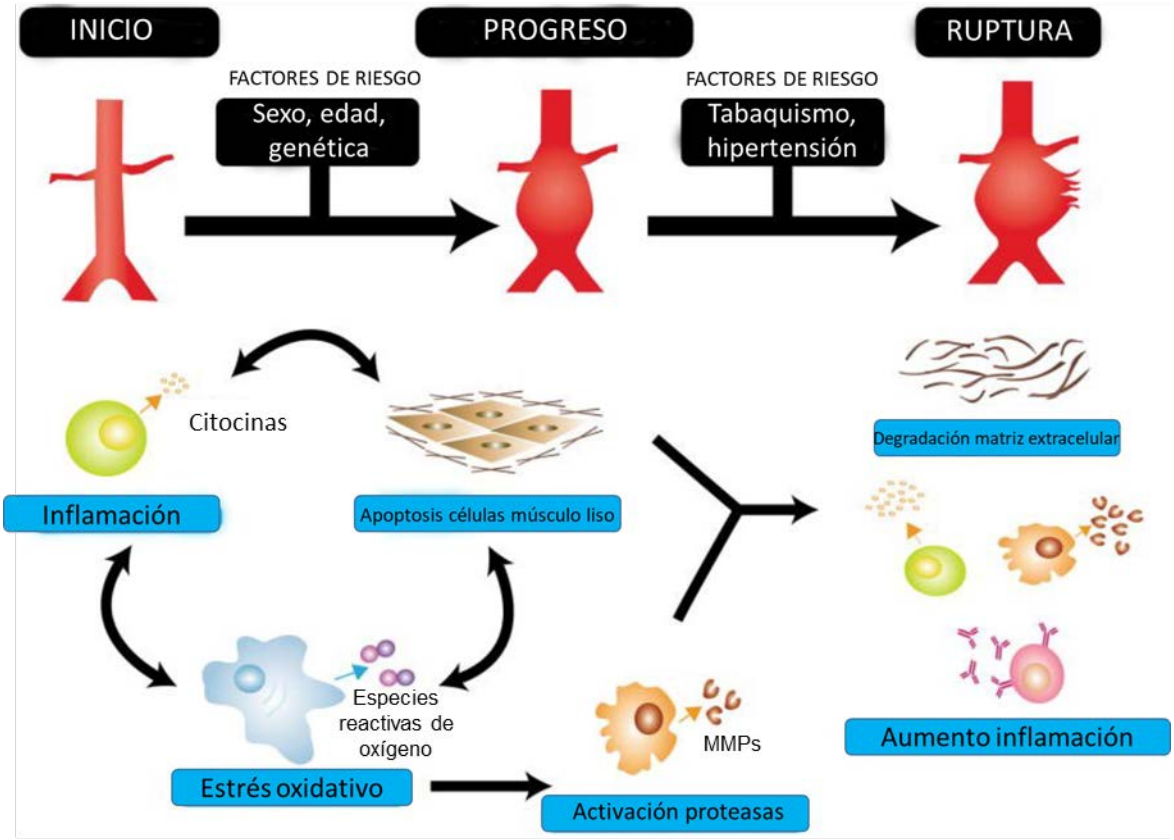

Figura 11. Esquema resumen de la patogenia del AAA. Se han identificado varios procesos biológicos y factores de riesgo que contribuyen a la patogénesis de AAA. Adaptado de Hu *et al.* 2017.

1.4.4.1 AAA y el sistema renina-angiotensina

Como se ha comentado anteriormente, la Ang-II es el principal péptido efector del SRA. Esta vía es importante en diferentes patologías cardiacas y se ha visto involucrada en la angiogénesis y el crecimiento vascular patológico (Willis *et al.* 2011). De hecho, un desajuste en este sistema ha sido asociado con la patogénesis del AAA (Malekzadeh *et al.* 2013).

Por otra parte, el SRA juega un papel importante en el inicio y la progresión de las enfermedades cardiovasculares y renales (Kaschina *et al.* 2017). Así, muchas enfermedades cardiovasculares presentan una hiperactivación del SRA, un mecanismo fisiopatológico

importante que ha sido propuesto como diana terapéutica. De este modo, la estimulación excesiva de los receptores AT_1 produce crecimiento celular, estrés oxidativo e inflamación vascular, lo que puede conducir a una rigidez arterial y a acelerar el envejecimiento vascular. Al mismo tiempo, durante las últimas décadas se ha descrito el eje vasoprotector del SRA, a cuyos componentes se les han atribuido propiedades antioxidantes y anti-inflamatorias, promotoras de la vasodilatación y la concentración de sodio en la orina (natriuresis) y reductoras de la deposición de colágeno, atenuando de este modo la rigidez arterial y mejorando la función del endotelio. Actualmente, estos efectos se han adscrito a la acción del péptido Ang (1-7) generado por la enzima ECA-2 y su interacción con el receptor Mas, ya que pueden contrarrestar los efectos nocivos del eje Ang-II/AT_1. Una función importante que desempeña la ECA-2 es metabolizar Ang-I y la Ang-II para dar lugar a la formación del péptido Ang (1-7), disminuyendo de esta manera los niveles de Ang-II, tanto a nivel tisular como en sangre (Neves *et al.* 2018).

1.4.4.2 Angiogénesis

La angiogénesis es el proceso de formación de nuevos vasos sanguíneos a partir de la vasculatura ya existente. Este proceso es imprescindible en situaciones fisiológicas como el desarrollo embrionario, la reparación tisular y la curación de heridas. Los capilares son esenciales para el intercambio de nutrientes y metabolitos en los distintos tejidos, y por tanto, cambios en la actividad metabólica, producen cambios en la angiogénesis (Adair *et al.* 2010, Zhao *et al.* 2015).

El estudio sistemático de la angiogénesis se estableció a principios de la década de 1970, cuando Folkman estableció la hipótesis de que el crecimiento de los tumores era dependiente de este proceso (Folkman 1971). Igualmente, la angiogénesis tiene importancia en el contexto de las enfermedades cardiovasculares (Huang *et al.* 2014) y, en especial, en el desarrollo del AAA (Sano *et al.* 2014, Futami *et al.* 2015), en el cual se ha observado un aumento de determinadas citocinas proangiogénicas y una mayor neovascularización en la zona de ruptura (Escudero *et al.* 2015b, Martorell *et al.* 2016).

La inflamación y el ambiente de hipoxia son estímulos potenciales en el desarrollo de la angiogénesis. Se produce un influjo de macrófagos, la liberación de MMPs y la consiguiente migración de células endoteliales (Adair *et al.* 2010) y, por tanto, contribuye al

proceso de degradación de la pared del AAA (Futami *et al.* 2015). En el contexto de proliferación celular, los estímulos angiogénicos son factores de crecimiento y citocinas, especialmente VEGF, TGF-α y β, las angiopoyetinas, el factor de crecimiento epidermal y el factor de crecimiento de fibroblastos. Además de estos factores, las quimiocinas angiogénicas juegan un papel fundamental en el proceso (Yoo *et al.* 2013, Martorell *et al.* 2016).

Los acontecimientos que ocurren durante la angiogénesis se detallan en la **Figura 12** (Yoo *et al.* 2013).

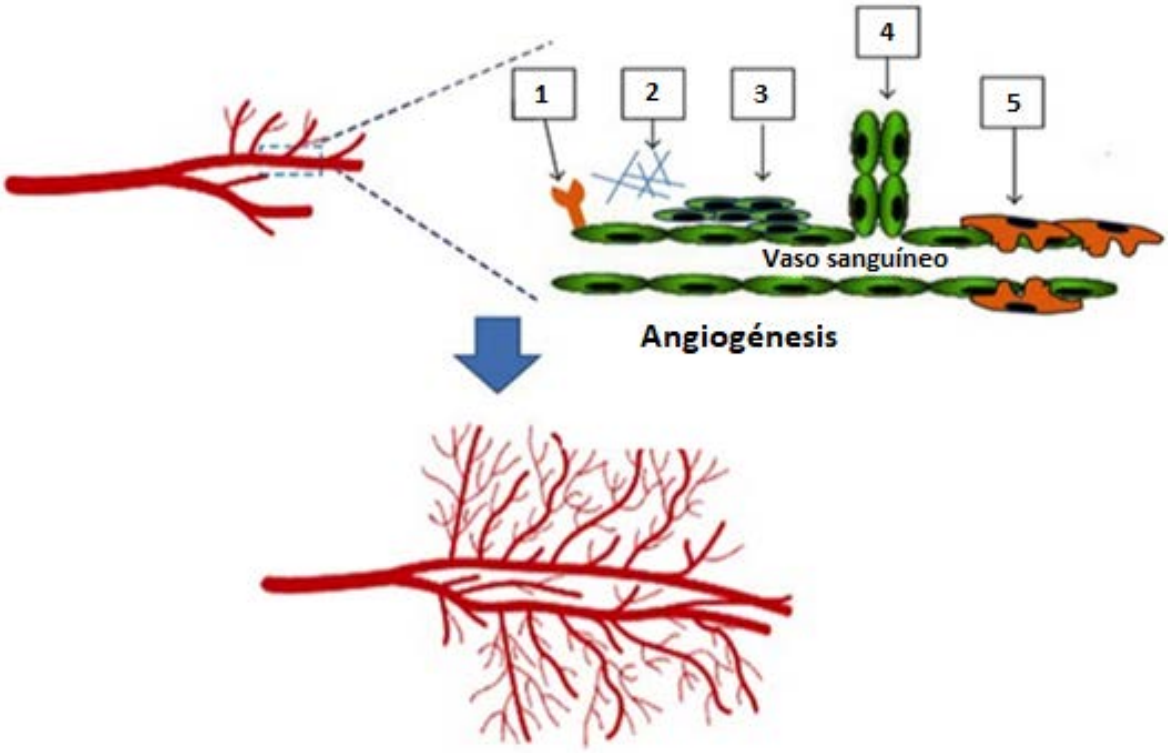

Figura 12. Etapas que intervienen en el proceso de angiogénesis. El proceso comienza con la unión de factores proangiogénicos como VEGF y el factor de crecimiento de fibroblastos al endotelio vascular activado (**1**). A continuación, comienza la degradación local de la matriz extracelular del vaso por la acción de las MMPs (**2**), favoreciendo la proliferación y migración en la dirección del estímulo de las células endoteliales del vaso (**3**). Posteriormente se produce la formación, elongación y reestructuración del nuevo vaso sanguíneo por la acción de las integrinas (**4**). Finalmente, se produce la estabilización del vaso disponiéndose la matriz en torno a los nuevos capilares (**5**). Adaptado de Yoo *et al.* 2013.

1.4.4.2.1 Quimiocinas implicadas en el control de la angiogénesis

Los miembros de la subfamilia C-X-C de quimiocinas tienen un papel importante tanto en la angiogénesis fisiológica como en la patológica, incluyendo la inflamación crónica (Mehrad *et al.* 2007). La familia C-X-C se caracteriza por su capacidad de comportarse de manera dispar en la regulación de la angiogénesis. El extremo N-terminal de la mayoría de estas quimiocinas contiene el denominado motivo ELR, con tres residuos característicos de aminoácidos: glutamina, leucina y arginina. Las quimiocinas que contienen este motivo son potentes promotores de la angiogénesis (Santoni *et al.* 2014). Dentro de esta familia cabe destacar los receptores CXCR1, cuyos únicos ligandos son IL-8/CXCL8 y CXCL6; y CXCR2, el receptor más angiogénico, al cual se unen el resto de quimiocinas que expresan el motivo ELR (Mehrad *et al.* 2007). Por contra, miembros de la subfamilia C-X-C que son inducibles por IFNγ y sin motivo ELR, suelen ser inhibidores de la angiogénesis (Santoni *et al.* 2014).

Además de la familia C-X-C, también es relevante la subfamilia C-C en este contexto, donde destacan fundamentalmente las quimiocinas RANTES/CCL5 y MCP-1/CCL2, que han sido implicadas en la angiogénesis. Se sabe que promueven indirectamente este proceso reclutando primero macrófagos al sitio de la inflamación o lesión, donde luego liberan citocinas proinflamatorias y factores de crecimiento que conducen a la formación de neovasos (Ridiandries *et al.* 2016).

1.4.4.2.1.1 CXCL16

La quimiocina CXCL16 es una glicoproteína transmembrana de pequeño tamaño (30 kDa) que pertenece a la familia C-X-C de las quimiocinas. Está constituida por 254 aminoácidos y estructuralmente está formada por cuatro dominios: un dominio quimiocina C-X-C, un dominio brazo tipo mucina, un dominio transmembrana y un dominio citoplasmático formado por una cola corta citoplasmática que contiene una tirosina potencialmente fosforilable (**Figura 13**) (Ludwig *et al.* 2007, Izquierdo *et al.* 2014).

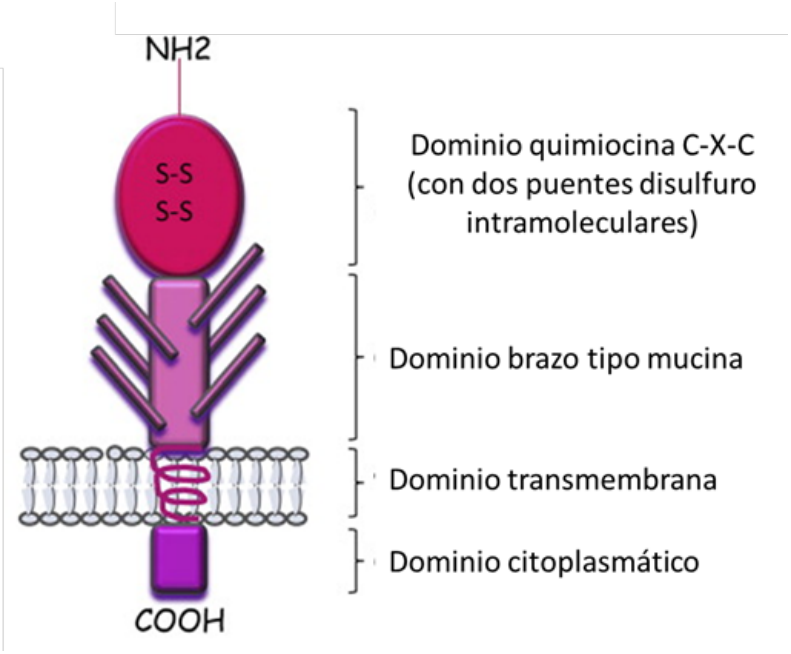

Figura 13. Representación esquemática de la estructura de la quimiocina CXCL16. La quimiocina CXCL16 es una molécula transmembrana que presenta varios dominios. Adaptado de Izquierdo *et al.* 2014.

La quimiocina CXCL16 interactúa con el receptor CXCR6, también conocido como Bonzo, STRL33 ó TYMSTR (Matloubian *et al.* 2000, Wilbanks *et al.* 2002). La fractalquina (CX_3CL1) y CXCL16 son las únicas quimiocinas con un comportamiento dual, ya que se expresan tanto unidas a la membrana celular como en forma soluble y comportándose como moléculas quimioatrayentes de diferentes poblaciones leucocitarias tras una ruptura proteolítica, por medio de la acción de dos proteasas con dominio metaloproteasa y desintegrina (ADAM), denominadas ADAM10 y ADAM17, también conocida como TACE (enzima convertidora de TNFα) (Ludwig *et al.* 2005, Schulte *et al.* 2007). Dichas proteasas están implicadas en numerosos procesos de ruptura proteolítica o *shedding*, y son las encargadas de llevar a cabo la acción enzimática que permite la conversión de la molécula transmembrana en un mediador soluble (Ludwig *et al.* 2005). ADAM10 es la encargada de llevar a cabo la escisión de CXCL16 de manera tanto constitutiva como inducible (Abel *et al.* 2004, Gough *et al.* 2004, Hundhausen *et al.* 2007), mientras que ADAM17 únicamente lo hace de manera inducida (Ludwig *et al.* 2005).

1.4.4.2.1.1.1 Expresión de CXCL16

La quimiocina CXCL16 se expresa tanto en el endotelio como en la musculatura lisa vascular, así como en los macrófagos, los linfocitos T y B, las células dendríticas y las plaquetas (Ludwig *et al.* 2007, Borst *et al.* 2012, Izquierdo *et al.* 2014, Marques *et al.* 2017). Además, su expresión es inducida por diversas citocinas proinflamatorias como TNFα e IFNγ (Wente *et al.* 2008, Marques *et al.* 2017).

1.4.4.2.1.1.2 Funciones de CXCL16

Las funciones de CXCL16 son diversas, tanto más en cuanto a su naturaleza dual. La forma soluble de CXCL16 actúa como factor quimiotáctico e induce la quimiotaxis de linfocitos T activados, como linfocitos $CD4^+$, Th1 y un subconjunto de linfocitos T $CD8^+$ (Tc1) al área de infección, así como células plasmáticas de la médula ósea por medio de la interacción con su receptor CXCR6 (Abel *et al.* 2004, Wuttge *et al.* 2004). Al mismo tiempo, promueve la proliferación de células vasculares (Lehrke *et al.* 2007), está implicada en la regulación de la angiogénesis (Wente *et al.* 2008, Isozaki *et al.* 2013, Yu *et al.* 2016), así como la transcripción de diferentes genes proinflamatorios (Chandrasekar *et al.* 2004, Zhuge *et al.* 2005).

Por el contrario, cuando CXCL16 se encuentra unida a membrana actúa como MAC atrayendo al endotelio leucocitos que expresan el receptor CXCR6, fundamentalmente linfocitos T, linfocitos NKT y monocitos (Abel *et al.* 2004, Shimaoka *et al.* 2004, Lehrke *et al.* 2007, Hofnagel *et al.* 2011). Además, puede actuar como receptor *scavenger* o "basurero" permitiendo la internalización de fosfatidilserina, bacterias y LDLox, facilitando con ello la formación de células espumosas durante el proceso aterosclerótico (**Figura 14**) (Wuttge *et al.* 2004, Lehrke *et al.* 2007, Izquierdo *et al.* 2014).

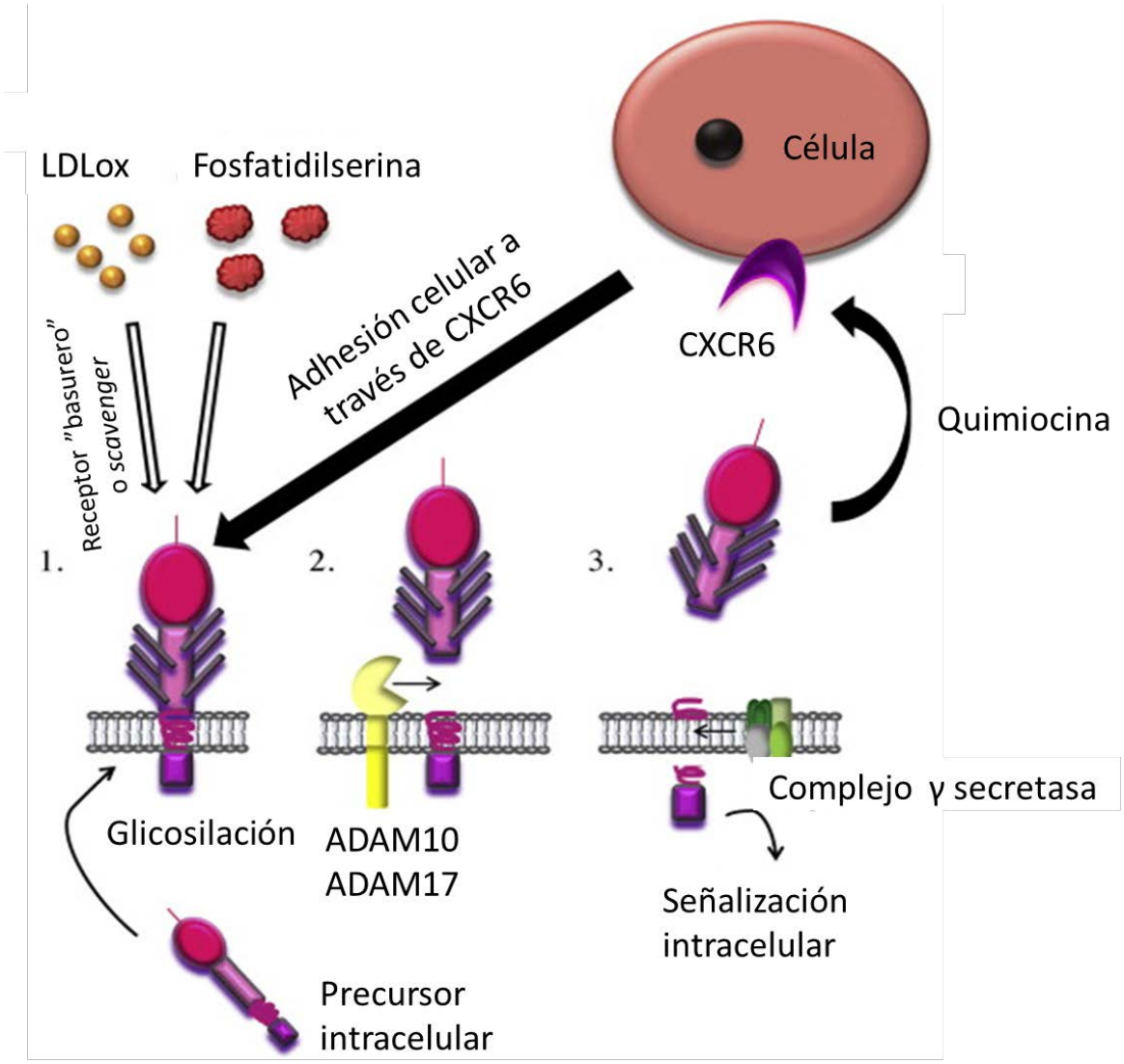

Figura 14. Representación esquemática de las funciones desempeñadas por la quimiocina CXCL16. Cuando la quimiocina CXCL16 se encuentra unida a membrana, actúa como receptor "basurero" o *scavenger* para permitir la captación de fosfatidilserina así como de LDLox (**1**). La escisión enzimática es debida a la actividad de las proteasas con dominio metaloproteasa y desintegrina, ADAM10 y ADAM17; cerca de la membrana celular se produce la liberación del ectodominio compuesto por el tallo tipo mucina y el dominio quimiocina (**2**). La secretasa γ rompe el dominio C-terminal, liberando así la parte soluble de CXCL16, actuando como quimioatrayente de células $CXCR6^{+}$ (**3**). Adaptado de Izquierdo *et al.* 2014.

1.4.4.2.1.1.3 CXCL16 en las enfermedades cardiovasculares

La quimiocina CXCL16 es capaz de atraer y promover la adhesión firme de linfocitos y monocitos al endotelio vascular, por lo que se considera que desempeña un papel fundamental en la inflamación vascular (Wuttge *et al.* 2004).

Por otro lado, se ha observado que algunos polimorfismos en el gen codificante de CXCL16 están asociados con la severidad de la enfermedad de las arterias coronarias (Lehrke *et al.* 2007). Además, estudios en pacientes han demostrados niveles séricos elevados de esta quimiocina en enfermedades cardiovasculares como las patologías arteriales crónicas y los síndromes coronarios agudos. Por ello, es considerada como un buen marcador de enfermedad inflamatoria y aterosclerosis (Izquierdo *et al.* 2014).

Sin embargo, existe cierta controversia acerca de su papel en el desarrollo de la aterosclerosis. En ratones deficientes en CXCL16 y LDLR, se ha observado una aceleración del proceso aterosclerótico, debido a la pérdida de función de la quimiocina CXCL16 como receptor basurero (Aslanian *et al.* 2006). Por el contrario, se ha detectado esta quimiocina en lesiones ateroscleróticas humanas tras endarterectomía y en ratones apoE$^{-/-}$ sometidos a una dieta hipercolesterolémica (Ludwig *et al.* 2007). También, se ha demostrado la expresión de CXCL16 en plaquetas y la modulación de las mismas bajo ciertos estímulos, incluyendo su activación y su adhesión a otros tipos celulares a través de la activación de su receptor CXCR6 (Seizer *et al.* 2011, Borst *et al.* 2012). Igualmente, se ha podido comprobar que CXCL16 participa en el proceso aterosclerótico mediante la regulación de la respuesta inflamatoria, el metabolismo lipídico y la aceleración de la vulnerabilidad de la placa (Xing *et al.* 2018).

En conjunto, estas evidencias sugieren un papel relevante de la quimiocina CXCL16 en la inflamación vascular y, particularmente, en diversos procesos ateroscleróticos.

2. OBJECTIVES

1. One of the earliest stages of atherogenesis is endothelial dysfunction, a proinflammatory and pro-thrombotic phenotype of the endothelium that leads to platelet activation and the adhesion and subsequent migration of leukocytes to the subendothelial space (Landmesser *et al.* 2004). Since primary hypercholesterolemia (PH) is associated with a higher risk of suffering further cardiovascular diseases and a low-grade of systemic inflammation seems to be involved in this response, **the first objective** of this thesis was to characterize the systemic inflammation associated to PH. More precisely, the study of the activation state of platelets and leukocytes, the presence of platelet-leukocyte aggregates, the detection of soluble inflammatory mediators and their functional consequences were evaluated in PH patients and age-matched controls.

2. Once established the previous study **the second objective** of this thesis was to evaluate the effect of an oral fat load (OFL) with a commercial preparation of long-chain triglycerides (the ω6/ω3 ratio is >20/1) on different immune parameters and its potential beneficial consequences 4 h after its administration to PH patients.

3. In this line, **the third objective** of this thesis was to characterize the role of CCL11/CCR3 axis in the systemic inflammation associated with PH and its involvement in the atherosclerotic lesion development. For this purpose, mice deficient in apolipoprotein E ($apoE^{-/-}$) and CCR3 receptor ($apoE^{-/-}CCR3^{-/-}$) were generated and studied.

4. Finally, angiotensin-II (Ang-II) is the main effector peptide of the renin-angiotensin system (RAS) and promotes leukocyte adhesion to the stimulated endothelium. Because RAS activation and Ang-II signaling are implicated in the abdominal aortic aneurysm (AAA), **the fourth objective** of this thesis was to investigate the possible involvement of CXCL16/CXCR6 axis in Ang-II-induced AAA formation.

3. MATERIAL AND METHODS

3.1 STUDIES IN PATIENTS WITH PRIMARY HYPERCHOLESTEROLEMIA (PH) AND AGE-MATCHED CONTROLS

The subsequent studies were performed following the principles outlined in the Declaration of Helsinki for the use of human subjects. The Clinical Research Ethics Committee of the University Clinic Hospital of Valencia, Spain, approved the protocol for these studies. All subjects signed the appropriate written informed consent to take part in the study.

3.1.1 Inclusion and exclusion criteria

A total of 43 subjects (22 PH patients and 21 age-matched control volunteers without PH) were recruited by the Endocrinology Unit of the University Clinic Hospital of Valencia, Spain, and included in the present thesis.

The enrolled subjects had to comply with a series of requirements to be considered for the study: diagnostic criteria for patients, inclusion criteria for healthy individuals and exclusion criteria for both groups. All of them are described in **Table 5**.

Table 5. Diagnostic, inclusion and exclusion criteria for participation in the study (Collado *et al.* 2018a).

Diagnostic criteria (PH patients)	**Inclusion criteria (Age-matched controls)**	**Exclusion criteria (Both groups)**
TC >260 mg/dL and/or LDL >160 mg/dL	TC <200 mg/dL and apoB <120 mg/dL	CVDs, hypertension, diabetes, chronic diseases or cancer
TG <150 mg/dL	TG <150 mg/dL	Smoking Alcohol consume >30 g/day
Genetic testing for *APOE* (Genotype E3/E3)	Fasting plasma glucose <100 mg/dL	Renal or hepatic insufficiency and hypothyroidism
	The absence of dyslipidemia, CVDs or diabetes	Pregnancy or lactation
	Genetic testing for *APOE* (Genotype E3/E3)	Infection, inflammatory disease (including asthma, allergy, and autoimmune deficiency) or drugs able to alter inflammation six weeks before the study

3.1.2 Determination of clinical and biochemical parameters

The study started at 8:30 a.m., and blood was withdrawn by venipuncture after a fasting period of at least 12 hours. Anthropometric parameters and blood pressure were measured using standardized procedures: body mass index (BMI; kg/m^2), waist circumference (midpoint between the edge lower rib and iliac crest; cm) and blood pressure (mmHg). For analysis, whole blood samples were either heparinized or withdrawn in ethylenediaminetetraacetic acid (EDTA) or sodium citrate and subsequently subjected to different analytical determinations, including complete biochemistry with glycemic and lipid profile, and renal function through the quantification of creatinine levels.

3.1.3 Oral fat load (OFL) test

After the first blood sampling (time 0; T0), patients with PH ingested a commercial liquid preparation of 50 g of a high-fat meal per m^2 of body surface prepared with a commercial long-chain triglycerides (TG) liquid preparation (Supracal®; SHS International, Liverpool, UK). Each 100 mL of the formula contained 50 g of fat (450 kcal), of which 9.6 g were saturated, 28.2 g monounsaturated and 10 g polyunsaturated, with a ω6/ω3 ratio >20/1. Fatty acid content and the complete composition can be obtained from SHS International, Nutricia website.

Patients were only allowed to drink water throughout the study. Four hours later, another blood sample was taken from every PH patient (time 4; T4).

3.1.4 Human *in vitro* cell culture studies

3.1.4.1 Isolation of human endothelial cells

Human umbilical arterial endothelial cells (HUAEC) were isolated from human umbilical cords obtained from the Gynecology and Obstetrician Unit of the University Clinic Hospital of Valencia, Spain. Most importantly, no more than 12 hours had elapsed since childbirth in all cases. Relatives of neonates signed the corresponding written informed consent.

Cells were isolated by collagenase treatment as explained elsewhere (Jaffe *et al.* 1973) and maintained in human endothelial cell basal medium-2 (EBM-2; Lonza Group,

Basel, Switzerland) supplemented with endothelial growth medium-2 (EGM-2; Lonza Group) including 10% fetal bovine serum (FBS; Biowest, Nuaillé, France). Cells were grown to confluence up to passage 1 to preserve endothelial features. Before every experiment, cells were incubated for 24 h in medium containing 2% FBS.

3.1.4.2 Leukocyte-endothelial cell interactions under flow conditions

The flow chamber procedure allows the visualization of cell adhesion under dynamic flow conditions, mimicking the physiological milieu. As shown in **Figure 15**, the parallel flow chamber system consists of a base plate with an entrance and an exit port through which media and cells are perfused. Coupled to this base plate, there are a vacuum pump and a gasket. At the base plate, there is a 35 mm diameter culture plate, on which the endothelial cell monolayer is grown. As a result, a flow channel is generated over the endothelial monolayer, with the infusion rate being regulated by a suction pump, thus emulating the blood flow over the human endothelium.

To measure leukocyte adhesion, HUAEC were seeded on 35 mm diameter pre-treated culture plates. Once confluence was reached, and after the correspondent addition of the different stimuli, the plates were placed in the parallel flow chamber (GlycoTech, Gaithersburg, MD).

The GlycoTech flow chamber was assembled and placed onto an inverted microscope stage, and the diluted whole blood was then perfused over the HUAEC monolayers. Leukocyte adhesion was determined after 7 min at 0.5 dyn/cm^2. Those cells which interacted with the surface of the endothelium were visualized and recorded (x20 objective, x10 eyepiece) using an inverted microscope (Axio Observer A1; ZEISS International, Oberkochen, Germany). At least five fields were recorded for 10 seconds each. Finally, images were recorded and saved on a computer for further analyses.

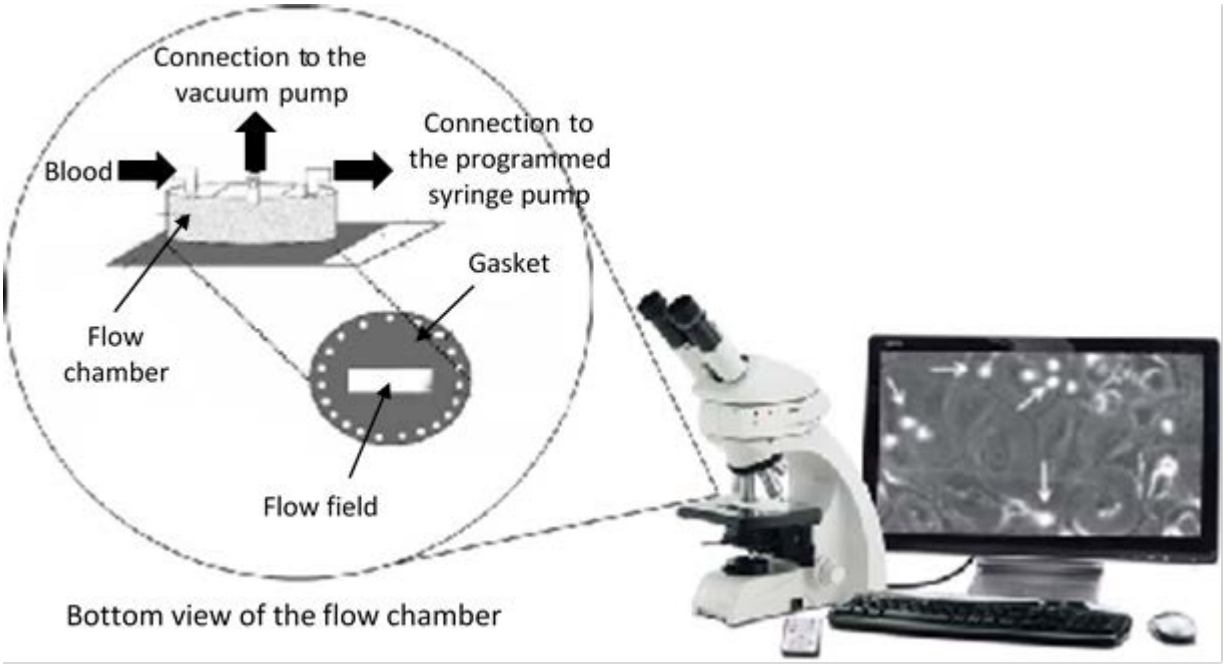

Figure 15. Parallel flow chamber system.

3.1.4.2.1 Flow chamber experimental protocols

Before starting each assay, Hank's balanced salt solution (HBSS; Lonza Group) tempered at 37ºC, was perfused to adjust the flow at a rate of 0.156 mL/min (corresponding to a shear stress of 0.5 dyn/cm^2). Whole blood from PH patients and age-matched controls was diluted 1:10 in HBSS and perfused over HUAEC monolayers, stimulated or not with 20 ng/mL of tumor necrosis factor α (TNFα; Sigma-Aldrich, St. Louis, MO) for 24 h. Experiments were carried out in heparinized whole blood incubated or not with EDTA (10 mM, for 15 min, 37ºC; PanReac AppliChem GmbH, Darmstadt, Germany) to evaluate the contribution of platelets to leukocyte adhesion (Postea *et al.* 2012).

3.1.5 Flow cytometry studies

3.1.5.1 Experimental protocols

Blood samples from PH patients and age-matched controls were taken and collected in BD Vacutainer® blood collection tubes (BD Biosciences, San Jose, CA) containing sodium citrate (3.2%), or in BD Vacutainer® PST™ II tubes with lithium/heparin as anticoagulant agents (17 IU/mL; BD Biosciences).

Primary antibodies conjugated with diverse fluorochromes (detailed in **Table 6**), were used to detect different cell surface markers. Heparinized or EDTA-treated whole blood was stained with saturated amounts of antibodies as indicated by the manufacturers. Then, the samples were gently shaken and incubated for 30 min at room temperature in the dark. Afterward, lysis buffer (BD FACS™ lysing solution 10x concentrate; BD Biosciences) was added to each tube to lyse red blood cells (RBCs). Subsequently, all samples were run in a FACSVerse™ flow cytometer (BD Biosciences) and data analyzed with FlowJo® v10.0.7 software (FlowJo LLC, Ashland, OR).

Table 6. Antibodies used for flow cytometry human experiments.

Antibody − Fluorochrome	Clone	Isotype	Manufacturer
CD41 – CF-Blue™	HIP8	IgG_1	IMMUNOSTEP
PAC-1 – FITC	PAC-1	Mouse IgM	BD Biosciences
P-selectin (CD62P) − APC	HI62P	IgG_1	IMMUNOSTEP
CD193 (CCR3) – PE	5E8	Mouse IgG_{2B}	BD Biosciences
CD45 − PB™	HI30	Mouse IgG_1	BioLegend
CD16 – FITC	3G8	Mouse IgG_1	BD Biosciences
CD41 – PE/Cy™7	HIP8	Mouse IgG_1	BioLegend
CD69 – PE	FN50	IgG_1	IMMUNOSTEP
CD3 – APC	33-2A3	Mouse IgG_{2A}	IMMUNOSTEP
CD14 − APC	47-3D6	Mouse IgG_{2A}	IMMUNOSTEP
CD16 – APC	3G8	Mouse IgG_1	IMMUNOSTEP
CD117 (c-kit) − BV421™	104D2	Mouse IgG_1	BioLegend
FcεRIα − FITC	CRA1	Mouse IgG_{2B}	MACS Miltenyi Biotec
CD11b − PerCP/Cy™5.5	ICRF44	Mouse IgG_1	BioLegend
CD192 (CCR2) − BV421™	K036C2	Mouse IgG_{2A}	BioLegend
CD11b − PE	CBRM1/5	Mouse IgG_1	BioLegend
CX_3CR1 − PE	2A9-1	Rat IgG_{2B}	BioLegend
CD4 − V450	RPA-T4	Mouse IgG_1	BD Biosciences

CD8 − FITC	SK1	Mouse IgG_1	BD Biosciences
CD4 – PerCP/Cy™5.5	RPA-T4	Mouse IgG_1	BD Biosciences
CD183 (CXCR3) – Alexa Fluor® 488	1C6/CXCR3	Mouse IgG_1	BD Biosciences
CD196 (CCR6) − BV421™	11A9	Mouse IgG_1	BD Biosciences
CD69 − APC	FN50	Mouse IgG_1	BD Biosciences
CD4 − FITC	SK3	Mouse IgG_1	BD Biosciences
CD127 − Alexa Fluor® 647	HIL-7R-M21	Mouse IgG_1	BD Biosciences
CD25 − PE/Cy™7	2A3	Mouse IgG_1	BD Biosciences

3.1.5.2 Platelet analysis

3.1.5.2.1 Measurement of platelet activation

Platelet activation is determined by PAC-1^+ platelets, an indicator of activated integrin $\alpha_{IIb}\beta_3$, and the expression of P-selectin (CD62P). Therefore, to assess platelet activation, PAC-1^+ platelets and P-selectin expression were measured in platelets from PH patients and age-matched controls by flow cytometry. Samples of citrated blood, diluted 1:10 in glucose buffer (1 mg/mL glucose in phosphate-buffered saline; PBS containing 0.35% of bovine serum albumin, BSA; Sigma-Aldrich) (Murugappa *et al.* 2006), were incubated in the dark for 30 min with a 5-carboxyfluorescein (CF)-Blue™-conjugated monoclonal antibody (mAb) against human CD41 (clone HIP8, IgG_1; IMMUNOSTEP, Salamanca, Spain) and a fluorescein isothiocyanate (FITC)-conjugated mouse mAb against human PAC-1 (clone PAC-1, IgM; BD Biosciences) or with an allophycocyanin (APC)-conjugated mAb against human P-selectin (CD62P, clone HI62P, IgG_1; IMMUNOSTEP).

Firstly, the identification of platelets was carried out determining their morphology according to size and complexity (side scatter, SSC *vs.* forward scatter, FSC). Then, they were selected as the $CD41^+$ population, according to the gating strategy illustrated in **Figure 16** and expressed as the percentage of positive platelets.

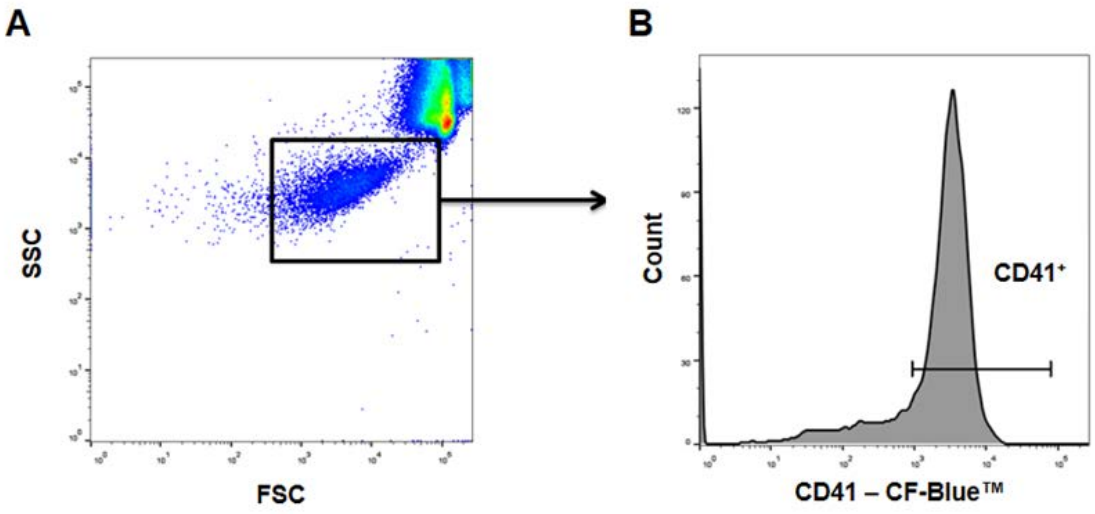

Figure 16. Gating strategy for human platelets in whole blood according to morphological properties and CD41 detection by flow cytometry. Platelets were gated according to a low side scatter (SSC) and forward scatter (FSC) in a logarithmic scale (**A**) and defined as $CD41^+$ population (**B**).

3.1.5.2.2 Determination of CCR3 expression in platelets

To determinate the expression of CCR3 on platelets' surface, citrated blood was incubated with a phycoerythrin (PE)-conjugated mouse mAb against human CD193 (CCR3, clone 5E8, IgG_{2B}; BD Biosciences) and a CF-Blue™-conjugated mAb against human CD41 (clone HIP8, IgG_1; IMMUNOSTEP). Samples were incubated for 30 min at room temperature in the dark. Then, morphology was determined with SSC *vs.* FSC that allowed the selection of the $CD41^+$ population and the determination of CCR3 expression. Platelets were selected according to the gating strategy illustrated before in **Figure 16** and expressed as the percentage of positive platelets.

3.1.5.3 Leukocyte subpopulations studies

3.1.5.3.1 Neutrophils and eosinophils

To assess the polymorphonuclear population present in blood samples, pacific blue (PB)™-conjugated mouse mAb against human CD45 (clone HI30, IgG_1; BioLegend, San Diego, CA) and a high SSC were combined to discard RBCs and select the neutrophil and eosinophil populations. These cells correspond to the subtypes with the highest granular

content. An analysis with a FITC-conjugated mouse mAb against human CD16 (clone 3G8, IgG_1; BD Biosciences) was first performed to distinguish them.

After the identification of the different neutrophil ($CD16^+$) and eosinophil ($CD16^-$) populations, the possible contribution of platelets was studied using two different experimental approaches. First, heparinized whole blood was analyzed to detect neutrophils and eosinophils attached to platelets. Second and in parallel, blood samples were incubated with 10 mM EDTA (PanReac AppliChem GmbH), for 15 min at 37ºC, to promote platelet dissociation as previously described (Postea *et al.* 2012). In both cases, a PE/Cy™7-conjugated mouse mAb against human CD41 (clone HIP8, IgG_1; BioLegend) was used to determine the granulocyte-platelet aggregates (**Figure 17**).

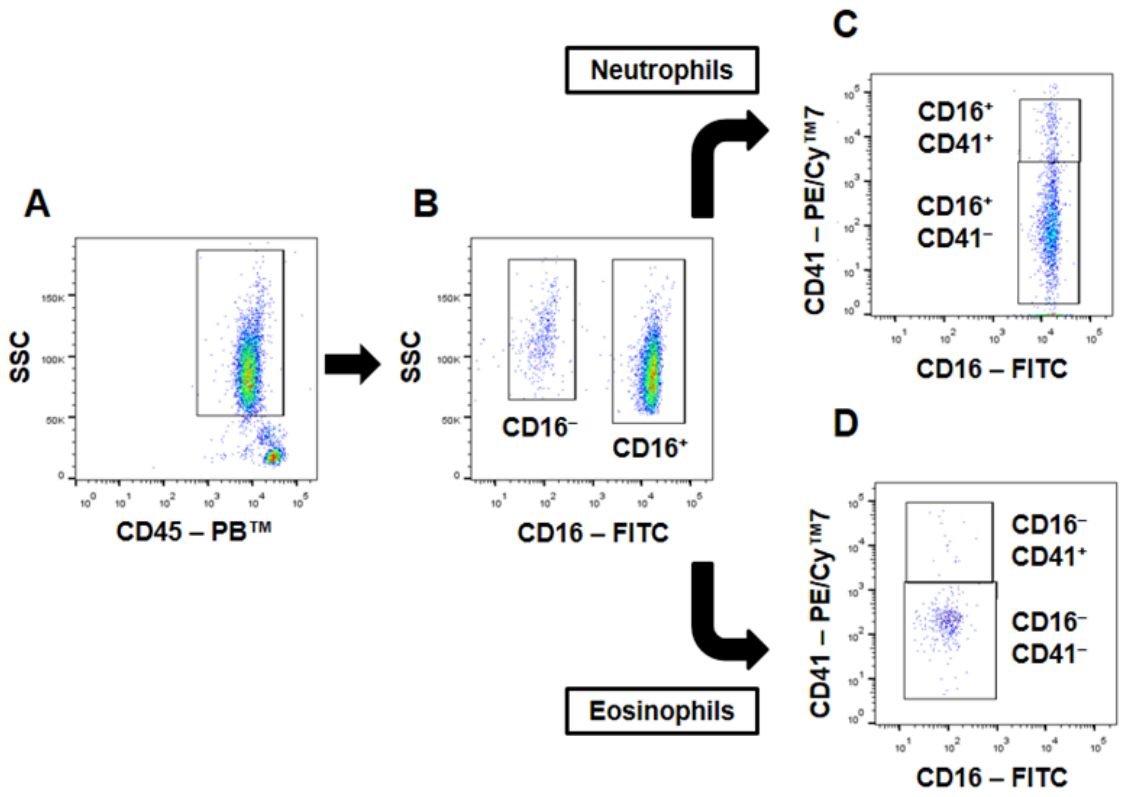

Figure 17. Gating strategy for human neutrophils and eosinophils in whole blood according to morphological properties and CD16 expression by flow cytometry. Populations were selected by CD45 labeling and morphology (high SSC; **A**). To differentiate cell populations, CD16 antibody was used, being neutrophils $CD16^+$ and eosinophils $CD16^-$ (**B**). In heparinized whole blood, neutrophil-platelet complexes were selected as $CD16^+CD41^+$ population from heparinized whole blood, and platelet-free neutrophils were gated as $CD16^+CD41^-$ from blood incubated with EDTA (**C**). Eosinophils bound to platelets in heparinized whole blood were selected as $CD16^-CD41^+$, whereas in samples treated with EDTA, platelet-depleted eosinophils were selected as $CD16^-CD41^-$ (**D**).

Subsequently, an analysis of the CCR3 receptor expression was performed using a PE-conjugated mouse mAb against human CCR3 (clone 5E8, IgG_{2B}; BD Biosciences) and determined the activation state in these cell populations with a PE-conjugated mAb against human CD69 (clone FN50, IgG_1; IMMUNOSTEP).

3.1.5.3.2 Progenitor mast cells and basophils

To determine progenitor mast cell and basophil populations, a mixture (negative lineage; LIN^-) composed of APC-conjugated mouse mAbs against human CD3 (clone 33-2A3, IgG_{2A}; IMMUNOSTEP), human CD14 (clone 47-3D6, IgG_{2A}; IMMUNOSTEP) and human CD16 (clone 3G8, IgG_1; IMMUNOSTEP) was used. The population with LIN^- corresponded to eosinophils, basophils and progenitor mast cells. A brilliant violet (BV)421™-conjugated mouse mAb against human CD117 (c-kit, clone 104D2, IgG_1; BioLegend), a FITC-conjugated mouse mAb against human high-affinity IgE receptor, (FcεRIα, clone CRA1, IgG_{2B}; MACS Miltenyi Biotec, Bergisch Gladbach, Germany), and a PerCP/Cy™5.5-conjugated mouse mAb against human integrin CD11b (clone ICRF44, IgG_1; BioLegend) were used to select only progenitor mast cells and basophils. Progenitor mast cell population correspond to $LIN^-CD11b^+c\text{-}kit^+Fc\varepsilon RI\alpha^+$ and basophil population to $LIN^-CD11b^+c\text{-}kit^-Fc\varepsilon RI\alpha^+$ (**Figure 18**).

The association of progenitor mast cells and basophils with platelets was studied using a PE/Cy™7-conjugated mouse mAb against human CD41 (clone HIP8, IgG_1; BioLegend) in heparinized whole blood incubated or not with EDTA. This was done to promote platelet dissociation as described before in **Section 3.1.5.3.1**. Expression analysis of the CCR3 receptor was carried out using a PE-conjugated mouse mAb against human CCR3 (clone 5E8, IgG_{2B}; BD Biosciences).

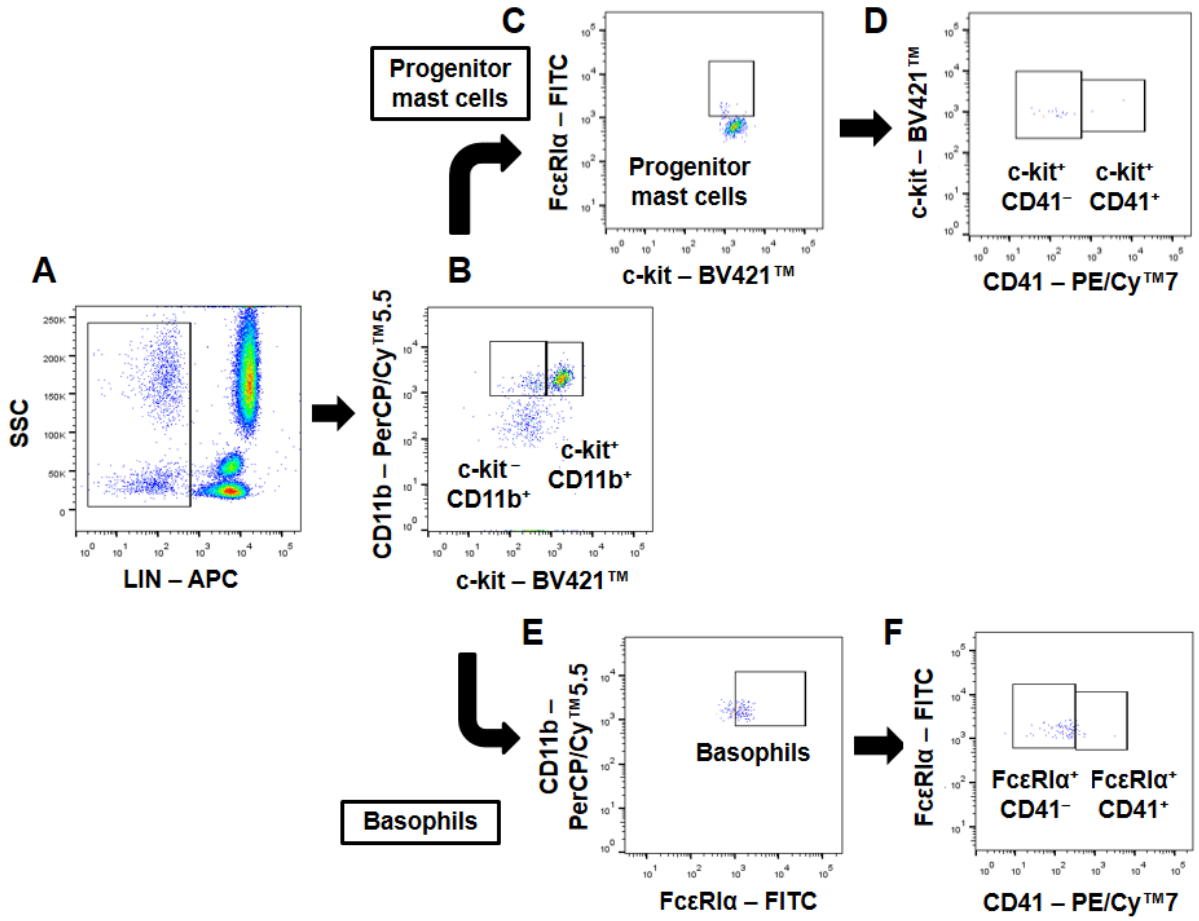

Figure 18. Gating strategy for human progenitor mast cells and basophils detection in whole blood by flow cytometry. Progenitor mast cells and basophils were selected with $CD3^-$, $CD14^-$, and $CD16^-$ (LIN^-) antibodies and SSC (**A**). Progenitor mast cells and basophils were differentiated with c-kit and CD11b markers (**B**). Progenitor mast cells were selected as $CD11b^+c\text{-}kit^+Fc\varepsilon RI\alpha^+$ (**C**) and then, progenitor mast cell-platelet complexes were selected as $CD11b^+c\text{-}kit^+Fc\varepsilon RI\alpha^+CD41^+$ population from heparinized whole blood, whereas in samples incubated with EDTA, platelet-free progenitor mast cells were identified as $CD11b^+c\text{-}kit^+Fc\varepsilon RI\alpha^+CD41^-$ (**D**). Subsequently, basophils were selected as $CD11b^+c\text{-}kit^-Fc\varepsilon RI\alpha^+$ (**E**). In heparinized whole blood, platelet-associated basophils were selected as $CD11b^+c\text{-}kit^-Fc\varepsilon RI\alpha^+CD41^+$, whereas in samples incubated with EDTA, the population unbound to platelets was selected as $CD11b^+c\text{-}kit^-Fc\varepsilon RI\alpha^+CD41^-$ (**F**).

3.1.5.3.3 Monocytes

An APC-conjugated mouse mAb against human CD14 (clone 47-3D6, IgG_{2A}; IMMUNOSTEP) was used to distinguish monocytes from the rest of the leukocyte populations and positive cells selected. Subsequently, in order to identify the different types of monocytes, the CD14 marker was confronted with a FITC-conjugated mouse mAb against human CD16 (clone 3G8, IgG_1; BD Biosciences) and a BV421™-conjugated mouse mAb

against human CD192 (CCR2, clone K036C2, IgG_{2A}; BioLegend) (**Figure 19**) (Shantsila *et al.* 2011), consequently three subpopulations of monocytes were differentiated as described in **Table 7**.

Table 7. Differential markers of monocyte subpopulations.

Markers	Cellular subpopulation
$CD14^+CD16^-CCR2^+$	Type 1 monocytes (Mon 1)
$CD14^+CD16^+CCR2^+$	Type 2 monocytes (Mon 2)
$CD14^+CD16^+CCR2^-$	Type 3 monocytes (Mon 3)

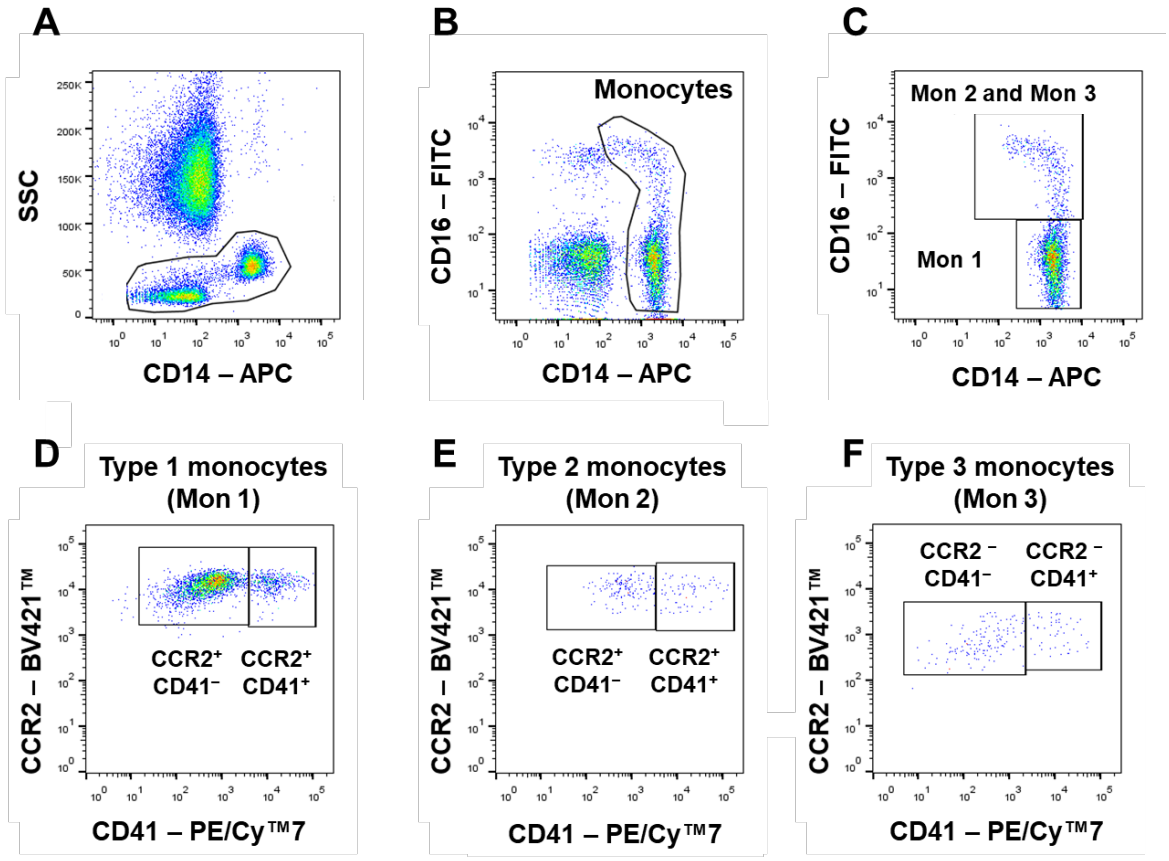

Figure 19. Gating strategy for human monocyte detection in whole blood by flow cytometry. Monocytes were selected by CD14 labeling and morphology (medium SSC; **A**). For the determination of monocyte subpopulations, CD16 and CCR2 markers were used (**B**–**F**). Monocytes-platelets complexes were selected as $CD14^+CD41^+$ population from heparinized whole blood, and platelet-free monocytes were gated as $CD14^+CD41^-$ from blood incubated with EDTA (**D**–**F**).

To determine the grade of activation of these cell populations, a PE-conjugated mouse mAb against human integrin CD11b (clone CBRM1/5, IgG_1; BioLegend) was used in all subpopulations. Similarly, the fractalkine receptor (CX_3CR1) expression was also determined in these three monocyte subpopulations using a PE-conjugated rat mAb against human CX_3CR1 (clone 2A9-1, IgG_{2B}; BioLegend).

3.1.5.3.4 T lymphocytes

The markers CD3 (T lymphocytes), CD4 (T helper lymphocytes; Th) and CD8 (cytotoxic T lymphocytes) were used to identify the lymphocyte population within the leukocytes present in peripheral blood. The gating strategy consisted in a selection using an APC-conjugated mouse mAb against human CD3 (clone 33-2A3, IgG_{2A}; IMMUNOSTEP), a V450-conjugated mouse mAb against human CD4 (clone RPA-T4, IgG_1; BD Biosciences), and finally, a FITC-conjugated mouse mAb against human CD8 (clone SK1, IgG_1; BD Biosciences) (**Figure 20**). After the identification of the different lymphocyte subpopulations, the possible contribution of platelets was studied as previously described (**Section 3.1.5.3.1**). Then, an analysis of the activation state was determined by using a PE-conjugated mAb against human CD69 (clone FN50, IgG_1; IMMUNOSTEP).

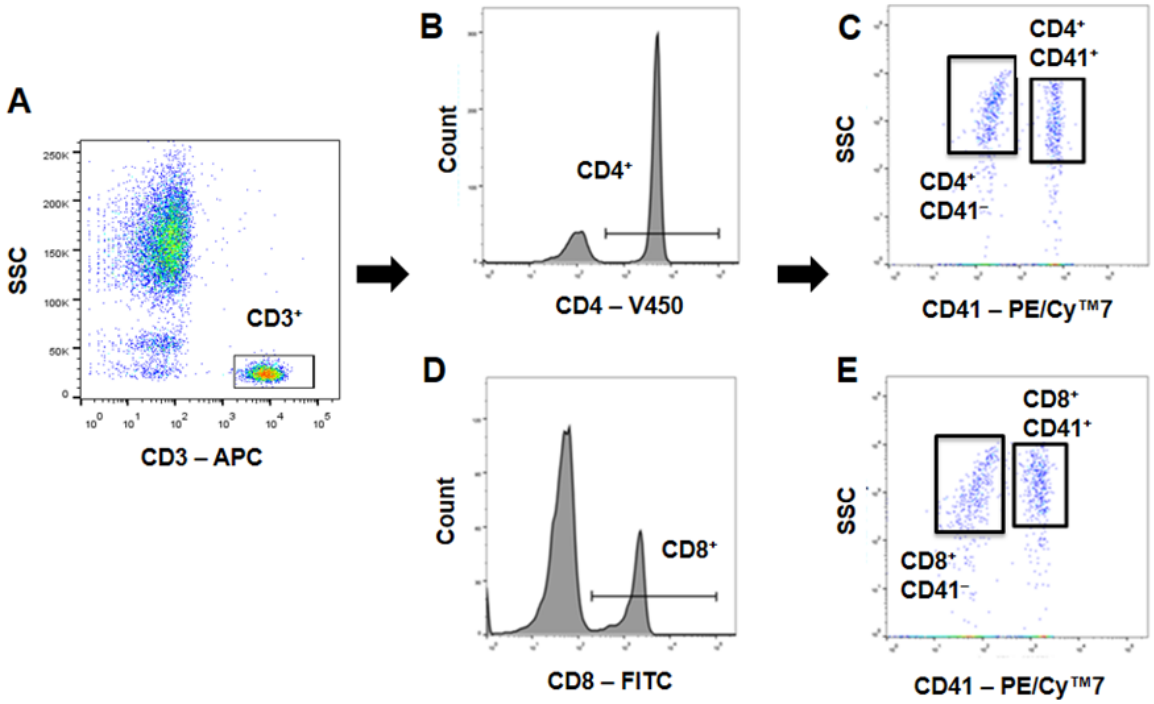

Figure 20. Gating strategy for human T lymphocytes detection in whole blood by flow cytometry. T lymphocytes were selected as $CD3^+$ population and with a low SSC (**A**). T helper (Th) lymphocytes were the $CD3^+CD4^+$ population (**B**). In heparinized whole blood, Th lymphocyte-platelet complexes were selected as $CD3^+CD4^+CD41^+$ population, while platelet-free Th lymphocytes were gated as $CD3^+CD4^+CD41^-$ from blood incubated with EDTA (**C**). Cytotoxic T lymphocytes were selected as $CD3^+CD8^+$ (**D**). In heparinized whole blood, cytotoxic T lymphocyte-platelet complexes were selected as $CD3^+CD8^+CD41^+$ population, while platelet-free cytotoxic T lymphocytes were gated as $CD3^+CD8^+CD41^-$ from blood incubated with EDTA (**E**).

3.1.5.3.5 T helper lymphocytes (Th)

To select the different Th lymphocyte subpopulations, a PerCP/Cy™5.5-conjugated mouse mAb against human CD4 (clone RPA-T4, IgG_1; BD Biosciences) was used first. Once detected, the subpopulations were identified as shown in **Table 8** with an Alexa Fluor® 488-conjugated mouse mAb against human CD183 (CXCR3, clone 1C6/CXCR3, IgG_1; BD Biosciences) and a BV421™-conjugated mouse mAb against human CD196 (CCR6, clone 11A9, IgG_1; BD Biosciences) (**Figure 21**).

Table 8. Differential markers of Th lymphocyte subpopulations.

Markers	Cellular subpopulation
$CXCR3^{+}CCR6^{-}$	Type 1 T helper (Th1)
$CXCR3^{-}CCR6^{-}$	Type 2 T helper (Th2)
$CXCR3^{-}CCR6^{+}$	Type 17 T helper (Th17)

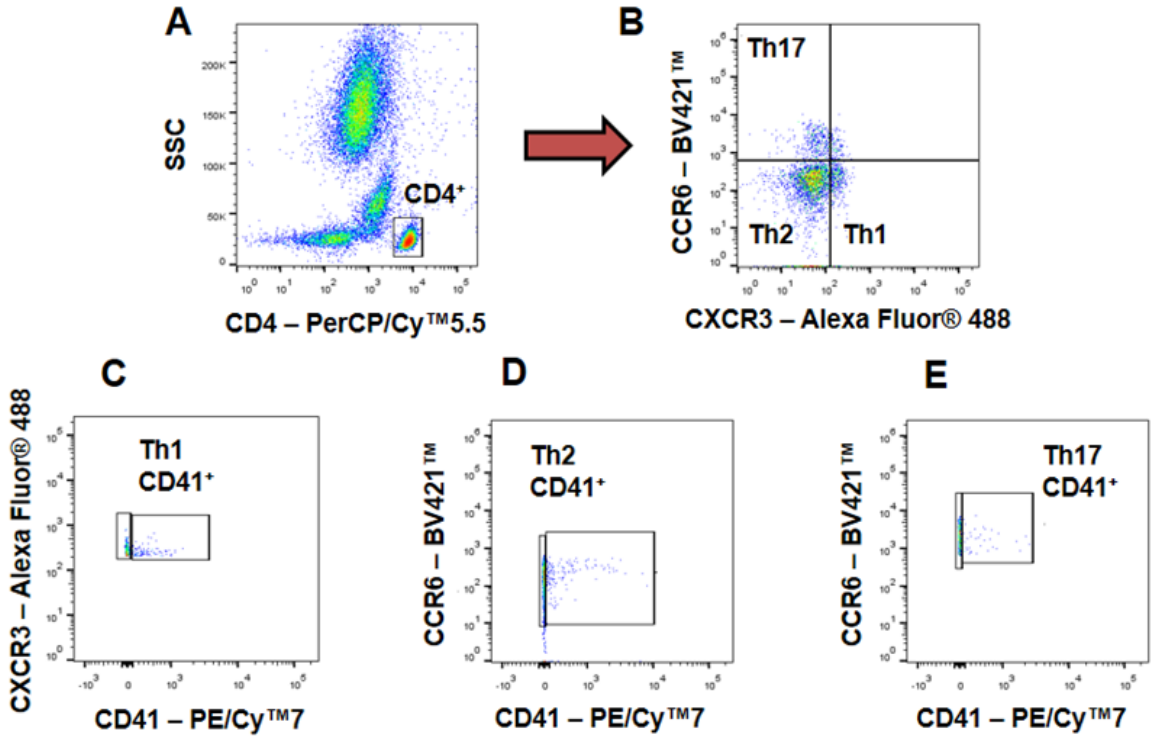

Figure 21. Gating strategy for human T helper (Th) lymphocytes detection in whole blood by flow cytometry. Th lymphocytes were selected as $CD4^{+}$ population and with a low SSC (**A**). Th lymphocyte subpopulations were detected with the markers CXCR3 and CCR6 (**B**). In heparinized whole blood, Th1 lymphocyte-platelet complexes were selected as $CXCR3^{+}CCR6^{-}CD41^{+}$ (**B** and **C**). Th2 lymphocyte-platelet complexes were selected as $CXCR3^{-}CCR6^{-}CD41^{+}$ (**B** and **D**), and Th17 lymphocyte-platelet complexes were selected as $CXCR3^{-}CCR6^{+}CD41^{+}$ (**B** and **E**).

Heparinized whole blood incubated or not with EDTA, was employed to determine lymphocyte-platelet complexes or platelet-free lymphocytes using a PE/Cy™7-conjugated mouse mAb against human CD41 (clone HIP8, IgG_1; BioLegend). Then, the expression of the CCR3 receptor and the grade of cell activation were measured using a PE-conjugated

mouse mAb against human CCR3 (clone 5E8, IgG_{2B}; BD Biosciences) and an APC-conjugated mouse mAb against human CD69 (clone FN50, IgG_1; BD Biosciences), respectively.

3.1.5.3.6 Regulatory T lymphocytes (Treg)

To identify the Treg population, a human regulatory T cell cocktail (BD Pharmingen™ Human Regulatory T Cell Cocktail; BD Biosciences) was used. Th lymphocytes were firstly identified with the marker CD4 (FITC-conjugated mouse mAb, clone SK3, IgG_1; BD Biosciences). An Alexa Fluor® 647-conjugated mouse mAb against human CD127 (clone HIL-7R-M21, IgG_1; BD Biosciences) and a PE/Cy™7-conjugated mouse mAb against human CD25 (clone 2A3, IgG_1; BD Biosciences) were used to determine the natural Treg cells (**Figure 22**). Two experiments were carried out in parallel: one with heparinized whole blood and the other with EDTA-treated blood, to determine Treg lymphocyte-platelet aggregates. For that purpose, a CF-Blue™-conjugated mAb against human CD41 (clone HIP8, IgG_1; IMMUNOSTEP) was employed.

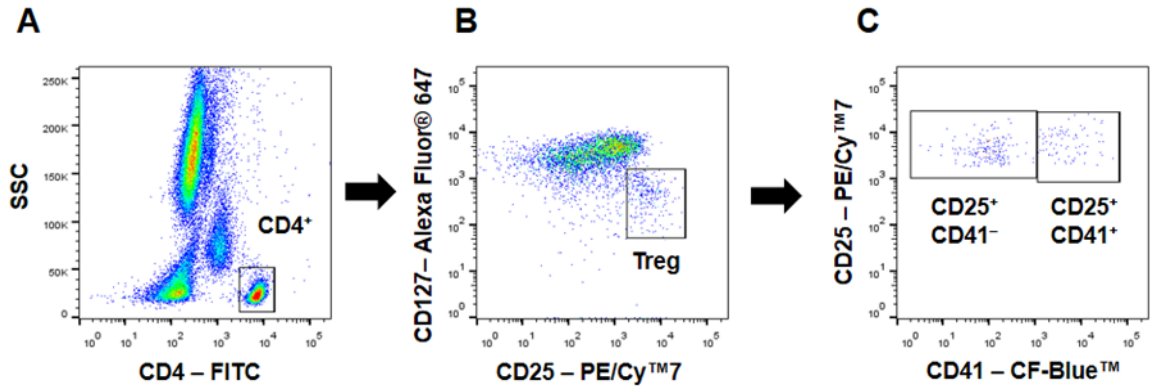

Figure 22. Gating strategy for human regulatory T lymphocytes (Treg) detection in whole blood by flow cytometry. Treg lymphocytes were selected as $CD4^+$ population and with a low SSC (**A**). Treg lymphocytes were detected with the markers CD127 and CD25 (**B**). Treg lymphocyte-platelet complexes were selected as $CD127^-CD25^+CD41^+$ population from heparinized whole blood, and platelet-free lymphocytes were gated as $CD127^-CD25^+CD41^-$ from blood incubated with EDTA (**C**).

3.1.5.4 Immunofluorescence studies

To visualize adherent platelet-leukocyte complexes with endothelial cells, immunofluorescence analysis was performed. HUAEC were grown up to confluence on glass coverslips and stimulated with TNFα (20 ng/mL; Sigma-Aldrich) for 24 h. Cells were incubated for 1 h at 37ºC with heparinized whole blood from patients with PH and age-matched controls, treated or not with EDTA as described before in **Section 3.1.5.3.1**. Afterward, cells were fixed with 4% paraformaldehyde (PFA; PanReac AppliChem GmbH) and blocked in PBS containing 1% BSA (Sigma-Aldrich). Subsequently, cells were incubated at room temperature for 2 h with an Alexa Fluor® 488-conjugated mouse mAb against human CD45 (1:50 dilution, clone HI30, IgG_1; BioLegend) and an APC-conjugated mAb against human CD41 (1:50 dilution, clone HIP8, IgG_1; IMMUNOSTEP) in 0.1% BSA-PBS. Nuclei from endothelial cells and leukocytes were counterstained with Hoechst dye (1:4000 dilution; Sigma-Aldrich). Images were captured with an Axio Observer A1 fluorescence microscope (ZEISS International).

3.1.5.5 Quantification of soluble metabolic and inflammatory markers

Heparinized whole blood (17 IU heparin/mL) from PH patients and age-matched controls was collected and centrifuged to obtain the plasma, which was stored at -80ºC. Human soluble adiponectin, leptin, ghrelin, interleukin (IL)-4, IL-5, IL-6, IL-8/CXCL8, IL-10, IL-12, IL-13, IL-25, IL-33, growth-regulated oncogene α (GROα)/CXCL1, fractalkine/CX_3CL1, TNFα, interferon γ (IFNγ), monocyte chemoattractant protein-1 (MCP-1)/CCL2, regulated upon activation, normal T cell expressed and secreted (RANTES)/CCL5, soluble P-selectin (sP-selectin), platelet factor-4 (PF-4)/CXCL4, eotaxin-1/CCL11, eotaxin-2/CCL24 and eotaxin-3/CCL26, were measured in plasma samples by enzyme-linked immunosorbent assay (ELISA; Human DuoSet® ELISA; R&D Systems, Inc., Minneapolis, MN) following manufacturer's instructions. Results were expressed as pg/mL or ng/mL of mediator in plasma.

3.2 ANIMAL STUDIES

All the experiments carried out with animals were in accordance with the principles outlined by the Guide for the Care and Use of Laboratory Animals, 8th edition, published by the National Institutes of Health (NIH, Department of Health and Human Services) of the United States (NIH publication No. 85-23, revised 2011) and approved by the Institutional Ethical Committee on Animal Experimentation of the University of Valencia, Spain.

The animals were bred, maintained under specific pathogen-free conditions and fed with autoclaved diet, with free access to water throughout the experimental period at a humidity of 60-65% and at a constant temperature of 22 ± 2ºC with a 12 h dark/light cycle. All efforts were made to minimize the number and suffering of the animals used.

3.2.1 Atherosclerosis model in apoE$^{-/-}$ mice

3.2.1.1 Generation of apoE$^{-/-}$CCR3$^{-/-}$ mice

Genotyping was carried out with mouse-tail DNA using the Maxwell® 16 Mouse Tail DNA purification kit (Promega, Madison, WI) following manufacturer's instructions. For that purpose, the Maxwell® 16 Instrument (Promega) was employed.

ApoE$^{-/-}$ C57BL/6 and CCR3$^{-/-}$ BALB/c mice were supplied by Charles River Laboratories, Inc. (Wilmington, MA). ApoE$^{-/-}$CCR3$^{-/-}$ C57BL/6 mice were obtained crossing apoE$^{-/-}$ C57BL/6 with CCR3$^{-/-}$ BALB/c mice.

Mice were genotyped and intercrossed during seven generations to obtain the expected genotypes and expand the populations generated: apoE$^{-/-}$CCR3$^{+/+}$ and apoE$^{-/-}$CCR3$^{-/-}$.

To analyze mice genotype, a polymerase chain reaction (PCR) analysis was carried out using specific primers (sequences [5'-3']) shown in **Table 9**. Primers oIMR 180, 181, 182 were used to determine the presence or absence of the *Apoe* gene while primers Ex2p5 FW and Ex2p5 RV were employed to verify the absence of the *Ccr3* gene. Finally, primers oIMR 3896 and oIMR 3897 were utilized to resolute the presence of the *Ccr3* gene.

Table 9. Sequences of primers used in the genotyping for *Apoe* and *Ccr3* genes.

Primer	Sequence [5'-3']
oIMR 180	GCCTAGCCGAGGGAGAGCCG
oIMR 181	TGTGACTTGGGAGCTCTGCAGC
oIMR 182	GCCGCCCCGACTGCATCT
Ex2p5 FW	CTTGCTGACCGCTTCCTCGTG
Ex2p5 RV	CATCATGTTGCCCAGGAGGCCG
oIMR 3896	TGGCATTCAACACAGATGAAA
oIMR 3897	CATGACCCCAGCTCTTTGAT

For each PCR sample, reagents listed in **Table 10** were added.

Table 10. PCR components.

Stock reagent	Volume [µL] per sample
Promega™ GoTaq™ Master Mix	12.5
Forward Primer	0.2
Reverse Primer	0.2
Nuclease-free water	9.1
DNA sample	2

Then, PCR tubes were placed in a SimpliAmp™ Thermal Cycler (Applied Biosystems, Thermo Fisher Scientific, Waltham, MA), and the PCR program shown in **Table 11** was run.

Table 11. PCR program.

Cycle step	Temperature [ºC]	Time [min]	Number of cycles
Initial denaturalization	94	5	1
Denaturalization	94	0.5	38
Annealing	62	0.5	
Extension	72	0.5	
Final extension	72	2	1
Hold	4	∞	

Gels were prepared with 2% agarose dissolved in Tris acetate-EDTA (TAE) buffer. After solidification, the gel was put into the electrophoresis chamber and covered with TAE buffer before sample loading. The gel was run at 120 V for 30 minutes.

A molecular range weight marker (Generuler^{TM} 1kb Plus DNA Ladder; Thermo Fisher Scientific, Waltham, MA) was used to determine the size of DNA.

3.2.1.2 Experimental protocol

Eight-week apoE$^{-/-}$CCR3$^{+/+}$ and apoE$^{-/-}$CCR3$^{-/-}$ male mice were bred for eight additionally weeks with either a control diet (2.8% fat; Panlab, S.L. - Harvard Apparatus, Barcelona, Spain) or with an atherogenic diet (10.8% fat, 0.75% cholesterol, S4892-E010; Ssniff Spezialdiäten GmbH, Soest, Germany).

3.2.1.3 Quantification of the atherosclerotic lesion

After this period, mice were sacrificed by anesthetic overdose with an intraperitoneal injection of a mixture of medetomidine hydrochloride (1 mg/mL; Orion Corporation, Espoo, Finland) and ketamine (50 mg/mL; Orion Corporation), and cut open ventrally. Left cardiac ventricles were perfused with 10 mL of PBS and exit through the severed right atrium. Aortas were isolated and cleaned *in situ* with PBS, fixed with 4% PFA (PanReac AppliChem GmbH) and kept overnight at 4ºC.

Then, samples were stained with Oil Red-O (0.2% Oil-Red-O in 78% methanol; Sigma-Aldrich) as described before (Landmesser *et al.* 2004, Avogaro *et al.* 2005). Images

were captured (Axio Observer A1 inverted microscope; ZEISS International), digitized and analyzed (ImageJ software, Windows free version; NIH, Bethesda, MD). Scoring was blindly performed on coded slides.

3.2.1.4 Histological analysis

Organs and tissues were removed from mice, washed with PBS, fixed with 4% PFA (PanReac AppliChem GmbH) overnight at 4ºC and paraffin-embedded for sectioning and further analyses (Escudero *et al.* 2015a).

Histological studies were performed on the aortic sigmoid valves, subcutaneous adipose tissue, and small intestine. Once organs were embedded in paraffin, they were cut into histological sections to carry out the subsequent studies. These slices were obtained employing a microtome (Leica RM2245; Leica Biosystems, Wetzlar, Germany) with a set thickness of 5 μm and mounted on microscope slides Superfrost® plus (Thermo Fisher Scientific). At least 20 slides, containing approximately four tissue cross-sections from each tissue and animal were examined (mean number of sections per mouse = 80 ± 5).

Once the histological sections obtained were dried, the area of interest was selected using a digital microscope (Leica DMD108; Leica Biosystems) with a 4x objective.

3.2.1.4.1 Hematoxylin and eosin stain

First, samples were hydrated and then immersed in filtered Harris hematoxylin (Sigma-Aldrich) and washed continuously in running water. Next, they were rapidly immersed in differentiation solution (0.25 mL concentrated hydrochloric acid in 100 mL 70% ethanol) followed by continuous washing in running water. Dyeing continued through sample immersion in 95% ethanol and then in eosin diluted 1:1 in 95% ethanol. A constant wash in water was carried out again and, finally, dehydration was accomplished in a series of ethanol baths of increasing concentrations, and a final xylene bath. Staining was completed with the assembly of the coverslips on the slides with the help of Bio-Mount synthetic based mounting media for histology and cytology (Bio-Optica, Milan, Italy).

3.2.1.4.2 Masson's trichrome stain

Masson's trichrome stain was used to define the area of connective tissue present in the atherosclerotic lesion, which is related to the stability of the atheromatous plaque. It is also useful to determine the necrotic *core* area, which correlates with the crystallization of cholesterol in the lesion (Luo *et al.* 2016).

Samples were immersed in Weigert's hematoxylin (Merck Millipore, Burlington, MA) and continuously washed in running water. Then, samples were stained with a solution of fuchsine (1:10 dilution; Sigma-Aldrich) followed with 1% acetic acid wash. Samples were then immersed in 5% phosphotungstic acid solution (Sigma-Aldrich) followed by immersion in light green solution (Sigma-Aldrich) and an additional 1% acetic acid wash. The staining procedure was finished with the assembly of the coverslips on the slides with Bio-Mount (Bio-Optica).

3.2.1.4.3 Toluidine blue stain

To detect mast cells, samples were hydrated and stained with toluidine blue solution (Toluidine Blue O; Sigma-Aldrich) for 2-3 minutes and washed with distilled water. Samples were dehydrated and the coverslips assembled on the slides with Bio-Mount (Bio-Optica).

3.2.1.5 Immunohistochemistry analysis

Inflammatory infiltration, smooth muscle formation, inflammatory mediators and receptors were measured in aortic sigmoid valves and small intestine.

After peroxidase inactivation (0.3% H_2O_2) and blockade of unspecific binding with goat serum (5% in PBS; Abcam, Cambridge, UK), samples were incubated overnight at 4ºC with the following primary antibodies: a rat mAb against mouse LAMP-2 (Mac-3, 1:100 dilution, clone M3/84, IgG_1; Santa Cruz Biotechnology, Inc., Dallas, TX) to detect macrophages and a rat mAb against mouse eotaxin-1 (CCL11, 1:40 dilution, clone 42285, IgG_{2A}; R&D Systems, Inc.). Specific labeling was assessed with a biotin-conjugated goat anti-rat antibody (1:500 dilution; Dako, Agilent Technologies, Santa Clara, CA). Then, samples were developed using a solution containing 3, 3'-diaminobenzidine (DAB; Dako, Agilent Technologies), counterstained with Harris hematoxylin (Sigma-Aldrich) and

dehydrated as described before in **Section 3.2.1.4.1**. Then, coverslips were assembled on the slides with Bio-Mount (Bio-Optica).

To detect smooth muscle cells (SMC), samples were incubated using an alkaline phosphatase mAb against α-smooth muscle actin (1:100 dilution, clone 1A4, IgG_{2A}; Sigma-Aldrich), followed by SIGMAFAST™ Fast Red TR/Naphthol AS-MX Tablets according to the manufacturer's instructions (Sigma-Aldrich).

Immunofluorescence assays were performed using a rabbit polyclonal antibody against human CD3 (1:50 dilution; Dako, Agilent Technologies), a goat polyclonal antibody against mouse CCR3 (1:100 dilution, IgG; Abcam), a rat mAb against mouse CD170 (SiglecF, 1:50 dilution, clone 1RNM44N, IgG_{2A}; Thermo Fisher Scientific). Specific labeling was detected with an Alexa Fluor® 488-conjugated goat anti-rabbit IgG (H+L) secondary antibody (1:500 dilution; Molecular Probes, Thermo Fisher Scientific, Waltham, MA), an Alexa Fluor® 594-conjugated chicken anti-goat IgG (H+L) secondary antibody (1:500 dilution; Molecular Probes, Thermo Fisher Scientific), an Alexa Fluor® 488-conjugated donkey anti-rabbit IgG (H+L) secondary antibody (1:500 dilution; Molecular Probes, Thermo Fisher Scientific) or an Alexa Fluor® 633-conjugated goat anti-rat IgG (H+L) secondary antibody (1:500 dilution; Molecular Probes, Thermo Fisher Scientific). Infiltration of lymphocytes $CD8^+$ and $CD4^+$ in the atherosclerotic lesion in $apoE^{-/-}CCR3^{+/+}$ and $apoE^{-/-}CCR3^{-/-}$ male mice was measured using an Alexa Fluor® 647-conjugated rat mAb against mouse CD8a (1:50 dilution, clone 53-6.7, IgG_{2A}; BioLegend) and an Alexa Fluor® 488-conjugated rat mAb against mouse CD4 (1:50 dilution, clone GK1.5, IgG_{2B}; BioLegend), respectively. They were incubated at room temperature for 2 h. Cell nuclei were counterstained with Hoechst dye (1:4000 dilution; Sigma-Aldrich). Then, the assembly was carried out with SlowFade® Gold antifade reagent (Molecular Probes, Thermo Fisher Scientific).

In order to confirm specificity of all antibodies, a rabbit IgG polyclonal isotype control (Abcam), a rat IgG_{2A} mAb isotype control (R&D Systems, Inc.), a rat IgG_{2B} Alexa Fluor® 488-conjugated isotype control (R&D Systems, Inc.), a rat IgG_{2A} Alexa Fluor® 647-conjugated antibody (R&D Systems, Inc.) or secondary antibodies only were used as negative controls.

Fields from each section were captured (Axio Observer A1 inverted microscope; ZEISS International), photographed (Olympus Camedia-C5060 Wide Zoom; Olympus, Tokyo, Japan), digitized, and analyzed (ImageJ software, Windows free version; NIH). Scoring was performed blinded on coded slides.

3.2.1.6 Measurement of lipid profile and glucose

Lipid levels and circulating glucose levels in the plasma of mice overnight-fasted were measured. Total cholesterol (TC) and TG were determined by enzymatic methods (Wako Pure Chemicals Industries, Ltd., Cape Charles, VA). High-density lipoprotein (HDL) cholesterol was also quantified with the same process as that used to measure TC, after the precipitation of apolipoprotein B (apoB) with dextran sulfate/$MgCl_2$ (Sigma-Aldrich) as previously described (Zieske *et al.* 2005).

Blood glucose was measured in blood samples using a Contour next USB Blood glucose meter (Bayer HealthCare Pharmaceuticals LLC, Berlin, Germany).

3.2.1.7 Plasma soluble metabolic and inflammatory markers detection

Heparinized whole blood from apoE$^{-/-}$CCR3$^{+/+}$ and apoE$^{-/-}$CCR3$^{-/-}$ male mice was collected, and plasma samples were obtained by centrifugation and stored at -80ºC. Mouse levels of soluble IL-4, IL-5, eotaxin-1/CCL11 and eotaxin-2/CCL24 in plasma, were measured using commercial ELISA kits and following manufacturer's instructions (Mouse DuoSet® ELISA; R&D Systems, Inc.). Results were expressed as pg/mL of mediator in plasma.

3.2.1.8 Reverse transcription polymerase chain reaction (RT-PCR)

3.2.1.8.1 RNA extraction

Organs and tissues were frozen at -20°C immediately after animal sacrifice for subsequent RNA extraction. RNA was extracted using TRIzol® Reagent (Invitrogen, Thermo Fisher Scientific, Waltham, MA) following the manufacturer's instructions. TRIzol® Reagent was placed together with the organs and tissues, and homogenization was carried out with an Ultra-Turrax (IKA-Werke GmbH, Staufen, Germany). Once samples were homogenized, chloroform was added, and the samples were shaken for 15 seconds in

the vortex. Then, they were centrifuged for 15 minutes at 15,000 g and 4ºC. Next, the mixture was separated into three different phases: a protein-containing organic phase (red due to phenol-chloroform) at the bottom, a genomic DNA-containing interface (purple), and an RNA-containing aqueous phase. The last one was transferred carefully into a new cold 1.5 mL microtube. Isopropanol was added and inverted several times to enable mixing. Then samples were incubated for 5-10 minutes to allow RNA precipitation and centrifuged at 12,000 g at 4ºC for 10 minutes. The supernatant was removed, and 70% ethanol was added afterwards. Samples were vortexed to allow RNA to be washed and then centrifuged again, at 7,500 g at 4ºC for 5 minutes. Finally, ethanol was removed, and the precipitate was resuspended in nuclease-free water (Thermo Fisher Scientific).

Subsequently, a NanoDrop spectrophotometer (ND-100 v3.7.1; Thermo Fisher Scientific) was used to determine the RNA concentration.

3.2.1.8.2 Reverse transcription (RT)

RT was performed with the High-Capacity cDNA Reverse Transcription kit (Applied Biosystems, Thermo Fisher Scientific) following the supplier's instructions.

After RNA extraction and concentration determination, RT of 1,000 ng of RNA per sample was carried out, using the MultiScribe™ Reverse Transcriptase (50 U/μL; Applied Biosystems, Thermo Fisher Scientific) in a SimpliAmp™ Thermal Cycler (Applied Biosystems, Thermo Fisher Scientific). The reagents shown in **Table 12** were used to prepare the mix for the RT.

Table 12. Master Mix components.

Reagent	Volume [µL] per sample
10x RT Buffer	2
25x dNTPs Mix (100 mM)	0.8
10x RT Random Primers	2
MultiScribe™ Reverse Transcriptase	1
Applied Biosystems™ RNase Inhibitor (20 U/µL)	1
Nuclease-free water	4.2
RNA sample	1,000 ng

10 µL of master mix and 10 µL of the sample, previously diluted in nuclease-free water, were used for each reaction, adjusting the concentration to 1,000 ng. Then, samples were brought to the SimpliAmp™ Thermal Cycler (Applied Biosystems, Thermo Fisher Scientific), and the following experimental conditions were applied (**Table 13**).

Table 13. RT program.

Step	Temperature [ºC]	Time [min]
Step 1	25	10
Step 2	37	120
Step 3	85	5
Step 4	4	∞

At the end of the process, the obtained cDNA was stored at -20ºC until further use.

3.2.1.8.3 Quantitative polymerase chain reaction (qPCR)

cDNA was amplified with specific probes for the genes shown in **Table 14**.

Table 14. Probes used for qPCR assay in atherosclerosis studies.

Gene	TaqMan™ Gene Expression Probe
Mouse Eotaxin-1 (Ccl11)	Mm00441238_m1
Mouse Eotaxin-2 (Ccl24)	Mm00444701_m1
Mouse Il-25	Mm00499822_m1
Mouse Il-33	Mm00505403_m1
Mouse Gapdh	Mm99999915_g1

Reactions were performed in an Optical 384-Well Reaction Plate with Barcode (MicroAmp™; Applied Biosystems, Thermo Scientific) using a 7900HT Real-Time PCR apparatus (Applied Biosystems, Thermo Fisher Scientific) and the TaqMan™ Universal PCR Master Mix (Applied Biosystems, Thermo Fisher Scientific). Applied Biosystems predesigned all probes. Both the probe of each gene and the endogenous control were used to prepare a mix (**Table 15**).

Table 15. Reagents used for qPCR.

Reagent	Volume [µL] per sample
TaqMan™ Universal PCR Master Mix	5
Probe	0.5
Nuclease-free water	2.5
cDNA	2

The PCR cycling program was performed as shown in **Table 16**.

Table 16. qPCR cycling protocol.

Step	Temperature [ºC]	Time	Number of cycles
UDG pre-treatment	50	2 min	1
Initial denaturation	95	10 min	1
Denaturation	95	15 s	40
Annealing/Extension	60	60 s	

The relative quantification of the different transcripts was determined with the $2^{-\Delta\Delta Ct}$ method, using glyceraldehyde 3-phosphate dehydrogenase (*Gapdh*) as endogenous control, and normalizing to the control group. Results were analyzed using the software provided by the manufacturer (QuantStudio™ Design & Analysis; Applied Biosystems, Thermo Fisher Scientific).

3.2.1.9 Flow cytometry studies

Heparinized whole blood, bone marrow and subcutaneous adipose tissue were employed for flow cytometry analyses.

To obtain the bone marrow, the femur was firstly removed and gently cleaned from the remaining tissues. The bone marrow was obtained cutting one side of the femur with a scalpel and centrifuging at 6,000 rpm for 1 min. It was finally resuspended in PBS and stored at 4ºC until its use. 10 µL of the sample was added per tube.

Subcutaneous adipose tissue was firstly digested to obtain isolated cells. For this purpose, adipose tissue was removed and put in a digestion buffer containing low-glucose Dulbecco's modified eagle's medium (DMEM; Lonza Group), 0.2 M 4-(2-hydroxyethyl)-1-piperazineethanesulfonic acid (HEPES; PanReac AppliChem GmbH) saline, 10 mg/mL fatty acid-poor BSA (Sigma-Aldrich) supplemented with 0.2 mg/mL Liberase™ (Liberase™ Research Grade medium Thermolysin concentration; Sigma-Aldrich) and 25 µg/mL DNAse I from bovine pancreas (Sigma-Aldrich). The mixture was kept at 37ºC for 30-40 minutes in gentle agitation. After the incubation, the digested subcutaneous adipose tissue was filtered, and 5 mL of 3% FBS in PBS was poured in each sample and then centrifuged 10 minutes at 1,000 g. Subsequently, the pellet was resuspended in 5 mL of 3%

FBS in PBS and centrifuged again at 1,500 rpm for 5 minutes. RBCs were lysed with lysis buffer (BD FACS™ lysing solution 10x concentrate; BD Biosciences). After 1 minute, the digestion product was centrifuged again for 5 minutes at 200 g and mixed with 125 µL of 3% FBS in PBS. Unspecific binding was blocked for 5 minutes with FCBlock antibody (MACS Miltenyi Biotec). 10 µL of the final product was put in each microtube with the respective antibodies and incubated for 30 minutes at room temperature in the dark. Afterward, all samples were run in a FACSVerse™ Flow Cytometer (BD Biosciences). The analytical software FlowJo® v10.0.7 (FlowJo LLC) was used for the analysis of the flow cytometry results.

3.2.1.9.1 Determination of the expression of cell surface markers by flow cytometry

To detect different cell surface markers, heparinized whole blood, bone marrow and subcutaneous adipose tissue samples were stained for 30 minutes with saturated amounts of different antibodies as specified by the manufacturers (**Table 17**).

Table 17. Antibodies used for flow cytometry mice experiments.

Antibody − Fluorochrome	Clone	Isotype	Manufacturer
CD193 (CCR3) − APC	83101	Rat IgG_{2A}	R&D Systems, Inc.
CD117 (c-kit) – V450	2B8	Rat IgG_{2B}	BD Biosciences
CD49d − PE	R1-2	Rat IgG_{2B}	BD Biosciences
FcεRIα − FITC	MAR-1	Armenian Hamster IgG	BioLegend
CD45 – V450	30-F11	Rat IgG_{2B}	BD Biosciences
SiglecF − PE	ES22-10D8	Rat IgG_1	IMMUNOSTEP
CD11c − FITC	HL3	Armenian Hamster IgG_1	BD Biosciences
CD3e − FITC	145-2C11	Armenian Hamster IgG_1	BD Biosciences
CD69 – V450	H1.2F3	Armenian Hamster IgG_1	BD Biosciences
F4/80 − FITC	BM8	Rat IgG_{2A}	BioLegend
CD11b – PerCP/Cy™5.5	M1/70	Rat IgG_{2B}	BD Biosciences
Arginase 1 − APC	Polyclonal	Sheep IgG	R&D Systems, Inc.

3.2.2 Abdominal aortic aneurysm (AAA) model in apoE$^{-/-}$ mice

3.2.2.1 Generation of apoE$^{-/-}$CXCR6$^{GFP/GFP}$ mice

Mice apoE$^{-/-}$ C57BL/6 and mice carrying a targeted (Galkina *et al.* 2007) green fluorescence protein (GFP) knock-in of the CXCR6 gene (CXCR6$^{GFP/GFP}$ C57BL/6) were supplied by Charles River Laboratories, Inc.

ApoE$^{-/-}$CXCR6$^{GFP/GFP}$ C57BL/6 mice were obtained by crossing apoE$^{-/-}$ C57BL/6 with CXCR6$^{GFP/GFP}$ C57BL/6 mice. ApoE$^{-/-}$CXCR6$^{GFP/+}$ C57BL/6 mice were obtained by crossing apoE$^{-/-}$ C57BL/6, and apoE$^{-/-}$CXCR6$^{GFP/GFP}$ C57BL/6 mice and male heterozygous apoE$^{-/-}$CXCR6$^{GFP/+}$ mice were used as controls. For genotyping, the following primers were used (**Table 18**).

Table 18. Sequences of primers used in the genotyping for *Apoe, Gfp* and *Cxcr6* genes.

Primer	Sequence [5'−3']
oIMR 180	GCCTAGCCGAGGGAGAGCCG
oIMR 181	TGTGACTTGGGAGCTCTGCAGC
oIMR 182	GCCGCCCCGACTGCATCT
GFP 5'	GTCGCCACCATGGTGAGCAAGGGC
GFP 3'	AGATCTCAGCGCCGGCGAAATGAA
CXCR6 5'	TTGCTTGCTCATTTGGGTGGTCTC
CXCR6 3'	GAAGAGATTCACACCGTTCCGGAT

Primers oIMR 180, 181, 182 were used to determine the presence or absence of *Apoe* gene; primers GFP 5' and GFP 3' were employed to resolute the absence of *Cxcr6* and primers CXCR6 5' and CXCR6 3' to verify the presence of *Cxcr6* gene.

Mice were genotyped and intercrossed, and the PCR was performed following the same protocol as previously described in **Section 3.2.1.1**.

3.2.2.2 Experimental protocol

12-weeks-old apoE$^{-/-}$, apoE$^{-/-}$CXCR6$^{GFP/+}$ and apoE$^{-/-}$CXCR6$^{GFP/GFP}$ male mice were used. Alzet® mini-osmotic pumps, model 2004 (Charles River Laboratories, Inc.) were implanted subcutaneously; angiotensin-II (Ang-II; Calbiochem, San Diego, CA) was infused at a rate of 1,000 ng/kg/min. Simultaneously, losartan (LKT Laboratories, Inc., St. Paul, MN), which works as an angiotensin-II receptor type 1 (AT_1) antagonist, was infused, in some apoE$^{-/-}$Ang-II-treated mice, at a rate of 30 mg/kg/day for 28 days. Losartan's dose was based on ranges previously used in rodents (Scalia *et al.* 2011). In the control mice group, the mini-osmotic pumps were implanted to release the vehicle (saline).

3.2.2.3 Aneurysm quantification

At the end of the experimental protocols, mice were anesthetized as previously described in **Section 3.2.1.3** and cut open ventrally. Left cardiac ventricles were perfused with 10 mL of PBS with an exit through the right atrium. The aorta was exposed under a dissecting microscope to remove the periadventitial tissue, and then, it was photographed with a Leica DMD108 digital microscope (Leica Biosystems). Suprarenal regions of the abdominal aorta were identified between the last pair of intercostal arteries and the right renal branch. The maximal outer diameter of the suprarenal aorta was measured *ex vivo* using the Leica software image processor. Scoring was performed blinded.

3.2.2.4 Immunohistochemistry analysis in mouse aorta

Suprarenal aorta samples were divided into two sequential regions (A and B) taking the maximal dilatation as a threshold, using a Leica DMD108 Digital microscope (Leica Biosystems). Region A was kept at -80ºC for molecular analyses. Region B was fixed in 4% PFA (PanReac AppliChem GmbH), embedded in paraffin, sectioned with a microtome (Leica RM2245; Leica Biosystems) and mounted on microscope slides Superfrost® plus (Thermo Fisher Scientific) (Collado *et al.* 2018b). At least ten slides of region B, containing approximately four tissue cross sections (5 µm thick) from each animal were examined (mean number of aortic sections per mouse = 40 ± 5). Inflammatory infiltration and microvessel formation in aortas were measured as described elsewhere (Zhang *et al.* 2009, Company *et al.* 2011). Briefly, after the blockade with goat serum (5% diluted in PBS; Abcam), aorta

cross sections were incubated overnight at 4ºC with the following primary antibodies: a rat mAb against mouse CD68 (1:50 dilution, clone FA-11, IgG_{2A}; Bio-Rad Laboratories, Hercules, CA), a rabbit polyclonal antibody against mouse CXCR6 (1:50 dilution; IMMUNOSTEP) and a rabbit polyclonal antibody against human CD3 (1:50 dilution; Dako, Agilent Technologies). Specific labeling was detected with an Alexa Fluor® 633-conjugated goat anti-rat IgG (H+L) secondary antibody (1:500 dilution; Molecular Probes, Thermo Fisher Scientific), an Alexa Fluor® 488-conjugated goat anti-rabbit IgG (H+L) secondary antibody (1:500 dilution; Molecular Probes, Thermo Fisher Scientific) or an Alexa Fluor® 594-conjugated goat anti-rabbit IgG (H+L) secondary antibody (1:500 dilution; Molecular Probes, Thermo Fisher Scientific), respectively. Cell nuclei were counterstained with Hoechst dye (1:4000 dilution; Sigma-Aldrich). CD31 staining was performed with a rabbit polyclonal antibody against mouse CD31 (1:50 dilution, IgG; Abcam). Specific labeling was detected using a labeled polymer-horseradish peroxidase (HRP)-conjugated anti-rabbit as a secondary antibody (1:500 dilution) as part of the EnVision^{+} System/HRP kit (Dako, Agilent Technologies). Samples were treated with a solution containing DAB (Dako, Agilent Technologies), then counterstained with Harris hematoxylin (Sigma-Aldrich) and dehydrated. Lymphocytes $CD8^{+}CXCR6^{+}$ and $CD4^{+}CXCR6^{+}$ in the AAA of $apoE^{-/-}CXCR6^{GFP/+}$ male mice were detected using an Alexa Fluor® 647-conjugated rat mAb against mouse CD8a (1:50 dilution, clone 53-6.7, IgG_{2A}; BioLegend) and an Alexa Fluor® 647-conjugated rat mAb against mouse CD4 (1:50 dilution, clone GK1.5, IgG_{2B}; BioLegend), respectively, and incubated at room temperature for 2 h. Cell nuclei were counterstained with Hoechst dye (1:4000 dilution; Sigma-Aldrich). Fields from each suprarenal aortic section were captured (Axio Observer A1 inverted microscope; ZEISS International), digitized, and analyzed (ImageJ software, Windows free version; NIH). Scoring was performed blinded on coded slides.

In order to confirm specificity of all antibodies, a rabbit IgG polyclonal isotype control (Abcam), a rat IgG_{2A} mAb isotype control (R&D Systems, Inc.), a rat IgG_{2B} Alexa Fluor® 647-conjugated isotype control (R&D Systems, Inc.), a rat IgG_{2A} Alexa Fluor® 647-conjugated antibody (R&D Systems, Inc.) or secondary antibodies only were used as negative controls.

3.2.2.5 Measurement of blood pressure and lipid profile

Systolic blood pressure (SBP) was measured in conscious mice using a non-invasive tail-cuff system (CODA-6; Kent Scientific Corporation, Torrington, CT). During the procedure, animals were placed in the retainer tube of a chamber that was kept at 37ºC (LE5510; Panlab S.L. - Harvard Apparatus) as previously described (Zhang *et al.* 2009). Mice were acclimated to the instrument for at least five consecutive days before baseline measurements and the implantation of the mini-osmotic pumps. All assessments were performed between 8 and 11 a.m. to avoid variations in blood pressure due to the circadian cycle.

Furthermore, each mouse received ten initial pressure readings to acclimate them to the procedure. Then, ten additional cycles were measured to obtain the systolic pressure. The criterion for data acceptance was the acquisition of at least 10 of 20 measurements and a standard deviation <30 mmHg for each session.

Lipid levels in mice plasma overnight-fasted were measured as explained previously in **Section 3.2.1.6**.

3.2.2.6 Analysis of Mcp-1, Cxcl16 and Vegf expression in the aortic aneurysm

RNA extraction, RT-PCR and finally qPCR were performed following the same protocol to that previously described in **Section 3.2.1.8**. Probes used are shown in **Table 19**.

Table 19. Probes used in qPCR assays in AAA studies.

Gene	TaqMan™ Gene Expression Probe
Mouse Mcp-1/Ccl2	Mm00441242_m1
Mouse Cxcl16	Mm00469712_m1
Mouse Vegf	Mm00437306_m1
Mouse Gapdh	Mm99999915_g1

3.2.2.7 Determination of cytokine and chemokine levels in plasma

To determine CXCL16, TNFα and IFNγ plasma levels, heparinized whole blood from apoE$^{-/-}$ male mice infused or not with Ang-II and treated or not with losartan, was collected, centrifuged to obtain plasma and stored at -80°C. Cytokine and chemokine levels were measured in plasma by commercial ELISA kits (Mouse DuoSet® ELISA, R&D Systems, Inc.) and the results expressed as pg/mL of cytokine and chemokine in plasma.

3.3 STATISTICAL ANALYSIS

All results were analyzed using the GraphPad Prism software version 6.0 (GraphPad Software, Inc., La Jolla, CA) and the values expressed as individual data points, percentages or mean ± standard error of the mean (SEM) when appropriate. For two-group comparisons, paired or unpaired Student's t-test was used in data that passed both normality (Kolmogorov-Smirnov test) and equal variance (Levene test) as appropriate; otherwise, a non-parametric Mann Whitney U test was performed. For comparisons among multiple groups, one-way or two-way analysis of variance (ANOVA) followed by *post hoc* analysis (Bonferroni test) was used in data that passed both normality and equal variance; otherwise, a non-parametric Kruskal-Wallis test followed by Dunn's *post hoc* analysis was used. Data were considered statistically significant at $p < 0.05$. Additionally, some correlations between experimental findings and clinical features were calculated using Spearman correlation method.

4. RESULTS

4.1 STUDY OF THE SYSTEMIC INFLAMMATION IN PATIENTS WITH PH AND ITS MODULATION BY AN OFL

A total of 43 subjects, 22 patients with PH (4 males and 18 females, aged 49 ± 2.7 years) and 21 age-matched control subjects without PH (5 males and 16 females, aged 48.8 ± 3.1 years) were included in the present study. The demographic, clinical and biochemical characteristics of PH patients and age-matched volunteers are shown in **Table 20**. No statistically significant differences were found with regards to age, gender, BMI, or waist circumference between the two groups (**Table 20**). By contrast, levels of TC, LDL, TG, and apoB were significantly higher in patients than in control subjects (**Table 20**).

Table 20. Clinical features of studied subjects.

	Control volunteers (*n* = 21)	**PH subjects (*n* = 22)**	***p*-value**
Age (years)	48.8 ± 2.7	49 ± 3.1	0.95
Gender M/F (%)	5/16 (23.8/76.2)	4/18 (18.2/81.8)	0.72
BMI (kg/m^2)	25.4 ± 0.7	25.7 ± 0.9	0.83
Waist circumference (cm)	85.3 ± 1.9	85.7 ± 2.2	0.90
SBP (mmHg)	115.9 ± 2.0	124.7 ± 3.6 *	**<0.05**
DBP (mmHg)	71.6 ± 1.8	78.5 ± 2.6 *	**<0.05**
Glucose (mg/dL)	86.7 ± 1.5	88.1 ± 1.9	0.57
TC levels (mg/dL)	206.1 ± 6.8	264.6 ± 8.9 **	**<0.01**
LDL levels (mg/dL)	130.6 ± 5.4	182.8 ± 6.2 **	**<0.01**
TG (mg/dL)	80.9 ± 7.3	109.7 ± 8.5 **	**<0.01**
HDL levels (mg/dL)	65.9 ± 2.5	63.4 ± 2.9	0.51
ApoB (mg/dL)	92.5 ± 4.1	127.4 ± 5.0 **	**<0.01**
GOT (U/L)	21.7 ± 0.9	22.8 ± 1.1	0.42
GPT (U/L)	18.3 ± 1.8	18.5 ± 1.1	0.90
Creatinine (mg/dL)	0.7 ± 0.0	0.7 ± 0.0	0.48
IgG (mg/dL)	966.7 ± 41.1	968.5 ± 34.4	0.97
IgM (mg/dL)	100.4 ± 7.6	125.8 ± 14.1	0.14
IgE total (IU/L)	42.6 ± 12.0	50.4 ± 16.9	0.71

M, male; F, female; BMI, body mass index; SBP, systolic blood pressure; DBP, diastolic blood pressure; TC, total cholesterol; LDL, low-density lipoprotein; TG, triglycerides; HDL, high-density lipoprotein; ApoB, apolipoprotein B; GOT, glutamic-oxalacetic transaminase; GPT, glutamate-pyruvate transaminase; Ig, immunoglobulin. Data are presented as mean ± SEM. *p <0.05 or **p <0.01 relative to values in the control group.

4.1.1 Platelet activation is enhanced in patients with PH and reduced by the OFL administration

We first determined the platelet activation state and levels of several mediators released upon their activation in blood samples from the two study groups using flow cytometry and ELISA. No significant differences in the number of circulating platelets were found between controls and patients (**Figure 23A**). By contrast, the percentage of platelets expressing PAC-1 and P-selectin (CD62P) was significantly higher in patients than in control subjects (**Figures 23B**, **C**, and **G**), indicating their activation state. Since P-selectin translocates to the cell surface upon cell activation, where it can be cleaved and released into the circulation as soluble P-selectin (sP-selectin), we also determined its circulating levels in plasma, finding that levels were significantly higher in the PH group than in the control one (**Figure 23D**). Similarly, circulating plasma levels of PF-4/CXCL4, a platelet chemokine released upon platelet activation, were significantly higher in PH patients than in controls (**Figure 23E**). No differences, however, were encountered between PH patients and control subjects for the levels of circulating RANTES/CCL5, a chemokine released by platelets and other immune cells when they are activated (**Figure 23F**).

When the OFL was administrated to these same PH patients, no changes were observed in the percentage of circulating platelets after 4 hours (**Figure 23A**); however, the percentage of platelets expressing PAC-1 and P-selectin (**Figures 23B**, **C**, and **G**), as well as levels of sP-selectin, PF-4/CXCL4 and RANTES/CCL5 (**Figures 23D–F**), were significantly reduced in those patients with PH.

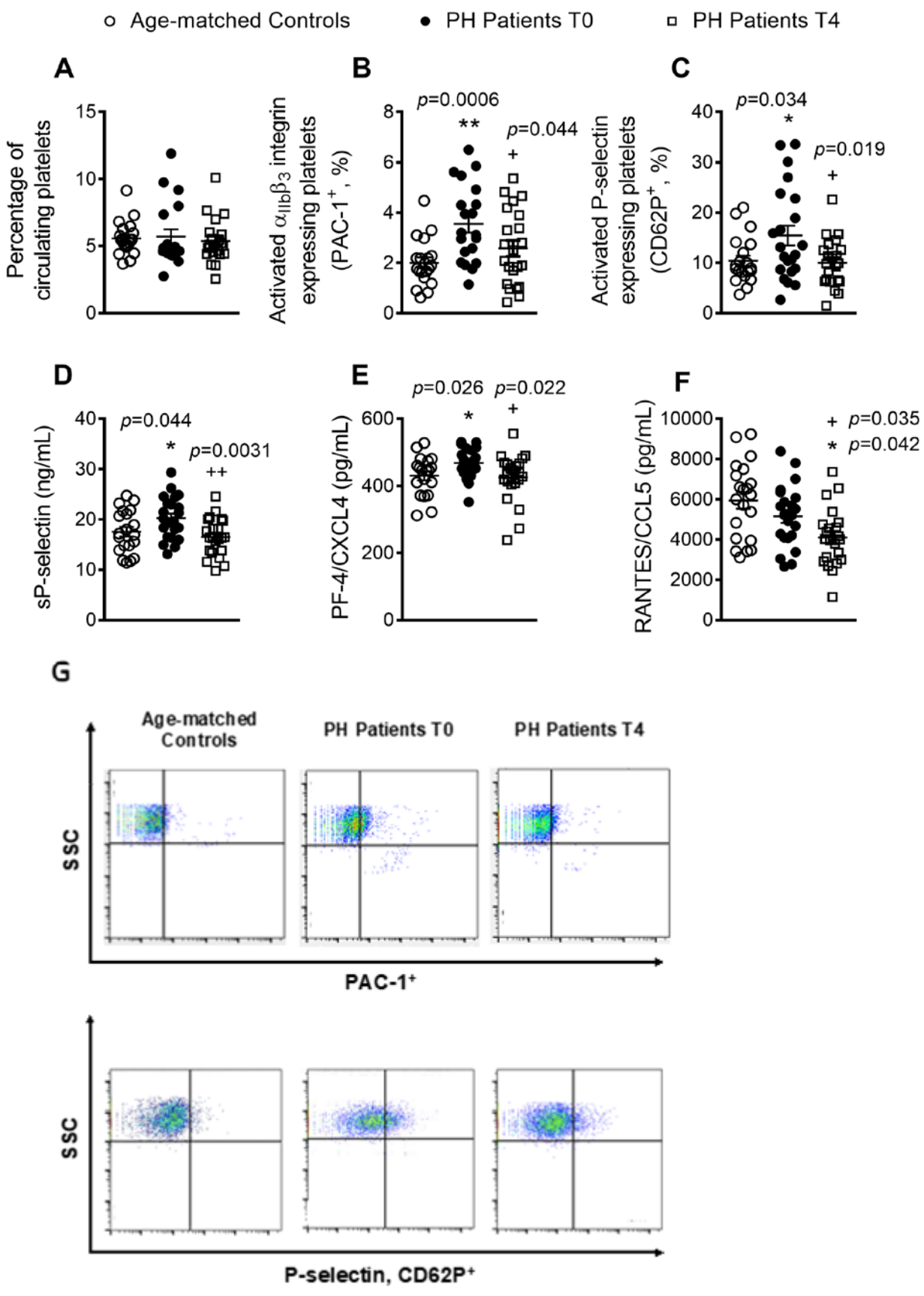
Age-matched Controls
PH Patients T0
PH Patients T4
A
Percentage of circulating platelets
B
Activated $\alpha_{IIb}\beta_3$ integrin expressing platelets (PAC-1$^+$, %)
p=0.0006
**
p=0.044
+
C
Activated P-selectin expressing platelets (CD62P$^+$, %)
p=0.034
*
p=0.019
+
D
sP-selectin (ng/mL)
p=0.044
*
p=0.0031
++
E
PF-4/CXCL4 (pg/mL)
p=0.026
*
p=0.022
+
F
RANTES/CCL5 (pg/mL)
+ p=0.035
* p=0.042
G
Age-matched Controls
PH Patients T0
PH Patients T4
SSC
PAC-1$^+$
SSC
P-selectin, CD62P$^+$

Figure 23. Platelet activation and related soluble markers are elevated in patients with PH and reduced by the OFL administration. Flow cytometry analysis of platelets stained with conjugated antibodies against CD41 (**A**), CD41 and PAC-1 (**B** and **G**), and CD41 and P-selectin (**C** and **G**). Results are expressed as the percentage of positive cells. sP-selectin (**D**), PF-4/CXCL4 (**E**), and RANTES/CCL5 (**F**) plasma levels (ng or pg/mL) were measured by ELISA (n = 21 control subjects and n = 22 PH patients). Values are expressed as mean ± SEM. *p <0.05 or **p <0.01 relative to values in the control group. +p <0.05 or ++p <0.01 relative to values in the PH group at time 0 (T0).

4.1.2 The percentage of platelet-neutrophil aggregates, activated neutrophils, and circulating levels of IL-8 are elevated in patients with PH. Some of these parameters are decreased after the OFL administration

Next, we evaluated several parameters related to the activation of different leukocyte subsets. No significant differences were found in the percentage of circulating neutrophils in heparinized whole blood between the two groups (**Figure 24A**); however, the percentage of platelet-neutrophil aggregates and activated neutrophils ($CD69^+$) was significantly higher in patients than in control subjects (**Figures 24B** and **C**). As some chemokines, such as GROα/CXCL1 and IL-8/CXCL8, can induce activation and chemotaxis of human neutrophils, we quantified their levels in plasma. Whereas no differences in the levels of GROα/CXCL1 were detected between the two groups (**Figure 24D**), plasma levels of IL-8/CXCL8 were significantly elevated in PH patients (**Figure 24E**). Of note, we found a significant association between the circulating levels of IL-8/CXCL8 and three clinical features of PH: apoB, LDL, and TC (**Figures 24F–H**).

When the OFL was administrated, no changes were observed in the percentage of circulating neutrophils, or the platelet-neutrophil aggregates (**Figures 24A** and **B**). Nevertheless, a faint, but not significant decrease in the activation state of neutrophils 4 hours after the OFL administration was observed (**Figure 24C**). Again, while no differences were found in plasma levels of GROα/CXCL1 in PH patients before and after OFL (**Figure 24D**), IL-8/CXCL8 levels were significantly decreased 4 h after the OFL administration (**Figure 24E**).

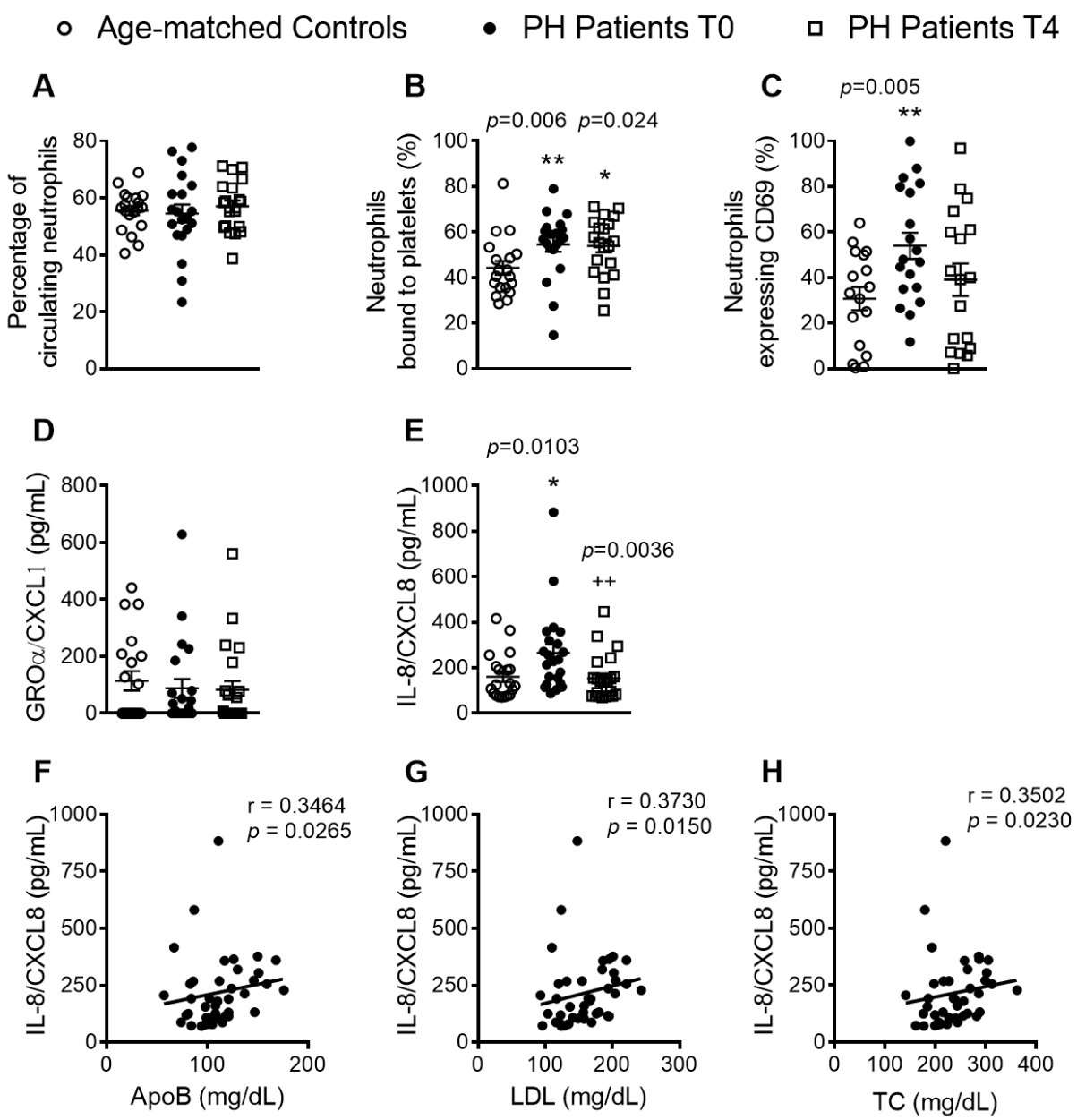

Figure 24. The percentage of platelet-neutrophil aggregates, activated neutrophils, and IL-8 circulating levels are higher in patients with PH, and some of these parameters are reduced after the OFL administration. Flow cytometry analysis of heparinized whole blood co-stained with specific markers for platelets and neutrophils (**A** and **B**). Neutrophils were also stained for CD69 (**C**). Results are expressed as the percentage of positive cells. GROα/CXCL1 (**D**) and IL-8/CXCL8 (**E**) plasma levels (pg/mL) were measured by ELISA (n = 21 control subjects and n = 22 PH patients). Values are expressed as mean ± SEM. *p <0.05 or **p <0.01 relative to values in the control group. ++p <0.01 relative to values in the PH group at T0. Correlations between circulating IL-8/CXCL8 and apoB (**F**), LDL (**G**), and TC (**H**) plasma levels.

4.1.3 Circulating Mon 3 monocytes, platelet-Mon 1 and 3 aggregates, activated Mon 1 and 2 monocytes, and plasma levels of MCP-1/CCL2 and CX_3CL1 are all elevated in patients with PH. The OFL administration decreases different parameters

Three monocyte subpopulations have been described in peripheral blood based on their differential expression of the cell surface markers CD14, CD16 and CCR2, as described in **Section 3.1.5.3.3** and **Table 7**. Whereas the percentage of circulating type 1 (Mon 1) and 2 (Mon 2) monocytes in blood was not different between patients and controls volunteers, as determined by flow cytometry, we found a significantly higher percentage of circulating type 3 (Mon 3) monocytes in the former group (**Figures 25A**, **D**, and **G**). When we analyzed platelet-monocyte aggregates, those established between platelets and Mon 1 and 3 monocytes were significantly elevated in patients with PH (**Figures 25B** and **H**), but no differences between groups were found in Mon 2 aggregates (**Figure 25E**). Moreover, the expression of CD11b integrin in Mon 1 and 2, but not in Mon 3 monocytes, was significantly higher in patients than in controls, indicating their activation state (**Figures 25C**, **F**, and **I**). Analysis of CX_3CR1 on the different monocyte subtypes from heparinized whole blood revealed that the percentage of Mon 1 monocytes expressing this receptor was significantly higher in patients than in controls (**Figure 25J**). After dissociating platelets with EDTA, we found that the percentage of all monocyte subtypes positive for CX_3CR1 was significantly higher in patients than in controls, with Mon 1 monocytes showing the highest percentage of CX_3CR1 expression (**Figure 25K**). In addition, the circulating levels of MCP-1/CCL2 and soluble fractalkine/CX_3CL1, ligands of CCR2 and CX_3CR1 receptors respectively and involved in mononuclear cell recruitment, were significantly higher in patients (**Figures 25L** and **M**), and a positive correlation was found between the circulating concentration of both chemokines and apoB, LDL, and TC levels in patients (**Figures 25N–S**).

After 4-hours OFL administration to PH patients, a significant decrease in the percentage of circulating monocytes could be observed, mainly in Mon 1 population (**Figure 25A**). In agreement with this observation, a marked decrease in MCP-1/CCL2 plasma levels was found in PH patients 4 hours after the OFL administration (**Figure 25L**).

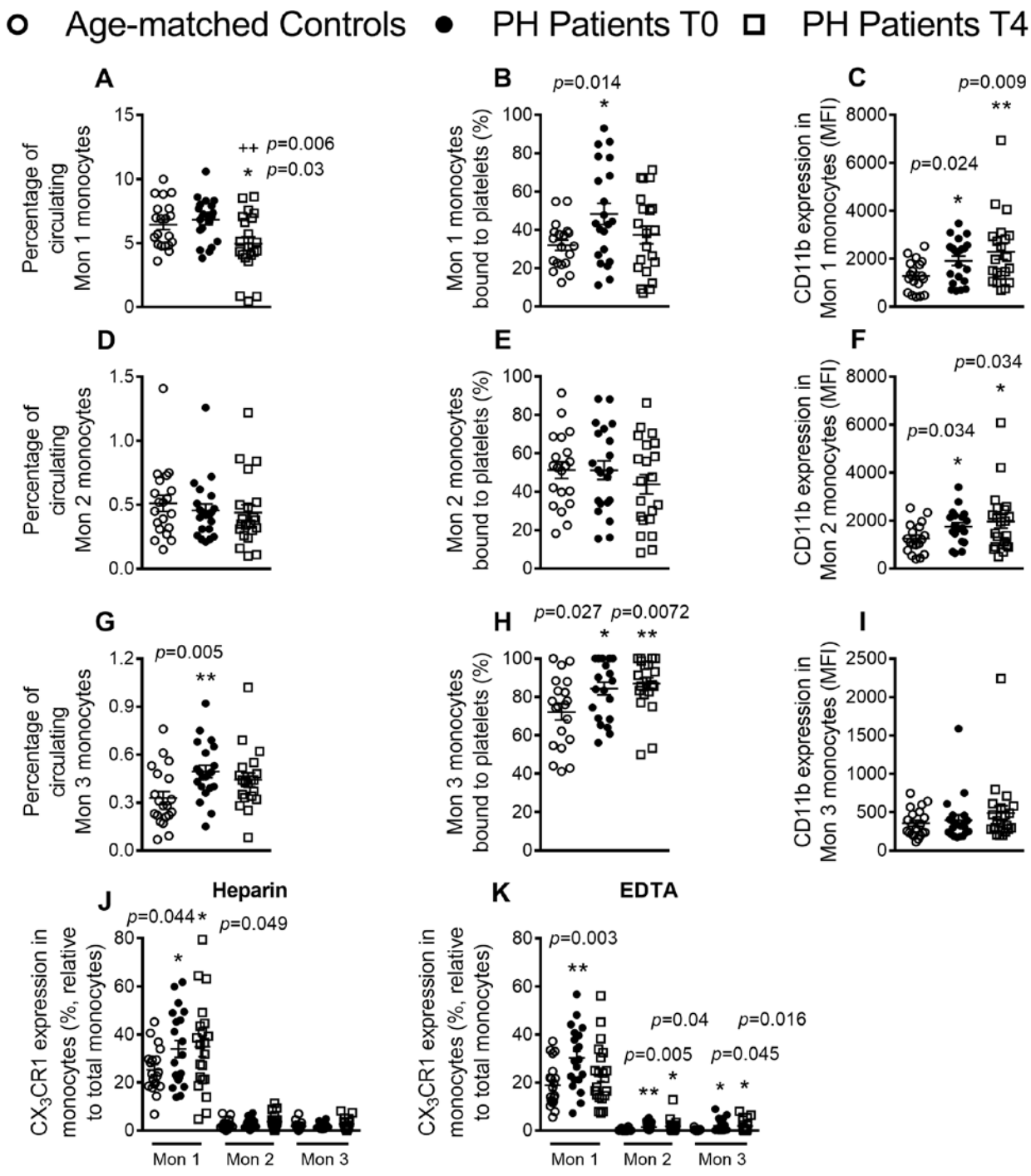
Age-matched Controls
PH Patients T0
PH Patients T4
A
Percentage of circulating Mon 1 monocytes
p=0.006
p=0.03
B
Mon 1 monocytes bound to platelets (%)
p=0.014
C
CD11b expression in Mon 1 monocytes (MFI)
p=0.024
p=0.009
D
Percentage of circulating Mon 2 monocytes
E
Mon 2 monocytes bound to platelets (%)
F
CD11b expression in Mon 2 monocytes (MFI)
p=0.034
p=0.034
G
Percentage of circulating Mon 3 monocytes
p=0.005
H
Mon 3 monocytes bound to platelets (%)
p=0.027
p=0.0072
I
CD11b expression in Mon 3 monocytes (MFI)
J
Heparin
CX3CR1 expression in monocytes (%, relative to total monocytes)
p=0.044
p=0.049
Mon 1
Mon 2
Mon 3
K
EDTA
CX3CR1 expression in monocytes (%, relative to total monocytes)
p=0.003
p=0.04
p=0.016
p=0.005
p=0.045
Mon 1
Mon 2
Mon 3

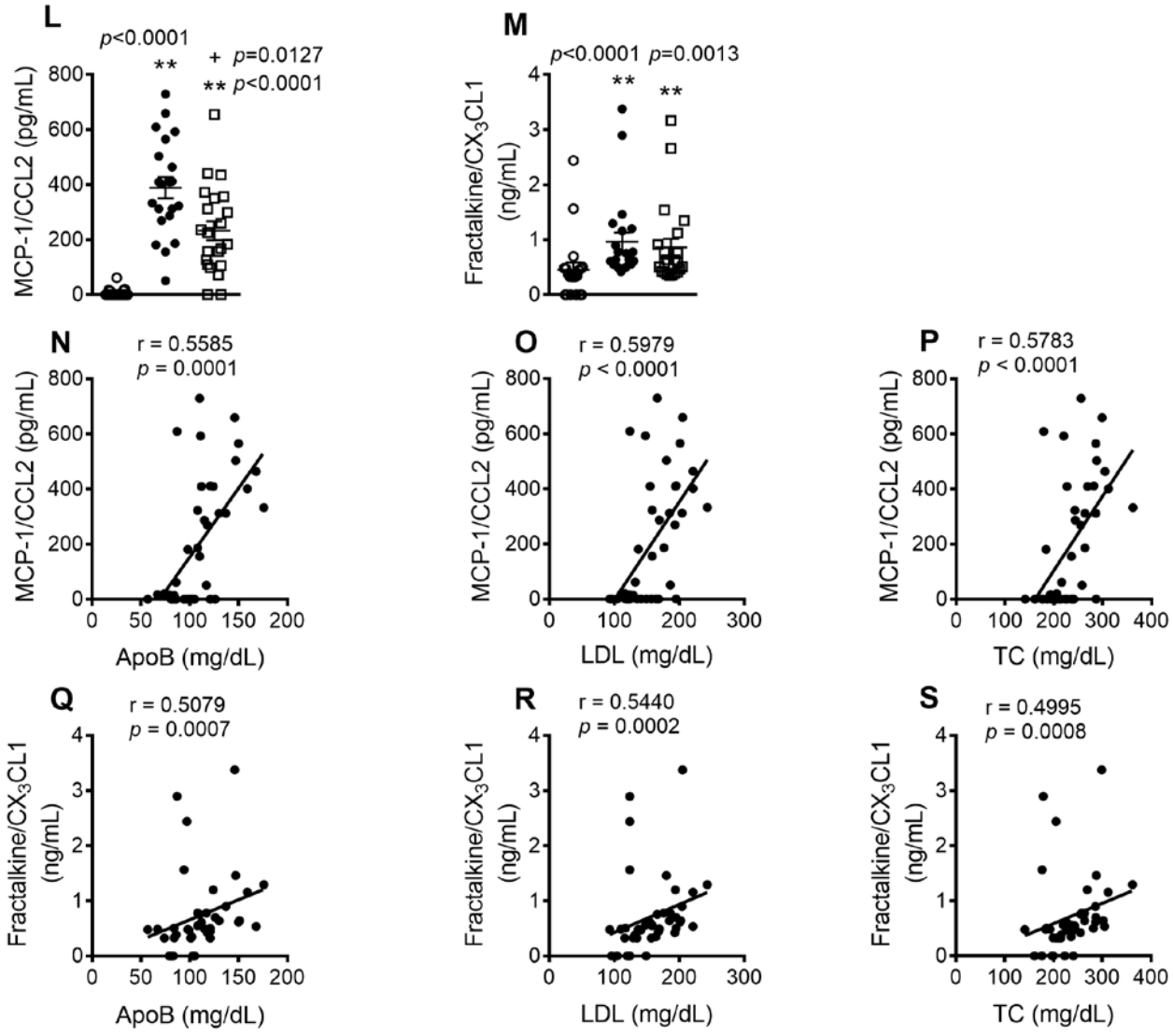

Figure 25. The percentage of circulating Mon 3 monocytes, platelet-Mon 1 and 3 aggregates, activated Mon 1 and 2 monocytes, and plasma levels of MCP-1/CCL2 and CX_3CL1, are elevated in PH patients. Some of these parameters are significantly affected by an OFL administration. Flow cytometry analysis of heparinized or EDTA-treated whole blood co-stained with specific markers for platelets and Mon 1, 2 and 3 monocytes (**A**, **B**, **D**, **E**, **G**, and **H**), CD11b integrin (**C**, **F**, and **I**), and also for CX_3CR1 in heparinized and EDTA-treated whole blood (**J** and **K**). Results are expressed as the percentage of positive cells or mean fluorescence intensity (MFI). MCP-1/CCL2 (**L**) and fractalkine/CX_3CL1 (**M**) plasma levels (pg or ng/mL) were measured by ELISA (n = 21 control subjects and n = 22 PH patients). Values are expressed as mean ± SEM. *p <0.05 or **p <0.01 relative to values in the control group. +p <0.05 or ++p <0.01 relative to values in the PH group at T0. Correlations between circulating MCP-1/CCL2 or fractalkine/CX_3CL1 and apoB (**N** and **Q**), LDL (**O** and **R**), and TC (**P** and **S**) plasma levels.

4.1.4 Circulating $CD4^+$ lymphocytes, platelet-lymphocyte ($CD4^+$ and $CD8^+$) aggregates and lymphocyte ($CD4^+$ and $CD8^+$) activation are significantly increased in patients with PH, but no changes in these parameters were detected after the OFL administration

Mature T cells express the general marker CD3, and also either CD4 or CD8 depending on the T cell type. Whereas no differences were found in circulating numbers of $CD3^+$ and $CD8^+$ lymphocytes between patients and controls, the number of $CD4^+$ lymphocytes was higher in the former group (**Figures 26A**, **D**, and **J**) and positively correlated with apoB, LDL, and TC levels (**Figures 26G–I**). Moreover, the percentage of $CD3^+$, $CD4^+$ and $CD8^+$ lymphocytes bound to platelets, and also their activation state ($CD69^+$), was higher in patients than in control subjects (**Figures 26B**, **C**, **E**, **F**, **K**, and **L**). Interestingly, a positive correlation was found between the percentage of $CD8^+CD69^+$ cells and the lipid profile (apoB, LDL, and TC levels) (**Figures 26M–O**).

Closer inspection of the different $CD4^+$ T lymphocyte subtypes revealed an increased number of circulating Th2 and Th17 lymphocytes, but not Th1 in PH patients (**Figures 27A**, **D**, and **G**). Furthermore, we found that the percentage of circulating platelet-Th lymphocyte aggregates of all three subtypes, as well as their activation state ($CD69^+$), was higher in patients than in controls (**Figures 27B**, **C**, **E**, **F**, **H**, and **I**). In contrast to $CD4^+$ cells, the percentage of circulating Treg lymphocytes (**Figure 27J**), as well as the Treg/Th17 ratio (**Figure 27L**), was significantly lower in patients. However, no differences were found between patients and controls in the percentage of circulating Treg lymphocyte-platelet aggregates (**Figure 27K**). Of note, whereas the circulating levels of IL-12, a cytokine involved in the differentiation of naïve T cells to Th1 lymphocytes, were significantly elevated in patients, plasma levels of IFNγ, a cytokine released by Th1 lymphocytes, were not different from those of control subjects (**Figures 27M** and **N**). By contrast, levels of the anti-inflammatory cytokines IL-4 and IL-10, which are mainly produced by Th2 and Treg lymphocytes, respectively, were significantly lower in the circulation of PH patients (**Figures 27O** and **P**). Indeed, an inverse correlation was found between IL-4 and IL-10 and the lipid profile associated with PH (**Figures 27Q–V**).

After the 4-hour OFL administration to PH patients, a tendency towards lower activation of $CD4^+$ lymphocytes was observed (**Figure 26F**); however, no significant differences were encountered when compared with T0 values in the remainder parameters determined either in global T cells (**Figures 26A**–**E**, **J**–**L**) or in the different Th lymphocyte subpopulations (**Figures 27A**–**I**). Of note, the percentage of circulating Treg lymphocytes was significantly increased 4 hours after the administration of the OFL (**Figure 27J**), although no differences in the percentage of Treg lymphocyte-platelet aggregates nor the Treg/Th17 ratio were found (**Figures 27K** and **L**, respectively). Plasma levels of the different soluble markers in the PH group were not affected by the administration of the OFL (**Figures 27M**–**P**).

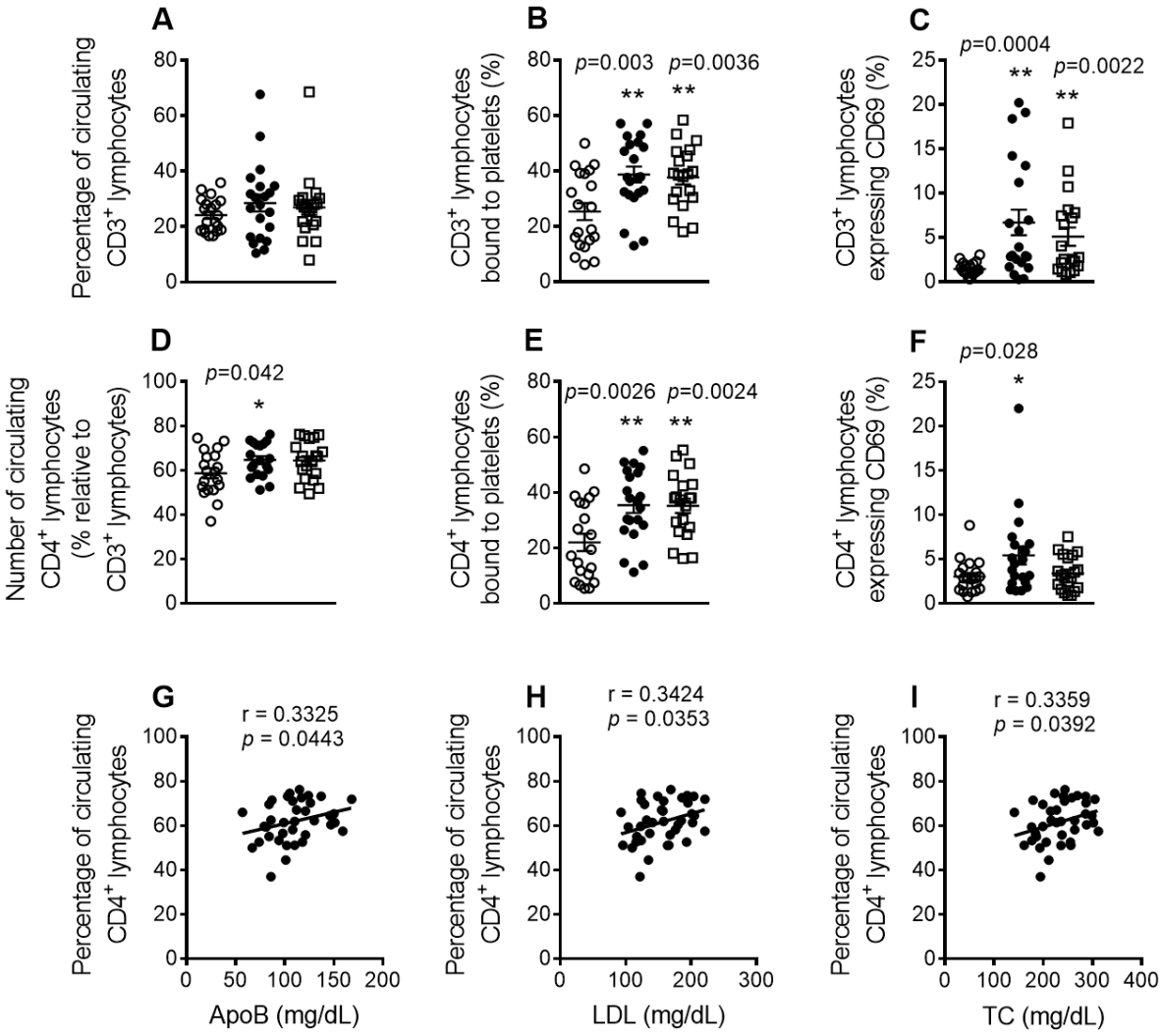

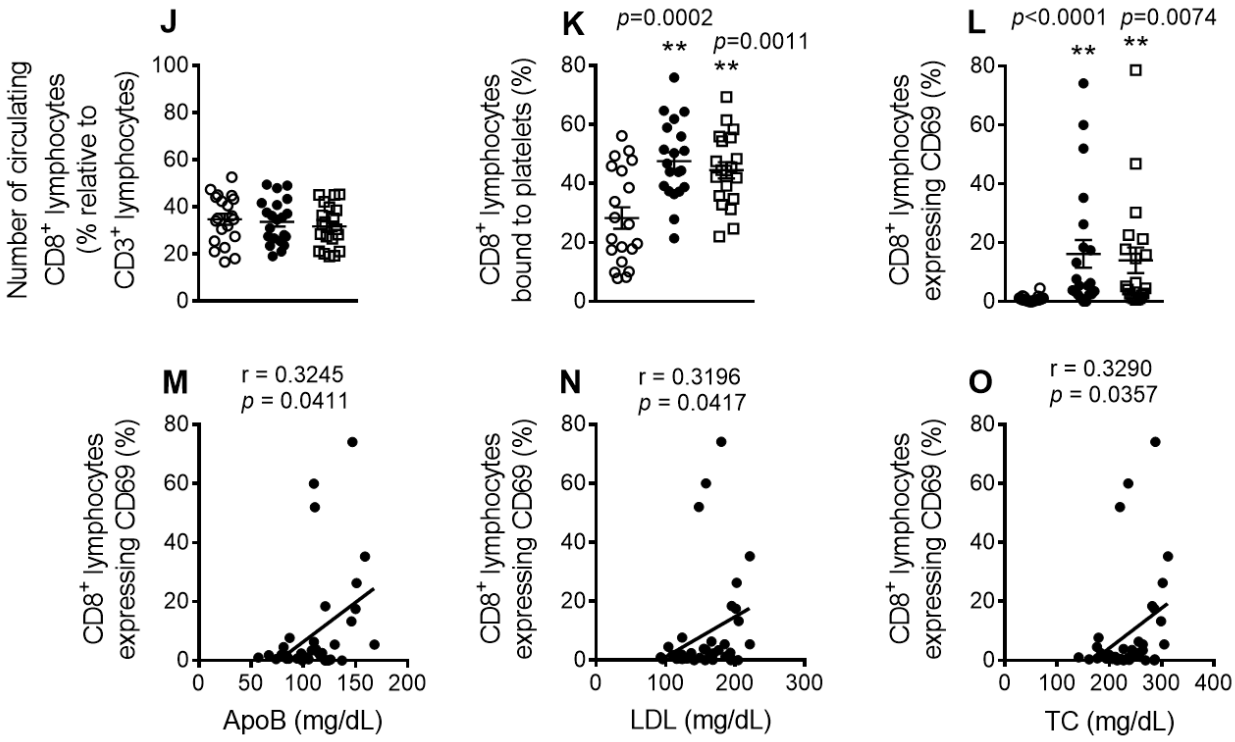

Figure 26. The percentage of circulating CD4⁺ lymphocytes, platelet-lymphocyte (CD4⁺ and CD8⁺) aggregates, and lymphocyte (CD4⁺ and CD8⁺) activation, are significantly elevated in patients with PH, but no changes in these parameters were detected after the OFL administration. Heparinized whole blood was co-stained with specific markers for CD3⁺, CD4⁺ and CD8⁺ lymphocytes (**A**, **B**, **D**, **E**, **J**, and **K**), as well as for CD69 (**C**, **F**, and **L**). Results are expressed as the percentage of positive cells (n = 21 control subjects and n = 22 PH patients). Values are expressed as mean ± SEM. *p <0.05 or **p <0.01 relative to values in the control group. Correlations between circulating CD4⁺ cells and activated CD8⁺ lymphocytes and apoB (**G** and **M**), LDL (**H** and **N**), and TC (**I** and **O**) plasma levels.

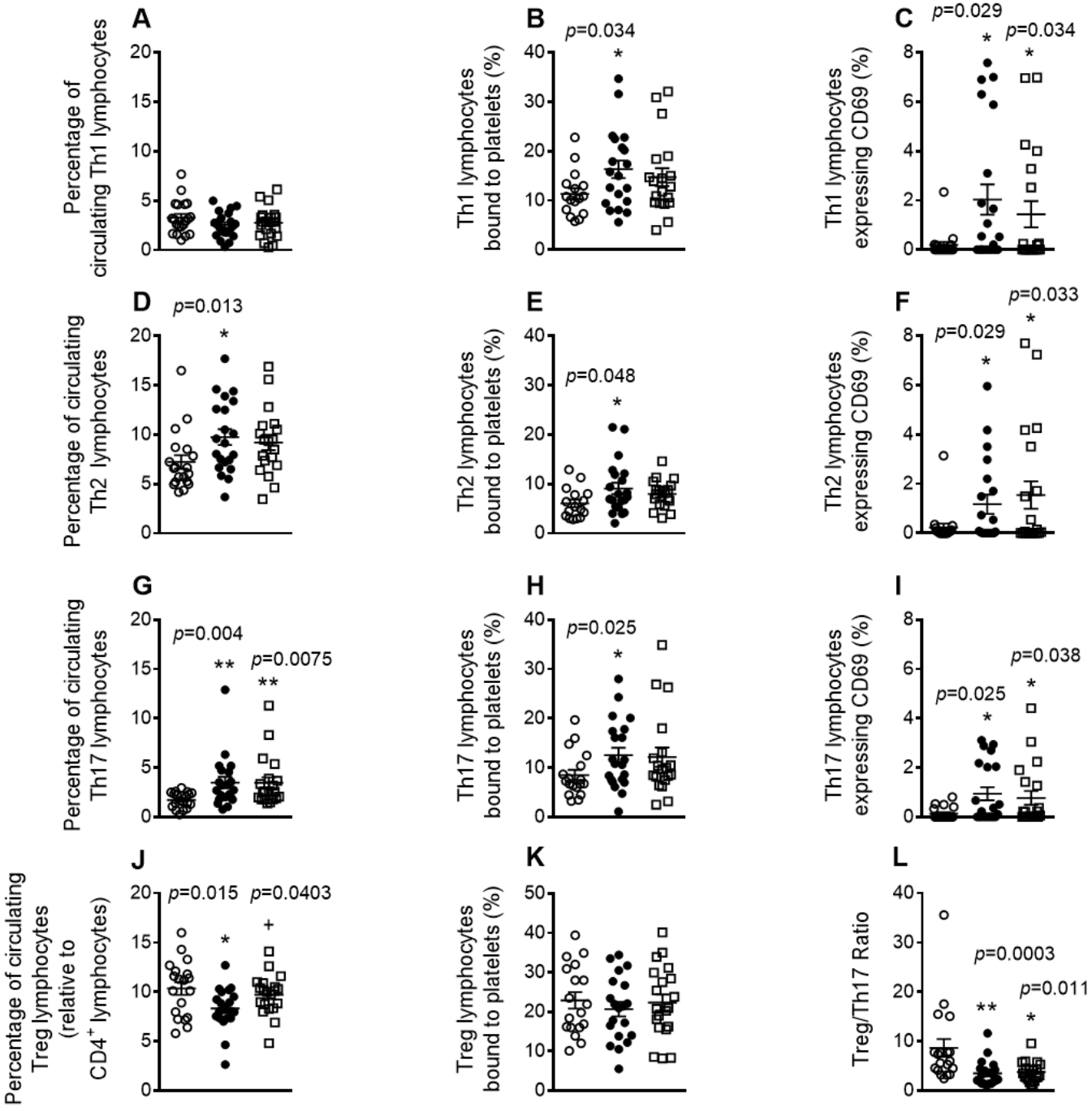
A
Percentage of circulating Th1 lymphocytes
B
Th1 lymphocytes bound to platelets (%)
p=0.034
C
Th1 lymphocytes expressing CD69 (%)
p=0.029
p=0.034
D
Percentage of circulating Th2 lymphocytes
p=0.013
E
Th2 lymphocytes bound to platelets (%)
p=0.048
F
Th2 lymphocytes expressing CD69 (%)
p=0.029
p=0.033
G
Percentage of circulating Th17 lymphocytes
p=0.004
p=0.0075
H
Th17 lymphocytes bound to platelets (%)
p=0.025
I
Th17 lymphocytes expressing CD69 (%)
p=0.025
p=0.038
J
Percentage of circulating Treg lymphocytes (relative to CD4+ lymphocytes)
p=0.015
p=0.0403
K
Treg lymphocytes bound to platelets (%)
L
Treg/Th17 Ratio
p=0.0003
p=0.011

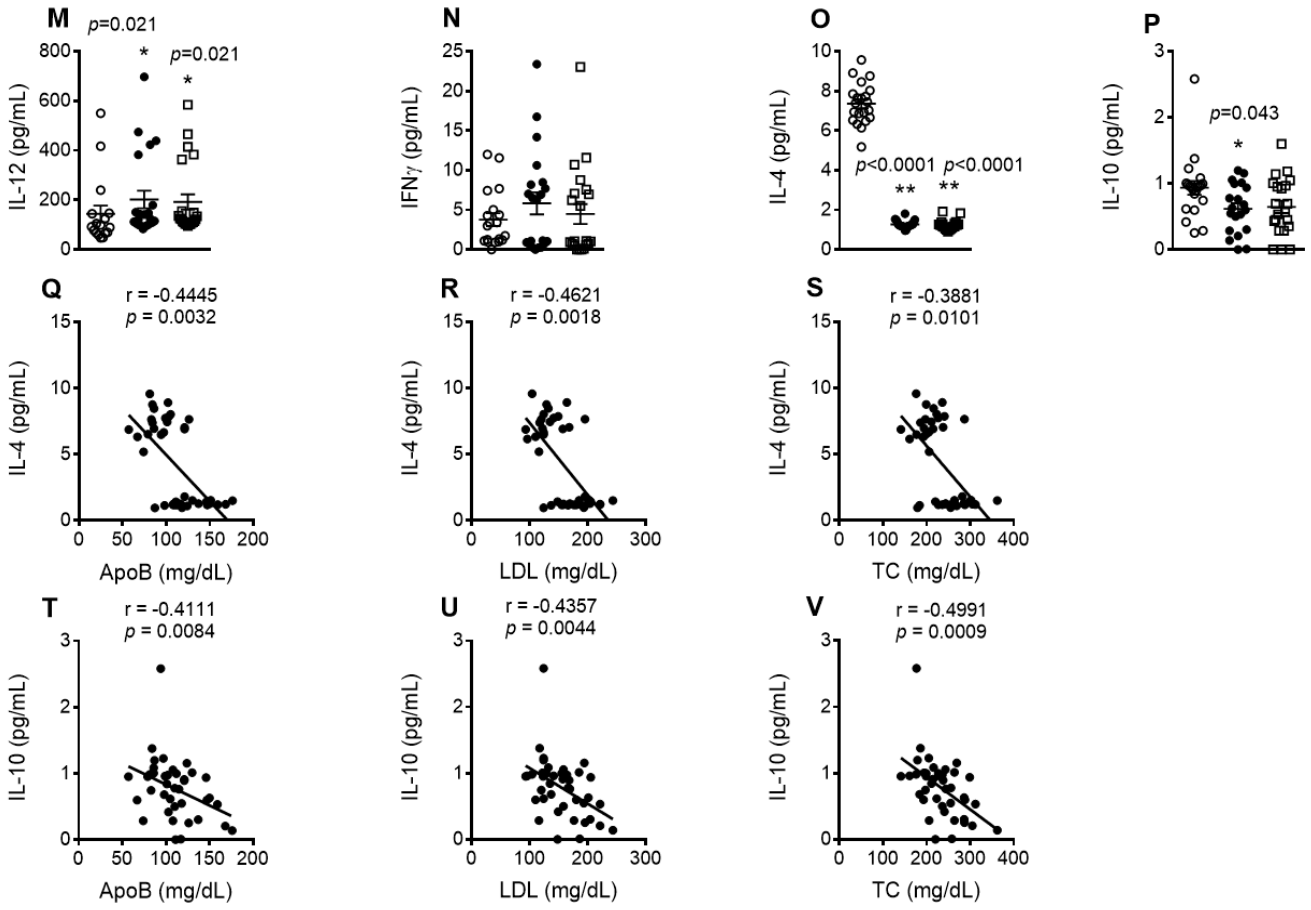

Figure 27. The percentage of circulating Th2 and Th17 lymphocytes, platelet-lymphocyte aggregates, lymphocyte activation and IL-12 circulating levels, are significantly increased in patients with PH, whereas the percentage of circulating Treg cells, Treg/Th17 ratio, and IL-4 and IL-10 plasma levels, are decreased. Administration of the OFL increased the percentage of circulating Treg cells in PH patients. Heparinized whole blood was co-stained with specific markers for platelets and Th1, Th2, Th17 and Treg lymphocytes (**A**, **B**, **D**, **E**, **G**, **H**, **J**, and **K**) as well as for CD69 (**C**, **F**, and **I**). Treg/Th17 ratio was also determined (**L**). Results are expressed as the percentage of positive cells. IL-12 (**M**), IFNγ (**N**), IL-4 (**O**), and IL-10 (**P**) plasma levels (pg/mL) were measured by ELISA (n = 21 control subjects and n = 22 PH patients). Values are expressed as mean ± SEM. *p <0.05 or **p <0.01 relative to values in the control group. +p <0.05 relative to values in the PH group at T0. Correlations between circulating IL-4 or IL-10 and apoB (**Q** and **T**), LDL (**R** and **U**), and TC (**S** and **V**) plasma levels.

4.1.5 Circulating levels of proinflammatory cytokines but no adipokines are increased in PH patients. TNFα plasma levels in PH are decreased by the OFL administration

Th17 lymphocytes produce TNFα and IL-6 (Olson *et al.* 2013), and an increase in the plasma levels of these proinflammatory cytokines has been reported before in patients with PH (Sampietro *et al.* 1997, Real *et al.* 2010a, Holven *et al.* 2014). We noted similar findings in our patient cohort (**Figures 28A** and **B**). Moreover, a positive association was found between IL-6 plasma levels and the levels of circulating apoB, LDL, and TC (**Figures 28C–E**). By contrast, no differences were found for the circulating levels of adiponectin, leptin or ghrelin between patients and controls (**Figures 28F–H**).

Of note, TNFα circulating levels were significantly reduced 4 hours after the administration of the OFL (**Figure 28A**), without affecting the plasma levels of IL-6 or the adipokines investigated (**Figures 28B**, **F**, **G**, and **H**).

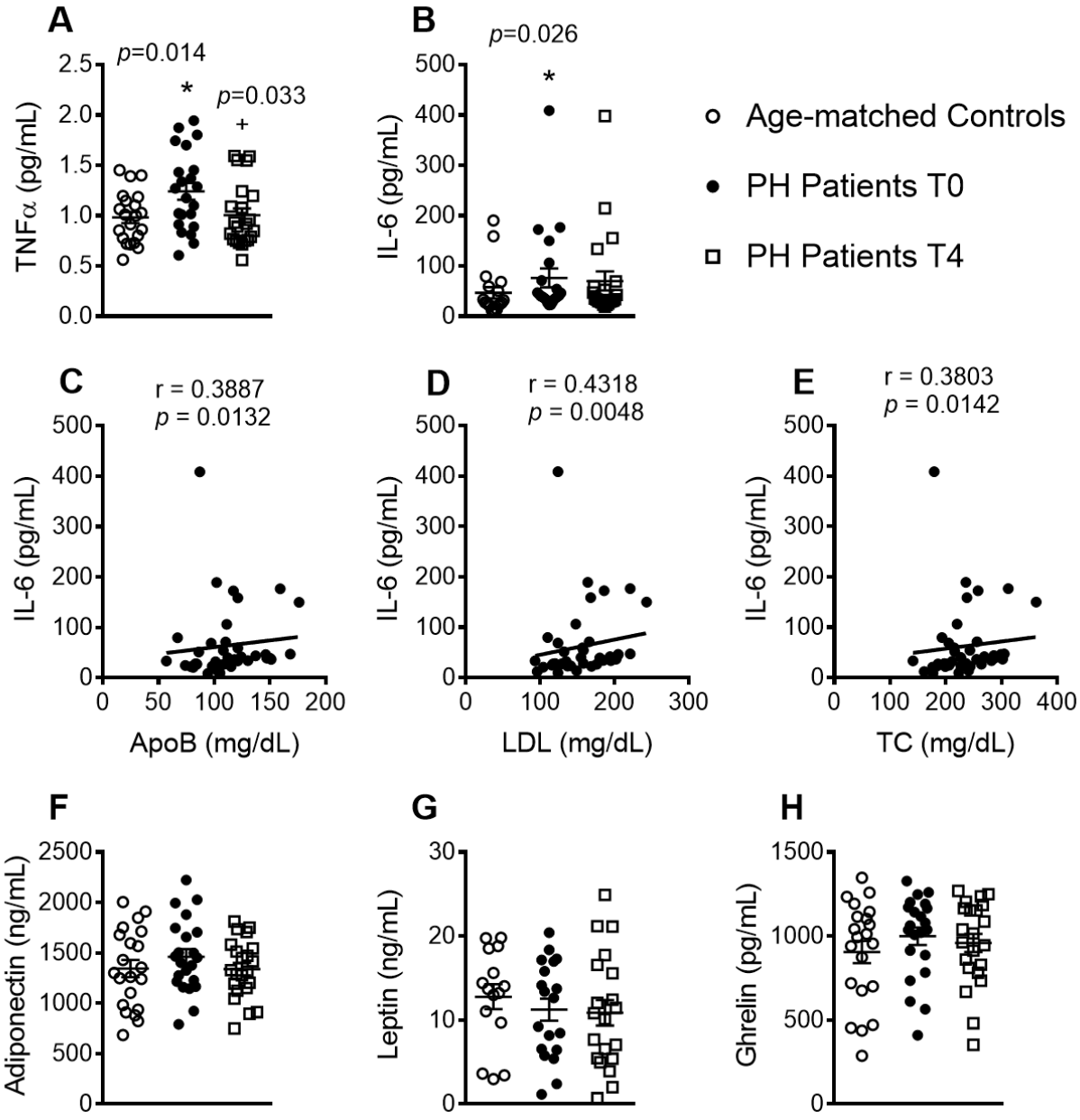

Figure 28. Increased circulating levels of proinflammatory cytokines but no adipokines in patients with PH. Administration of the OFL to PH patients reduced the circulating levels of TNFα. TNFα (**A**), IL-6 (**B**), adiponectin (**F**), leptin (**G**), and ghrelin (**H**) plasma levels (pg or ng/mL) were measured by ELISA (n = 21 control subjects and n = 22 PH patients). Values are expressed as mean ± SEM. *p <0.05 relative to values in the control group. +p <0.05 relative to values in the PH group at T0. Correlations between circulating IL-6 and apoB (**C**), LDL (**D**), and TC (**E**) plasma levels.

4.1.6 Circulating platelet-leukocyte aggregates and leukocytes from PH patients have increased adhesiveness to TNFα-stimulated HUAEC which is diminished by the OFL administration

Endothelial dysfunction is one of the earliest stages of atherogenesis and leads to the adhesion and the subsequent migration of leukocytes (Landmesser *et al.* 2004). Because TNFα is a central cytokine/adipokine in hypercholesterolemia (Sampietro *et al.* 1997, Hansen *et al.* 2019), we next explored the functional consequences of the elevated levels of TNFα in patients with PH. We first examined the adhesion of platelet-leukocyte aggregates and leukocytes alone to unstimulated or TNFα-stimulated HUAEC under dynamic flow conditions. To accomplish this, experiments were carried out with heparinized or EDTA-treated whole blood, which promotes the dissociation of platelets from leukocytes.

When heparinized, diluted whole blood from patients and controls was perfused across unstimulated HUAEC, leukocyte adhesiveness was significantly higher in the PH group (**Figure 29A**). After exposure of HUAEC to TNFα for 24 h, leukocyte adhesiveness increased in both groups and remained markedly elevated in the PH group (**Figure 29A**). Importantly, when platelets were disaggregated from leukocytes with EDTA, leukocyte adhesion was still considerably greater in the PH group than in the control group (**Figure 29B**), despite the significant decrease in the number of adhered leukocytes to stimulated HUAEC after platelet disaggregation (**Figures 29A** and **B**). In agreement with these observations, immunofluorescence studies revealed enhanced adherent platelet-leukocyte complexes to TNFα-stimulated endothelial cells from PH patients compared with age-matched controls (**Figures 29C** and **D**). Furthermore, when platelets were disaggregated from leukocytes with EDTA, leukocyte adhesion to TNFα-stimulated HUAEC was notably diminished, but this parameter was markedly higher in the PH group than in the control one (**Figures 29E** and **F**).

Interestingly, 4 hours after the OFL administration to patients with PH, a significant decrease in the number of leukocytes adhered to the endothelium was detected, either in heparinized or in platelet-disaggregated whole blood (**Figures 29A** and **B**).

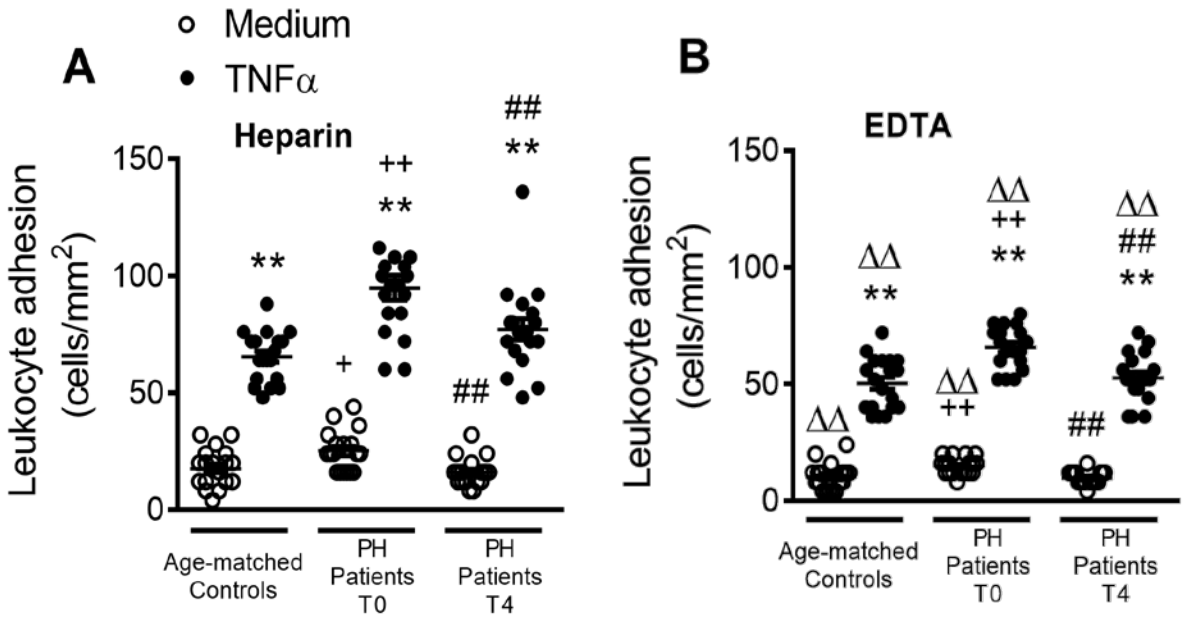
A
Medium
TNFα
Heparin
Leukocyte adhesion (cells/mm2)
150
100
50
0
**
+
++
**
##
**
Age-matched Controls
PH Patients T0
PH Patients T4
B
EDTA
Leukocyte adhesion (cells/mm2)
150
100
50
0
ΔΔ
**
ΔΔ
++
ΔΔ
++
**
##
ΔΔ
##
**
Age-matched Controls
PH Patients T0
PH Patients T4

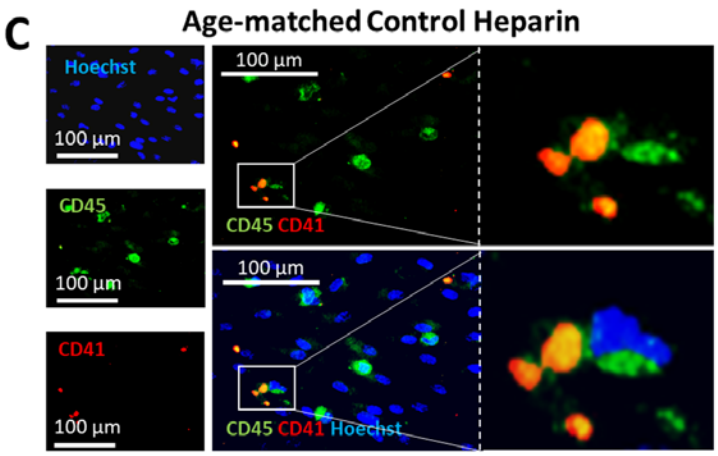
C
Age-matched Control Heparin
Hoechst
100 µm
CD45
CD41
CD45 CD41
CD45 CD41 Hoechst

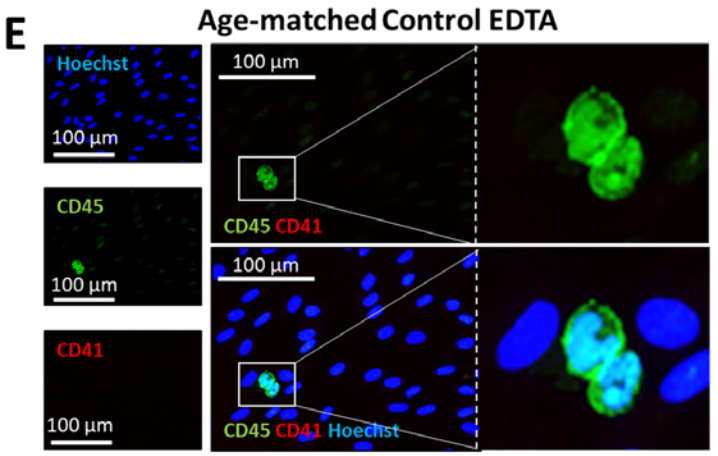
E
Age-matched Control EDTA
Hoechst
100 µm
CD45
CD41
CD45 CD41
CD45 CD41 Hoechst

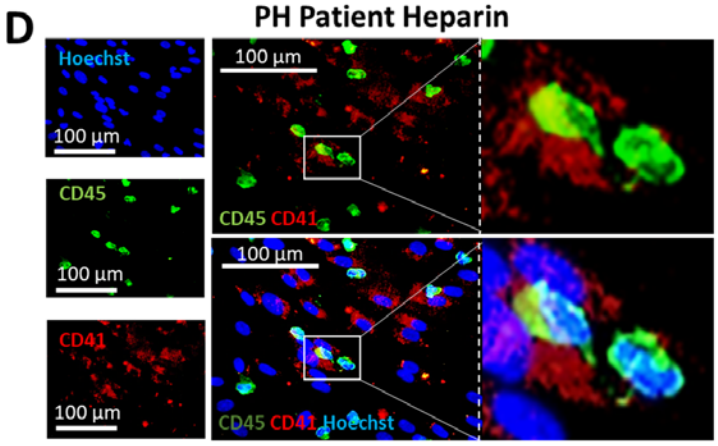
D
PH Patient Heparin
Hoechst
100 µm
CD45
CD41
CD45 CD41
CD45 CD41 Hoechst

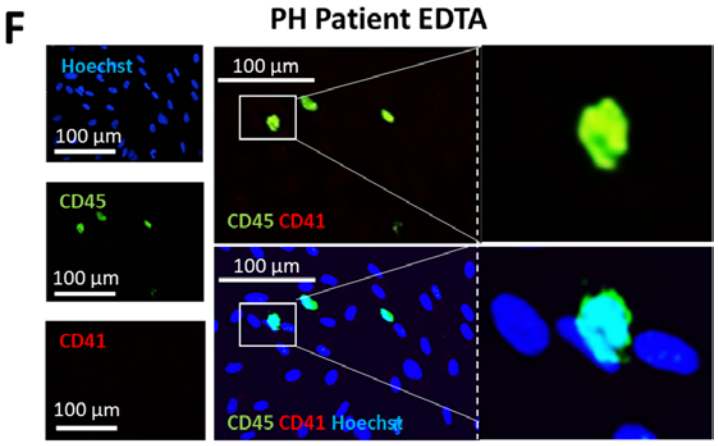
F
PH Patient EDTA
Hoechst
100 µm
CD45
CD41
CD45 CD41
CD45 CD41 Hoechst

Figure 29. Circulating platelet-leukocyte aggregates and leukocytes from PH patients show increased adhesiveness to TNFα-stimulated HUAEC, which is decreased by the OFL administration. HUAEC were stimulated or not with TNFα (20 ng/mL) for 24 h. Subsequently, whole blood from patients and controls, incubated without (**A**) or with EDTA (**B**), was perfused over the endothelial monolayers for 7 min at 0.5 dyn/cm^2 and leukocyte adhesion quantified (cells/mm^2). Values are expressed as mean ± SEM (n = 21 control subjects and n = 22 PH patients). **p <0.01 relative to values in the medium group; ##p <0.01 relative to respective values at T0; +p <0.05 or ++p <0.01 relative to respective values in the control group; ΔΔp <0.01 relative to respective values in the heparin group. Immunofluorescence analysis showing adherent platelet-leukocyte complexes to TNFα-stimulated HUAEC (**C**–**F**). Cells were incubated for 1 hour at 37ºC with heparinized whole blood from age-matched controls and patients with PH incubated with or without EDTA. Then, cells were fixed with 4% PFA and blocked in PBS containing 1% BSA. After that, cells were incubated for 2 h with an Alexa Fluor® 488-conjugated mouse mAb against human CD45 (1:50 dilution, green) and an APC-conjugated mAb against human CD41 (1:50 dilution, red). Nuclei of endothelial cells and leukocytes were stained with Hoechst dye (1:4000, blue). Images were captured with an Axio Observer A1 fluorescence microscope (ZEISS International).

4.2 STUDY OF THE ROLE OF CCL11/CCR3 AXIS IN PH AND ATHEROSCLEROSIS DEVELOPMENT

4.2.1 Increased circulating plasma levels of eotaxin-1/CCL11 and eotaxin-3/CCL26 and decreased plasma levels of IL-5 in patients with PH compared to age-matched controls

First, plasma levels of eotaxin-1/CCL11, eotaxin-2/CCL24, eotaxin-3/CCL26, IL-5, IL-13, IL-25, and IL-33 were determined by ELISA in 21 control subjects and 22 PH patients. Surprisingly, increased levels of circulating eotaxin-1/CCL11 and eotaxin-3/CCL26 were detected in PH patients compared to control volunteers (**Figures 30A** and **C**). Additionally, both of them positively correlated with three clinical features of PH such as apoB, LDL, and TC plasma content (**Figures 30D**–**I**). Nevertheless, no differences were found between groups in circulating levels of eotaxin-2/CCL24 (**Figure 30B**).

Since eotaxin-1/CCL11 and eotaxin-3/CCL26 signal exclusively through the CCR3 receptor, which is constitutively expressed at high levels in eosinophils (Daugherty *et al.* 1996), we next determined circulating levels of other eosinophil-related cytokines. Unexpectedly, plasma concentrations of IL-5 were notably lower in patients with PH than in age-matched controls (**Figure 30J**). In contrast, no significant differences were detected between both groups in plasma levels of IL-13, IL-25 or IL-33 (**Figures 30K**–**M**).

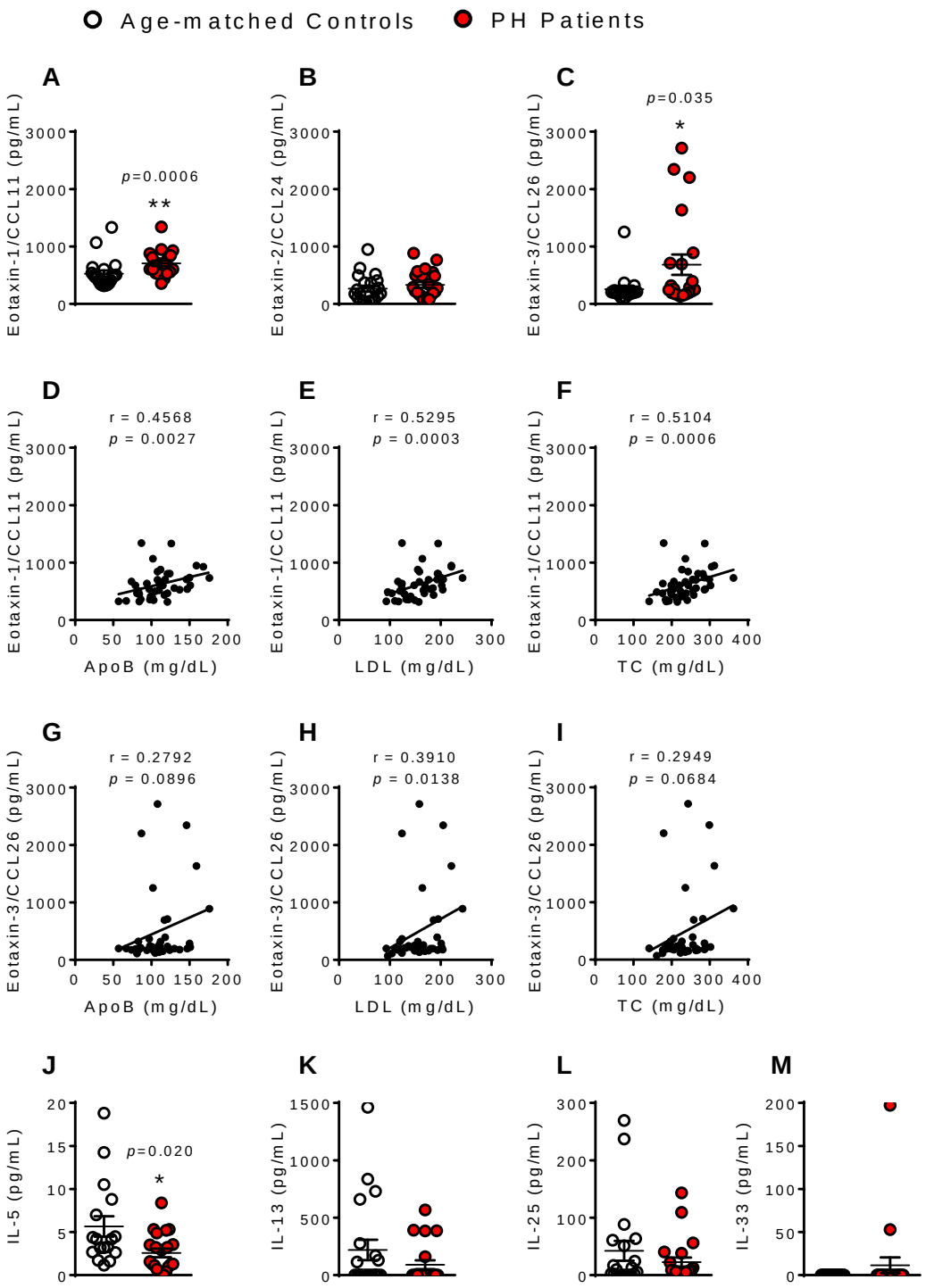

Figure 30. Increased circulating plasma levels of eotaxin-1/CCL11 and eotaxin-3/CCL26 and decreased plasma levels of IL-5 in patients with PH compared to age-matched controls. Eotaxin-1/CCL11 (**A**), eotaxin-2/CCL24 (**B**), eotaxin-3/CCL26 (**C**), IL-5 (**J**), IL-13 (**K**), IL-25 (**L**), and IL-33 (**M**) plasma levels (pg/mL) were determined by ELISA (n = 21 control subjects and n = 22 PH patients). Values are expressed as mean ± SEM. *p <0.05 or **p <0.01 relative to values in the control group. Correlations between circulating eotaxin-1/CCL11 and eotaxin-3/CCL26 plasma levels and apoB (**D** and **G**), LDL (**E** and **H**), and TC (**F** and **I**).

4.2.2 The percentage of circulating CCR3-expressing cells were significantly increased in PH patients compared with control subjects

CCR3 receptor serves as the primary chemokine receptor responsible for eosinophil trafficking to tissues in diseased and healthy conditions (Daugherty *et al.* 1996); therefore, we next evaluated CCR3 expression in different CCR3-expressing leukocytes in PH patients and age-matched controls.

Increased percentage of CCR3-expressing leukocytes and enhanced CCR3 leukocyte expression were found in heparinized whole blood from PH patients compared with age-matched controls (Heparin; **Figures 31A** and **B**). Similar observations were detected when platelets were dissociated from leukocytes (EDTA; **Figures 31A** and **B**).

To determine which circulating CCR3-expressing cells were significantly elevated in PH patients, a more in-depth analysis of CCR3 expression on platelets and CCR3-expressing leukocytes was carried out. Platelets express functional CCR3 receptors (Clemetson *et al.* 2000); however, no differences between PH patients and age-matched controls were encountered in the percentage of circulating platelets (**Figure 31C**), the percentage of CCR3-expressing platelets (**Figure 31D**) or CCR3 platelet expression (**Figure 31E**).

When eosinophils were analyzed, we first found a significantly increased percentage of circulating eosinophils ($CCR3^+$) in PH patients compared with age-matched controls (**Figure 31F**). Nevertheless, CCR3 eosinophil expression was similar in PH patients and control volunteers (**Figure 31G**). Of note, the percentage of circulating eosinophils were found to positively correlate with apoB, LDL, and TC plasma levels (**Figures 31H–J**).

Mast cells are resident tissue cells that, when activated, express the CCR3 receptor (Price *et al.* 2003). Nevertheless, progenitor mast cells, which are defined as $CD45^+Lin^-c\text{-}kit^+Fc\varepsilon RI\alpha^+$ cells (Nagai *et al.* 2013), also express the CCR3 receptor (Li *et al.* 2001). In this regard, we observed a significant increase in the percentage of circulating progenitor mast cells in PH patients compared to age-matched controls (**Figure 31K**). While an enhanced percentage of CCR3-expressing progenitor mast cells were encountered in PH individuals when platelets were dissociated (EDTA; **Figure 31L**), only an increased in CCR3 expression was detected in PH patients when platelets were bound (Heparin; **Figure 31M**).

In contrast, even though basophils also highly express the CCR3 receptor (Uguccioni *et al.* 1997), the percentage of circulating basophils was significantly lower in PH patients than in age-matched controls (**Figure 31N**). When platelets were dissociated from them (EDTA), increased percentage of circulating $CCR3^+$ basophils was found in PH individuals (**Figure 31O**), but then, no differences in CCR3 expression between the subjects investigated were detected (**Figure 31P**).

Finally, the expression of CCR3 was studied in Th2 lymphocytes, since they also express the CCR3 receptor (Sallusto *et al.* 1997). As illustrated in **Figure 31Q**, the percentage of circulating Th2 lymphocytes was unexpectedly higher in patients with PH than in age-matched controls. However, the percentage of $CCR3^+$ Th2 lymphocytes (EDTA; **Figure 31R**) and CCR3 expression in Th2 lymphocytes (EDTA; **Figure 31S**) was significantly lower in PH patients. In both cases, only when Th2 lymphocytes were unbound to platelets. Notably, while the number of circulating Th2 lymphocytes was positively correlated with plasma levels of apoB, LDL, and TC (**Figures 31T**–**V**), the percentage of CCR3-expressing Th2 cells was negatively correlated with these lipid parameters (**Figures 31W**–**Y**).

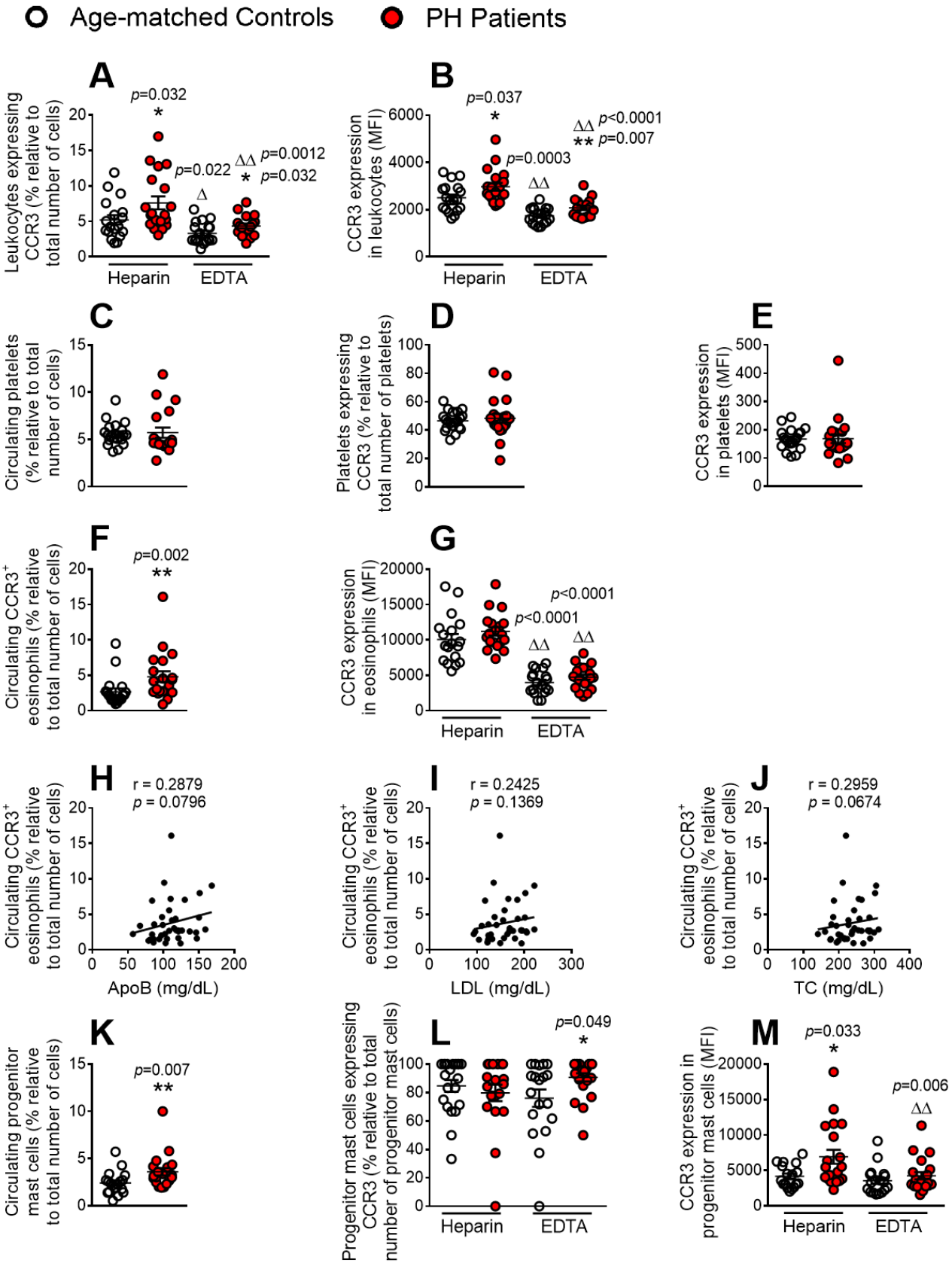
Age-matched Controls
PH Patients
A
Leukocytes expressing CCR3 (% relative to total number of cells)
p=0.032
p=0.022
p=0.0012
p=0.032
Heparin
EDTA
B
CCR3 expression in leukocytes (MFI)
p=0.037
p=0.0003
p<0.0001
p=0.007
C
Circulating platelets (% relative to total number of cells)
D
Platelets expressing CCR3 (% relative to total number of platelets)
E
CCR3 expression in platelets (MFI)
F
Circulating CCR3+ eosinophils (% relative to total number of cells)
p=0.002
G
CCR3 expression in eosinophils (MFI)
p<0.0001
p<0.0001
H
r = 0.2879
p = 0.0796
ApoB (mg/dL)
I
r = 0.2425
p = 0.1369
LDL (mg/dL)
J
r = 0.2959
p = 0.0674
TC (mg/dL)
K
Circulating progenitor mast cells (% relative to total number of cells)
p=0.007
L
Progenitor mast cells expressing CCR3 (% relative to total number of progenitor mast cells)
p=0.049
M
CCR3 expression in progenitor mast cells (MFI)
p=0.033
p=0.006

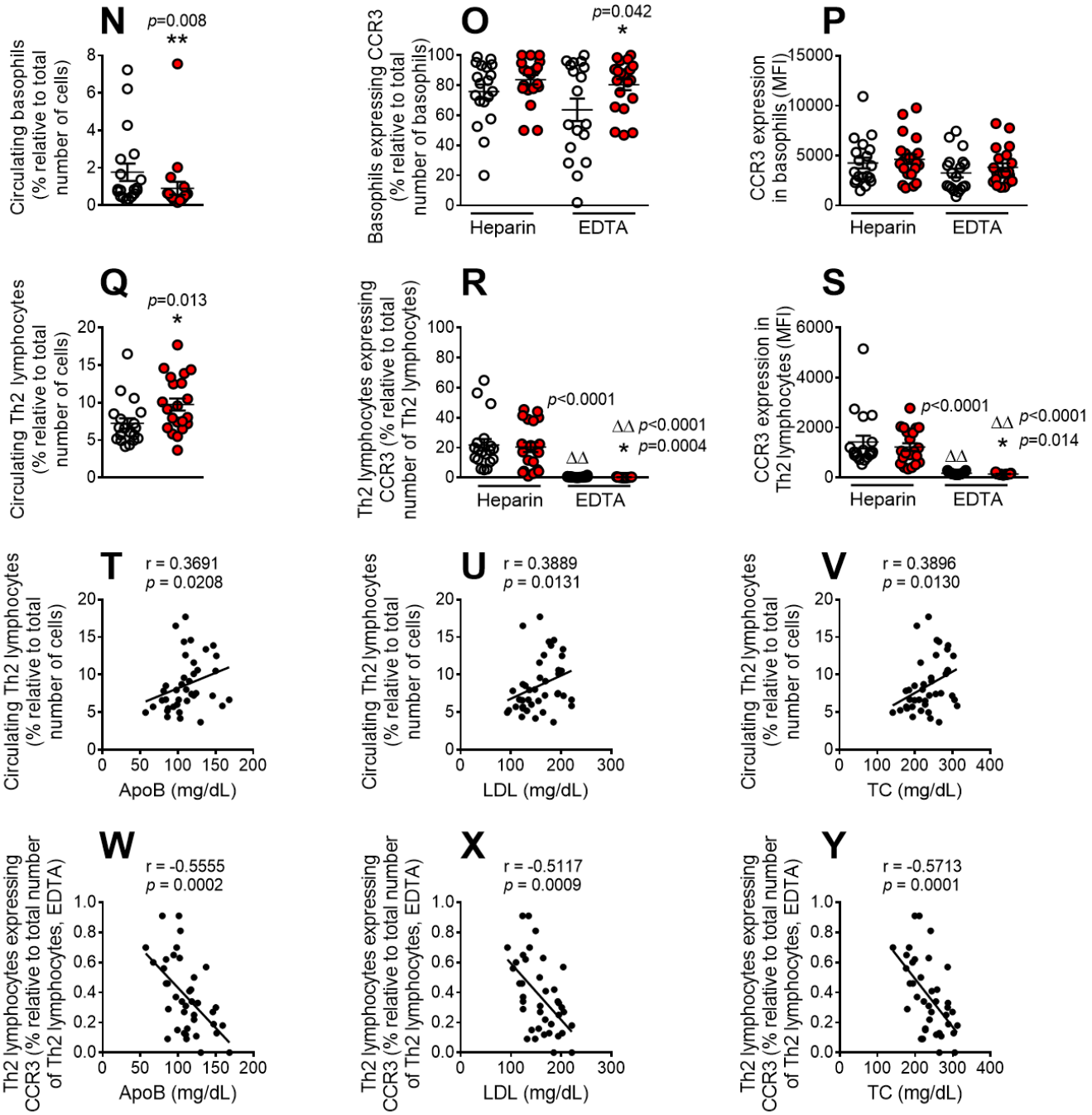

Figure 31. The percentage of circulating CCR3-expressing cells were significantly increased in PH patients compared with control subjects. Heparinized or EDTA-treated whole blood was co-stained with specific markers for leukocytes (**A** and **B**), platelets (**C**–**E**, **G**, **L**, **M**, **O**, **P**, **R**, and **S**), eosinophils (**F** and **G**), progenitor mast cells (**K**–**M**), basophils (**N**–**P**), and Th2 lymphocytes (**Q**–**S**), as well as CCR3 (**A**, **B**, **D**–**G**, **L**, **M**, **O**, **P**, **R**, and **S**), and analyzed by flow cytometry. Results are presented as MFI or the percentage of positive cells. Values are expressed as mean ± SEM (n = 21 control subjects and n = 22 PH patients). *p <0.05 or **p <0.01 relative to values in the control group. Δp <0.05 or $\Delta\Delta p$ <0.01 relative to values in the heparinized group. Correlations between the percentage of circulating eosinophils, Th2 lymphocytes, circulating CCR3-expressing Th2 cells and apoB (**H**, **T**, and **W**), LDL (**I**, **U**, and **X**), and TC (**J**, **V**, and **Y**).

4.2.3 The circulating levels of eotaxin-1/CCL11, the percentage of circulating CCR3-expressing leukocytes and eosinophils were significantly increased in atherogenic diet-fed apoE$^{-/-}$ animals, while plasma levels of IL-4 were decreased under atherogenic conditions

We next measured circulating levels of eotaxin-1/CCL11, eotaxin-2/CCL24, IL-4, and IL-5 by ELISA in apoE$^{-/-}$ mice fed with a high-fat diet or a control diet for two months. Remarkably, and in agreement with human data, elevated plasma levels of eotaxin-1/CCL11 were observed in apoE$^{-/-}$ mice fed with a high-fat diet for two months (**Figure 32A**), whereas plasma levels of IL-4 were notably decreased (**Figure 32C**). No significant differences were detected between groups in plasma levels of eotaxin-2/CCL24 (**Figure 32B**) and IL-5 (**Figure 32D**).

Then, we evaluated the percentage of different circulating leukocyte subpopulations expressing CCR3 by flow cytometry. In heparinized whole blood, increased percentage of CCR3-expressing leukocytes and an enhanced CCR3 leukocyte expression were found in apoE$^{-/-}$ mice fed with an atherogenic diet (**Figures 32E** and **F**).

The percentage of circulating SiglecF^{+} eosinophils and the percentage of SiglecF^{+}CCR3^{+} eosinophils was increased in atherogenic diet-fed apoE$^{-/-}$ mice (**Figures 32G** and **H**); however, no differences were found in the percentage of circulating progenitor mast cells between groups (**Figure 32J**). Additionally, there were neither differences in CCR3 eosinophil expression (**Figure 32I**), nor in the percentage of progenitor mast cells expressing CCR3 between groups (**Figures 32K** and **L**).

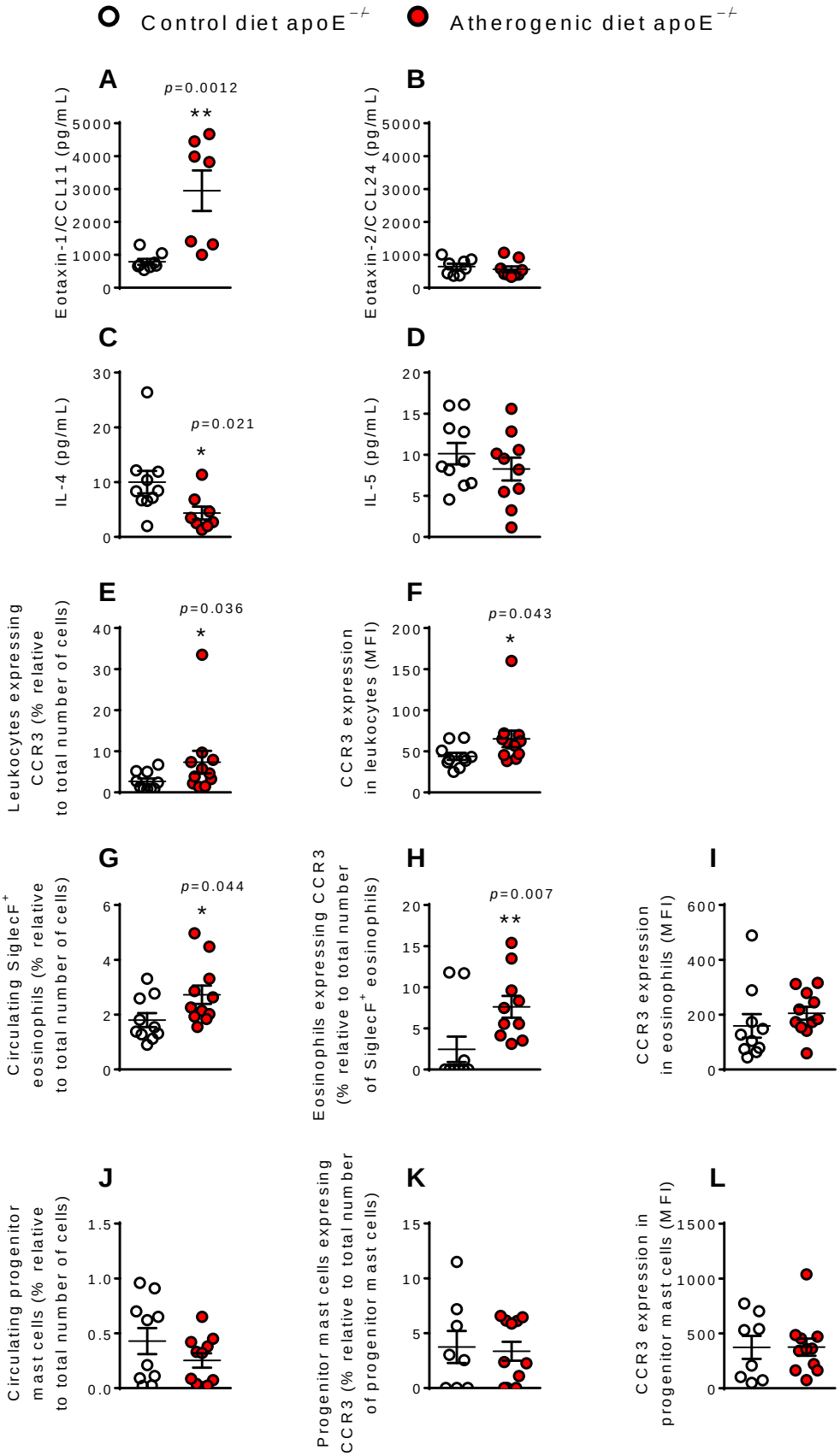
Control diet apoE−/−
Atherogenic diet apoE−/−
A
p=0.0012
**
Eotaxin-1/CCL11 (pg/mL)
5000
4000
3000
2000
1000
0
B
Eotaxin-2/CCL24 (pg/mL)
5000
4000
3000
2000
1000
0
C
p=0.021
*
IL-4 (pg/mL)
30
20
10
0
D
IL-5 (pg/mL)
20
15
10
5
0
E
p=0.036
*
Leukocytes expressing CCR3 (% relative to total number of cells)
40
30
20
10
0
F
p=0.043
*
CCR3 expression in leukocytes (MFI)
200
150
100
50
0
G
p=0.044
*
Circulating SiglecF+ eosinophils (% relative to total number of cells)
6
4
2
0
H
p=0.007
**
Eosinophils expressing CCR3 (% relative to total number of SiglecF+ eosinophils)
20
15
10
5
0
I
CCR3 expression in eosinophils (MFI)
600
400
200
0
J
Circulating progenitor mast cells (% relative to total number of cells)
1.5
1.0
0.5
0.0
K
Progenitor mast cells expresing CCR3 (% relative to total number of progenitor mast cells)
15
10
5
0
L
CCR3 expression in progenitor mast cells (MFI)
1500
1000
500
0

Figure 32. The circulating levels of eotaxin-1/CCL11, the percentage of circulating CCR3-expressing leukocytes and eosinophils were significantly increased in atherogenic diet-fed apoE$^{-/-}$ animals, while plasma levels of IL-4 were decreased under atherogenic conditions. ApoE$^{-/-}$ mice were subjected to a control or an atherogenic diet for two months. Eotaxin-1/CCL11 (**A**), eotaxin-2/CCL24 (**B**), IL-4 (**C**), and IL-5 (**D**) plasma levels (pg/mL) were determined by ELISA. Heparinized whole blood was co-stained with specific markers for leukocytes (**E** and **F**), eosinophils (**G**–**I**), and progenitor mast cells (**J**–**L**), as well as CCR3 (**E**, **F**, **H**, **I**, **K**, and **L**), and analyzed by flow cytometry. Results are presented as MFI or the percentage of positive cells (n = 7–11 animals per group). Values are expressed as mean ± SEM. *p <0.05 or **p <0.01 relative to values in the control diet-fed group.

4.2.4 Two months with a high-fat diet markedly increased the atherosclerotic lesion formation, the inflammatory infiltrates and the synthesis of collagen fibers in apoE$^{-/-}$CCR3$^{-/-}$ animals compared with apoE$^{-/-}$CCR3$^{+/+}$ mice fed with the same diet

To investigate the relevance of the CCL11/CCR3 axis in atherosclerosis development, apoE$^{-/-}$CCR3$^{-/-}$ mice were generated. Then both, apoE$^{-/-}$CCR3$^{+/+}$ and apoE$^{-/-}$CCR3$^{-/-}$ mice were subjected to a high-fat diet for two months.

First, the study of the macroscopic lesion using the Oil Red-O staining from apoE$^{-/-}$CCR3$^{+/+}$ and apoE$^{-/-}$CCR3$^{-/-}$ mice revealed a clear increase in the atherosclerotic lesion either in the aortic arch or in the thoracic aorta in those animals subjected to a high-fat diet for two months (**Figures 33A**–**C**). Surprisingly, the lesion was significantly higher in apoE$^{-/-}$CCR3$^{-/-}$ mice than in apoE$^{-/-}$CCR3$^{+/+}$ fed with the atherogenic diet (**Figures 33A**–**C**). In contrast, no differences between groups were found when they were subjected to a control diet for the same period (**Figures 33A**–**C**).

The quantification of the atherosclerotic lesion in the aortic sinus showed similar results (**Figures 33D**–**F**). ApoE$^{-/-}$CCR3$^{-/-}$ mice fed with an atherogenic diet had a significant increase in both, the intima/media ratio and lesion area compared to their respective controls (apoE$^{-/-}$CCR3$^{+/+}$; **Figures 33D**–**F**). These two parameters were enhanced by 45% and 26%, respectively, in apoE$^{-/-}$CCR3$^{-/-}$ mice *vs.* apoE$^{-/-}$CCR3$^{+/+}$ mice (**Figures 33E** and **F**).

Immunohistochemical studies showed augmented infiltration of macrophages (Mac-3^{+} cells) and T lymphocytes (CD3^{+} cells) in the atherosclerotic lesion of mice fed with an atherogenic diet *vs.* that found in those subjected to a control diet (**Figures 33D**, **G**–**J**) in both genotypes. Again, both macrophage and T cell infiltration was significantly higher in

apoE$^{-/-}$CCR3$^{-/-}$ mice than in apoE$^{-/-}$CCR3$^{+/+}$ mice fed with a high-fat diet (46% and 55%, respectively; **Figures 33G** and **H**). The increase in T lymphocytes was mainly due to CD8^{+} lymphocytes (**Figure 33J**). In contrast, no differences were found in the number of infiltrated CD4^{+} lymphocytes between both genotypes (**Figure 33I**).

Although a significant increase in the synthesis of collagen fibers, necrotic *core* area, and infiltrated vascular SMC within the atherosclerotic lesion was detected in animals subjected to an atherogenic diet *vs.* those who do not (**Figures 33K**–**M**), only the collagen area was markedly enhanced in apoE$^{-/-}$CCR3$^{-/-}$ mice *vs.* apoE$^{-/-}$CCR3$^{+/+}$ mice subjected to a high-fat diet (**Figure 33K**).

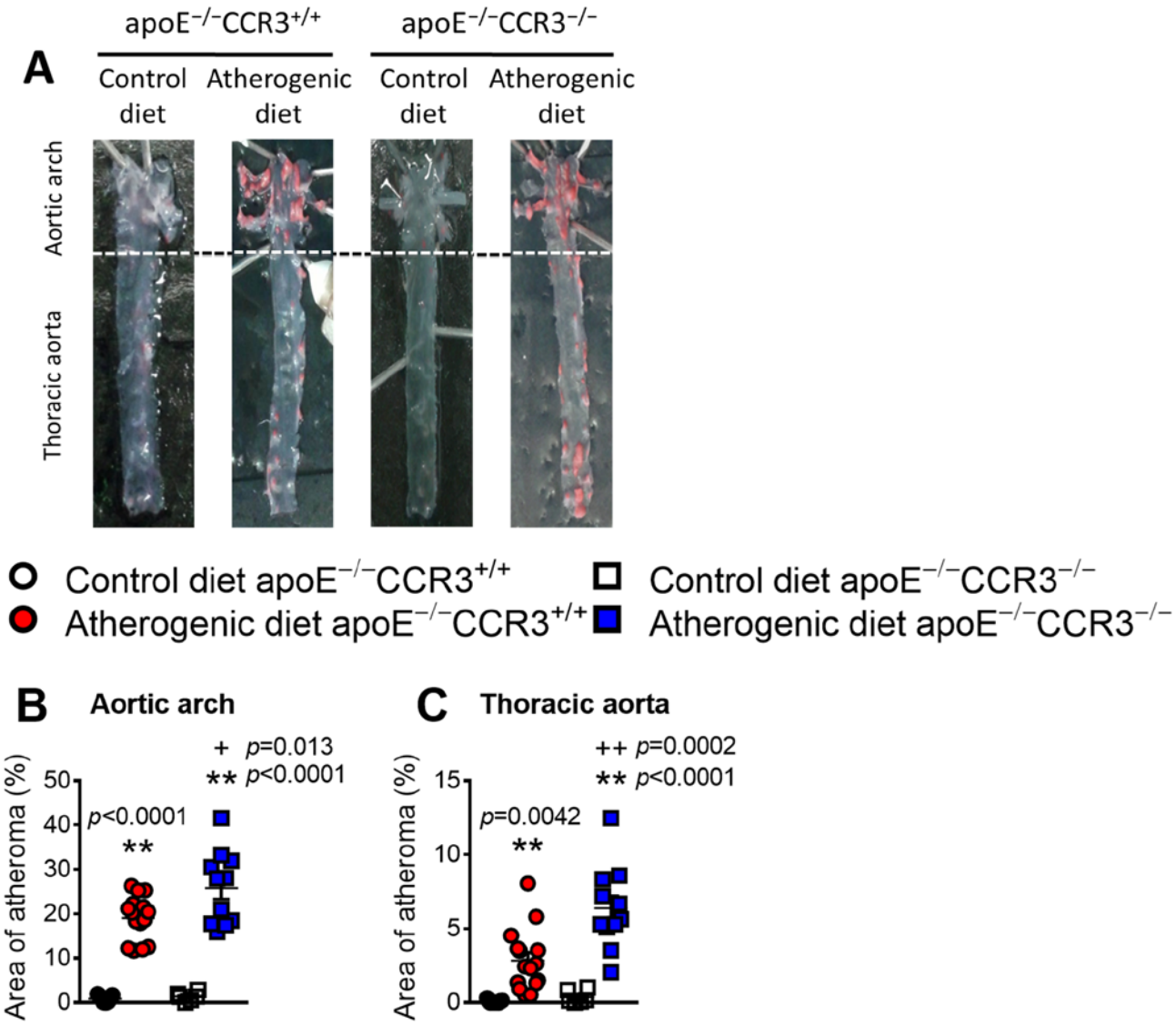

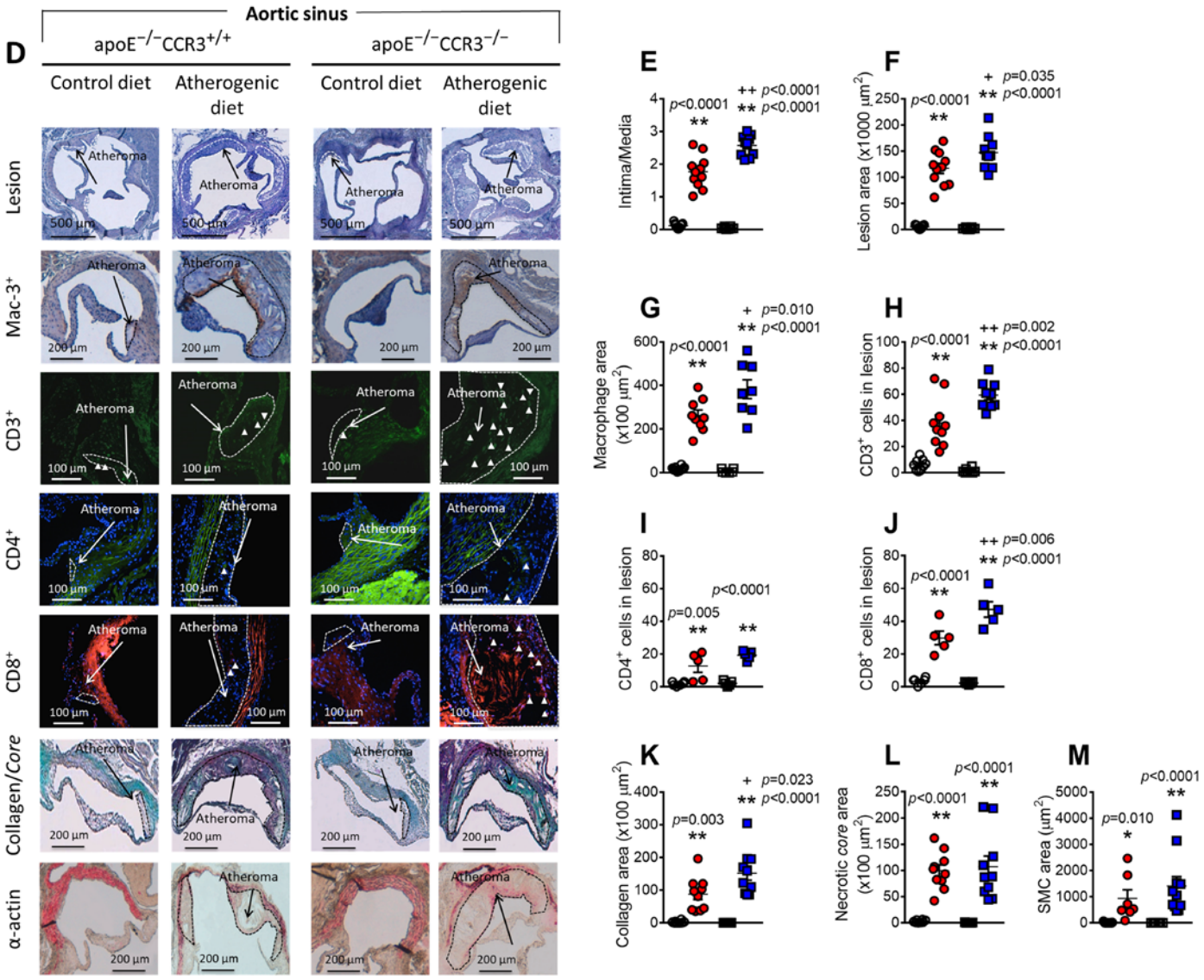

Figure 33. Two months with a high-fat diet markedly increased the atherosclerotic lesion formation, the inflammatory infiltrates and the synthesis of collagen fibers in apoE$^{-/-}$CCR3$^{-/-}$ animals compared with apoE$^{-/-}$CCR3$^{+/+}$ mice fed with the same diet. ApoE$^{-/-}$CCR3$^{+/+}$ and apoE$^{-/-}$CCR3$^{-/-}$ mice were subjected to a control or an atherogenic diet for two months. Representative images of Oil-Red stained aortas (**A**), atheroma lesion in the aortic arch (**B**), and in the thoracic aorta (**C**). The discontinuous lines delineate the limits of the atherosclerotic lesion (**D**). Intima/media ratio (**E**), lesion area (**F**), Mac-3^{+} macrophages (**G**), CD3^{+} T-cells (**H**), CD4^{+} lymphocytes (**I**), CD8^{+} lymphocytes (**J**), collagen area (**K**), necrotic *core* area (**L**), and smooth muscle cell infiltration (SMC; **M**) were determined in the aortic sinus. Representative photomicrographs of aortic sinus cross-sections of stained macrophages (Mac-3^{+}; brown staining), CD3^{+}, CD4^{+}, and CD8^{+} T cells (white arrowheads), Masson's staining (collagen; green staining), and α-actin (red staining) for control or atherogenic diet-fed mice. Black and white arrows point to the atheroma. Immunoreactivity was visualized using an Alexa Fluor® 488 secondary antibody (green) and an Alexa Fluor® 647 secondary antibody (red), respectively. Nuclei were stained with Hoechst dye (blue). Results are expressed as mean ± SEM (n = 8–11 animals per group). *p <0.05 or **p <0.01 relative to values animals subjected to a control diet; +p <0.05 or ++p <0.01 relative to values in apoE$^{-/-}$CCR3$^{+/+}$ animals subjected to an atherogenic diet.

4.2.5 Two months under a high-fat diet increased the expression of eotaxin-1/CCL11, the number of mast cells and SiglecF^{+}CCR3^{+} eosinophils in the atherosclerotic lesion of apoE$^{-/-}$CCR3$^{+/+}$ mice

Immunohistochemical analyses demonstrated that apoE$^{-/-}$CCR3$^{+/+}$ mice fed with an atherogenic diet had significantly increased eotaxin-1/CCL11 expression within the atherosclerotic lesion compared with those animals fed with a control diet (**Figures 34A–C**). The expression of CCL11 was virtually absent in apoE$^{-/-}$CCR3$^{-/-}$ mice subjected or not to a high-fat diet (**Figures 34A–C**).

In addition, a higher number of mast cells in the atherosclerotic lesion were detected in both genotypes when they were subjected to an atherogenic diet (**Figures 34A** and **D**), and the numbers were significantly higher in apoE$^{-/-}$CCR3$^{-/-}$ mice than in apoE$^{-/-}$CCR3$^{+/+}$ mice (**Figure 34D**).

Finally, a significant increase of SiglecF^{+}CCR3^{+} cells was observed in the atherosclerotic lesion of apoE$^{-/-}$CCR3$^{+/+}$ mice subjected to an atherogenic diet for two months compared with those mice under a control diet (**Figure 34E**).

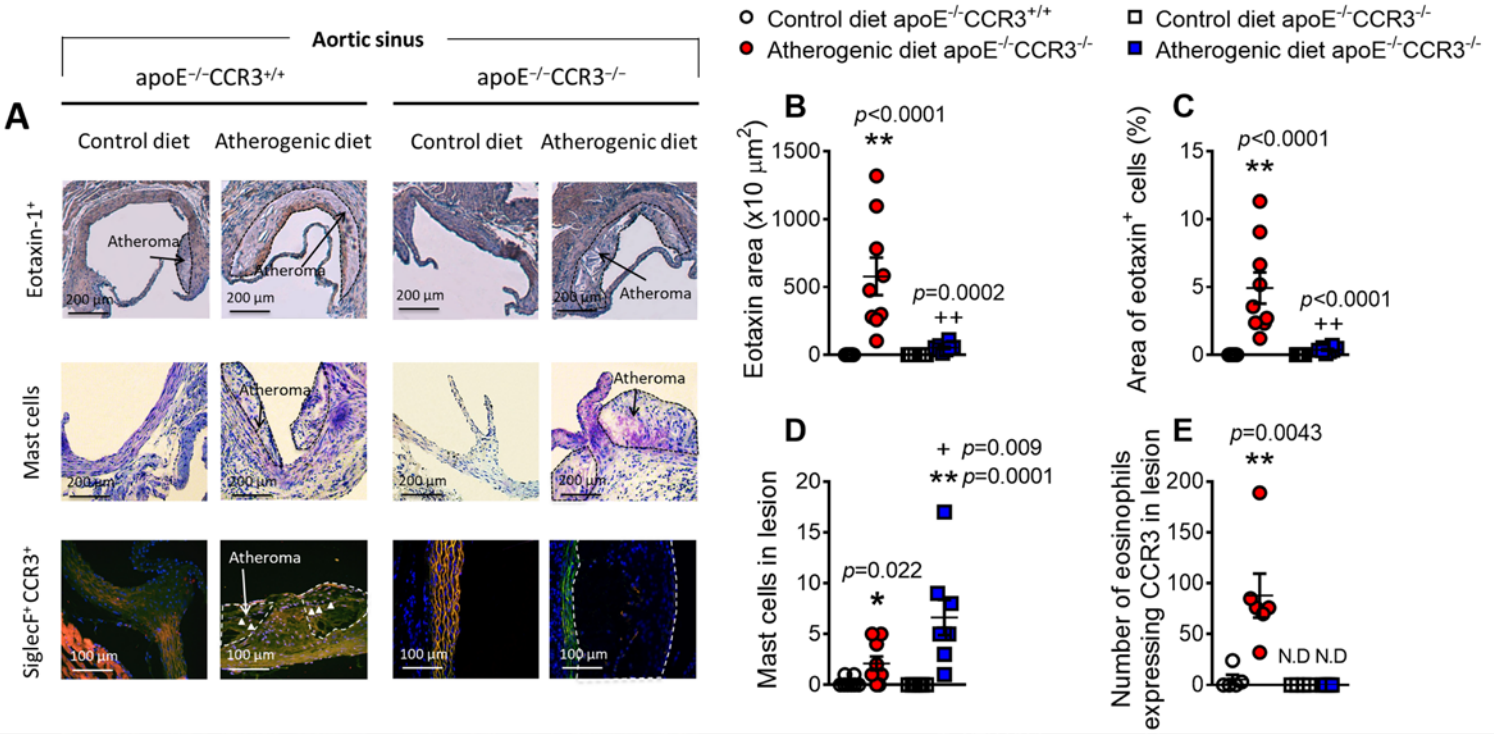

Figure 34. Two months under a high-fat diet increased the expression of eotaxin-1/CCL11, the number of mast cells and SiglecF^{+}CCR3^{+} eosinophils in the atherosclerotic lesion of apoE$^{-/-}$CCR3$^{+/+}$ mice. ApoE$^{-/-}$CCR3$^{+/+}$ and apoE$^{-/-}$CCR3$^{-/-}$ mice were subjected to a control or an atherogenic diet for two months. Representative images of aortic sinus cross-sections (**A**). Eotaxin-1 area (brown staining; **B**), the area of eotaxin-1 (CCL11)$^{+}$ cells (brown staining; **C**), the number of mast cells within the lesion (purple staining; **D**), and the number of eosinophils (SiglecF^{+}CCR3^{+}, white arrowheads; **E**) were determined in the aortic sinus. Discontinuous lines delineate the limits of the atherosclerotic lesion. Black and white arrows point to the atheroma. Immunoreactivity was visualized using an Alexa Fluor® 488 secondary antibody (green) and an Alexa Fluor® 594 secondary antibody (red) respectively. Nuclei were stained with Hoechst dye (blue). Values are expressed as mean ± SEM (n = 8–11 animals per group). *p <0.05 or **p <0.01 relative to values animals subjected to a control diet; +p <0.05 or ++p <0.01 relative to values in apoE$^{-/-}$CCR3$^{+/+}$ animals subjected to an atherogenic diet. N.D = No detected.

4.2.6 Decreased percentage of CCR3-expressing eosinophils and mast cells was observed in subcutaneous adipose tissue of apoE$^{-/-}$CCR3$^{+/+}$ mice subjected to a high-fat diet

First, the histological examination of subcutaneous adipose tissue was carried out by hematoxylin/eosin staining. Adipocyte size was determined and found that the adipocyte area of those apoE$^{-/-}$CCR3$^{-/-}$ animals fed with an atherogenic diet was significantly reduced compared to apoE$^{-/-}$CCR3$^{-/-}$ mice fed with a control diet (**Figures 35A** and **B**). Additionally, different leukocyte subpopulations were analyzed in subcutaneous adipose tissue by flow cytometry. Although no differences in the number of SiglecF^{+} eosinophils were found between groups (**Figure 35C**), the percentage of CCR3-expressing cells such as eosinophil and mast cell populations was drastically decreased in apoE$^{-/-}$CCR3$^{+/+}$ mice subjected to a high-fat diet (**Figures 35D** and **E**). Moreover, the percentage of alternative-activated macrophages (AAM) was significantly impaired in animals under an atherogenic diet for two months regardless of the genotype (**Figures 35F** and **G**). Inasmuch, the activation state of CD3^{+} lymphocytes (CD69^{+}) was significantly increased in these apoE$^{-/-}$CCR3$^{+/+}$ mice subjected to a high-fat diet (**Figure 35H**). In apoE$^{-/-}$CCR3$^{-/-}$ mice, no differences in the activation state of CD3^{+} lymphocytes (CD69^{+}) was observed when animals were subjected to a control or an atherogenic diet (**Figure 35H**). Furthermore, CD3^{+} activation was significantly lower in this genotype compared to that observed in apoE$^{-/-}$CCR3$^{+/+}$ mice subjected to an atherogenic diet.

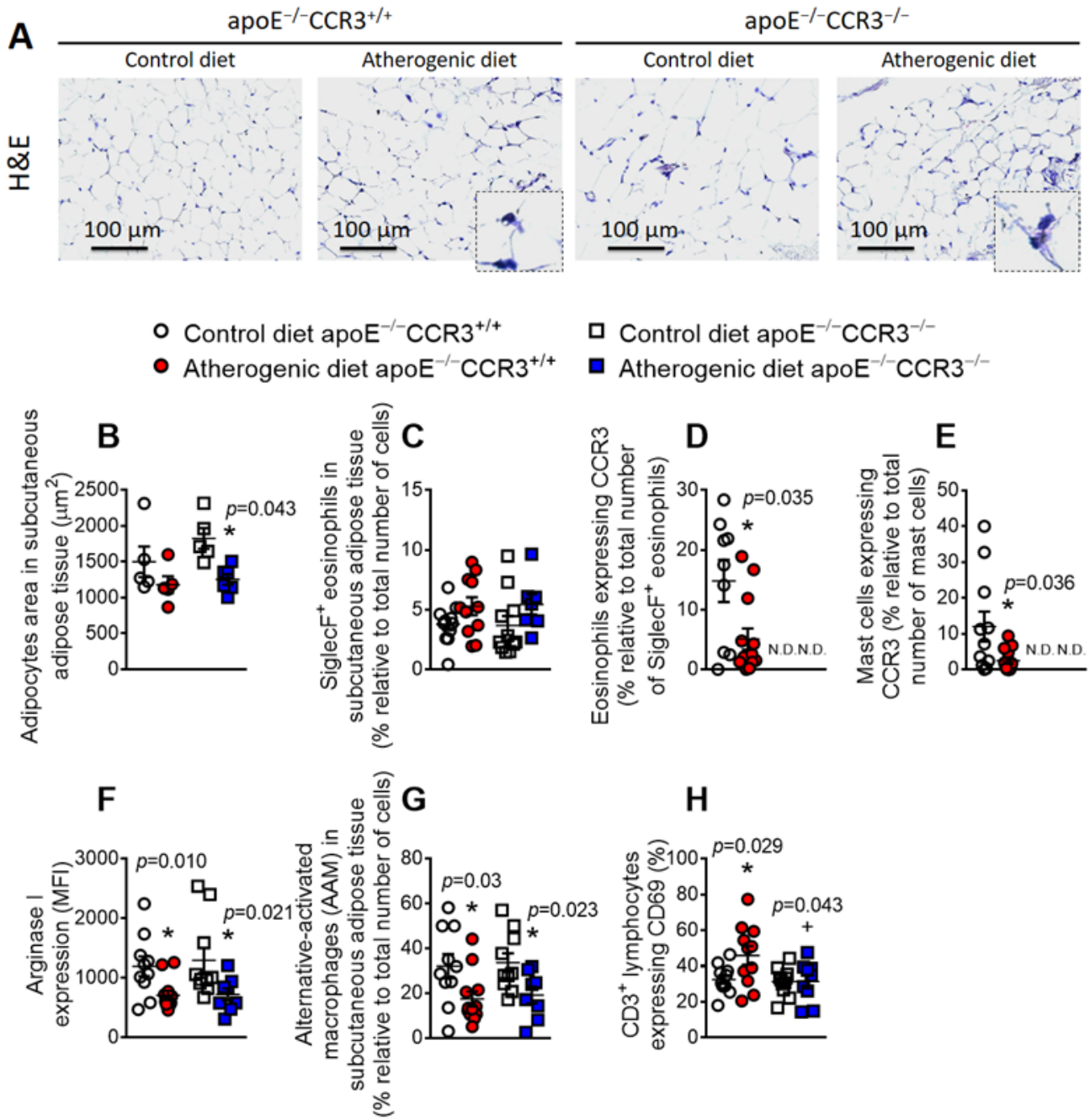

Figure 35. Decreased percentage of CCR3-expressing eosinophils and mast cells was observed in subcutaneous adipose tissue of apoE$^{-/-}$CCR3$^{+/+}$ mice subjected to a high-fat diet. ApoE$^{-/-}$CCR3$^{+/+}$ and apoE$^{-/-}$CCR3$^{-/-}$ mice were subjected to a control or an atherogenic diet for two months. Representative images of subcutaneous adipose tissue in paraffin-embedded cross-sections (**A**). Hematoxylin/eosin (H&E) staining was performed to measure the adipocyte area (**B**). Subcutaneous adipose tissue samples were analyzed by flow cytometry and co-stained with specific markers for eosinophils (**C** and **D**), mast cells (**E**), alternative-activated macrophages (AAM; **F** and **G**), and CD3^{+} lymphocytes (**H**), as well as CCR3 (**D** and **E**) and CD69 (**H**). Results are presented as MFI or the percentage of positive cells (n = 10–15 animals per group). Values are expressed as mean ± SEM. *p <0.05 relative to values of animals subjected to a control diet; +p <0.05 relative to values of apoE$^{-/-}$CCR3$^{+/+}$ animals subjected to an atherogenic diet. N.D = No detected.

4.2.7 ApoE$^{-/-}$CCR3$^{+/+}$ mice fed with a high-fat diet showed an increased number of eosinophils, *villi* length, and *Eotaxin-1* mRNA levels

To determine whether CCR3 and a two-month high-fat diet affect the intestinal epithelium, we next examined the small intestines of apoE$^{-/-}$CCR3$^{+/+}$ and apoE$^{-/-}$CCR3$^{-/-}$ mice subjected or not to an atherogenic diet. Histologically, the small intestine exhibited marked proliferative changes in the *villi* length in apoE$^{-/-}$CCR3$^{+/+}$ mice fed with a high-fat diet, with an ectopic crypt formation in those apoE$^{-/-}$CCR3$^{-/-}$ mice subjected to the same diet (**Figures 36A**–**C**). Interestingly, a higher number of SiglecF^{+} eosinophils was found in the small intestine of apoE$^{-/-}$CCR3$^{+/+}$ mice subjected to a high-fat diet (**Figures 36A** and **D**), while apoE$^{-/-}$CCR3$^{-/-}$ mice showed decreased numbers of eosinophils when they were subjected to the same diet (**Figure 36D**). In contrast, the number of mast cells was significantly higher in those animals lacking the CCR3 receptor, and this number was further increased when they were fed with a high-fat diet (**Figures 36A** and **E**).

Moreover, mRNA expression of *Eotaxin-1/Ccl11*, *Eotaxin-2/Ccl24*, *Il-25*, and *Il-33* was studied in the small intestine of apoE$^{-/-}$CCR3$^{+/+}$ and apoE$^{-/-}$CCR3$^{-/-}$ mice subjected or not to an atherogenic diet during two months (**Figures 36F**–**I**). Only *Eotaxin-1/Ccl11* mRNA expression was significantly increased in the small intestine from apoE$^{-/-}$CCR3$^{+/+}$ group fed with an atherogenic diet compared with its control group (**Figure 36F**), and in the absence of CCR3 receptor, no significant differences in this parameter were encountered. Nevertheless, no differences were detected between genotypes in mRNA levels of *Eotaxin-2/Ccl24*, *Il-25*, and *Il-33* when they were subjected or not to an atherogenic diet (**Figures 36G**–**I**).

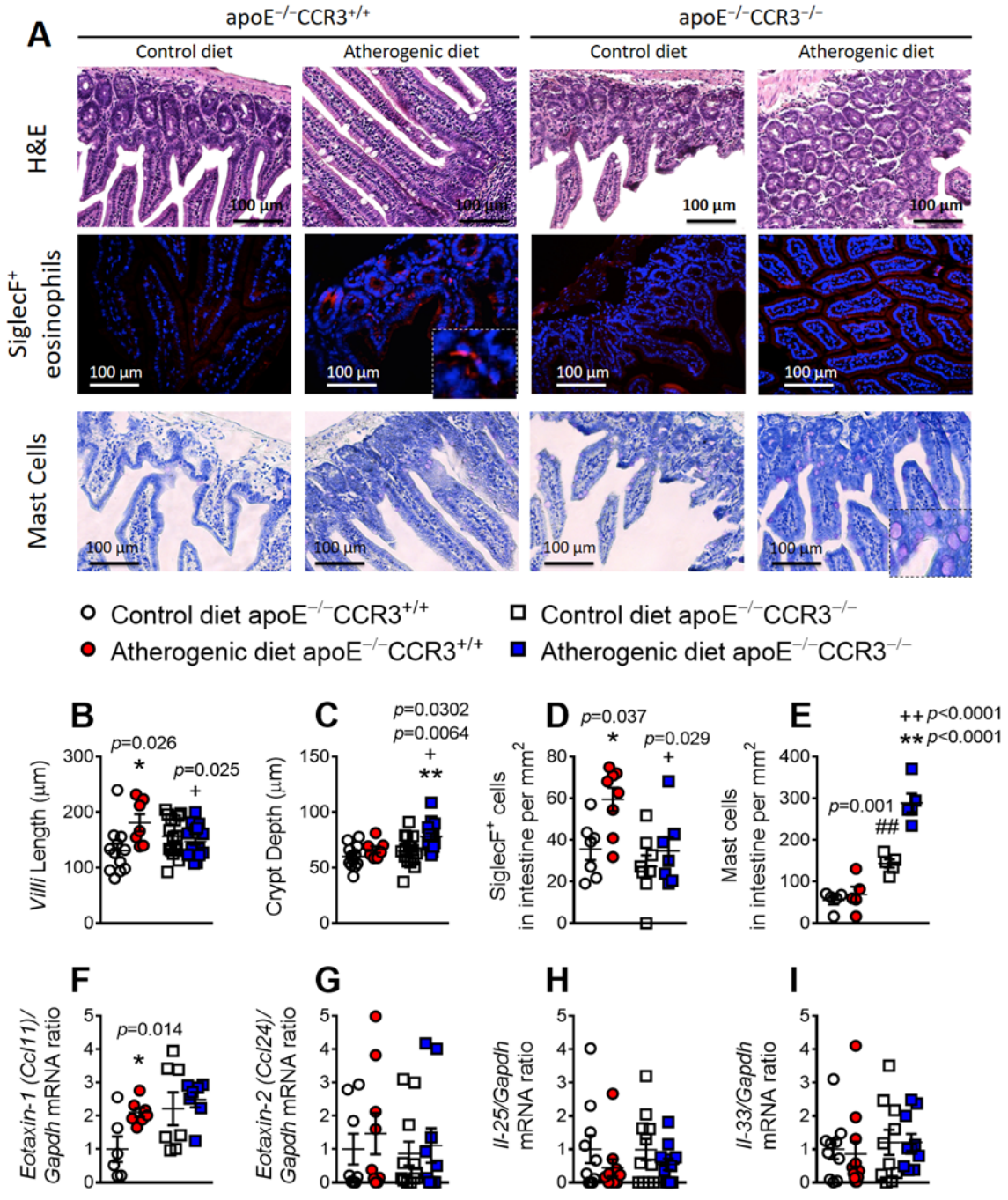

Figure 36. The number of eosinophils, *villi* length, and the mRNA levels of *Eotaxin-1* were higher in apoE$^{-/-}$CCR3$^{+/+}$ mice fed with a high-fat diet. ApoE$^{-/-}$CCR3$^{+/+}$ and apoE$^{-/-}$CCR3$^{-/-}$ mice were subjected to a control or an atherogenic diet for two months. Representative images of small intestine cross-sections (**A**). Hematoxylin and eosin (H&E) staining was performed to measure *villi* length (**B**) and crypt depth (**C**). The number of SiglecF^{+} eosinophils (**D**) and mast cells (**E**) were determined. Gene expression of *Eotaxin-1* (*Ccl11*; **F**), *Eotaxin-2* (*Ccl24*; **G**), *Il-25* (**H**), and *Il-33* (**I**) in the intestine were analyzed by RT-PCR. Results are expressed as mean ± SEM (n = 5–11 animals per group). *p <0.05 or **p <0.01 relative to values of animals subjected to a control diet; +p <0.05 or ++p <0.01 relative to values in apoE$^{-/-}$CCR3$^{+/+}$ animals subjected to an atherogenic diet; ##p <0.01 relative to values in apoE$^{-/-}$CCR3$^{+/+}$ mice subjected to a control diet.

4.2.8 The circulating levels of eotaxin-1/CCL11 increased in atherogenic diet-fed apoE$^{-/-}$CCR3$^{+/+}$ animals but decreased in apoE$^{-/-}$CCR3$^{-/-}$ mice. Augmented percentage of eosinophils and mast cells in the bone marrow of apoE$^{-/-}$CCR3$^{-/-}$ mice subjected to an atherogenic diet

Circulating levels of eotaxin-1/CCL11, eotaxin-2/CCL24, IL-4, and IL-5 were measured by ELISA in both genotypes, fed or not with an atherogenic diet. Interestingly, decreased plasma levels of eotaxin-1/CCL11 (**Figure 37A**), IL-4 (**Figure 37C**), and IL-5 (**Figure 37D**) were observed in apoE$^{-/-}$CCR3$^{-/-}$ mice fed with a high-fat diet for two months compared to apoE$^{-/-}$CCR3$^{+/+}$ mice fed with the same diet, whereas no significant differences were detected between groups in plasma levels of eotaxin-2/CCL24 (**Figure 37B**).

When the bone marrow was analyzed by flow cytometry, though the number of SiglecF^{+} eosinophils and mast cells in apoE$^{-/-}$CCR3$^{+/+}$ mice fed with an atherogenic diet did not significantly differ from those fed with a control diet (**Figures 37E** and **G**, respectively), there were a significant increase in apoE$^{-/-}$CCR3$^{-/-}$ mice fed with a high-fat diet (**Figures 37E** and **G)**; whereas the number of CCR3-expressing eosinophils and mast cells were significantly increased in apoE$^{-/-}$CCR3$^{+/+}$ mice fed with the same diet (**Figures 37F** and **H**).

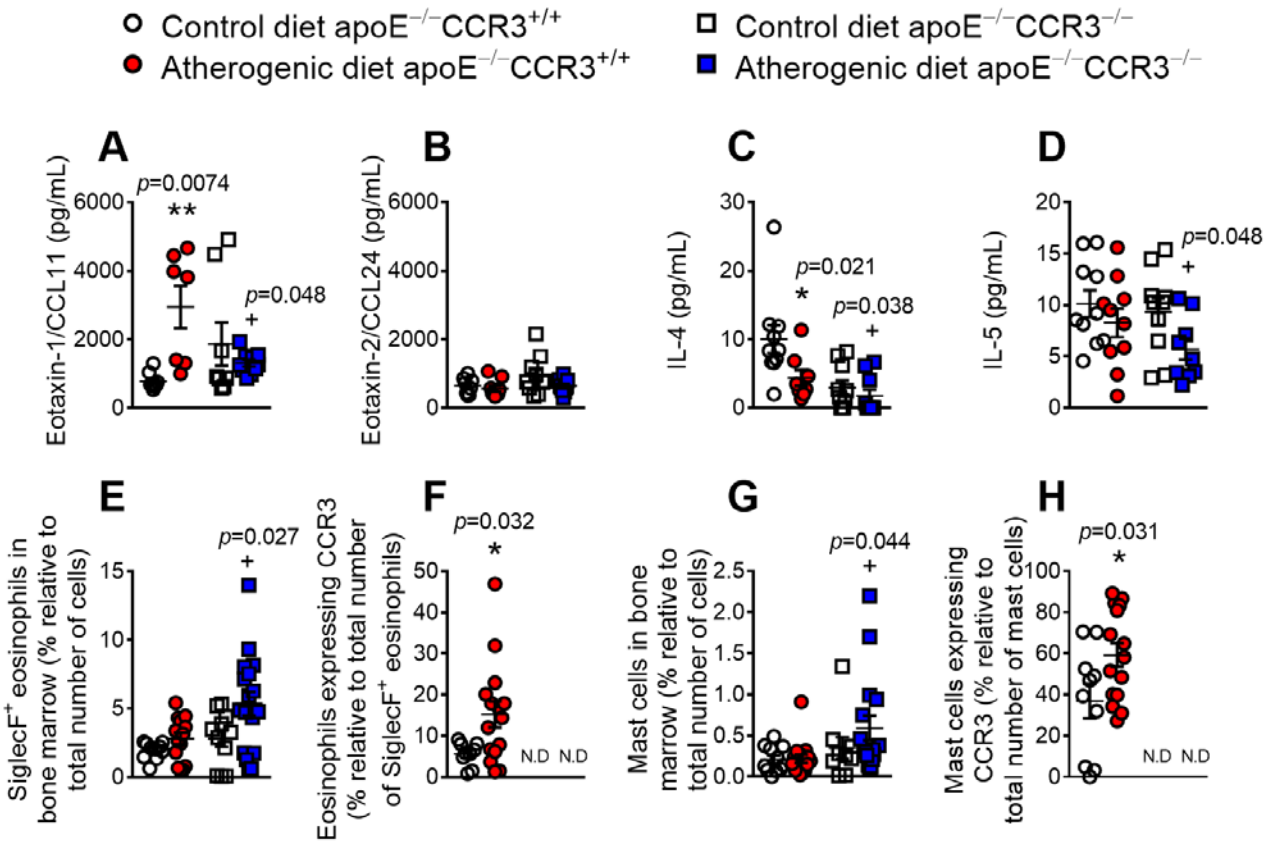

Figure 37. The circulating levels of eotaxin-1 increased in atherogenic diet-fed apoE$^{-/-}$CCR3$^{+/+}$ animals but decreased in apoE$^{-/-}$CCR3$^{-/-}$ mice. Augmented percentage of eosinophils and mast cells in the bone marrow of apoE$^{-/-}$CCR3$^{-/-}$ mice fed with an atherogenic diet. ApoE$^{-/-}$CCR3$^{+/+}$ and apoE$^{-/-}$CCR3$^{-/-}$ mice were subjected to a control or an atherogenic diet for two months. Eotaxin-1/CCL11 (**A**), eotaxin-2/CCL24 (**B**), IL-4 (**C**), and IL-5 (**D**) plasma levels (pg/mL) were determined by ELISA. Bone marrow was co-stained with specific markers for eosinophils (**E** and **F**) and mast cells (**G** and **H**), as well as CCR3 (**F** and **H**), and analyzed by flow cytometry. Results are presented as the percentage of positive cells (n = 6–15 animals per group). Values are expressed as mean ± SEM. *p <0.05 or **p <0.01 relative to values of animals subjected to a control diet; +p <0.05 relative to values in apoE$^{-/-}$CCR3$^{+/+}$ animals subjected to an atherogenic diet. N.D = No detected.

4.2.9 Two-month high-fat diet feeding increased the levels of TC and TG and decreased the levels of HDL cholesterol in apoE$^{-/-}$CCR3$^{+/+}$ and apoE$^{-/-}$CCR3$^{-/-}$ mice

ApoE$^{-/-}$CCR3$^{+/+}$ and apoE$^{-/-}$CCR3$^{-/-}$ mice subjected to a control diet showed TC levels around 220 mg/dL. After two months with a high-fat diet, these levels significantly increased, reaching values close to 460 mg/dL (**Table 21**). A similar profile was found for plasma LDL, very low-density lipoprotein (VLDL) or TG (**Table 21**). HDL cholesterol levels decreased in both genotypes after two months of atherogenic diet (**Table 21**).

Table 21. Biochemical parameters in mice fed or not with an atherogenic diet for two months.

	ApoE$^{-/-}$CCR3$^{+/+}$	**ApoE$^{-/-}$CCR3$^{+/+}$**	**ApoE$^{-/-}$CCR3$^{-/-}$**	**ApoE$^{-/-}$CCR3$^{-/-}$**
	Control diet	**Atherogenic diet**	**Control diet**	**Atherogenic diet**
Weight (g)	28.1 ± 0.5	29.4 ± 0.7	25.2 ± 0.5 ++	26.7 ± 0.4 ++
Glucose (mg/dL)	64.3 ± 4.6	97.2 ± 8.3 *	79.3 ± 8.6	86.5 ± 5.4
TC levels (mg/dL)	214.5 ± 11.2	468.6 ± 23.7 **	226.9 ± 19.9	466.3 ± 19.3 **
LDL levels (mg/dL)	152.9 ± 14.2	395.6 ± 25.1 **	161.7 ± 21.7	388.4 ± 22.8 **
TG (mg/dL)	116.3 ± 8.8	236.1 ± 18.1 **	131.9 ± 6.5	249.8 ± 19.3 **
HDL levels (mg/dL)	38.3 ± 5.2	24.9 ± 3.0 *	38.8 ± 4.1	25.4 ± 1.8 *
VLDL levels (mg/dL)	23.2 ± 1.8	47.2 ± 3.6 **	26.4 ± 1.3	49.9 ± 3.9 **
Ratio HDL/LDL	0.4 ± 0.1	0.1 ± 0.0 *	0.3 ± 0.1	0.1 ± 0.0 *
Ratio HDL/TC	0.2 ± 0.0	0.1 ± 0.0 **	0.2 ± 0.0	0.1 ± 0.0 **
Ratio TG/HDL	3.8 ± 0.6	12.5 ± 1.9 **	3.8 ± 0.4	11.0 ± 1.2 **

TC, total cholesterol; LDL, low-density lipoprotein; TG, triglycerides; HDL, high-density lipoprotein; VLDL, very low-density lipoprotein. Data are presented as mean ± SEM of 10–15 animals per group. *p <0.05 or **p <0.01 relative to values in the control group. ++p <0.01 relative to values in apoE$^{-/-}$CCR3$^{+/+}$ group.

4.3 STUDY OF THE ROLE OF CXCR6 RECEPTOR IN ABDOMINAL AORTIC ANEURYSM FORMATION

4.3.1 Chronic administration of an AT_1 receptor antagonist, losartan reduces Ang-II–induced AAA formation in apoE$^{-/-}$ mice

We evaluated the effect of the Ang-II AT_1 receptor antagonist losartan on experimentally induced AAA formation. Accordingly, apoE$^{-/-}$ mice were infused subcutaneously with Ang-II (1000 ng/kg/min) or vehicle (saline) for 28 days, inducing the development of AAA in Ang-II infused mice (**Figure 38A**). Ang-II-infused mice had a larger maximal external diameter of the suprarenal aorta than saline-infused mice; this diameter was significantly reduced in mice cotreated with 30 mg/kg/day of losartan (Ang-II, 2.2 ± 0.2 mm *vs.* losartan, 1.4 ± 0.1 mm; **Figure 38B**).

Immunohistochemical analyses of suprarenal aortic sections showed that Ang-II infusion promoted the recruitment of CD68$^+$, CD3$^+$ and CXCR6$^+$ cells in the adventitia and media, which was substantially decreased in animals cotreated with losartan (**Figures 38C–F**). Likewise, an increase in the number of CD31$^+$ capillary vessels in suprarenal aortas was also detected, being significantly lower in mice cotreated with losartan (**Figures 38C** and **G**). Additionally, the mRNA expression of *Mcp-1 (Ccl2)*, *Cxcl16* and *Vegf* in the suprarenal aorta of Ang-II-infused apoE$^{-/-}$ mice was significantly diminished in animals cotreated with losartan (**Figures 38H–J**). Moreover, circulating levels of soluble CXCL16 and TNFα, but not IFNγ, were significantly elevated in animals infused with Ang-II but were dramatically decreased by losartan coadministration (**Figures 38K–M**). Finally, Ang-II infusion caused a significant increase in systolic blood pressure, which was lower in animals cotreated with losartan (**Table 22**). However, losartan administration failed to alter the lipid profile in apoE$^{-/-}$ mice chronically infused with Ang-II (**Table 22**).

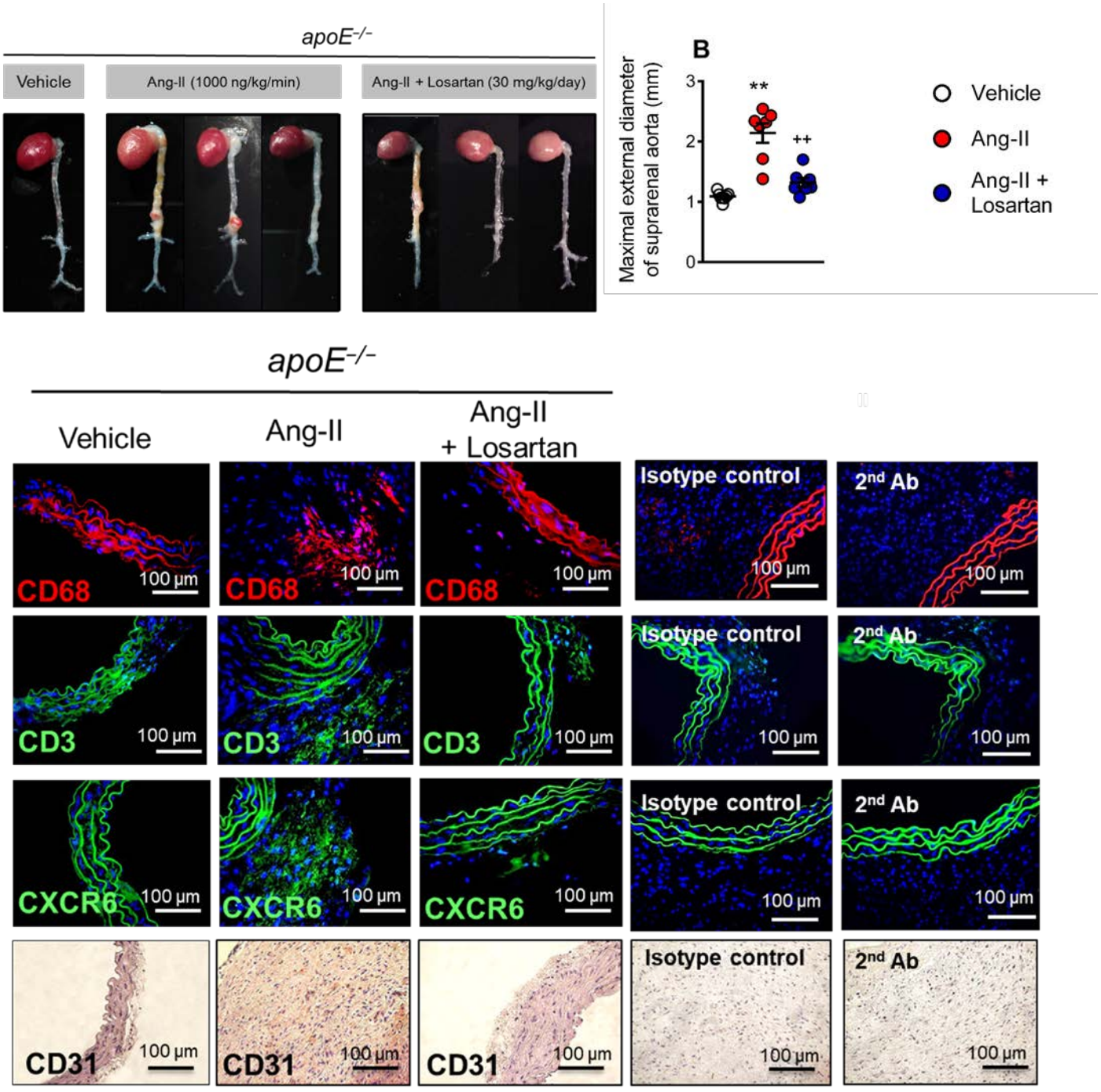
apoE-/-
Vehicle
Ang-II (1000 ng/kg/min)
Ang-II + Losartan (30 mg/kg/day)
B
Maximal external diameter of suprarenal aorta (mm)
**
++
Vehicle
Ang-II
Ang-II + Losartan
C
apoE-/-
Vehicle
Ang-II
Ang-II + Losartan
CD68
CD3
CXCR6
CD31
Isotype control
2nd Ab
100 µm

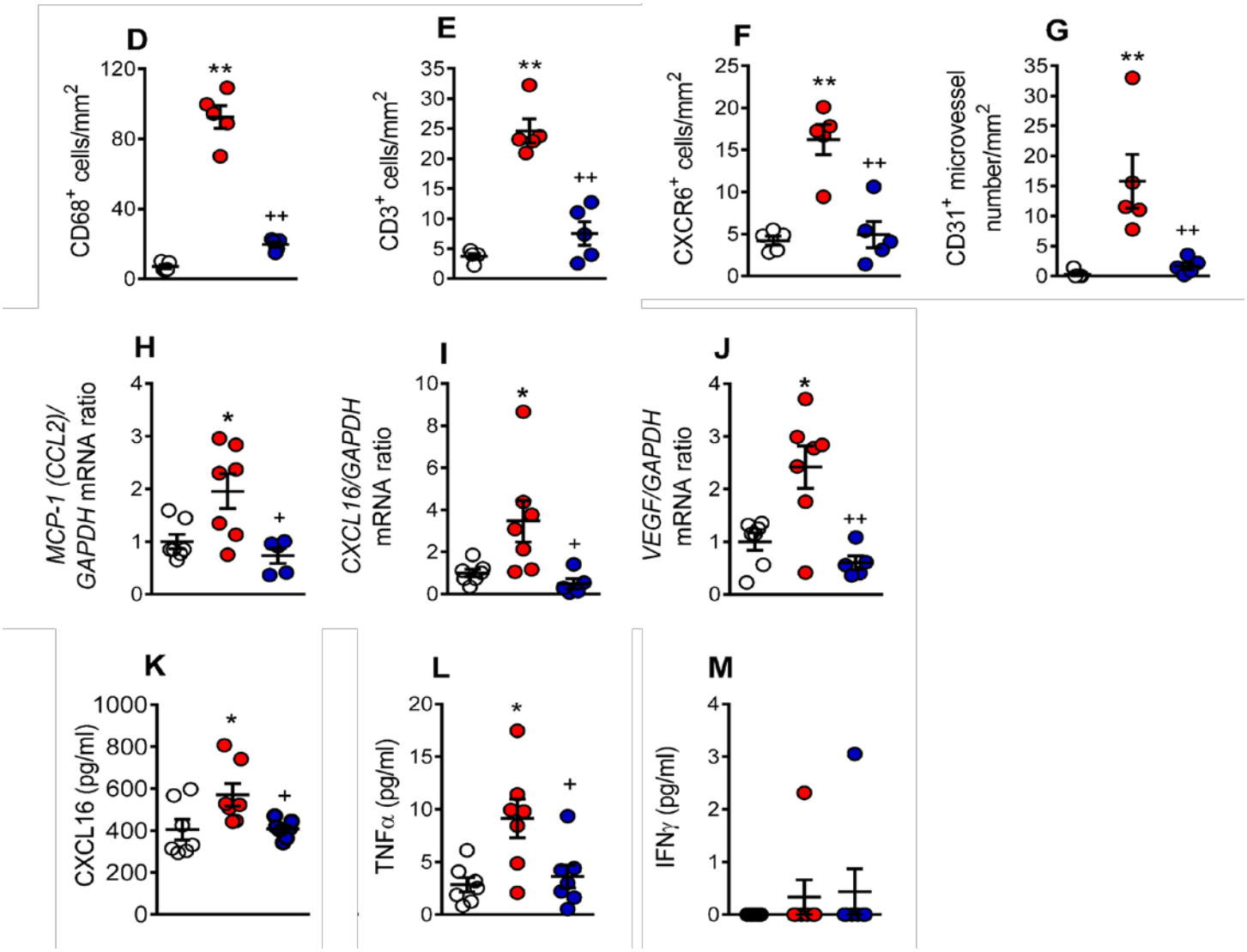

Figure 38. Chronic administration of losartan decreases Ang-II-induced AAA formation in apoE$^{-/-}$ mice. Representative aortas from apoE$^{-/-}$ mice. The gross appearance of the aortas was photographed digitally (**A**), and the maximal external diameter of the suprarenal aorta was measured (**B**). Representative photomicrographs of stained macrophages (CD68^{+}), T lymphocytes (CD3^{+}), CXCR6^{+} cells and CD31^{+} microvessels in aortic cross sections (**C**). Immunoreactivity was visualized using an Alexa Fluor® 633 secondary antibody (red) and an Alexa Fluor® 488 secondary antibody (green), respectively. Nuclei were stained with Hoechst dye (blue). (**D**–**G**) Number of CD68^{+} cells (**D**), CD3^{+} cells (**E**), CXCR6^{+} cells (**F**), and CD31^{+} microvessels (**G**) per mm^2 in aortic aneurysm sections. (**H**–**J**) Gene expression of *Mcp-1* (*Ccl2*; **H**), *Cxcl16* (**I**), and *Vegf* (**J**) in AAA lesions analyzed by RT-PCR. CXCL16 (**K**), TNFα (**L**), and IFNγ (**M**) plasma levels were measured by ELISA (n = 5–7 animals per group). *p <0.05 or **p <0.01 relative to values in vehicle-infused mice; +p <0.05 or ++p <0.01 relative to values in Ang-II-infused animals without losartan.

4.3.2 CXCR6 deficiency reduces aortic dilatation and inflammation in Ang-II–induced AAA

We next generated apoE$^{-/-}$CXCR6$^{GFP/+}$ and apoE$^{-/-}$CXCR6$^{GFP/GFP}$ mice to evaluate the relevance of the CXCL16/CXCR6 axis in the progress of AAA. Ang-II infusion for 28 days provoked an increase in suprarenal aorta expansion and diameter in both groups (**Figures 39A** and **B**); however, aortic development was markedly smaller in apoE$^{-/-}$CXCR6$^{GFP/GFP}$ mice than in apoE$^{-/-}$CXCR6$^{GFP/+}$ mice, with the former group having a significantly smaller maximum diameter of the suprarenal aorta. Interestingly, the Ang-II-induced inflammatory infiltrates (CD68^{+}, CD3^{+}, and CXCR6^{+} cells) and neovascularization (CD31^{+} vessels) was also significantly lower in apoE$^{-/-}$CXCR6$^{GFP/GFP}$ mice (**Figures 39D–G**). Additionally, whereas *Mcp-1 (Ccl2)*, *Cxcl16*, and *Vegf* mRNA expression was markedly elevated in the suprarenal aortas of apoE$^{-/-}$CXCR6$^{GFP/+}$ mice treated with Ang-II, it was significantly lower in apoE$^{-/-}$CXCR6$^{GFP/GFP}$ mice subjected to the same stimulus (**Figures 39H–J**). Of note, the immunofluorescence analyses revealed a marked increase in CD8^{+}CXCR6^{+} but not in CD4^{+}CXCR6^{+} lymphocyte infiltration in the AAA lesion of apoE$^{-/-}$CXCR6$^{GFP/+}$ mice (**Figures 40A–C**). Nevertheless, neither the rise in blood pressure induced by Ang-II nor the lipid profile was affected by CXCR6 (**Table 22**).

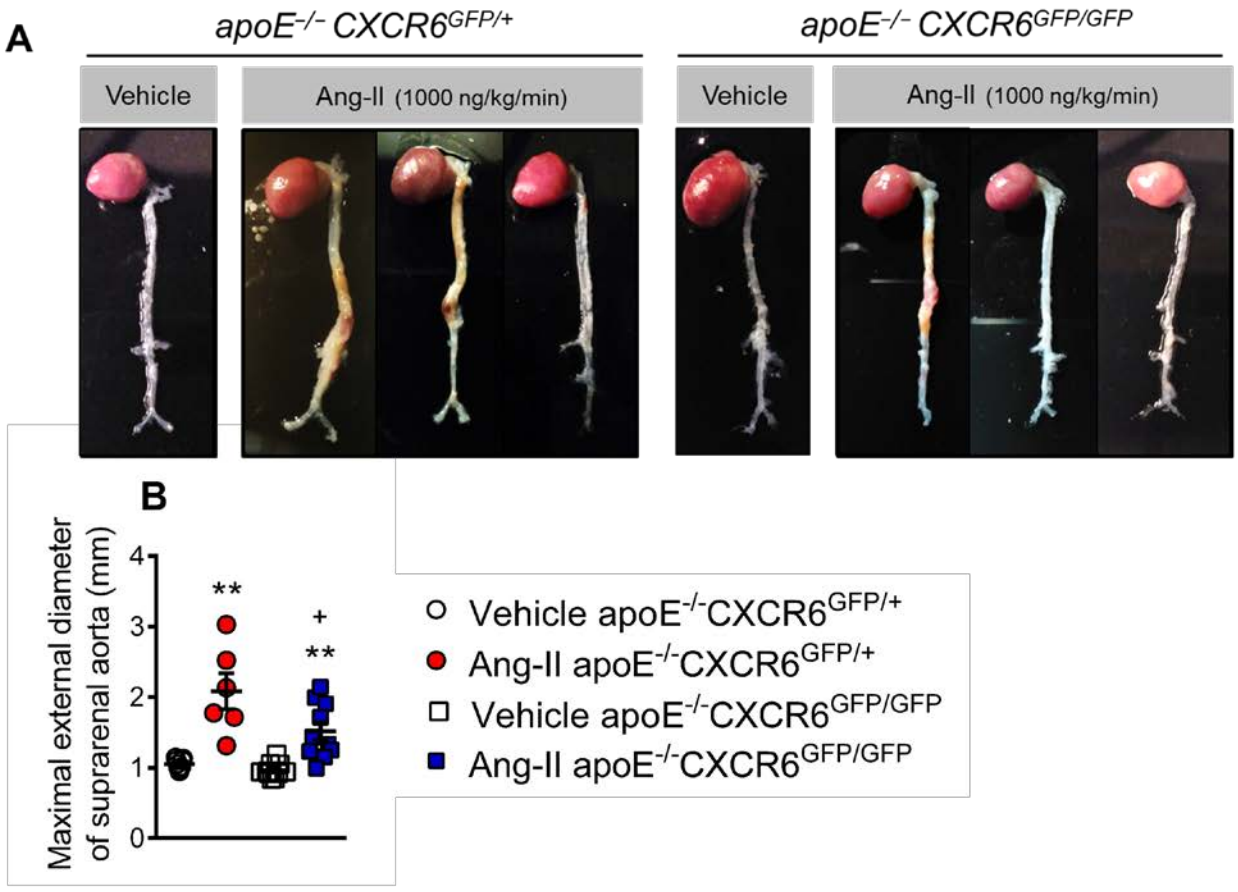
A
apoE-/- CXCR6GFP/+
apoE-/- CXCR6GFP/GFP
Vehicle
Ang-II (1000 ng/kg/min)
Vehicle
Ang-II (1000 ng/kg/min)
B
Maximal external diameter of suprarenal aorta (mm)
0
1
2
3
4
**
**
+
Vehicle apoE-/-CXCR6GFP/+
Ang-II apoE-/-CXCR6GFP/+
Vehicle apoE-/-CXCR6GFP/GFP
Ang-II apoE-/-CXCR6GFP/GFP

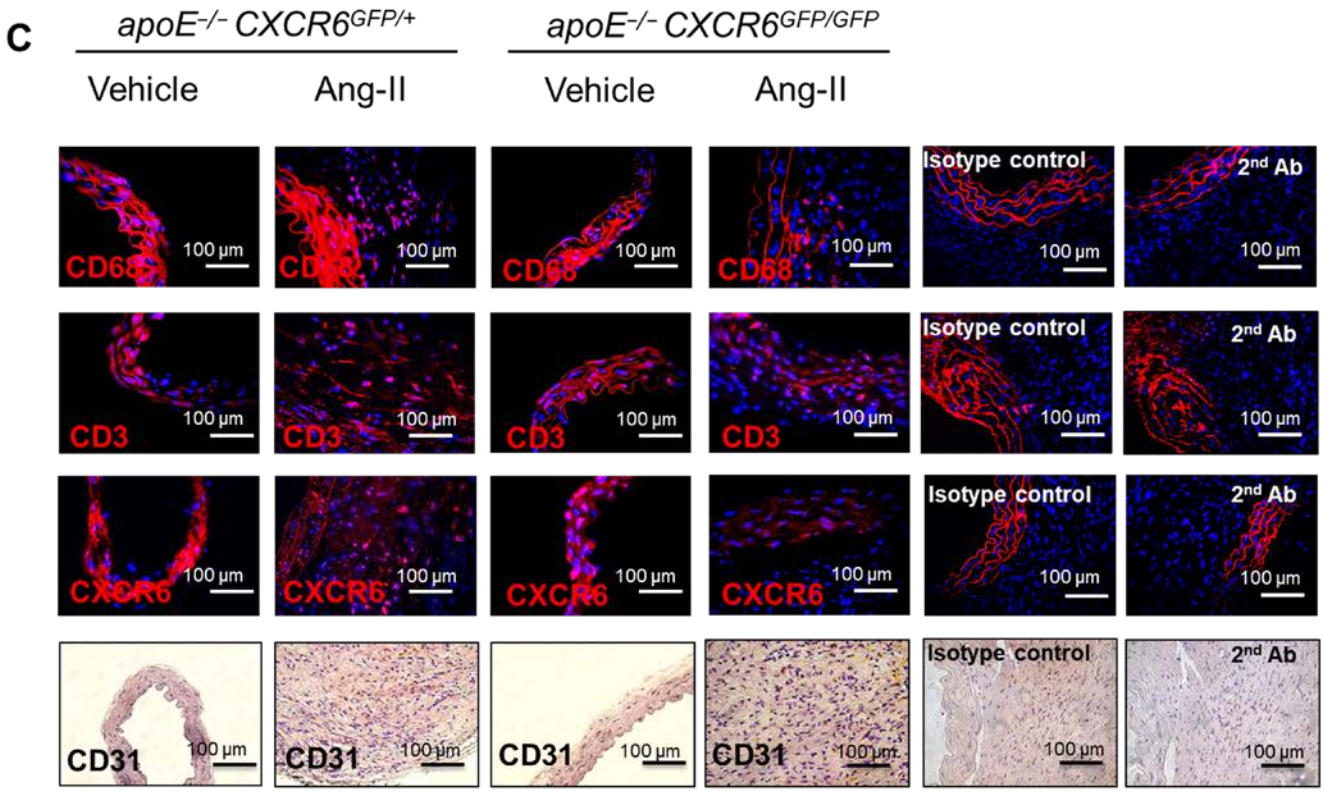
C
apoE-/- CXCR6GFP/+
apoE-/- CXCR6GFP/GFP
Vehicle
Ang-II
Vehicle
Ang-II
CD68
CD3
CXCR6
CD31
Isotype control
2nd Ab
100 µm

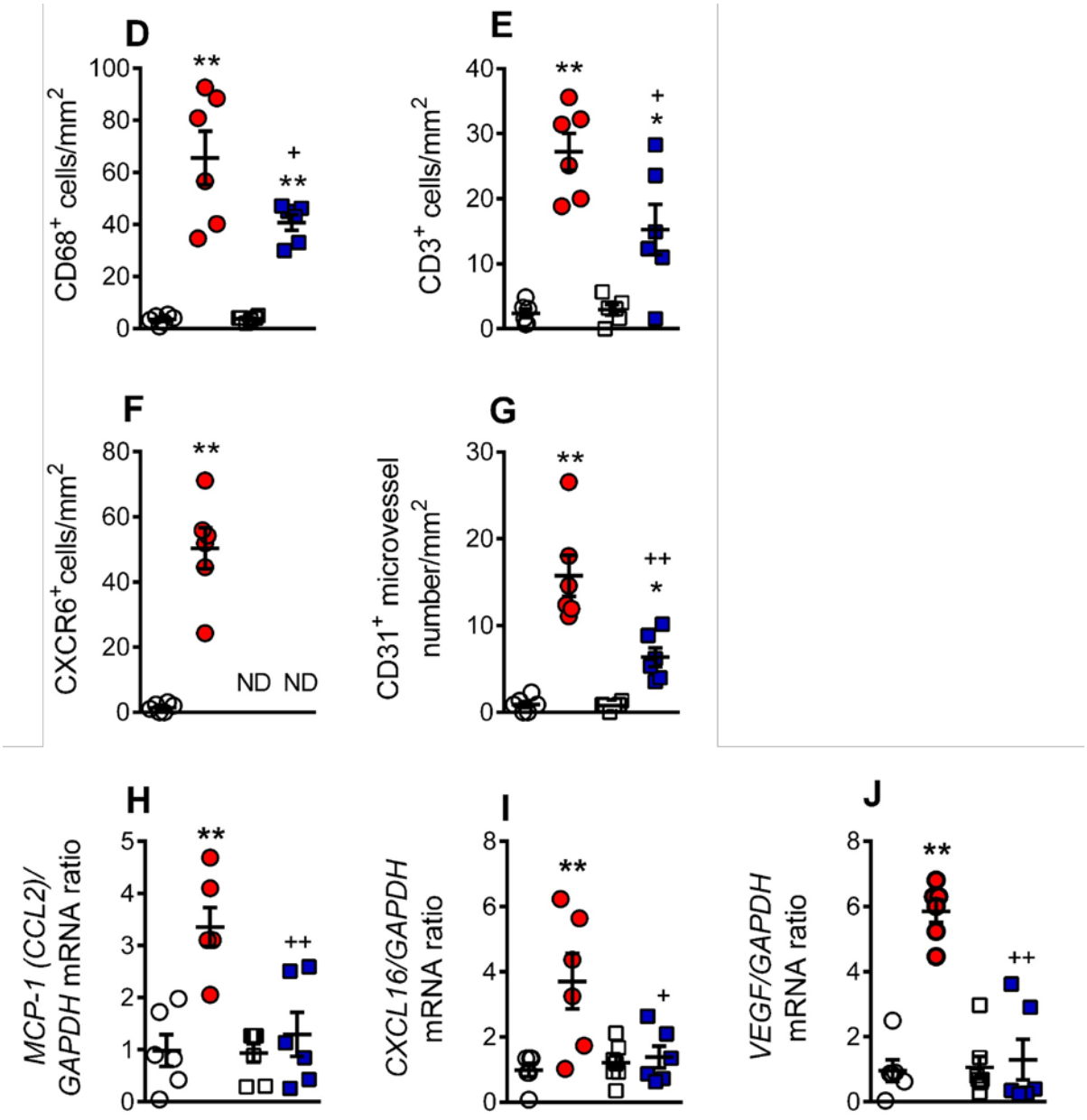

Figure 39. CXCR6 deficiency reduces aortic dilatation and inflammation in AAA induced by Ang-II in apoE$^{-/-}$ mice. Representative aortas from apoE$^{-/-}$CXCR6$^{GFP/+}$ and apoE$^{-/-}$CXCR6$^{GFP/GFP}$ mice. The gross appearances of the aortas were photographed digitally (**A**), and the maximal external diameter of the suprarenal aorta was measured (**B**). Representative photomicrographs of stained macrophages (CD68^{+}), T lymphocytes (CD3^{+}), CXCR6^{+} cells and CD31^{+} microvessels in aortic cross sections (**C**). Immunoreactivity was visualized using an Alexa Fluor® 633 secondary antibody (red) and an Alexa Fluor® 594 secondary antibody (red), respectively. Nuclei were stained with Hoechst dye (blue). (**D**–**G**) Number of CD68^{+} cells (**D**), CD3^{+} cells (**E**), CXCR6^{+} cells (**F**), and CD31^{+} microvessels (**G**) per mm^2 in aortic aneurysm sections. (**H**–**J**) Gene expression of *Mcp-1* (*Ccl2*; **H**), *Cxcl16* (**I**), and *Vegf* (**J**) in the suprarenal aortas analyzed by RT-PCR (n = 6–10 animals per group). *p <0.05 or **p <0.01 relative to values in vehicle-infused mice; +p <0.05 or ++p <0.01 relative to values in the Ang-II group in apoE$^{-/-}$CXCR6$^{GFP/+}$ mice. N.D = No detected.

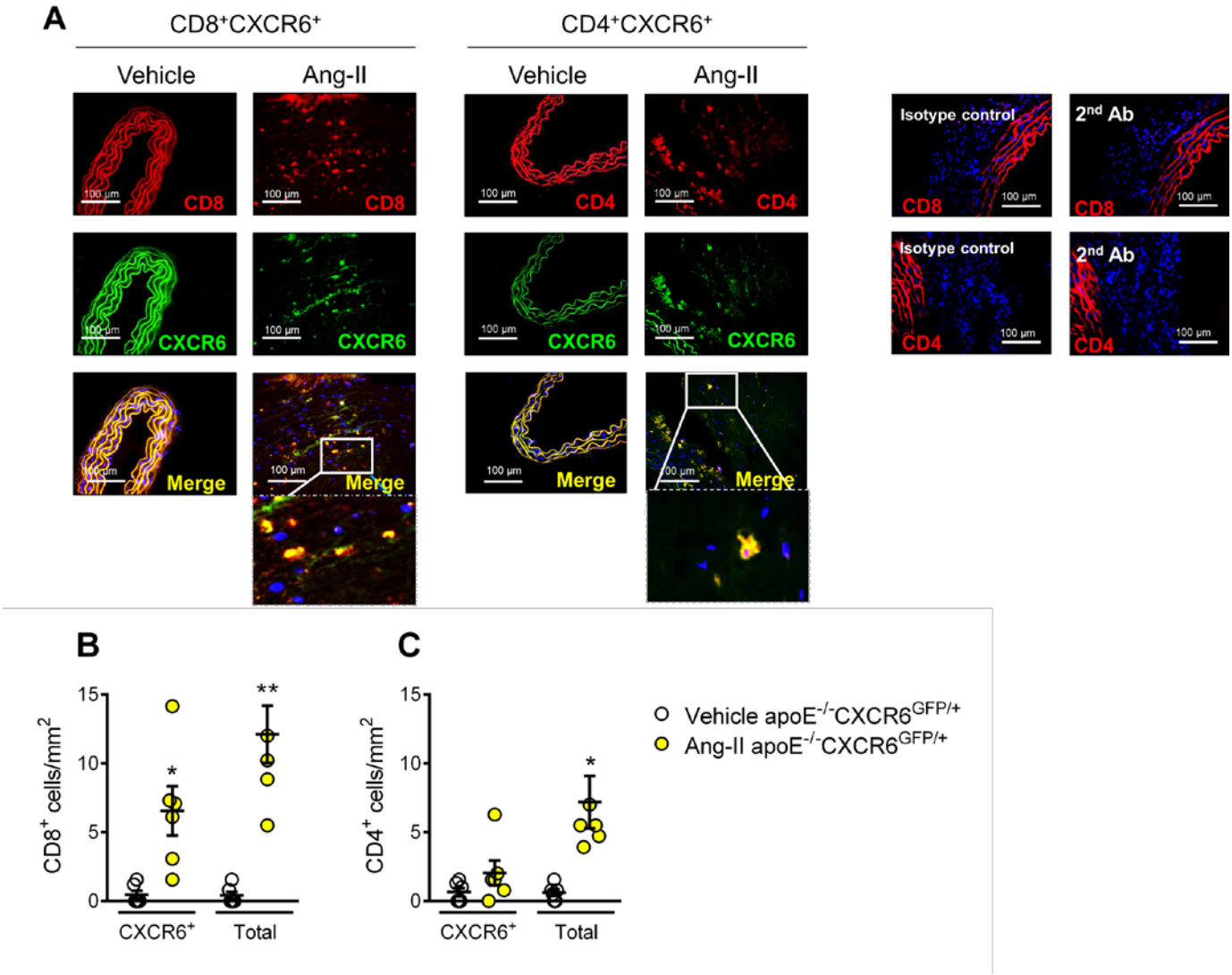

Figure 40. Increased infiltration of CD8$^+$CXCR6$^+$ but no CD4$^+$CXCR6$^+$ lymphocytes in AAA lesion in apoE$^{-/-}$CXCR6$^{GFP/+}$ mice. Representative photomicrographs of CD8$^+$, CD4$^+$, CXCR6$^+$, CD8$^+$CXCR6$^+$ and CD4$^+$CXCR6$^+$ lymphocytes in aortic cross sections of vehicle and Ang-II-infused apoE$^{-/-}$CXCR6$^{GFP/+}$ mice (**A**). CD4 and CD8 immunoreactivity were visualized using an Alexa Fluor® 647 antibody (red), and CXCR6 immunoreactivity was visualized by GFP protein (green). Nuclei were stained with Hoechst dye (blue). Total CD8$^+$CXCR6$^+$ and CD8$^+$ lymphocytes per mm^2 in aortic aneurysm sections (**B**). Total CD4$^+$CXCR6$^+$ and CD4$^+$ lymphocytes per mm^2 in aortic aneurysm sections (**C**). Results are expressed as mean ± SEM (n = 6–10 animals per group). *p <0.05 or **p <0.01 *vs.* vehicle-infused apoE$^{-/-}$CXCR6$^{GFP/+}$ mice.

		SBP (mmHg)	TC levels (mg/dL)	HDL levels (mg/dL)	TG (mg/dL)
ApoE$^{-/-}$	Control	117.8 ± 4.6	159.5 ± 14.2	54.3 ± 3.2	66.3 ± 3.5
	Ang-II	161.2 ± 8.8 **	163.5 ± 12.3	50.4 ± 3.3	63.8 ± 3.4
	Ang-II + Losartan	132.9 ± 9.7 +	156.3 ± 10.2	50.3 ± 5.4	60.6 ± 3.1
ApoE$^{-/-}$ CXCR6$^{GFP/+}$	Control	127.6 ± 12.6	180.3 ± 12.5	47.2 ± 4.9	61.1 ± 4.8
	Ang-II	164.8 ± 10.9 *	161.1 ± 18.5	45.2 ± 4.8	66.5 ± 14.1
ApoE$^{-/-}$ CXCR6$^{GFP/GFP}$	Control	129.7 ± 6.4	174.9 ± 11.7	46.9 ± 4.3	64.8 ± 7.4
	Ang-II	184.7 ± 10.4 **	183.2 ± 10	46.9 ± 4.9	64.7 ± 4.8

Table 22. Ang-II infusion increases systolic blood pressure (SBP) but not TC, HDL or TG levels in apoE$^{-/-}$, apoE$^{-/-}$CXCR6$^{GFP/+}$ and apoE$^{-/-}$CXCR6$^{GFP/GFP}$ mice. Data are presented as mean ± SEM of 5–10 animals per group. *p <0.05 or **p <0.01 relative to values in control mice infused with saline. +p <0.05 relative to values in apoE$^{-/-}$ mice infused with Ang-II. SBP, systolic blood pressure; TC, total cholesterol; HDL, high-density lipoprotein; TG, triglycerides.

5. DISCUSSION

5.1 STUDY OF THE SYSTEMIC INFLAMMATION IN PATIENTS WITH PH AND ITS MODULATION BY AN OFL

PH is associated with the risk of developing arteriosclerosis and the likelihood of future ischemic severe events. Previous studies have provided evidence of low systemic inflammation in patients with hypercholesterolemia (Sampietro *et al.* 1997, Chironi *et al.* 2006, Real *et al.* 2010a, Holven *et al.* 2014, Cortes *et al.* 2016, Hansen *et al.* 2019). Here, we carried out a detailed characterization of different immune players and soluble inflammatory markers in PH and correlated these data with the circulating levels of key lipid components (apoB, LDL, and TC). The enhanced inflammatory status of PH reported herein has functional consequences, as illustrated for circulating platelet-bound leukocytes, which have increased adhesiveness to dysfunctional arterial endothelium, a prominent feature of the atherogenic process. Furthermore, administration of an OFL to PH patients partially decreased the systemic inflammatory response associated with PH.

Platelet activation is known to be associated with atherogenesis and cardiovascular morbidity (von Hundelshausen *et al.* 2014). Indeed, upon their activation, platelets express specific cell adhesion molecules such as P-selectin and release several inflammatory chemokines, including PF-4/CXCL4 or RANTES/CCL5 (von Hundelshausen *et al.* 2014). We have shown that patients with PH present a pro-thrombotic state characterized by increased platelet activation (P-selectin^{+} and PAC-1^{+} platelets). However, 4 hours after the administration of the lipid OFL, platelet activation was reduced, evidencing the potential anti-thrombotic effect of the administered treatment. While hypercholesterolemia has been previously associated with platelet activation (Chironi *et al.* 2006, Barale *et al.* 2018), we found that patients have both increased circulating levels of sP-selectin and PF-4/CXCL4, which are involved in multiple atherogenic processes. Indeed, different platelet surface molecules such as GPIIb/IIIa (recognized by PAC-1) or P-selectin are critically involved in the interaction of platelets to endothelial cells and leukocytes (von Hundelshausen *et al.* 2014), all of which are central for atherosclerotic lesion formation. Again, the OFL decreased the circulating levels of several inflammatory mediators linked to platelet activation such as sP-selectin, PF-4/CXCL4 and RANTES/CCL5. Taken together, it seems that this treatment impaired the pro-thrombotic state associated with PH.

To gain insight into the immune state of the hypercholesterolemic environment of PH, we examined different leukocyte subtypes. An increase in leukocyte activation *in vitro* has been reported in subjects at high cardiovascular risk (hyperlipidemia) (Mazor *et al.* 2008). In our study, whereas no differences in the percentage of circulating neutrophils were detected between patients and controls, a clear increase in the percentage of activated cells ($CD69^+$) was observed, suggesting the existence of a pro-atherogenic state. This is consistent with our finding of increased circulating levels of IL-8/CXCL8, which is involved in neutrophil activation, in the PH group, as has been reported previously, albeit in patients with familial hypercholesterolemia (Cortes *et al.* 2016). Also, the plasma concentrations of this chemokine positively correlated with the circulating levels of key lipids in PH: apoB, LDL, and TC. Overall, these results indicate that IL-8 might have utility as a biomarker of atherosclerotic risk in PH. On the other hand, after 4 hours of treatment of PH patients with an OFL, a slight though not significant decrease in the percentage of activated neutrophils ($CD69^+$) was detected which was in agreement with the substantial reduction encountered in the circulating levels of IL-8/CXCL8, evidencing an improvement in the immune state.

Human monocytes are a heterogeneous cell population that is commonly classified into three subtypes: classical $CD14^+CD16^-CCR2^+$ (Mon 1), intermediate $CD14^+CD16^+CCR2^+$ (Mon 2), and nonclassical $CD14^+CD16^+CCR2^-$ (Mon 3) (Weber *et al.* 2016). There is evidence to support that adults with PH have a proinflammatory imbalance in circulating monocyte subpopulations (Mon 1) (Fadini *et al.* 2014), although another study has indicated that the levels of Mon 2 and/or Mon 3 subtypes were increased in hyperlipidemia and associated with atherosclerosis development (Wu *et al.* 2017). We found that only the percentage of the nonclassical/Mon 3 subtype was increased in patients over controls, and this positively correlated with the circulating levels of apoB, LDL, and TC. By contrast, Mon 1 and Mon 2 subtypes, both of which express the CCR2 receptor, were significantly activated in patients. We also show, for the first time, an increase in the percentage of CX_3CR1 expression on Mon 1 monocytes in heparinized whole blood, and on all monocyte subsets when platelets were dissociated. In line with these observations, studies of atherosclerosis in mice suggest that both inflammatory (similar to human Mon 1) and patrolling (comparable to human Mon 3) monocytes are involved in disease progression (Kratofil *et al.* 2017). In humans, different studies have noted increases in circulating $CD16^+$

monocytes in cardiovascular disease (Kratofil *et al.* 2017), which are possibly linked to disease outcome (Urra *et al.* 2009). After 4 hours of OFL administration, a significant decrease was observed in the percentage of circulating monocytes, mainly in the percentage of Mon 1.

On the other hand, there is also evidence to support that mobilized classical monocytes from the bone marrow mature into nonclassical monocytes through an intermediate subset. How these different monocyte subtypes correlate with disease pathogenesis and clinical outcomes in PH is, however, unknown. Nevertheless, it is likely that those subtypes expressing both CCR2 and CX_3CR1 are more prone to migrate from the circulation into arterial walls through the interaction with their cognate ligands MCP-1/CCL2 and CX_3CL1, the circulating levels of which were significantly elevated in patients and correlated positively with plasma apoB, LDL, and TC content. In this regard, MCP-1 levels were reduced after 4 hours of OFL, which may be related to the reduced percentage of circulating Mon 1 monocytes.

To the best of our knowledge, the associations we have found between T lymphocytes and PH have never previously been reported. Four findings are worthy of mention. First, the percentage of circulating $CD4^+$ cells was significantly higher in PH patients than controls and directly correlated with the levels of apoB, LDL, and TC. Of note, this increase was likely due to the increased numbers of circulating Th2 and Th17 cells. Second, most of the T cell subpopulations in patients displayed an activated state, and positive correlations were found between the percentage of $CD8^+CD69^+$ cells and key lipid features of the disease. Third, the percentage of circulating Treg cells and the Treg/Th17 ratio was decreased in PH patients. Finally, whereas IL-12, TNFα and IL-6 plasma levels were increased in patients, levels of the anti-inflammatory cytokines IL-4 and IL-10 were decreased and inversely correlated with the levels of apoB, LDL, and TC. These observations, overall, link the cellular and molecular inflammatory profile to a possible pro-atherogenic environment.

Along with this line, it is well known that both $CD4^+$ and $CD8^+$ T cells are involved in atherosclerosis development (Ketelhuth *et al.* 2016). While the role of Th2 cells in atherogenesis remains debated (Ketelhuth *et al.* 2016), it has recently been shown that patients with coronary artery atherosclerosis had an impaired Treg/Th17 ratio together with

reduced serum levels of IL-10 (Ding *et al.* 2016). Th17 cells repress the function of Treg cells, contributing to an inflammatory milieu. Moreover, whereas Th17 cells can produce the inflammatory cytokines TNFα and IL-6 (Olson *et al.* 2013), Treg cells generate and release the anti-inflammatory cytokine IL-10. It is therefore tempting to speculate that there is a conversion of Treg cells into Th17 cells in PH. Finally, although IL-4 is a classic Th2 cytokine, the decreased levels found in patients suggest an alternative cellular origin of this cytokine. Indeed, potential sources of IL-4 are double-positive CD4/CD8 lymphocytes, basophils or natural killer T cells (Quandt *et al.* 2014, Yoshimoto 2018), whose circulating levels may be decreased in this pathology, although this requires further investigation. When the immune status of PH patients was analyzed 4 h after the administration of the OFL, a significant decrease in circulating TNFα concentrations and an increase in the percentage of Treg was observed, which may contribute to the anti-inflammatory environment exerted by this treatment. Nevertheless, neither the Treg/Th17 ratio nor circulating levels of IL-10 were improved although it is feasible that the latter would change if the determination were done at a later time point.

Finally, we used the dynamic model of the flow chamber to explore the functional consequences of platelet-leukocyte-endothelium (heparin) or leukocyte-endothelium (EDTA) interactions, finding that adhesion of platelet-leukocyte aggregates to HUAEC, stimulated or not with TNFα, was significantly higher in the patient group. The increased adhesion to functional (no stimulated) endothelium was likely due to neutrophil, and monocyte activation and consequent over-expression of CD11b/CD18 integrin, which interacts with the constitutively expressed intercellular cell adhesion molecule-1 in the endothelium. Furthermore, platelets seem to be critical for leukocyte adhesion to dysfunctional (stimulated) arterial endothelium, as leukocyte-endothelium interactions were significantly impaired when platelets were dissociated with EDTA. It is widely accepted that activated platelets can mediate the endothelial adhesion of circulating leukocytes, a characteristic feature of the dysfunctional endothelium (Landmesser *et al.* 2004, Rius *et al.* 2013a, Rius *et al.* 2013b, Marques *et al.* 2017, Furio *et al.* 2018). We also found a significant enhancement in the percentage of platelet-leukocyte aggregates, which were established with almost all the leukocyte subsets investigated in a background of PH. The increased number of these aggregates has been detected in the peripheral circulation of patients with unstable

angina or other coronary diseases, and they have been considered a predictive factor of acute myocardial infarction (Michelson *et al.* 2001). This platelet-leukocyte interaction is in all probability due to the interaction of platelet P-selectin with its ligand, PSGL-1, present on leukocyte surfaces, which in turns facilitates the contact between these aggregates and the dysfunctional endothelium, a key event in arteries prone to arteriosclerotic lesion development (Landmesser *et al.* 2004). Inasmuch, when these parameters were evaluated after 4 h administration of the OFL, diminished adhesion of both platelet-leukocyte (heparin) and leukocyte (EDTA) to the dysfunctional arterial endothelium was observed, reinforcing the potential beneficial anti-inflammatory effect of the lipid load treatment in patients with this metabolic disorder.

In summary, the low-grade systemic inflammation associated with PH is accompanied by a pro-thrombotic state with heightened platelet activation and associated circulating soluble markers. This platelet activation state in PH, together with the activation of different leukocyte subsets, results in the formation of platelet-leukocyte aggregates and their adhesion to dysfunctional arterial endothelium, suggesting a possible link between systemic inflammation and cardiovascular disease development in this metabolic disorder. Moreover, the positive correlations between key lipid features of PH and different circulating proinflammatory mediators (IL-8, MCP-1, fractalkine or IL-6) and the negative correlations between these lipids and anti-inflammatory cytokines (IL-4 and IL-10) might be used as potential markers of cardiovascular disease. Finally, the administration of an OFL has a beneficial impact on the pro-thrombotic and proinflammatory state of PH patients, although further long-term studies in animal models are required. Nevertheless, the modulation of the cellular and inflammatory molecular components in PH, as well as the lipid profile, might be crucial to prevent further cardiovascular complications.

5.2 STUDY OF THE ROLE OF THE CCL11/CCR3 AXIS IN PH AND ATHEROSCLEROSIS DEVELOPMENT

PH is a metabolic disorder which is associated with the risk of developing early arteriosclerosis and the likelihood of suffering further ischemic severe events. Previous studies in PH patients have provided evidence of some signs of a low-grade of systemic inflammation in this lipid disorder (Sampietro *et al.* 1997, Real *et al.* 2010a, Holven *et al.* 2014, Cortes *et al.* 2016, Collado *et al.* 2018a). In the current thesis and for the first time, we found that the circulating levels of two inflammatory mediators not yet linked to this metabolic disease, the C-C chemokines eotaxin-1/CCL11 and eotaxin-3/CCL26, were significantly elevated in PH patients. Of note, eotaxin-1/CCL11 and eotaxin-3/CCL26 plasma concentrations positively correlated with the altered circulating levels of key lipid components of this disease (apoB, LDL, and TC). Therefore, these results led us to examine the different cell populations that might be affected by these chemokines.

Both eotaxin-1/CCL11 and eotaxin-3/CCL26 only signal through the CCR3 receptor (Combadiere *et al.* 1996, Kitaura *et al.* 1996, Petkovic *et al.* 2004) and consequently, increased CCR3 expression on platelet-bound or unbound (EDTA) leukocytes and the percentage of circulating $CCR3^+$ cells were encountered in PH patients compared with control individuals. Further analyses of the potential $CCR3^+$ populations revealed relevant and novel information. First, as eotaxins are key eosinophil chemoattractants, we found enhanced circulating numbers of eosinophils, a hematological feature not previously described in PH patients. Second, the percentage of both progenitor mast cells and Th2 lymphocytes were also increased in these patients. In contrast, neither the percentage of platelets nor basophils were enhanced. In fact, the latter was found to be significantly decreased in people with this metabolic disorder. Furthermore, while the percentages of $CCR3^+$ eosinophils, progenitor mast cells and basophils were increased in PH patients, $CCR3^+$ platelets or Th2 lymphocytes either remained unmodified or decreased. Finally, both the percentage of circulating eosinophils and Th2 lymphocytes positively correlated with plasma apoB, LDL, and TC content, three key clinical features of PH.

In this human setting and given that Th2 lymphocytes are capable of generating and release cytokines such as IL-4, IL-5 or IL-13 (Fallon *et al.* 2002), the decreased

concentrations of IL-4 and IL-5 in patients *vs.* control subjects suggest an origin of these cytokines other than Th2 lymphocytes (Quandt *et al.* 2014). Indeed, alternative IL-4 sources could be basophils, which are considered IL-4-producers under infection conditions (Min *et al.* 2004, van Panhuys *et al.* 2011) and circulating levels of this cells are decreased in PH patients. Nevertheless, further studies are required to confirm such contention.

Although eotaxin-1/CCL11 has been detected in humans and mice's atherosclerotic lesions (Haley *et al.* 2000, Kraaijeveld *et al.* 2007), its role in this pathology remains mostly unknown. Therefore, to try to understand the remarkable observations here described in PH patients, we first investigated whether some of these findings were reproduced in apoE$^{-/-}$ mice subjected to an atherogenic diet. Indeed, significantly higher plasma levels of eotaxin-1/CCL11 and percentage of circulating CCR3-expressing leukocytes were found in apoE$^{-/-}$ mice subjected to a high-fat diet compared with those under a control diet. This increased percentage of CCR3^{+} cells was due to augmented numbers of circulating eosinophils since the percentage of circulating progenitor mast cells remained unchanged in both groups, and murine Th2 lymphocytes do not express CCR3 receptor (Romagnani 2002).

Given that the literature indicates that eosinophils are rarely present in the atherosclerotic lesion, but eotaxin-1/CCL11 is (Haley *et al.* 2000, Kraaijeveld *et al.* 2007), we next generated a double-deficient mice in apoE and the eotaxin receptor, CCR3 (apoE$^{-/-}$CCR3$^{-/-}$) to try to clarify the role of the CCL11/CCR3 axis in this pathological condition. Thus, both apoE$^{-/-}$CCR3$^{+/+}$ and apoE$^{-/-}$CCR3$^{-/-}$ mice were subjected for two months to either a control or an atherogenic diet.

As expected, the quantification of the atherosclerotic lesion revealed that the lesion in the aortic arch of the apoE$^{-/-}$CCR3$^{+/+}$ and apoE$^{-/-}$CCR3$^{-/-}$ mice was very evident in those animals subjected to the atherogenic diet and practically absent in mice undergoing control diet. Surprisingly, the lesion in the apoE$^{-/-}$CCR3$^{-/-}$ group was, in turn, significantly higher than that detected in apoE$^{-/-}$CCR3$^{+/+}$ mice. Further analyses of the lesions showed that apoE$^{-/-}$CCR3$^{-/-}$ mice had higher and significant infiltration of macrophages and T lymphocytes in the lesions than their respective controls when both were subjected to a hypercholesterolemic diet. Immunodetection of eotaxin-1 in the aortic sinus of all animals, subjected or not to an atherogenic diet showed, that eotaxin-1 was only detected in

apoE$^{-/-}$CCR3$^{+/+}$ mice subjected to an atherogenic diet but not in those subjected to a control diet or in apoE$^{-/-}$CCR3$^{-/-}$ mice fed with a hypercholesterolemic diet. Therefore, it is feasible that the lack of eotaxin-1 in the lesion of apoE$^{-/-}$CCR3$^{-/-}$ mice results in increased macrophage numbers since eotaxin-1/CCL11 acts as an antagonist of CCR2 receptor, which is expressed on the surface of proinflammatory monocytes (Ogilvie *et al.* 2001), and its ligand (MCP-1/CCL2) is involved in the mononuclear cell infiltration into the atherosclerotic lesion (Gonzalez-Quesada *et al.* 2009). The higher number of T lymphocytes was mainly due to CD8^{+} lymphocytes, which are reported to promote atherosclerosis, the release of proinflammatory cytokines such as IFNγ that affect monocyte recruitment, and provoke the activation of cytolytic pathways inducing the death of both smooth muscle and endothelial cells (van Duijn *et al.* 2018).

One essential question that now arises is the source of eotaxin-1 under a hypercholesterolemic scenario. While Haley *et al.* 2000, indicated that its expression was predominant in regions rich in vascular SMC, our group did not detect it in those areas. Inasmuch, our results suggest that a CCR3-expressing cell is likely the source of eotaxin. In this regard, we have described for the first time the presence of eosinophils in the lesion. Moreover, mast cells were also present, which are known to express CCR3 receptor when activated (Forsythe *et al.* 2003, Juremalm *et al.* 2005) and are widely localized in the atherosclerotic lesion, mainly in the adventitial layer and in the regions prone to rupture (Bot *et al.* 2015). In fact, the interaction of eotaxin-1 with its CCR3 receptor can induce mast cell migration (Forsythe *et al.* 2003, Juremalm *et al.* 2005). Nevertheless, both eosinophils and mast cells are potential sources of eotaxin-1/CCL11 (Hogaboam *et al.* 1998, Lampinen *et al.* 2004). Since increased mast cell numbers and decreased eosinophil infiltration were encountered in the lesion of apoE$^{-/-}$CCR3$^{-/-}$ mice subjected to an atherogenic diet compared with those found in apoE$^{-/-}$CCR3$^{+/+}$ mice subjected to the same diet, it is tempting to speculate that eosinophils are one of the key sources of eotaxin-1 in this hypercholesterolemic environment.

Since inflammation is a crucial feature of obesity (Schipper *et al.* 2012) and increased circulating levels of eotaxin-1 have been detected in obese individuals (Vasudevan *et al.* 2006), we next analyzed the subcutaneous adipose tissue from apoE$^{-/-}$CCR3$^{+/+}$ and apoE$^{-/-}$CCR3$^{-/-}$ mice, fed or not with an atherogenic diet. Adipocyte size was found to be

smaller in atherogenic diet-fed animals than in those under control diet. While an increased size of adipocytes has been usually associated to inflammation, others have suggested that in subcutaneous adipose tissue, an increased proportion of small (relative-to-large) adipose cells, independently predict the expression of inflammatory genes (McLaughlin *et al.* 2010). Based on the recent findings, it is feasible that these small cells may be dysfunctional and inflammatory. However, it is also possible that the increased proportion of small cells may reflect impaired adipogenesis, putting storage stress on the existing large adipose cells, which in turn would promote inflammation (McLaughlin *et al.* 2010).

Furthermore, CCR3-expressing cells in subcutaneous adipose tissue were mainly due to eosinophils and mast cells whose numbers were decreased in those animals fed with an atherogenic diet. Interestingly, the percentage of AAM was also significantly impaired in those mice. In this regard, AAM improve insulin sensitivity, but eosinophils are required for monocyte polarization to this anti-inflammatory macrophage state (Wu *et al.* 2011). The absence of eosinophils leads to adiposity and systemic insulin resistance, implying a protective role of this leukocyte population in the metabolic homeostasis (Jung *et al.* 2014). Likewise, it is well known that eosinophils are produced in the bone marrow and they migrate to peripheral tissues including the adipose tissue and the lamina of the intestine through the expression of the CCR3 receptor (Jung *et al.* 2014).

During the last decade, the composition of gut microbiota has been shown to be critical in disease development, including cardiovascular disorders (Tang *et al.* 2017). Therefore, to understand the role of the CCL11/CCR3 axis in atherosclerosis, we also analyzed the small intestine of apoE$^{-/-}$CCR3$^{+/+}$ and apoE$^{-/-}$CCR3$^{-/-}$ mice fed or not with an atherogenic diet. When animals were fed with a high-fat diet, the length of the *villi* increased in apoE$^{-/-}$CCR3$^{+/+}$ mice compared with those under a control diet. However, apoE$^{-/-}$CCR3$^{-/-}$ subjected to the same diet showed decreased in *villi* length. In contrast and under these conditions, crypt size in apoE$^{-/-}$CCR3$^{-/-}$ mice was higher than in apoE$^{-/-}$CCR3$^{+/+}$ mice. Notably, the number of gut eosinophils was increased in apoE$^{-/-}$CCR3$^{+/+}$ mice fed with the atherogenic diet compared with those under the control diet which correlated with the increased *Eotaxin-1* mRNA expression in the tissue. Conversely, a lower number of eosinophils were found in apoE$^{-/-}$CCR3$^{-/-}$ subjected to a high-fat diet. Therefore, additional analyses are required to accurately detect eotaxin-1/CCL11 protein expression in the gut of

both genotypes. Eosinophils have long been considered effector cells with a protective role against parasitic infections. However, they are also associated with numerous inflammatory diseases. Indeed, several lines of evidence indicate that eosinophils are multifunctional leukocytes involved in biologic processes in the gastrointestinal tract (Jung *et al.* 2014). Nevertheless, to date, clear conclusion from these results cannot be achieved, and further studies are now in progress to understand their role in the gut under a pro-atherogenic environment.

By contrast, while no differences were found in the number of mast cells in apoE$^{-/-}$CCR3$^{+/+}$ mice, there was an increased number of them in apoE$^{-/-}$CCR3$^{-/-}$ mice, especially in those animals fed with a high-fat diet. Mast cells are tissue-resident immune cells and exert different functions. In health, they protect from microorganisms; in disease, they can release mediators that participate in the inflammatory bowel response leading to mucosa activation and the infiltration of additional inflammatory cells (Hamilton *et al.* 2014). Nevertheless, it is likely that those mast cells will be in a low activation state since, in those animals (apoE$^{-/-}$CCR3$^{-/-}$ mice), CCR3 receptor is not expressed and it is a critical marker of mast cell activation.

Finally, apoE$^{-/-}$CCR3$^{+/+}$ mice fed with an atherogenic diet had an increased number of eosinophils and CCR3^{+} mast cells in the bone marrow. In contrast, apoE$^{-/-}$CCR3$^{-/-}$ mice, under similar conditions, have even higher amounts of both cell types. Moreover, circulating plasma levels of CCL11/eotaxin-1, IL-4, and IL-5 were drastically decreased in apoE$^{-/-}$CCR3$^{-/-}$ animals under atherogenic conditions. It is possible that impaired eotaxin-1 and IL-5 circulating levels impede the egress of eosinophils from the bone marrow since both mediators are required for proper eosinophil circulation and infiltration *in vivo* (Collins *et al.* 1995). Taken together these intriguing observations, it seems that CCL11/CCR3 axis exerts a protective effect against the development of atherosclerotic lesions under hypercholesterolemic conditions. In fact, administration of an atherogenic diet provokes increased numbers of circulating eosinophils, their infiltration in the atherogenic lesion and gut, but impairs their accumulation in the subcutaneous adipose tissue. Therefore, further studies evaluating eosinophil role and behavior in a hypercholesterolemic environment are required to understand the contribution of these immune players in the atherogenic process.

5.3 STUDY OF THE ROLE OF CXCR6 RECEPTOR IN ABDOMINAL AORTIC ANEURYSM FORMATION

Previous *in vitro* studies carried out by our research group showed a relevant role of the CXCL16/CXCR6 axis in the initial attachment of leukocytes to the dysfunctional arterial endothelium. To understand the potential contribution of this axis in an *in vivo* inflammatory environment, we infused Ang-II into $CXCR6^{GFP/+}$ mice for 14 days and found an increase in the adhesion of leukocytes to the cremasteric arterioles. This response was dampened in $CXCR6^{GFP/GFP}$ mice lacking a functional CXCR6 receptor. Furthermore, decreased monocyte and T lymphocyte activation was detected in $CXCR6^{GFP/GFP}$ mice subjected to the same stimulus. These initial observations led us to suspect that the CXCL16/CXCR6 axis was probably involved in pathologies associated with vascular inflammation in which Ang-II plays a crucial role.

In this regard, the role of RAS in the AAA pathogenesis is widely accepted (Daugherty *et al.* 2006, Zhang *et al.* 2009); however, pharmacological treatment options focused on the modulation of this system are limited. In particular, the role of CXCL16 in this pathology has been scarcely investigated. In the only study performed so far, an increase in *Cxcl16* mRNA expression was detected in $CaCl_2$-induced AAA (Ren *et al.* 2014). Interestingly, chronic blockade of the AT_1 receptor with losartan reduced AAA formation; this was accompanied by impaired monocyte, T lymphocyte, and $CXCR6^+$ cell infiltration into the AAA lesion. Moreover, decreased *Cxcl16* mRNA expression within the aneurismal lesion and circulating levels of the soluble chemokine were detected in losartan-treated animals. Since both cell types, monocytes, and T lymphocytes, express the CXCR6 receptor (Ludwig *et al.* 2007), it is tempting to speculate that the decreased endothelial expression of CXCL16 is partly responsible for the reduced cellularity within the lesion. Nonetheless, other chemokines such as MCP-1/CCL2 are likely involved in the aneurismal mononuclear cell infiltration as Ang-II can promote MCP-1/CCL2 generation and release (Mateo *et al.* 2006), and neutralization CCL2/CCR2 axis has been shown to halt Ang-II-induced AAA development (Daugherty *et al.* 2010).

We also detected ameliorated angiogenesis in animals treated with losartan, measured as the number of $CD31^+$ capillary vessels. Inflammatory cells recruitment can be driven by

newly formed vessels, thus amplifying the angiogenic and inflammatory processes both, as these leukocyte subtypes are able to release growth factors and pro-angiogenic chemokines. In this sense, CXCL16 can promote endothelial proliferation, migration, and tube formation (Zhuge *et al.* 2005, Wente *et al.* 2008). Additionally, $CXCR6^+$ cells produce angiogenic factors such as VEGF and IL-8 (Wang *et al.* 2008), and CXCR6 deficiency results in profound decreases in T cell and monocyte in the arthritic joint, which has seen to correlate with impaired vessel formation (Isozaki *et al.* 2013). Furthermore, a strong correlation between CXCR6 expression and cancer aggressiveness has been linked to angiogenic processes (Wang *et al.* 2008, Gao *et al.* 2012). More recently, the simultaneous neutralization of CXCL16 and MCP-1/CCL2 activity has been shown to significantly inhibit tube formation in venous endothelial cells (Han *et al.* 2014).

We generated $apoE^{-/-}$ mice with a CXCR6 deficiency to better understand the role of the CXCL16/CXCR6 axis in an AAA milieu. Deficiency in CXCR6 markedly attenuated AAA formation, an effect unrelated to systolic blood pressure or plasma cholesterol concentrations. Decreased lesion formation was associated with a reduction in macrophages, T lymphocytes and $CXCR6^+$ cell infiltrates, and neovascularization; and also with impaired *Mcp-1 (Ccl2)*, *Cxcl16* and *Vegf* mRNA expression. Thus, $CXCR6^+$ cells are likely additional sources of inflammatory and angiogenic mediators, including CXCL16. Notably, immunofluorescence analyses revealed a marked increase in $CD8^+CXCR6^+$ but not in $CD4^+CXCR6^+$ lymphocyte infiltration in the AAA lesion of $apoE^{-/-}CXCR6^{GFP/+}$ mice, which resembles the pattern encountered in circulating CXCR6-expressing platelet-lymphocyte aggregates in metabolic syndrome patients (Collado *et al.* 2018b). Furthermore, $CD8^+$ T cells are known to release inflammatory cytokines, promoting the recruitment of monocytes; and to produce the cytolysis of SMC and endothelial cells (van Duijn *et al.* 2018). Moreover, IFNγ producing $CD8^+$ T cells, but not $CD4^+$ T cells, have been reported to promote the development of AAA in mice by enhancing cellular apoptosis and MMPs activity (Zhou *et al.* 2013).

Therefore, CXCL16/CXCR6 axis plays a functional role in AAA formation, and pharmacological modulation of this axis may positively affect the cardiovascular outcome in those disorders linked to RAS activation.

6. CONCLUSIONS

1. PH is accompanied by a low-grade of systemic inflammation and associated to platelet and leukocyte activation which results in the formation of platelet-leukocyte aggregates and their adhesion to dysfunctional arterial endothelium, suggesting a possible link between systemic inflammation and cardiovascular disease development in this metabolic disorder.

2. The positive correlations between key lipid features of PH and different circulating proinflammatory mediators (IL-8, MCP-1, fractalkine or IL-6) and the negative correlations between these lipids and anti-inflammatory cytokines (IL-4 and IL-10) might be used as potential markers of cardiovascular disease.

3. The administration of a lipid OFL has a beneficial impact on the pro-thrombotic and inflammatory status of PH patients. Therefore, the modulation of the cellular and inflammatory molecular components in PH, as well as the lipid profile, might be crucial to prevent further cardiovascular complications.

4. ApoE$^{-/-}$ mice subjected to an atherogenic diet and PH patients have increased levels of circulating eotaxin-1 (CCL11) and eosinophils than their respective controls.

5. Studies in apoE$^{-/-}$CCR3$^{-/-}$ and apoE$^{-/-}$CCR3$^{+/+}$ mice fed with an atherogenic diet for two months suggest that eotaxin-1 (CCL11)/CCR3 axis may exert a protective effect in the development of the atherosclerotic process under hypercholesterolemic conditions.

6. CXCL16/CXCR6 axis plays a functional role in the AAA formation. ApoE$^{-/-}$ mice lacking functional CXCR6 receptor had a lower incidence of AAA, impaired macrophage, CD3^{+}, and CXCR6^{+} cell infiltration and neovascularization than control animals, which was accompanied by decreased *Mcp-1/Ccl2*, *Cxcl16* and *Vegf* mRNA expression within the lesion. Therefore, pharmacological modulation of this axis may prevent or even delay the progression of this cardiovascular disorder linked to RAS activation.

7. REFERENCES

Abadier, M. and Ley, K. (2017). P-selectin glycoprotein ligand-1 in T cells. *Curr Opin Hematol* **24**(3): 265-273.

Abel, S., Hundhausen, C., Mentlein, R., Schulte, A., Berkhout, T. A., Broadway, N., Hartmann, D., Sedlacek, R., Dietrich, S., Muetze, B., Schuster, B., Kallen, K. J., Saftig, P., Rose-John, S. and Ludwig, A. (2004). The transmembrane CXC-chemokine ligand 16 is induced by IFN-gamma and TNF-alpha and shed by the activity of the disintegrin-like metalloproteinase ADAM10. *J Immunol* **172**(10): 6362-6372.

Abu Nabah, Y. N., Losada, M., Estelles, R., Mateo, T., Company, C., Piqueras, L., Lopez-Gines, C., Sarau, H., Cortijo, J., Morcillo, E. J., Jose, P. J. and Sanz, M. J. (2007). CXCR2 blockade impairs angiotensin II-induced CC chemokine synthesis and mononuclear leukocyte infiltration. *Arterioscler Thromb Vasc Biol* **27**(11): 2370-2376.

Adair, T. H. and Montani, J. P. (2010). Integrated Systems Physiology: from Molecule to Function to Disease. Angiogenesis. San Rafael (CA), Morgan & Claypool Life Sciences

Copyright (c) 2010 by Morgan & Claypool Life Sciences.

Ahmad, Z., Adams-Huet, B., Chen, C. and Garg, A. (2012). Low prevalence of mutations in known loci for autosomal dominant hypercholesterolemia in a multiethnic patient cohort. *Circ Cardiovasc Genet* **5**(6): 666-675.

Ahmadi, Z., Hassanshahi, G., Khorramdelazad, H., Zainodini, N. and Koochakzadeh, L. (2016). An Overlook to the Characteristics and Roles Played by Eotaxin Network in the Pathophysiology of Food Allergies: Allergic Asthma and Atopic Dermatitis. *Inflammation* **39**(3): 1253-1267.

Alcazar, R., Ruiz-Ortega, M. and Egido, J. (2003). [Angiotensin II : a key peptide in vascular and renal failure]. *Nefrologia* **23 Suppl 4**: 27-35.

Alvarez, A., Cerda-Nicolas, M., Naim Abu Nabah, Y., Mata, M., Issekutz, A. C., Panes, J., Lobb, R. R. and Sanz, M. J. (2004). Direct evidence of leukocyte adhesion in arterioles by angiotensin II. *Blood* **104**(2): 402-408.

Alvarez, A. and Sanz, M. J. (2001). Reactive oxygen species mediate angiotensin II-induced leukocyte-endothelial cell interactions in vivo. *J Leukoc Biol* **70**(2): 199-206.

Andersen, L. H., Miserez, A. R., Ahmad, Z. and Andersen, R. L. (2016). Familial defective apolipoprotein B-100: A review. *J Clin Lipidol* **10**(6): 1297-1302.

Angarica, V. E., Orozco, M. and Sancho, J. (2016). Exploring the complete mutational space of the LDL receptor LA5 domain using molecular dynamics: linking SNPs with disease phenotypes in familial hypercholesterolemia. *Hum Mol Genet* **25**(6): 1233-1246.

Anjum, A. and Powell, J. T. (2012). Is the incidence of abdominal aortic aneurysm declining in the 21st century? Mortality and hospital admissions for England & Wales and Scotland. *Eur J Vasc Endovasc Surg* **43**(2): 161-166.

Ashley, N. T., Weil, Z. M. and Nelson, R. J. (2012). Inflammation: Mechanisms, Costs, and Natural Variation. *Annual Review of Ecology, Evolution, and Systematics* **43**(1): 385-406.

Aslanian, A. M. and Charo, I. F. (2006). Targeted disruption of the scavenger receptor and chemokine CXCL16 accelerates atherosclerosis. *Circulation* **114**(6): 583-590.

Avogaro, A. and de Kreutzenberg, S. V. (2005). Mechanisms of endothelial dysfunction in obesity. *Clin Chim Acta* **360**(1-2): 9-26.

Back, M., Weber, C. and Lutgens, E. (2015). Regulation of atherosclerotic plaque inflammation. *J Intern Med* **278**(5): 462-482.

Badimon, L. and Vilahur, G. (2014). Thrombosis formation on atherosclerotic lesions and plaque rupture. *J Intern Med* **276**(6): 618-632.

Bakogiannis, C., Sachse, M., Stamatelopoulos, K. and Stellos, K. (2017). Platelet-derived chemokines in inflammation and atherosclerosis. *Cytokine*.

Balakumar, P. and Jagadeesh, G. (2014). A century old renin-angiotensin system still grows with endless possibilities: AT1 receptor signaling cascades in cardiovascular physiopathology. *Cell Signal* **26**(10): 2147-2160.

Barale, C., Frascaroli, C., Senkeev, R., Cavalot, F. and Russo, I. (2018). Simvastatin Effects on Inflammation and Platelet Activation Markers in Hypercholesterolemia. *Biomed Res Int* **2018**: 6508709.

Baum, S. J. and Cannon, C. P. (2018). PCSK9 inhibitor valuation: A science-based review of the two recent models. *Clin Cardiol*.

Benjamin, E. J., Blaha, M. J., Chiuve, S. E., Cushman, M., Das, S. R., Deo, R., de Ferranti, S. D., Floyd, J., Fornage, M., Gillespie, C., Isasi, C. R., Jiménez, M. C., Jordan, L. C., Judd, S. E., Lackland, D., Lichtman, J. H., Lisabeth, L., Liu, S., Longenecker, C. T., Mackey, R. H., Matsushita, K., Mozaffarian, D., Mussolino, M. E., Nasir, K., Neumar, R. W., Palaniappan, L., Pandey, D. K., Thiagarajan, R. R., Reeves, M. J., Ritchey, M., Rodriguez, C. J., Roth, G. A., Rosamond, W. D., Sasson, C., Towfighi, A., Tsao, C. W., Turner, M. B., Virani, S. S., Voeks, J. H., Willey, J. Z., Wilkins, J. T., Wu, J. H. Y., Alger, H. M., Wong, S. S. and Muntner, P. (2017). Heart Disease and Stroke Statistics—2017. *Circulation* **135**(10): e146-603.

Bennett, M. R., Sinha, S. and Owens, G. K. (2016). Vascular Smooth Muscle Cells in Atherosclerosis. *Circ Res* **118**(4): 692-702.

Berberich, A. J. and Hegele, R. A. (2017). Lomitapide for the treatment of hypercholesterolemia. *Expert Opin Pharmacother* **18**(12): 1261-1268.

Bertoncello, N., Moreira, R. P., Arita, D. Y., Aragao, D. S., Watanabe, I. K., Dantas, P. S., Santos, R., Mattar-Rosa, R., Yokota, R., Cunha, T. S. and Casarini, D. E. (2015). Diabetic Nephropathy Induced by Increased Ace Gene Dosage Is Associated with High Renal Levels of Angiotensin (1-7) and Bradykinin. *J Diabetes Res* **2015**: 674047.

Blanchet, X., Langer, M., Weber, C., Koenen, R. R. and von Hundelshausen, P. (2012). Touch of chemokines. *Front Immunol* **3**: 175.

Borst, O., Munzer, P., Gatidis, S., Schmidt, E. M., Schonberger, T., Schmid, E., Towhid, S. T., Stellos, K., Seizer, P., May, A. E., Lang, F. and Gawaz, M. (2012). The inflammatory chemokine CXC motif ligand 16 triggers platelet activation and adhesion via CXC motif receptor 6-dependent phosphatidylinositide 3-kinase/Akt signaling. *Circ Res* **111**(10): 1297-1307.

Bot, I., Shi, G. P. and Kovanen, P. T. (2015). Mast cells as effectors in atherosclerosis. *Arterioscler Thromb Vasc Biol* **35**(2): 265-271.

Brasier, A. R., Recinos, A., 3rd and Eledrisi, M. S. (2002). Vascular inflammation and the renin-angiotensin system. *Arterioscler Thromb Vasc Biol* **22**(8): 1257-1266.

Camare, C., Pucelle, M., Negre-Salvayre, A. and Salvayre, R. (2017). Angiogenesis in the atherosclerotic plaque. *Redox Biol* **12**: 18-34.

Carbone, F., Mach, F. and Montecucco, F. (2015). Update on the role of neutrophils in atherosclerotic plaque vulnerability. *Curr Drug Targets* **16**(4): 321-333.

Clemetson, K. J., Clemetson, J. M., Proudfoot, A. E., Power, C. A., Baggiolini, M. and Wells, T. N. (2000). Functional expression of CCR1, CCR3, CCR4, and CXCR4 chemokine receptors on human platelets. *Blood* **96**(13): 4046-4054.

Collado, A., Marques, P., Domingo, E., Perello, E., Gonzalez-Navarro, H., Martinez-Hervas, S., Real, J. T., Piqueras, L., Ascaso, J. F. and Sanz, M. J. (2018a). Novel Immune Features of the Systemic Inflammation Associated with Primary Hypercholesterolemia: Changes in Cytokine/Chemokine Profile, Increased Platelet and Leukocyte Activation. *J Clin Med* **8**(1).

Collado, A., Marques, P., Escudero, P., Rius, C., Domingo, E., Martinez-Hervas, S., Real, J. T., Ascaso, J. F., Piqueras, L. and Sanz, M. J. (2018b). Functional role of endothelial CXCL16/CXCR6-platelet-leucocyte axis in angiotensin II-associated metabolic disorders. *Cardiovasc Res* **114**(13): 1764-1775.

Collins, C., Guilluy, C., Welch, C., O'Brien, E. T., Hahn, K., Superfine, R., Burridge, K. and Tzima, E. (2012). Localized tensional forces on PECAM-1 elicit a global mechanotransduction response via the integrin-RhoA pathway. *Curr Biol* **22**(22): 2087-2094.

Collins, P. D., Marleau, S., Griffiths-Johnson, D. A., Jose, P. J. and Williams, T. J. (1995). Cooperation between interleukin-5 and the chemokine eotaxin to induce eosinophil accumulation in vivo. *J Exp Med* **182**(4): 1169-1174.

Combadiere, C., Ahuja, S. K. and Murphy, P. M. (1996). Cloning and functional expression of a human eosinophil CC chemokine receptor. *J Biol Chem* **271**(18): 11034.

Company, C., Piqueras, L., Naim Abu Nabah, Y., Escudero, P., Blanes, J. I., Jose, P. J., Morcillo, E. J. and Sanz, M. J. (2011). Contributions of ACE and mast cell chymase to endogenous angiotensin II generation and leucocyte recruitment in vivo. *Cardiovasc Res* **92**(1): 48-56.

Coronato, S., Laguens, G. and Di Girolamo, V. (2012). [Role of metalloproteinases and their inhibitors in tumors]. *Medicina (B Aires)* **72**(6): 495-502.

Cortes, R., Ivorra, C., Martinez-Hervas, S., Pedro, T., Gonzalez-Albert, V., Artero, A., Adam, V., Garcia-Garcia, A. B., Ascaso, J. F., Real, J. T. and Chaves, F. J. (2016). Postprandial Changes in Chemokines Related to Early Atherosclerotic Processes in Familial Hypercholesterolemic Subjects: A Preliminary Study. *Arch Med Res* **47**(1): 33-39.

Cortes, R., Martinez-Hervas, S., Ivorra, C., De Marco, G., Gonzalez-Albert, V., Rojo-Martinez, G., Saez, G., Carmena, R., Ascaso, J. F., Real, J. T. and Chaves, F. J. (2014). Enhanced reduction in oxidative stress and altered glutathione and thioredoxin system

response to unsaturated fatty acid load in familial hypercholesterolemia. *Clin Biochem* **47**(18): 291-297.

Cuevas, C. A., Gonzalez, A. A., Inestrosa, N. C., Vio, C. P. and Prieto, M. C. (2015). Angiotensin II increases fibronectin and collagen I through the beta-catenin-dependent signaling in mouse collecting duct cells. *Am J Physiol Renal Physiol* **308**(4): F358-365.

Chandrasekar, B., Bysani, S. and Mummidi, S. (2004). CXCL16 signals via Gi, phosphatidylinositol 3-kinase, Akt, I kappa B kinase, and nuclear factor-kappa B and induces cell-cell adhesion and aortic smooth muscle cell proliferation. *J Biol Chem* **279**(5): 3188-3196.

Chaudhary, R., Garg, J., Shah, N. and Sumner, A. (2017). PCSK9 inhibitors: A new era of lipid lowering therapy. *World J Cardiol* **9**(2): 76-91.

Chen, C. and Khismatullin, D. B. (2015). Oxidized Low-Density Lipoprotein Contributes to Atherogenesis via Co-activation of Macrophages and Mast Cells. *PLoS One* **10**(3).

Chen, L., Deng, H., Cui, H., Fang, J., Zuo, Z., Deng, J., Li, Y., Wang, X. and Zhao, L. (2018). Inflammatory responses and inflammation-associated diseases in organs. *Oncotarget* **9**(6): 7204-7218.

Chen, P. Y., Qin, L., Li, G., Tellides, G. and Simons, M. (2016). Smooth muscle FGF/TGFbeta cross talk regulates atherosclerosis progression. *EMBO Mol Med* **8**(7): 712-728.

Cheng, C., Chrifi, I., Pasterkamp, G. and Duckers, H. J. (2013). Biological mechanisms of microvessel formation in advanced atherosclerosis: the big five. *Trends Cardiovasc Med* **23**(5): 153-164.

Chironi, G., Dosquet, C., Del-Pino, M., Denarie, N., Megnien, J. L., Drouet, L., Bal dit Sollier, C., Levenson, J. and Simon, A. (2006). Relationship of circulating biomarkers of inflammation and hemostasis with preclinical atherosclerotic burden in nonsmoking hypercholesterolemic men. *Am J Hypertens* **19**(10): 1025-1031.

Chistiakov, D. A., Orekhov, A. N. and Bobryshev, Y. V. (2015). Contribution of neovascularization and intraplaque haemorrhage to atherosclerotic plaque progression and instability. *Acta Physiol (Oxf)* **213**(3): 539-553.

Cho, J. G., Lee, A., Chang, W., Lee, M. S. and Kim, J. (2018). Endothelial to Mesenchymal Transition Represents a Key Link in the Interaction between Inflammation and Endothelial Dysfunction. *Front Immunol* **9**: 294.

Daniels, D. (2014). Frontiers in Neuroscience

Diverse Roles of Angiotensin Receptor Intracellular Signaling Pathways in the Control of Water and Salt Intake. Neurobiology of Body Fluid Homeostasis: Transduction and Integration. L. A. De Luca, Jr., J. V. Menani and A. K. Johnson. Boca Raton (FL), CRC Press/Taylor & Francis

(c) 2014 by Taylor & Francis Group, LLC.

Daugherty, A., Rateri, D. L. and Cassis, L. A. (2006). Role of the renin-angiotensin system in the development of abdominal aortic aneurysms in animals and humans. *Ann N Y Acad Sci* **1085**: 82-91.

Daugherty, A., Rateri, D. L., Charo, I. F., Owens, A. P., Howatt, D. A. and Cassis, L. A. (2010). Angiotensin II infusion promotes ascending aortic aneurysms: attenuation by CCR2 deficiency in apoE-/- mice. *Clin Sci (Lond)* **118**(11): 681-689.

Daugherty, B. L., Siciliano, S. J., DeMartino, J. A., Malkowitz, L., Sirotina, A. and Springer, M. S. (1996). Cloning, expression, and characterization of the human eosinophil eotaxin receptor. *J Exp Med* **183**(5): 2349-2354.

Davis, F. M., Rateri, D. L., Balakrishnan, A., Howatt, D. A., Strickland, D. K., Muratoglu, S. C., Haggerty, C. M., Fornwalt, B. K., Cassis, L. A. and Daugherty, A. (2015a). Smooth muscle cell deletion of low-density lipoprotein receptor-related protein 1 augments angiotensin II-induced superior mesenteric arterial and ascending aortic aneurysms. *Arterioscler Thromb Vasc Biol* **35**(1): 155-162.

Davis, F. M., Rateri, D. L. and Daugherty, A. (2015b). Abdominal aortic aneurysm: novel mechanisms and therapies. *Curr Opin Cardiol* **30**(6): 566-573.

de Kloet, A. D. (2017). Protective Angiotensin Type 2 Receptors in the Brain and Hypertension. **19**(6): 46.

de la Serna, F. (2014). Novedades en el sistema renina-angiotensina. *Insuficiencia cardíaca* **9**(1): 31-35.

de Munnik, S. M., Smit, M. J., Leurs, R. and Vischer, H. F. (2015). Modulation of cellular signaling by herpesvirus-encoded G protein-coupled receptors. *Front Pharmacol* **6**.

de Paulis, A., Annunziato, F., Di Gioia, L., Romagnani, S., Carfora, M., Beltrame, C., Marone, G. and Romagnani, P. (2001). Expression of the chemokine receptor CCR3 on human mast cells. *Int Arch Allergy Immunol* **124**(1-3): 146-150.

de Vries, M. R. and Quax, P. H. (2016). Plaque angiogenesis and its relation to inflammation and atherosclerotic plaque destabilization. *Curr Opin Lipidol* **27**(5): 499-506.

Deanfield, J. E., Halcox, J. P. and Rabelink, T. J. (2007). Endothelial function and dysfunction: testing and clinical relevance. *Circulation* **115**(10): 1285-1295.

Defesche, J. C., Gidding, S. S., Harada-Shiba, M., Hegele, R. A., Santos, R. D. and Wierzbicki, A. S. (2017). Familial hypercholesterolaemia. *Nat Rev Dis Primers* **3**: 17093.

Di Gennaro, A. and Haeggstrom, J. Z. (2014). Targeting leukotriene B4 in inflammation. *Expert Opin Ther Targets* **18**(1): 79-93.

Didion, S. P. (2017). Cellular and Oxidative Mechanisms Associated with Interleukin-6 Signaling in the Vasculature. *Int J Mol Sci* **18**(12).

Ding, J. W., Zheng, X. X., Zhou, T., Tong, X. H., Luo, C. Y. and Wang, X. A. (2016). HMGB1Modulates the Treg/Th17 Ratio in Atherosclerotic Patients. *J Atheroscler Thromb* **23**(6): 737-745.

Eguchi, S., Kawai, T., Scalia, R. and Rizzo, V. (2018). Understanding Angiotensin II Type 1 Receptor Signaling in Vascular Pathophysiology. *Hypertension*.

Eichel, K. and von Zastrow, M. (2018). Subcellular Organization of GPCR Signaling. *Trends Pharmacol Sci* **39**(2): 200-208.

Elsner, J., Escher, S. E. and Forssmann, U. (2004). Chemokine receptor antagonists: a novel therapeutic approach in allergic diseases. *Allergy* **59**(12): 1243-1258.

Ellis, B., Li, X. C., Miguel-Qin, E., Gu, V. and Zhuo, J. L. (2012). Review: Evidence for a functional intracellular angiotensin system in the proximal tubule of the kidney. *Am J Physiol Regul Integr Comp Physiol* **302**(5): R494-509.

Escudero, P., Martinez de Maranon, A., Collado, A., Gonzalez-Navarro, H., Hermenegildo, C., Peiro, C., Piqueras, L. and Sanz, M. J. (2015a). Combined sub-optimal doses of rosuvastatin and bexarotene impair angiotensin II-induced arterial mononuclear cell adhesion through inhibition of Nox5 signaling pathways and increased RXR/PPARalpha and RXR/PPARgamma interactions. *Antioxid Redox Signal* **22**(11): 901-920.

Escudero, P., Navarro, A., Ferrando, C., Furio, E., Gonzalez-Navarro, H., Juez, M., Sanz, M. J. and Piqueras, L. (2015b). Combined treatment with bexarotene and rosuvastatin reduces angiotensin-II-induced abdominal aortic aneurysm in apoE(-/-) mice and angiogenesis. *Br J Pharmacol* **172**(12): 2946-2960.

Fadini, G. P., Simoni, F., Cappellari, R., Vitturi, N., Galasso, S., Vigili de Kreutzenberg, S., Previato, L. and Avogaro, A. (2014). Pro-inflammatory monocyte-macrophage polarization imbalance in human hypercholesterolemia and atherosclerosis. *Atherosclerosis* **237**(2): 805-808.

Fallon, P. G., Jolin, H. E., Smith, P., Emson, C. L., Townsend, M. J., Fallon, R., Smith, P. and McKenzie, A. N. (2002). IL-4 induces characteristic Th2 responses even in the combined absence of IL-5, IL-9, and IL-13. *Immunity* **17**(1): 7-17.

Fava, C. and Montagnana, M. (2018). Atherosclerosis Is an Inflammatory Disease which Lacks a Common Anti-inflammatory Therapy: How Human Genetics Can Help to This Issue. A Narrative Review. *Front Pharmacol* **9**.

Ferrario, C. M. and Mullick, A. E. (2017). Renin angiotensin aldosterone inhibition in the treatment of cardiovascular disease. *Pharmacol Res* **125**(Pt A): 57-71.

Fitzgerald, K., Frank-Kamenetsky, M., Shulga-Morskaya, S., Liebow, A., Bettencourt, B. R., Sutherland, J. E., Hutabarat, R. M., Clausen, V. A., Karsten, V., Cehelsky, J., Nochur, S. V., Kotelianski, V., Horton, J., Mant, T., Chiesa, J., Ritter, J., Munisamy, M., Vaishnaw, A. K., Gollob, J. A. and Simon, A. (2014). Effect of an RNA interference drug on the synthesis of proprotein convertase subtilisin/kexin type 9 (PCSK9) and the concentration of serum LDL cholesterol in healthy volunteers: a randomised, single-blind, placebo-controlled, phase 1 trial. *Lancet* **383**(9911): 60-68.

Folkman, J. (1971). Tumor angiogenesis: therapeutic implications. *N Engl J Med* **285**(21): 1182-1186.

Forsythe, P. and Befus, A. D. (2003). CCR3: a key to mast cell phenotypic and functional diversity? *Am J Respir Cell Mol Biol* **28**(4): 405-409.

Fountain, J. H. and Lappin, S. L. (2018). Physiology, Renin Angiotensin System. StatPearls. Treasure Island (FL), StatPearls Publishing

StatPearls Publishing LLC.

Furio, E., Garcia-Fuster, M. J., Redon, J., Marques, P., Ortega, R., Sanz, M. J. and Piqueras, L. (2018). CX3CR1/CX3CL1 Axis Mediates Platelet-Leukocyte Adhesion to Arterial Endothelium in Younger Patients with a History of Idiopathic Deep Vein Thrombosis. *Thromb Haemost* **118**(3): 562-571.

Futami, K., Sano, H., Kitabayashi, T., Misaki, K., Nakada, M., Uchiyama, N. and Ueda, F. (2015). Parent artery curvature influences inflow zone location of unruptured sidewall internal carotid artery aneurysms. *AJNR Am J Neuroradiol* **36**(2): 342-348.

Galkina, E., Harry, B. L., Ludwig, A., Liehn, E. A., Sanders, J. M., Bruce, A., Weber, C. and Ley, K. (2007). CXCR6 promotes atherosclerosis by supporting T-cell homing, interferon-gamma production, and macrophage accumulation in the aortic wall. *Circulation* **116**(16): 1801-1811.

Gao, Q., Zhao, Y. J., Wang, X. Y., Qiu, S. J., Shi, Y. H., Sun, J., Yi, Y., Shi, J. Y., Shi, G. M., Ding, Z. B., Xiao, Y. S., Zhao, Z. H., Zhou, J., He, X. H. and Fan, J. (2012). CXCR6 upregulation contributes to a proinflammatory tumor microenvironment that drives metastasis and poor patient outcomes in hepatocellular carcinoma. *Cancer Res* **72**(14): 3546-3556.

Gao, S. and Liu, J. (2017). Association between circulating oxidized low-density lipoprotein and atherosclerotic cardiovascular disease. *Chronic Dis Transl Med* **3**(2): 89-94.

Gerhardt, T. and Ley, K. (2015). Monocyte trafficking across the vessel wall. *Cardiovasc Res* **107**(3): 321-330.

Gimbrone, M. A. and García-Cardeña, G. (2016). Endothelial Cell Dysfunction and the Pathobiology of Atherosclerosis. *Circ Res* **118**(4): 620-636.

Gokalp, D., Tuzcu, A., Bahceci, M., Arikan, S., Pirinccioglu, A. G. and Bahceci, S. (2009). Levels of proinflammatory cytokines and hs-CRP in patients with homozygous familial hypercholesterolaemia. *Acta Cardiol* **64**(5): 603-609.

Golebiewska, E. M. and Poole, A. W. (2015). Platelet secretion: From haemostasis to wound healing and beyond. *Blood Rev* **29**(3): 153-162.

Gonzalez-Quesada, C. and Frangogiannis, N. G. (2009). Monocyte chemoattractant protein-1/CCL2 as a biomarker in acute coronary syndromes. *Curr Atheroscler Rep* **11**(2): 131-138.

Gough, P. J., Garton, K. J., Wille, P. T., Rychlewski, M., Dempsey, P. J. and Raines, E. W. (2004). A disintegrin and metalloproteinase 10-mediated cleavage and shedding regulates the cell surface expression of CXC chemokine ligand 16. *J Immunol* **172**(6): 3678-3685.

Gresele, P., Falcinelli, E., Sebastiano, M. and Momi, S. (2017). Matrix Metalloproteinases and Platelet Function. *Prog Mol Biol Transl Sci* **147**: 133-165.

Haley, K. J., Lilly, C. M., Yang, J. H., Feng, Y., Kennedy, S. P., Turi, T. G., Thompson, J. F., Sukhova, G. H., Libby, P. and Lee, R. T. (2000). Overexpression of eotaxin and the CCR3 receptor in human atherosclerosis: using genomic technology to identify a potential novel pathway of vascular inflammation. *Circulation* **102**(18): 2185-2189.

Hamilton, M. J., Frei, S. M. and Stevens, R. L. (2014). The multifaceted mast cell in inflammatory bowel disease. *Inflamm Bowel Dis* **20**(12): 2364-2378.

Han, E. C., Lee, J., Ryu, S. W. and Choi, C. (2014). Tumor-conditioned Gr-1(+)CD11b(+) myeloid cells induce angiogenesis through the synergistic action of CCL2 and CXCL16 in vitro. *Biochem Biophys Res Commun* **443**(4): 1218-1225.

Hansen, M., Kuhlman, A. C. B., Sahl, R. E., Kelly, B., Morville, T., Dohlmann, T. L., Chrois, K. M., Larsen, S., Helge, J. W. and Dela, F. (2019). Inflammatory biomarkers in patients in Simvastatin treatment: No effect of co-enzyme Q10 supplementation. *Cytokine* **113**: 393-399.

Hansson, G. K., Libby, P. and Tabas, I. (2015). Inflammation and plaque vulnerability. *J Intern Med* **278**(5): 483-493.

Hedrick, C. C. (2015). Lymphocytes in Atherosclerosis. *Arterioscler Thromb Vasc Biol* **35**(2): 253-257.

Hofnagel, O., Engel, T., Severs, N. J., Robenek, H. and Buers, I. (2011). SR-PSOX at sites predisposed to atherosclerotic lesion formation mediates monocyte-endothelial cell adhesion. *Atherosclerosis* **217**(2): 371-378.

Hogaboam, C., Kunkel, S. L., Strieter, R. M., Taub, D. D., Lincoln, P., Standiford, T. J. and Lukacs, N. W. (1998). Novel role of transmembrane SCF for mast cell activation and eotaxin production in mast cell-fibroblast interactions. *J Immunol* **160**(12): 6166-6171.

Holven, K. B., Damas, J. K., Yndestad, A., Waehre, T., Ueland, T., Halvorsen, B., Heggelund, L., Sandberg, W. J., Semb, A. G., Froland, S. S., Ose, L., Nenseter, M. S. and Aukrust, P. (2006). Chemokines in children with heterozygous familiar hypercholesterolemia: selective upregulation of RANTES. *Arterioscler Thromb Vasc Biol* **26**(1): 200-205.

Holven, K. B., Narverud, I., Lindvig, H. W., Halvorsen, B., Langslet, G., Nenseter, M. S., Ulven, S. M., Ose, L., Aukrust, P. and Retterstol, K. (2014). Subjects with familial hypercholesterolemia are characterized by an inflammatory phenotype despite long-term intensive cholesterol lowering treatment. *Atherosclerosis* **233**(2): 561-567.

Horton, J. D., Cohen, J. C. and Hobbs, H. H. (2009). PCSK9: a convertase that coordinates LDL catabolism. *J Lipid Res* **50**(Suppl): S172-177.

Howard, D. P., Banerjee, A., Fairhead, J. F., Handa, A., Silver, L. E. and Rothwell, P. M. (2015). Age-specific incidence, risk factors and outcome of acute abdominal aortic aneurysms in a defined population. *Br J Surg* **102**(8): 907-915.

Hu, C., Zhu, K., Li, J., Wang, C. and Lai, L. (2017). Molecular targets in aortic aneurysm for establishing novel management paradigms. *J Thorac Dis* **9**(11): 4708-4722.

Huang, M. M., Guo, A. B., Sun, J. F., Chen, X. L. and Yin, Z. Y. (2014). Angiotensin II promotes the progression of human gastric cancer. *Mol Med Rep* **9**(3): 1056-1060.

Hundhausen, C., Schulte, A., Schulz, B., Andrzejewski, M. G., Schwarz, N., von Hundelshausen, P., Winter, U., Paliga, K., Reiss, K., Saftig, P., Weber, C. and Ludwig, A. (2007). Regulated shedding of transmembrane chemokines by the disintegrin and metalloproteinase 10 facilitates detachment of adherent leukocytes. *J Immunol* **178**(12): 8064-8072.

Inoue, T., Croce, K., Morooka, T., Sakuma, M., Node, K. and Simon, D. I. (2011). Vascular Inflammation and Repair: Implications for Reendothelialization, Restenosis, and Stent Thrombosis. *JACC Cardiovasc Interv* **4**(10): 1057-1066.

Insull, W., Jr. (2009). The pathology of atherosclerosis: plaque development and plaque responses to medical treatment. *Am J Med* **122**(1 Suppl): S3-s14.

Isozaki, T., Arbab, A. S., Haas, C. S., Amin, M. A., Arendt, M. D., Koch, A. E. and Ruth, J. H. (2013). Evidence that CXCL16 is a potent mediator of angiogenesis and is involved in endothelial progenitor cell chemotaxis : studies in mice with K/BxN serum-induced arthritis. *Arthritis Rheum* **65**(7): 1736-1746.

Ivetic, A. (2018). A head-to-tail view of L-selectin and its impact on neutrophil behaviour. *Cell Tissue Res* **371**(3): 437-453.

Izquierdo, M. C., Martin-Cleary, C., Fernandez-Fernandez, B., Elewa, U., Sanchez-Nino, M. D., Carrero, J. J. and Ortiz, A. (2014). CXCL16 in kidney and cardiovascular injury. *Cytokine Growth Factor Rev* **25**(3): 317-325.

Jackson, L., Eldahshan, W., Fagan, S. C. and Ergul, A. (2018). Within the Brain: The Renin Angiotensin System. *Int J Mol Sci* **19**(3).

Jaffe, E. A., Nachman, R. L., Becker, C. G. and Minick, C. R. (1973). Culture of human endothelial cells derived from umbilical veins. Identification by morphologic and immunologic criteria. *J Clin Invest* **52**(11): 2745-2756.

Jain, T., Nikolopoulou, E. A., Xu, Q. and Qu, A. (2018). Hypoxia inducible factor as a therapeutic target for atherosclerosis. *Pharmacol Ther* **183**: 22-33.

Jenne, C. N. and Kubes, P. (2015). Platelets in inflammation and infection. *Platelets* **26**(4): 286-292.

Jung, Y. and Rothenberg, M. E. (2014). Roles and regulation of gastrointestinal eosinophils in immunity and disease. *J Immunol* **193**(3): 999-1005.

Juremalm, M. and Nilsson, G. (2005). Chemokine receptor expression by mast cells. *Chem Immunol Allergy* **87**: 130-144.

Kaschina, E., Namsolleck, P. and Unger, T. (2017). AT2 receptors in cardiovascular and renal diseases. *Pharmacol Res* **125**(Pt A): 39-47.

Kawai, T., Forrester, S. J., O'Brien, S., Baggett, A., Rizzo, V. and Eguchi, S. (2017). AT1 receptor signaling pathways in the cardiovascular system. *Pharmacol Res* **125**(Pt A): 4-13.

Ketelhuth, D. F. and Hansson, G. K. (2016). Adaptive Response of T and B Cells in Atherosclerosis. *Circ Res* **118**(4): 668-678.

Kitaura, M., Nakajima, T., Imai, T., Harada, S., Combadiere, C., Tiffany, H. L., Murphy, P. M. and Yoshie, O. (1996). Molecular cloning of human eotaxin, an eosinophil-selective CC chemokine, and identification of a specific eosinophil eotaxin receptor, CC chemokine receptor 3. *J Biol Chem* **271**(13): 7725-7730.

Koenen, R. R. and Weber, C. (2011). Chemokines: established and novel targets in atherosclerosis. *EMBO Mol Med* **3**(12): 713-725.

Kojima, Y., Weissman, I. L. and Leeper, N. J. (2017). The Role of Efferocytosis in Atherosclerosis. *Circulation* **135**(5): 476-489.

Kolaczkowska, E. and Kubes, P. (2013). Neutrophil recruitment and function in health and inflammation. *Nat Rev Immunol* **13**(3): 159-175.

Kraaijeveld, A. O., de Jager, S. C., van Berkel, T. J., Biessen, E. A. and Jukema, J. W. (2007). Chemokines and atherosclerotic plaque progression: towards therapeutic targeting? *Curr Pharm Des* **13**(10): 1039-1052.

Kratofil, R. M., Kubes, P. and Deniset, J. F. (2017). Monocyte Conversion During Inflammation and Injury. *Arterioscler Thromb Vasc Biol* **37**(1): 35-42.

Kwak, B. R., Bäck, M., Bochaton-Piallat, M. L., Caligiuri, G., Daemen, M., Davies, P. F., Hoefer, I. E., Holvoet, P., Jo, H., Krams, R., Lehoux, S., Monaco, C., Steffens, S., Virmani, R., Weber, C., Wentzel, J. J. and Evans, P. C. (2014). Biomechanical factors in atherosclerosis: mechanisms and clinical implications(). *Eur Heart J* **35**(43): 3013-3020.

Lam, F. W., Vijayan, K. V. and Rumbaut, R. E. (2015). Platelets and Their Interactions with Other Immune Cells. *Compr Physiol* **5**(3): 1265-1280.

Lampinen, M., Carlson, M., Hakansson, L. D. and Venge, P. (2004). Cytokine-regulated accumulation of eosinophils in inflammatory disease. *Allergy* **59**(8): 793-805.

Landmesser, U., Hornig, B. and Drexler, H. (2004). Endothelial function: a critical determinant in atherosclerosis? *Circulation* **109**(21 Suppl 1): Ii27-33.

Langslet, G., Emery, M. and Wasserman, S. M. (2015). Evolocumab (AMG 145) for primary hypercholesterolemia. *Expert Rev Cardiovasc Ther* **13**(5): 477-488.

Lawrance, I. C., Rogler, G., Bamias, G., Breynaert, C., Florholmen, J., Pellino, G., Reif, S., Speca, S. and Latella, G. (2017). Cellular and Molecular Mediators of Intestinal Fibrosis. *J Crohns Colitis* **11**(12): 1491-1503.

Legler, D. F. and Thelen, M. (2018). New insights in chemokine signaling. *F1000Res* **7**: 95.

Lehrke, M., Millington, S. C., Lefterova, M., Cumaranatunge, R. G., Szapary, P., Wilensky, R., Rader, D. J., Lazar, M. A. and Reilly, M. P. (2007). CXCL16 is a marker of inflammation, atherosclerosis, and acute coronary syndromes in humans. *J Am Coll Cardiol* **49**(4): 442-449.

Lertkiatmongkol, P., Liao, D., Mei, H., Hu, Y. and Newman, P. J. (2016). Endothelial functions of PECAM-1 (CD31). *Curr Opin Hematol* **23**(3): 253-259.

Ley, K. (2011). Monocyte and Macrophage Dynamics during Atherogenesis. **31**(7): 1506-1516.

Ley, K., Laudanna, C., Cybulsky, M. I. and Nourshargh, S. (2007). Getting to the site of inflammation: the leukocyte adhesion cascade updated. *Nat Rev Immunol* **7**(9): 678-689.

Li, J. and Ley, K. (2015). Lymphocyte migration into atherosclerotic plaque. *Arterioscler Thromb Vasc Biol* **35**(1): 40-49.

Li, Y., Li, L., Wadley, R., Reddel, S. W., Qi, J. C., Archis, C., Collins, A., Clark, E., Cooley, M., Kouts, S., Naif, H. M., Alali, M., Cunningham, A., Wong, G. W., Stevens, R. L. and Krilis, S. A. (2001). Mast cells/basophils in the peripheral blood of allergic individuals who

are HIV-1 susceptible due to their surface expression of CD4 and the chemokine receptors CCR3, CCR5, and CXCR4. *Blood* **97**(11): 3484-3490.

Libby, P. (2012). Inflammation in atherosclerosis. *Arterioscler Thromb Vasc Biol* **32**(9): 2045-2051.

Libby, P. and Hansson, G. K. (2015). Inflammation and Immunity in Diseases of the Arterial Tree: Players and Layers. *Circ Res* **116**(2): 307-311.

Libby, P., Lichtman, A. H. and Hansson, G. K. (2013). Immune effector mechanisms implicated in atherosclerosis: from mice to humans. *Immunity* **38**(6): 1092-1104.

Lievens, D. and von Hundelshausen, P. (2011). Platelets in atherosclerosis. *Thromb Haemost* **106**(5): 827-838.

Liu, X., Men, P., Wang, Y., Zhai, S., Zhao, Z. and Liu, G. (2017a). Efficacy and Safety of Lomitapide in Hypercholesterolemia. *Am J Cardiovasc Drugs* **17**(4): 299-309.

Liu, Z., Yago, T., Zhang, N., Panicker, S. R., Wang, Y., Yao, L., Mehta-D'souza, P., Xia, L., Zhu, C. and McEver, R. P. (2017b). L-selectin mechanochemistry restricts neutrophil priming in vivo. *Nat Commun* **8**: 15196.

Ludwig, A., Schulte, A., Schnack, C., Hundhausen, C., Reiss, K., Brodway, N., Held-Feindt, J. and Mentlein, R. (2005). Enhanced expression and shedding of the transmembrane chemokine CXCL16 by reactive astrocytes and glioma cells. *J Neurochem* **93**(5): 1293-1303.

Ludwig, A. and Weber, C. (2007). Transmembrane chemokines: versatile 'special agents' in vascular inflammation. *Thromb Haemost* **97**(5): 694-703.

Luo, Y., Cui, D., Yu, X., Chen, S., Liu, X., Tang, H., Wang, X. and Liu, L. (2016). Modeling of Mechanical Stress Exerted by Cholesterol Crystallization on Atherosclerotic Plaques. *PLoS One* **11**(5): e0155117.

Luster, A. D. and Rothenberg, M. E. (1997). Role of the monocyte chemoattractant protein and eotaxin subfamily of chemokines in allergic inflammation. *J Leukoc Biol* **62**(5): 620-633.

Malekzadeh, S., Fraga-Silva, R. A., Trachet, B., Montecucco, F., Mach, F. and Stergiopulos, N. (2013). Role of the renin-angiotensin system on abdominal aortic aneurysms. *Eur J Clin Invest* **43**(12): 1328-1338.

Mancuso, M. E. and Santagostino, E. (2017). Platelets: much more than bricks in a breached wall. *Br J Haematol* **178**(2): 209-219.

Manne, B. K. (2017). Platelet Secretion in Inflammatory and Infectious Diseases. **28**(2): 155-164.

Marki, A., Buscher, K., Mikulski, Z., Pries, A. and Ley, K. (2018). Rolling neutrophils form tethers and slings under physiologic conditions in vivo. *J Leukoc Biol* **103**(1): 67-70.

Marques, P., Collado, A., Escudero, P., Rius, C., González, C., Servera, E., Piqueras, L. and Sanz, M. J. (2017). Cigarette Smoke Increases Endothelial CXCL16-Leukocyte CXCR6 Adhesion In Vitro and In Vivo. Potential Consequences in Chronic Obstructive Pulmonary Disease. *Front Immunol* **8**.

Marsch, E., Sluimer, J. C. and Daemen, M. J. (2013). Hypoxia in atherosclerosis and inflammation. *Curr Opin Lipidol* **24**(5): 393-400.

Martorell, S., Hueso, L., Gonzalez-Navarro, H., Collado, A., Sanz, M. J. and Piqueras, L. (2016). Vitamin D Receptor Activation Reduces Angiotensin-II-Induced Dissecting Abdominal Aortic Aneurysm in Apolipoprotein E-Knockout Mice. *Arterioscler Thromb Vasc Biol* **36**(8): 1587-1597.

Mateo, T., Abu Nabah, Y. N., Abu Taha, M., Mata, M., Cerda-Nicolas, M., Proudfoot, A. E., Stahl, R. A., Issekutz, A. C., Cortijo, J., Morcillo, E. J., Jose, P. J. and Sanz, M. J. (2006). Angiotensin II-induced mononuclear leukocyte interactions with arteriolar and venular endothelium are mediated by the release of different CC chemokines. *J Immunol* **176**(9): 5577-5586.

Mateo, T., Naim Abu Nabah, Y., Losada, M., Estelles, R., Company, C., Bedrina, B., Cerda-Nicolas, J. M., Poole, S., Jose, P. J., Cortijo, J., Morcillo, E. J. and Sanz, M. J. (2007). A critical role for TNFalpha in the selective attachment of mononuclear leukocytes to angiotensin-II-stimulated arterioles. *Blood* **110**(6): 1895-1902.

Matloubian, M., David, A., Engel, S., Ryan, J. E. and Cyster, J. G. (2000). A transmembrane CXC chemokine is a ligand for HIV-coreceptor Bonzo. *Nat Immunol* **1**(4): 298-304.

Mazor, R., Shurtz-Swirski, R., Farah, R., Kristal, B., Shapiro, G., Dorlechter, F., Cohen-Mazor, M., Meilin, E., Tamara, S. and Sela, S. (2008). Primed polymorphonuclear leukocytes constitute a possible link between inflammation and oxidative stress in hyperlipidemic patients. *Atherosclerosis* **197**(2): 937-943.

McEver, R. P. (2010). Rolling back neutrophil adhesion. *Nat Immunol* **11**(4): 282-284.

McEver, R. P. (2015). Selectins: initiators of leucocyte adhesion and signalling at the vascular wall. *Cardiovasc Res* **107**(3): 331-339.

McLaughlin, T., Deng, A., Yee, G., Lamendola, C., Reaven, G., Tsao, P. S., Cushman, S. W. and Sherman, A. (2010). Inflammation in subcutaneous adipose tissue: relationship to adipose cell size. *Diabetologia* **53**(2): 369-377.

Mehrad, B., Keane, M. P. and Strieter, R. M. (2007). Chemokines as mediators of angiogenesis. *Thromb Haemost* **97**(5): 755-762.

Mestas, J. and Ley, K. (2008). Monocyte-endothelial cell interactions in the development of atherosclerosis. *Trends Cardiovasc Med* **18**(6): 228-232.

Michel, J. B., Martin-Ventura, J. L., Egido, J., Sakalihasan, N., Treska, V., Lindholt, J., Allaire, E., Thorsteinsdottir, U., Cockerill, G. and Swedenborg, J. (2011). Novel aspects of the pathogenesis of aneurysms of the abdominal aorta in humans. *Cardiovasc Res* **90**(1): 18-27.

Michelson, A. D., Barnard, M. R., Krueger, L. A., Valeri, C. R. and Furman, M. I. (2001). Circulating monocyte-platelet aggregates are a more sensitive marker of in vivo platelet activation than platelet surface P-selectin: studies in baboons, human coronary intervention, and human acute myocardial infarction. *Circulation* **104**(13): 1533-1537.

Min, B., Prout, M., Hu-Li, J., Zhu, J., Jankovic, D., Morgan, E. S., Urban, J. F., Jr., Dvorak, A. M., Finkelman, F. D., LeGros, G. and Paul, W. E. (2004). Basophils produce IL-4 and

accumulate in tissues after infection with a Th2-inducing parasite. *J Exp Med* **200**(4): 507-517.

Minton, K. (2018). Chemokines: Moving on up. *Nat Rev Immunol* **18**(1): 1.

Mitroulis, I. (2015). Leukocyte integrins: Role in leukocyte recruitment and as therapeutic targets in inflammatory disease. **0**: 123-135.

Mitroulis, I., Alexaki, V. I., Kourtzelis, I., Ziogas, A., Hajishengallis, G. and Chavakis, T. (2015). Leukocyte integrins: role in leukocyte recruitment and as therapeutic targets in inflammatory disease. *Pharmacol Ther* **147**: 123-135.

Miyagaki, T., Sugaya, M., Fujita, H., Ohmatsu, H., Kakinuma, T., Kadono, T., Tamaki, K. and Sato, S. (2010). Eotaxins and CCR3 interaction regulates the Th2 environment of cutaneous T-cell lymphoma. *J Invest Dermatol* **130**(9): 2304-2311.

Miyazaki, T. and Miyazaki, A. (2017). Defective Protein Catabolism in Atherosclerotic Vascular Inflammation. *Front Cardiovasc Med* **4**: 79.

Mollazadeh, H., Carbone, F., Montecucco, F., Pirro, M. and Sahebkar, A. (2018). Oxidative burden in familial hypercholesterolemia. *J Cell Physiol*.

Moreno, P. R. and Kini, A. (2012). Resolution of inflammation, statins, and plaque regression. *JACC Cardiovasc Imaging* **5**(2): 178-181.

Moro-García, M. A., Mayo, J. C., Sainz, R. M. and Alonso-Arias, R. (2018). Influence of Inflammation in the Process of T Lymphocyte Differentiation: Proliferative, Metabolic, and Oxidative Changes. *Front Immunol* **9**.

Morris, P. B., Ference, B. A., Jahangir, E., Feldman, D. N., Ryan, J. J., Bahrami, H., El-Chami, M. F., Bhakta, S., Winchester, D. E., Al-Mallah, M. H., Sanchez Shields, M., Deedwania, P., Mehta, L. S., Phan, B. A. and Benowitz, N. L. (2015). Cardiovascular Effects of Exposure to Cigarette Smoke and Electronic Cigarettes: Clinical Perspectives From the Prevention of Cardiovascular Disease Section Leadership Council and Early Career Councils of the American College of Cardiology. *J Am Coll Cardiol* **66**(12): 1378-1391.

Muller, W. A. (2014). How Endothelial Cells Regulate Transmigration of Leukocytes in the Inflammatory Response. *Am J Pathol* **184**(4): 886-896.

Murakami, M. and Hirano, T. (2012). The molecular mechanisms of chronic inflammation development. *Front Immunol* **3**: 323.

Murugappa, S. and Kunapuli, S. P. (2006). The role of ADP receptors in platelet function. *Front Biosci* **11**: 1977-1986.

Nagai, K., Tahara-Hanaoka, S., Morishima, Y., Tokunaga, T., Imoto, Y., Noguchi, E., Kanemaru, K., Imai, M., Shibayama, S., Hizawa, N., Fujieda, S., Yamagata, K. and Shibuya, A. (2013). Expression and function of Allergin-1 on human primary mast cells. *PLoS One* **8**(10): e76160.

Nahrendorf, M. and Swirski, F. K. (2015). Lifestyle effects on hematopoiesis and atherosclerosis. *Circ Res* **116**(5): 884-894.

Nehme, A. and Zibara, K. (2017). Cellular distribution and interaction between extended renin-angiotensin-aldosterone system pathways in atheroma. *Atherosclerosis* **263**: 334-342.

Neves, M. F., Cunha, A. R., Cunha, M. R., Gismondi, R. A. and Oigman, W. (2018). The Role of Renin-Angiotensin-Aldosterone System and Its New Components in Arterial Stiffness and Vascular Aging. *High Blood Press Cardiovasc Prev*.

Nigro, P., Abe, J. and Berk, B. C. (2011). Flow shear stress and atherosclerosis: a matter of site specificity. *Antioxid Redox Signal* **15**(5): 1405-1414.

Nording, H. M., Seizer, P. and Langer, H. F. (2015). Platelets in inflammation and atherogenesis. *Front Immunol* **6**: 98.

Ogilvie, P., Bardi, G., Clark-Lewis, I., Baggiolini, M. and Uguccioni, M. (2001). Eotaxin is a natural antagonist for CCR2 and an agonist for CCR5. *Blood* **97**(7): 1920-1924.

Olson, N. C., Sallam, R., Doyle, M. F., Tracy, R. P. and Huber, S. A. (2013). T helper cell polarization in healthy people: implications for cardiovascular disease. *J Cardiovasc Transl Res* **6**(5): 772-786.

Ouwerkerk, W., Voors, A. A., Anker, S. D., Cleland, J. G., Dickstein, K., Filippatos, G., van der Harst, P., Hillege, H. L., Lang, C. C., Ter Maaten, J. M., Ng, L. L., Ponikowski, P., Samani, N. J., van Veldhuisen, D. J., Zannad, F., Metra, M. and Zwinderman, A. H. (2017). Determinants and clinical outcome of uptitration of ACE-inhibitors and beta-blockers in patients with heart failure: a prospective European study. *Eur Heart J* **38**(24): 1883-1890.

Pant, S., Deshmukh, A., Gurumurthy, G. S., Pothineni, N. V., Watts, T. E., Romeo, F. and Mehta, J. L. (2014). Inflammation and atherosclerosis--revisited. *J Cardiovasc Pharmacol Ther* **19**(2): 170-178.

Pantzaris, N. D., Karanikolas, E., Tsiotsios, K. and Velissaris, D. (2017). Renin Inhibition with Aliskiren: A Decade of Clinical Experience. *J Clin Med* **6**(6).

Papapanagiotou, A., Daskalakis, G., Siasos, G., Gargalionis, A. and Papavassiliou, A. G. (2016). The Role of Platelets in Cardiovascular Disease: Molecular Mechanisms. *Curr Pharm Des* **22**(29): 4493-4505.

Pedro, T., Martinez-Hervas, S., Tormo, C., Garcia-Garcia, A. B., Saez-Tormo, G., Ascaso, J. F., Chaves, F. J., Carmena, R. and Real, J. T. (2013). Oxidative stress and antioxidant enzyme values in lymphomonocytes after an oral unsaturated fat load test in familial hypercholesterolemic subjects. *Transl Res* **161**(1): 50-56.

Pejic, R. N. (2014). Familial hypercholesterolemia. *Ochsner J* **14**(4): 669-672.

Periayah, M. H., Halim, A. S. and Mat Saad, A. Z. (2017). Mechanism Action of Platelets and Crucial Blood Coagulation Pathways in Hemostasis. *Int J Hematol Oncol Stem Cell Res* **11**(4): 319-327.

Petkovic, V., Moghini, C., Paoletti, S., Uguccioni, M. and Gerber, B. (2004). Eotaxin-3/CCL26 is a natural antagonist for CC chemokine receptors 1 and 5. A human chemokine with a regulatory role. *J Biol Chem* **279**(22): 23357-23363.

Piepoli, M. F., Hoes, A. W., Brotons, C., Hobbs, R. F. D. and Corra, U. (2018). Main messages for primary care from the 2016 European Guidelines on cardiovascular disease prevention in clinical practice. *Eur J Gen Pract* **24**(1): 51-56.

Piqueras, L., Kubes, P., Alvarez, A., O'Connor, E., Issekutz, A. C., Esplugues, J. V. and Sanz, M. J. (2000). Angiotensin II induces leukocyte-endothelial cell interactions in vivo via AT(1) and AT(2) receptor-mediated P-selectin upregulation. *Circulation* **102**(17): 2118-2123.

Ponath, P. D., Qin, S., Post, T. W., Wang, J., Wu, L., Gerard, N. P., Newman, W., Gerard, C. and Mackay, C. R. (1996). Molecular cloning and characterization of a human eotaxin receptor expressed selectively on eosinophils. *J Exp Med* **183**(6): 2437-2448.

Postea, O., Vasina, E. M., Cauwenberghs, S., Projahn, D., Liehn, E. A., Lievens, D., Theelen, W., Kramp, B. K., Butoi, E. D., Soehnlein, O., Heemskerk, J. W., Ludwig, A., Weber, C. and Koenen, R. R. (2012). Contribution of platelet CX(3)CR1 to platelet-monocyte complex formation and vascular recruitment during hyperlipidemia. *Arterioscler Thromb Vasc Biol* **32**(5): 1186-1193.

Price, K. S., Friend, D. S., Mellor, E. A., De Jesus, N., Watts, G. F. and Boyce, J. A. (2003). CC chemokine receptor 3 mobilizes to the surface of human mast cells and potentiates immunoglobulin E-dependent generation of interleukin 13. *Am J Respir Cell Mol Biol* **28**(4): 420-427.

Privratsky, J. R., Paddock, C. M., Florey, O., Newman, D. K., Muller, W. A. and Newman, P. J. (2011). Relative contribution of PECAM-1 adhesion and signaling to the maintenance of vascular integrity. *J Cell Sci* **124**(9): 1477-1485.

Quandt, D., Rothe, K., Scholz, R., Baerwald, C. W. and Wagner, U. (2014). Peripheral CD4CD8 double positive T cells with a distinct helper cytokine profile are increased in rheumatoid arthritis. *PLoS One* **9**(3): e93293.

Rafieian-Kopaei, M., Setorki, M., Doudi, M., Baradaran, A. and Nasri, H. (2014). Atherosclerosis: Process, Indicators, Risk Factors and New Hopes. *Int J Prev Med* **5**(8): 927-946.

Rahimi, N. (2017). Defenders and Challengers of Endothelial Barrier Function. *Front Immunol* **8**: 1847.

Rankin, S. M., Conroy, D. M. and Williams, T. J. (2000). Eotaxin and eosinophil recruitment: implications for human disease. *Mol Med Today* **6**(1): 20-27.

Ransohoff, R. M. (2009). Chemokines and chemokine receptors: standing at the crossroads of immunobiology and neurobiology. *Immunity* **31**(5): 711-721.

Rasini, E., Cosentino, M., Marino, F., Legnaro, M., Ferrari, M., Guasti, L., Venco, A. and Lecchini, S. (2006). Angiotensin II type 1 receptor expression on human leukocyte subsets: a flow cytometric and RT-PCR study. *Regul Pept* **134**(2-3): 69-74.

Real, J. T., Martinez-Hervas, S., Garcia-Garcia, A. B., Civera, M., Pallardo, F. V., Ascaso, J. F., Vina, J. R., Chaves, F. J. and Carmena, R. (2010a). Circulating mononuclear cells nuclear factor-kappa B activity, plasma xanthine oxidase, and low grade inflammatory markers in adult patients with familial hypercholesterolaemia. *Eur J Clin Invest* **40**(2): 89-94.

Real, J. T., Martinez-Hervas, S., Tormos, M. C., Domenech, E., Pallardo, F. V., Saez-Tormo, G., Redon, J., Carmena, R., Chaves, F. J., Ascaso, J. F. and Garcia-Garcia, A. B. (2010b). Increased oxidative stress levels and normal antioxidant enzyme activity in circulating

mononuclear cells from patients of familial hypercholesterolemia. *Metabolism* **59**(2): 293-298.

Reis, S. P., Majdalany, B. S., AbuRahma, A. F., Collins, J. D., Francois, C. J., Ganguli, S., Gornik, H. L., Kendi, A. T., Khaja, M. S., Norton, P. T., Sutphin, P. D., Rybicki, F. J. and Kalva, S. P. (2017). ACR Appropriateness Criteria((R)) Pulsatile Abdominal Mass Suspected Abdominal Aortic Aneurysm. *J Am Coll Radiol* **14**(5s): S258-s265.

Reite, A., Soreide, K., Ellingsen, C. L., Kvaloy, J. T. and Vetrhus, M. (2015). Epidemiology of ruptured abdominal aortic aneurysms in a well-defined Norwegian population with trends in incidence, intervention rate, and mortality. *J Vasc Surg* **61**(5): 1168-1174.

Ren, J., Wang, Q., Morgan, S., Si, Y., Ravichander, A., Dou, C., Kent, K. C. and Liu, B. (2014). Protein kinase C-delta (PKCdelta) regulates proinflammatory chemokine expression through cytosolic interaction with the NF-kappaB subunit p65 in vascular smooth muscle cells. *J Biol Chem* **289**(13): 9013-9026.

Riambau, V., Guerrero, F., Montana, X. and Gilabert, R. (2007). [Abdominal aortic aneurysm and renovascular disease]. *Rev Esp Cardiol* **60**(6): 639-654.

Ridiandries, A., Tan, J. T. M. and Bursill, C. A. (2016). The Role of CC-Chemokines in the Regulation of Angiogenesis. *Int J Mol Sci* **17**(11).

Rius, C., Company, C., Piqueras, L., Cerda-Nicolas, J. M., Gonzalez, C., Servera, E., Ludwig, A., Morcillo, E. J. and Sanz, M. J. (2013a). Critical role of fractalkine (CX3CL1) in cigarette smoke-induced mononuclear cell adhesion to the arterial endothelium. *Thorax* **68**(2): 177-186.

Rius, C., Piqueras, L., Gonzalez-Navarro, H., Albertos, F., Company, C., Lopez-Gines, C., Ludwig, A., Blanes, J. I., Morcillo, E. J. and Sanz, M. J. (2013b). Arterial and venous endothelia display differential functional fractalkine (CX3CL1) expression by angiotensin-II. *Arterioscler Thromb Vasc Biol* **33**(1): 96-104.

Romagnani, S. (2002). Cytokines and chemoattractants in allergic inflammation. *Mol Immunol* **38**(12-13): 881-885.

Ross, A. C. (2017). Impact of chronic and acute inflammation on extra- and intracellular iron homeostasis. *Am J Clin Nutr* **106**(Suppl 6): 1581s-1587s.

Ross, R. (1999). Atherosclerosis--an inflammatory disease. *N Engl J Med* **340**(2): 115-126.

Rouchaud, A., Brandt, M. D., Rydberg, A. M., Kadirvel, R., Flemming, K., Kallmes, D. F. and Brinjikji, W. (2016). Prevalence of Intracranial Aneurysms in Patients with Aortic Aneurysms. *AJNR Am J Neuroradiol* **37**(9): 1664-1668.

Ruddy, J. M., Ikonomidis, J. S. and Jones, J. A. (2016). Multidimensional Contribution of Matrix Metalloproteinases to Atherosclerotic Plaque Vulnerability: Multiple Mechanisms of Inhibition to Promote Stability. *J Vasc Res* **53**(1-2): 1-16.

Ruff, A., Patel, K., Joyce, J. R., Gornik, H. L. and Rothberg, M. B. (2016). The use of pre-existing CT imaging in screening for abdominal aortic aneurysms. *Vasc Med* **21**(6): 515-519.

Sahay, M. and Sahay, R. K. (2012). Low renin hypertension. *Indian J Endocrinol Metab* **16**(5): 728-739.

Salcedo, R., Young, H. A., Ponce, M. L., Ward, J. M., Kleinman, H. K., Murphy, W. J. and Oppenheim, J. J. (2001). Eotaxin (CCL11) induces in vivo angiogenic responses by human CCR3+ endothelial cells. *J Immunol* **166**(12): 7571-7578.

Sallusto, F., Mackay, C. R. and Lanzavecchia, A. (1997). Selective expression of the eotaxin receptor CCR3 by human T helper 2 cells. *Science* **277**(5334): 2005-2007.

Sampietro, T., Tuoni, M., Ferdeghini, M., Ciardi, A., Marraccini, P., Prontera, C., Sassi, G., Taddei, M. and Bionda, A. (1997). Plasma cholesterol regulates soluble cell adhesion molecule expression in familial hypercholesterolemia. *Circulation* **96**(5): 1381-1385.

Sano, M., Sasaki, T., Hirakawa, S., Sakabe, J., Ogawa, M., Baba, S., Zaima, N., Tanaka, H., Inuzuka, K., Yamamoto, N., Setou, M., Sato, K., Konno, H. and Unno, N. (2014). Lymphangiogenesis and angiogenesis in abdominal aortic aneurysm. *PLoS One* **9**(3): e89830.

Santoni, M., Bracarda, S., Nabissi, M., Massari, F., Conti, A., Bria, E., Tortora, G., Santoni, G. and Cascinu, S. (2014). CXC and CC Chemokines as Angiogenic Modulators in Nonhaematological Tumors. *Biomed Res Int* **2014**.

Sata, M. and Fukuda, D. (2010). Crucial role of renin-angiotensin system in the pathogenesis of atherosclerosis. *J Med Invest* **57**(1-2): 12-25.

Saunders, R., Siddiqui, S., Kaur, D., Doe, C., Sutcliffe, A., Hollins, F., Bradding, P., Wardlaw, A. and Brightling, C. E. (2009). Fibrocyte localization to the airway smooth muscle is a feature of asthma. *J Allergy Clin Immunol* **123**(2): 376-384.

Scalia, R., Gong, Y., Berzins, B., Freund, B., Feather, D., Landesberg, G. and Mishra, G. (2011). A novel role for calpain in the endothelial dysfunction induced by activation of angiotensin II type 1 receptor signaling. *Circ Res* **108**(9): 1102-1111.

Schipper, H. S., Prakken, B., Kalkhoven, E. and Boes, M. (2012). Adipose tissue-resident immune cells: key players in immunometabolism. *Trends Endocrinol Metab* **23**(8): 407-415.

Scholten, D. J., Canals, M., Maussang, D., Roumen, L., Smit, M. J., Wijtmans, M., de Graaf, C., Vischer, H. F. and Leurs, R. (2012). Pharmacological modulation of chemokine receptor function. *Br J Pharmacol* **165**(6): 1617-1643.

Schulte, A., Schulz, B., Andrzejewski, M. G., Hundhausen, C., Mletzko, S., Achilles, J., Reiss, K., Paliga, K., Weber, C., John, S. R. and Ludwig, A. (2007). Sequential processing of the transmembrane chemokines CX3CL1 and CXCL16 by alpha- and gamma-secretases. *Biochem Biophys Res Commun* **358**(1): 233-240.

Seimon, T. and Tabas, I. (2009). Mechanisms and consequences of macrophage apoptosis in atherosclerosis. *J Lipid Res* **50**(Suppl): S382-387.

Seizer, P., Stellos, K., Selhorst, G., Kramer, B. F., Lang, M. R., Gawaz, M. and May, A. E. (2011). CXCL16 is a novel scavenger receptor on platelets and is associated with acute coronary syndrome. *Thromb Haemost* **105**(6): 1112-1114.

Sellers, S. L., Milad, N., Chan, R., Mielnik, M., Jermilova, U., Huang, P. L., de Crom, R., Hirota, J. A., Hogg, J. C., Sandor, G. G., Van Breemen, C., Esfandiarei, M., Seidman, M. A. and Bernatchez, P. (2018). Inhibition of Marfan Syndrome Aortic Root Dilation by Losartan:

Role of Angiotensin II Receptor Type 1-Independent Activation of Endothelial Function. *Am J Pathol* **188**(3): 574-585.

Shang, W., Qian, S., Fang, L., Han, Y. and Zheng, C. (2017). Association study of inflammatory cytokine and chemokine expression in hand foot and mouth disease. *Oncotarget* **8**(45): 79425-79432.

Shantsila, E., Wrigley, B., Tapp, L., Apostolakis, S., Montoro-Garcia, S., Drayson, M. T. and Lip, G. Y. (2011). Immunophenotypic characterization of human monocyte subsets: possible implications for cardiovascular disease pathophysiology. *J Thromb Haemost* **9**(5): 1056-1066.

Shen, A., Nieves-Cintron, M., Deng, Y., Shi, Q., Chowdhury, D., Qi, J., Hell, J. W., Navedo, M. F. and Xiang, Y. K. (2018). Functionally distinct and selectively phosphorylated GPCR subpopulations co-exist in a single cell. *Nat Commun* **9**(1): 1050.

Shihata, W. A., Michell, D. L., Andrews, K. L. and Chin-Dusting, J. P. (2016). Caveolae: A Role in Endothelial Inflammation and Mechanotransduction? *Front Physiol* **7**: 628.

Shimaoka, T., Nakayama, T., Fukumoto, N., Kume, N., Takahashi, S., Yamaguchi, J., Minami, M., Hayashida, K., Kita, T., Ohsumi, J., Yoshie, O. and Yonehara, S. (2004). Cell surface-anchored SR-PSOX/CXC chemokine ligand 16 mediates firm adhesion of CXC chemokine receptor 6-expressing cells. *J Leukoc Biol* **75**(2): 267-274.

Singh, K. D. and Karnik, S. S. (2016). Angiotensin Receptors: Structure, Function, Signaling and Clinical Applications. *J Cell Signal* **1**(2).

Singh, S. and Bittner, V. (2015). Familial hypercholesterolemia--epidemiology, diagnosis, and screening. *Curr Atheroscler Rep* **17**(2): 482.

Sluimer, J. C. and Daemen, M. J. (2009). Novel concepts in atherogenesis: angiogenesis and hypoxia in atherosclerosis. *J Pathol* **218**(1): 7-29.

Smabrekke, B., Rinde, L. B., Hindberg, K., Hald, E. M., Vik, A., Wilsgaard, T., Lochen, M. L., Njolstad, I., Mathiesen, E. B., Hansen, J. B. and Braekkan, S. (2016). Atherosclerotic Risk Factors and Risk of Myocardial Infarction and Venous Thromboembolism; Time-Fixed versus Time-Varying Analyses. The Tromso Study. *PLoS One* **11**(9): e0163242.

Sniderman, A. D., Tsimikas, S. and Fazio, S. (2014). The severe hypercholesterolemia phenotype: clinical diagnosis, management, and emerging therapies. *J Am Coll Cardiol* **63**(19): 1935-1947.

Soehnlein, O. and Lindbom, L. (2010). Phagocyte partnership during the onset and resolution of inflammation. *Nat Rev Immunol* **10**(6): 427-439.

Soto, B., Gallastegi-Mozos, T., Rodriguez, C., Martinez-Gonzalez, J., Escudero, J. R., Vila, L. and Camacho, M. (2017). Circulating CCL20 as a New Biomarker of Abdominal Aortic Aneurysm. *Sci Rep* **7**(1): 17331.

Sprague, A. H. and Khalil, R. A. (2009). Inflammatory Cytokines in Vascular Dysfunction and Vascular Disease. *Biochem Pharmacol* **78**(6): 539-552.

Sreeramkumar, V., Adrover, J. M., Ballesteros, I., Cuartero, M. I., Rossaint, J., Bilbao, I., Nacher, M., Pitaval, C., Radovanovic, I., Fukui, Y., McEver, R. P., Filippi, M. D., Lizasoain,

I., Ruiz-Cabello, J., Zarbock, A., Moro, M. A. and Hidalgo, A. (2014). Neutrophils scan for activated platelets to initiate inflammation. *Science* **346**(6214): 1234-1238.

Steinbacher, T., Kummer, D. and Ebnet, K. (2018). Junctional adhesion molecule-A: functional diversity through molecular promiscuity. *Cell Mol Life Sci* **75**(8): 1393-1409.

Stone, M. J., Hayward, J. A., Huang, C., Z, E. H. and Sanchez, J. (2017). Mechanisms of Regulation of the Chemokine-Receptor Network. *Int J Mol Sci* **18**(2).

Sumners, C., de Kloet, A. D., Krause, E. G., Unger, T. and Steckelings, U. M. (2015). Angiotensin type 2 receptors: blood pressure regulation and end organ damage. *Curr Opin Pharmacol* **21**: 115-121.

Tabas, I., Garcia-Cardena, G. and Owens, G. K. (2015). Recent insights into the cellular biology of atherosclerosis. *J Cell Biol* **209**(1): 13-22.

Tang, W. H., Kitai, T. and Hazen, S. L. (2017). Gut Microbiota in Cardiovascular Health and Disease. *Circ Res* **120**(7): 1183-1196.

Tavori, H., Giunzioni, I., Linton, M. F. and Fazio, S. (2013). Loss of plasma proprotein convertase subtilisin/kexin 9 (PCSK9) after lipoprotein apheresis. *Circ Res* **113**(12): 1290-1295.

Tissino, E., Benedetti, D., Herman, S. E. M., ten Hacken, E., Ahn, I. E., Chaffee, K. G., Rossi, F. M., Dal Bo, M., Bulian, P., Bomben, R., Bayer, E., Härzschel, A., Gutjahr, J. C., Postorino, M., Santinelli, E., Ayed, A., Zaja, F., Chiarenza, A., Pozzato, G., Chigaev, A., Sklar, L. A., Burger, J. A., Ferrajoli, A., Shanafelt, T. D., Wiestner, A., Del Poeta, G., Hartmann, T. N., Gattei, V. and Zucchetto, A. (2018). Functional and clinical relevance of VLA-4 (CD49d/CD29) in ibrutinib-treated chronic lymphocytic leukemia. *J Exp Med* **215**(2): 681-697.

Tousoulis, D., Oikonomou, E., Economou, E. K., Crea, F. and Kaski, J. C. (2016). Inflammatory cytokines in atherosclerosis: current therapeutic approaches. *Eur Heart J* **37**(22): 1723-1732.

Trussoni, C. E., Tabibian, J. H., Splinter, P. L. and O'Hara, S. P. (2015). Lipopolysaccharide (LPS)-Induced Biliary Epithelial Cell NRas Activation Requires Epidermal Growth Factor Receptor (EGFR). *PLoS One* **10**(4): e0125793.

Tse, K., Tse, H., Sidney, J., Sette, A. and Ley, K. (2013). T cells in atherosclerosis. *Int Immunol* **25**(11): 615-622.

Turner, J. D., Pionnier, N., Furlong-Silva, J., Sjoberg, H., Cross, S., Halliday, A., Guimaraes, A. F., Cook, D. A. N., Steven, A., Van Rooijen, N., Allen, J. E., Jenkins, S. J. and Taylor, M. J. (2018). Interleukin-4 activated macrophages mediate immunity to filarial helminth infection by sustaining CCR3-dependent eosinophilia. *PLoS Pathog* **14**(3): e1006949.

Uguccioni, M., Mackay, C. R., Ochensberger, B., Loetscher, P., Rhis, S., LaRosa, G. J., Rao, P., Ponath, P. D., Baggiolini, M. and Dahinden, C. A. (1997). High expression of the chemokine receptor CCR3 in human blood basophils. Role in activation by eotaxin, MCP-4, and other chemokines. *J Clin Invest* **100**(5): 1137-1143.

Urra, X., Villamor, N., Amaro, S., Gomez-Choco, M., Obach, V., Oleaga, L., Planas, A. M. and Chamorro, A. (2009). Monocyte subtypes predict clinical course and prognosis in human stroke. *J Cereb Blood Flow Metab* **29**(5): 994-1002.

van der Vorst, E. P., Doring, Y. and Weber, C. (2015a). Chemokines. *Arterioscler Thromb Vasc Biol* **35**(11): e52-56.

van der Vorst, E. P. C., Döring, Y. and Weber, C. (2015b). Chemokines and their receptors in Atherosclerosis. *J Mol Med (Berl)* **93**(9): 963-971.

van Duijn, J., Kuiper, J. and Slutter, B. (2018). The many faces of CD8+ T cells in atherosclerosis. *Curr Opin Lipidol* **29**(5): 411-416.

van Gils, J. M., Zwaginga, J. J. and Hordijk, P. L. (2009). Molecular and functional interactions among monocytes, platelets, and endothelial cells and their relevance for cardiovascular diseases. *J Leukoc Biol* **85**(2): 195-204.

van Panhuys, N., Prout, M., Forbes, E., Min, B., Paul, W. E. and Le Gros, G. (2011). Basophils are the major producers of IL-4 during primary helminth infection. *J Immunol* **186**(5): 2719-2728.

Vanhoutte, P. M., Shimokawa, H., Feletou, M. and Tang, E. H. (2017). Endothelial dysfunction and vascular disease - a 30th anniversary update. *Acta Physiol (Oxf)* **219**(1): 22-96.

Vass, M., Kooistra, A. J., Yang, D., Stevens, R. C., Wang, M. W. and de Graaf, C. (2018). Chemical Diversity in the G Protein-Coupled Receptor Superfamily. *Trends Pharmacol Sci*.

Vasudevan, A. R., Wu, H., Xydakis, A. M., Jones, P. H., Smith, E. O., Sweeney, J. F., Corry, D. B. and Ballantyne, C. M. (2006). Eotaxin and obesity. *J Clin Endocrinol Metab* **91**(1): 256-261.

Vijaynagar, B., Bown, M. J., Sayers, R. D. and Choke, E. (2013). Potential role for anti-angiogenic therapy in abdominal aortic aneurysms. *Eur J Clin Invest* **43**(7): 758-765.

Volpe, M., Savoia, C., De Paolis, P., Ostrowska, B., Tarasi, D. and Rubattu, S. (2002). The renin-angiotensin system as a risk factor and therapeutic target for cardiovascular and renal disease. *J Am Soc Nephrol* **13 Suppl 3**: S173-178.

von Hundelshausen, P. and Schmitt, M. M. N. (2014). Platelets and their chemokines in atherosclerosis—clinical applications. *Front Physiol* **5**.

Wang, J., Lu, Y., Wang, J., Koch, A. E., Zhang, J. and Taichman, R. S. (2008). CXCR6 induces prostate cancer progression by the AKT/mammalian target of rapamycin signaling pathway. *Cancer Res* **68**(24): 10367-10376.

Warner, N., Burberry, A., Pliakas, M., McDonald, C. and Nunez, G. (2014). A genome-wide small interfering RNA (siRNA) screen reveals nuclear factor-kappaB (NF-kappaB)-independent regulators of NOD2-induced interleukin-8 (IL-8) secretion. *J Biol Chem* **289**(41): 28213-28224.

Watanabe, T., Barker, T. A. and Berk, B. C. (2005). Angiotensin II and the endothelium: diverse signals and effects. *Hypertension* **45**(2): 163-169.

Weber, C. and Noels, H. (2011). Atherosclerosis: current pathogenesis and therapeutic options. *Nat Med* **17**(11): 1410-1422.

Weber, C., Shantsila, E., Hristov, M., Caligiuri, G., Guzik, T., Heine, G. H., Hoefer, I. E., Monaco, C., Peter, K., Rainger, E., Siegbahn, A., Steffens, S., Wojta, J. and Lip, G. Y. (2016). Role and analysis of monocyte subsets in cardiovascular disease. Joint consensus document of the European Society of Cardiology (ESC) Working Groups "Atherosclerosis & Vascular Biology" and "Thrombosis". *Thromb Haemost* **116**(4): 626-637.

Wente, M. N., Gaida, M. M., Mayer, C., Michalski, C. W., Haag, N., Giese, T., Felix, K., Bergmann, F., Giese, N. A. and Friess, H. (2008). Expression and potential function of the CXC chemokine CXCL16 in pancreatic ductal adenocarcinoma. *Int J Oncol* **33**(2): 297-308.

White, G. E., Iqbal, A. J. and Greaves, D. R. (2013). CC chemokine receptors and chronic inflammation--therapeutic opportunities and pharmacological challenges. *Pharmacol Rev* **65**(1): 47-89.

Wilbanks, A. M., Laporte, S. A., Bohn, L. M., Barak, L. S. and Caron, M. G. (2002). Apparent loss-of-function mutant GPCRs revealed as constitutively desensitized receptors. *Biochemistry* **41**(40): 11981-11989.

Wilkins, E., Wilson, L., Wickramasinghe, K., Bhatnagar, P., Leal, J., Luengo-Fernandez, R., Burns, R., Rayner, M. and Townsend, N. (2017). European cardiovascular disease statistics 2017. *European Heart Network: Brussels, Belgium*.

Willems, L. I. and Ijzerman, A. P. (2010). Small molecule antagonists for chemokine CCR3 receptors. *Med Res Rev* **30**(5): 778-817.

Willis, L. M., El-Remessy, A. B., Somanath, P. R., Deremer, D. L. and Fagan, S. C. (2011). Angiotensin receptor blockers and angiogenesis: clinical and experimental evidence. *Clin Sci (Lond)* **120**(8): 307-319.

Wong, N. D., Zhao, Y., Patel, R., Patao, C., Malik, S., Bertoni, A. G., Correa, A., Folsom, A. R., Kachroo, S., Mukherjee, J., Taylor, H. and Selvin, E. (2016). Cardiovascular Risk Factor Targets and Cardiovascular Disease Event Risk in Diabetes: A Pooling Project of the Atherosclerosis Risk in Communities Study, Multi-Ethnic Study of Atherosclerosis, and Jackson Heart Study. *Diabetes Care* **39**(5): 668-676.

Wu, D., Molofsky, A. B., Liang, H. E., Ricardo-Gonzalez, R. R., Jouihan, H. A., Bando, J. K., Chawla, A. and Locksley, R. M. (2011). Eosinophils sustain adipose alternatively activated macrophages associated with glucose homeostasis. *Science* **332**(6026): 243-247.

Wu, H. and Ballantyne, C. M. (2017). Dyslipidaemia: PCSK9 inhibitors and foamy monocytes in familial hypercholesterolaemia. *Nat Rev Cardiol* **14**(7): 385-386.

Wu, W., Jin, Y. and Carlsten, C. (2018). Inflammatory health effects of indoor and outdoor particulate matter. *J Allergy Clin Immunol* **141**(3): 833-844.

Wuttge, D. M., Zhou, X., Sheikine, Y., Wagsater, D., Stemme, V., Hedin, U., Stemme, S., Hansson, G. K. and Sirsjo, A. (2004). CXCL16/SR-PSOX is an interferon-gamma-regulated chemokine and scavenger receptor expressed in atherosclerotic lesions. *Arterioscler Thromb Vasc Biol* **24**(4): 750-755.

Xing, J., Liu, Y. and Chen, T. (2018). Correlations of chemokine CXCL16 and TNF-alpha with coronary atherosclerotic heart disease. *Exp Ther Med* **15**(1): 773-776.

Yamada, H., Hirai, K., Miyamasu, M., Iikura, M., Misaki, Y., Shoji, S., Takaishi, T., Kasahara, T., Morita, Y. and Ito, K. (1997). Eotaxin is a potent chemotaxin for human basophils. *Biochem Biophys Res Commun* **231**(2): 365-368.

Yang, Z., Yang, F., Zhang, D., Liu, Z., Lin, A., Liu, C., Xiao, P., Yu, X. and Sun, J. P. (2017). Phosphorylation of G Protein-Coupled Receptors: From the Barcode Hypothesis to the Flute Model. *Mol Pharmacol* **92**(3): 201-210.

Yoo, S. Y. and Kwon, S. M. (2013). Angiogenesis and its therapeutic opportunities. *Mediators Inflamm* **2013**: 127170.

Yoshimoto, T. (2018). The Hunt for the Source of Primary Interleukin-4: How We Discovered That Natural Killer T Cells and Basophils Determine T Helper Type 2 Cell Differentiation In Vivo. *Front Immunol* **9**: 716.

Yu, X., Zhao, R., Lin, S., Bai, X., Zhang, L., Yuan, S. and Sun, L. (2016). CXCL16 induces angiogenesis in autocrine signaling pathway involving hypoxia-inducible factor 1alpha in human umbilical vein endothelial cells. *Oncol Rep* **35**(3): 1557-1565.

Zabel, B. A., Rott, A. and Butcher, E. C. (2015). Leukocyte chemoattractant receptors in human disease pathogenesis. *Annu Rev Pathol* **10**: 51-81.

Zernecke, A. and Weber, C. (2010). Chemokines in the vascular inflammatory response of atherosclerosis. *Cardiovasc Res* **86**(2): 192-201.

Zernecke, A. and Weber, C. (2014). Chemokines in atherosclerosis: proceedings resumed. *Arterioscler Thromb Vasc Biol* **34**(4): 742-750.

Zhang, H. and Baker, A. (2017). Recombinant human ACE2: acing out angiotensin II in ARDS therapy. *Crit Care* **21**(1): 305.

Zhang, X., Sun, D., Song, J. W., Zullo, J., Lipphardt, M., Coneh-Gould, L. and Goligorsky, M. S. (2018). Endothelial cell dysfunction and glycocalyx - A vicious circle. *Matrix Biol*.

Zhang, Y., Naggar, J. C., Welzig, C. M., Beasley, D., Moulton, K. S., Park, H. J. and Galper, J. B. (2009). Simvastatin inhibits angiotensin II-induced abdominal aortic aneurysm formation in apolipoprotein E-knockout mice: possible role of ERK. *Arterioscler Thromb Vasc Biol* **29**(11): 1764-1771.

Zhao, Q. and Li, Z. (2015). Angiogenesis. *Biomed Res Int* **2015**: 135861.

Zhao, T., Bernstein, K. E., Fang, J. and Shen, X. Z. (2017). Angiotensin-converting enzyme affects the presentation of MHC class II antigens. *Lab Invest* **97**(7): 764-771.

Zhou, H. F., Yan, H., Cannon, J. L., Springer, L. E., Green, J. M. and Pham, C. T. (2013). CD43-mediated IFN-gamma production by CD8+ T cells promotes abdominal aortic aneurysm in mice. *J Immunol* **190**(10): 5078-5085.

Zhuge, X., Murayama, T., Arai, H., Yamauchi, R., Tanaka, M., Shimaoka, T., Yonehara, S., Kume, N., Yokode, M. and Kita, T. (2005). CXCL16 is a novel angiogenic factor for human umbilical vein endothelial cells. *Biochem Biophys Res Commun* **331**(4): 1295-1300.

Zieske, A. W., Tracy, R. P., McMahan, C. A., Herderick, E. E., Homma, S., Malcom, G. T., McGill, H. C., Jr. and Strong, J. P. (2005). Elevated serum C-reactive protein levels and advanced atherosclerosis in youth. *Arterioscler Thromb Vasc Biol* **25**(6): 1237-1243.

Zimmer, S., Grebe, A. and Latz, E. (2015). Danger signaling in atherosclerosis. *Circ Res* **116**(2): 323-340.